

Antibody Based Strategies For Multiplexed Diagnostics

by

Krupa Arun Navalkar

A Dissertation Presented in Partial Fulfillment
of the Requirements for the Degree
Doctor of Philosophy

Approved April 2014 by the
Graduate Supervisory Committee:

Stephen Albert Johnston, Co-Chair
Phillip Stafford, Co-Chair
Kathryn Sykes
Bertram Jacobs

ARIZONA STATE UNIVERSITY

August 2014

ABSTRACT

Peptide microarrays are to proteomics as sequencing is to genomics. As microarrays become more content-rich, higher resolution proteomic studies will parallel deep sequencing of nucleic acids. Antigen-antibody interactions can be studied at a much higher resolution using microarrays than was possible only a decade ago. My dissertation focuses on testing the feasibility of using either the Immunosignature platform, based on non-natural peptide sequences, or a pathogen peptide microarray, which uses bioinformatically-selected peptides from pathogens for creating sensitive diagnostics. Both diagnostic applications use relatively little serum from infected individuals, but each approaches diagnosis of disease differently. The first project compares pathogen epitope peptide (life-space) and non-natural (random-space) peptide microarrays while using them for the early detection of Coccidioidomycosis (Valley Fever). The second project uses NIAID category A, B and C priority pathogen epitope peptides in a multiplexed microarray platform to assess the feasibility of using epitope peptides to simultaneously diagnose multiple exposures using a single assay. Cross-reactivity is a consistent feature of several antigen-antibody based immunodiagnostics. This work utilizes microarray optimization and bioinformatic approaches to distill the underlying disease specific antibody signature pattern. Circumventing inherent cross-reactivity observed in antibody binding to peptides was crucial to achieve the goal of this work to accurately distinguishing multiple exposures simultaneously.

DEDICATION

To my family and friends

ACKNOWLEDGMENTS

I am deeply indebted to Dr. Stephen Albert Johnston and Dr. Phillip Stafford for having mentored me throughout my dissertation and for the wonderful opportunity of optimizing peptide microarray based infectious disease diagnostics. I am grateful to them for their tireless efforts at steering my dissertation to its fruition and for never failing to help address empirical phenomenon encountered through this work.

I would like to thank my committee members Dr. Kathryn Sykes and Dr. Bertram Jacobs for helping broaden the scope of my work. I wish to also thank previous committee members, Dr. Mitchell Magee and Dr. Jeffrey Touchman for being part of my committee. Dr. Mitchell Magee was involved in the initial phases of the Valley Fever peptide microarray diagnostic project and introduced me to the corpus of prior research performed on the subject.

I would like to thank our collaborators Dr. John Galgiani for contributing valuable, well-characterized, Valley Fever patient sera from the Valley Fever Center for Excellence at University of Arizona. I would also like to thank Dr. Ian Lipkin at Columbia University for providing Herpes virus infected human patient sera. I would like to thank Dr. Anders Sjöstedt, Umeå University for having kindly contributed *Francisella tularensis subsp. holarctica (LVS)* vaccine recipient human serum samples. I am grateful to Lawrence Livermore National Laboratory for providing infected patient sera for West Nile virus and Malaria infections originally acquired by them from SeraCare.

I am grateful to Dr. Rebecca Halperin for helping design the analysis strategy for the pathogen proteome peptide array. She was kind enough to implement my suggestions regarding di-peptide inversions in her program GuiTope. I am grateful to Dr. Bart

Legutki for his scientific input and suggestions throughout my dissertation. I am grateful to Kevin Brown for writing programs to query and retrieve outputs from B-cell epitope prediction algorithms hosted on the Immune Epitope Database (IEDB) website. I wish to thank John Lainson for helping design the ‘*VF-diagnostic*’ sub-array and for processing sera for the project on random peptide Immunosignature microarrays. I thank Elizabeth Lambert, Mara Gardner and Dr. Bart Legutki for processing patient serum samples on the random peptide microarrays as per protocol. I thank Sara Matsumoto and Daniel Wrapp for helping analyze microarray slide image data and Jameson Berry for processing an Influenza PR8 ELISA.

I wish to thank all my lab members Preston Hunter, Dr. Kurt Whittemore, Dr. Nidhi Gupta, Pattie Madjidi, Penny Gwynne, Dr. Andrey Loskutov, Loren Howell, Tien Olson, Lori Phillips, Felicia Craciunescu, Lu Wang, Dr. Luhui Shen, Dr. Zhan-gong Zhao and Dr. Chris Diehnelt for always being willing to help. I wish to thank Dr. Neal Woodbury for providing critical suggestions on the Valley Fever publication and the DTRA-1 project.

This dissertation would not have been possible without the funding support from the Chemical Biological Technologies Directorate contract HDTRA-11-1-0010 from the Department of Defense Chemical and Biological Defense program through the Defense Threat Reduction Agency (DTRA) to Dr. Stephen Albert Johnston.

I am grateful to Mrs. Renate Mittelman, Dr. Rosemary Renaut, Dr. Zdzislaw Jackiewicz and Dr. Scott Bingham for always guiding me throughout my time at ASU. I am grateful to always have the continuing support of my family and friends.

TABLE OF CONTENTS

	Page
LIST OF TABLES.....	xiii
LIST OF FIGURES.....	xvii
PREFACE.....	xxviii
CHAPTER	
1. INTRODUCTION.....	1
Project Overview	1
Peptide Microarray As Clinical Diagnostics.....	1
Advantages Of Using Peptide Microarrays.....	2
Project I: Valley Fever Immunosignaturing Diagnostic	4
Multiplexed Diagnostics For Human Pathogens And Bio-Threat Agents.....	10
Cross-Reactive Components Of The Humoral Antibody Response To An Infection	14
Project II: Multiplexed Priority Pathogen Proteome Peptide Array.....	16
2. APPLICATION OF IMMUNOSIGNATURES TO DIAGNOSIS OF VALLEY FEVER.....	18
Abstract	18
Background	18
Methods.....	18
Results	19
Conclusion.....	19

CHAPTER	Page
Abbreviations	19
Introduction	20
Methods	23
Serum Samples Used In This Study	23
Confounding Infection Samples	23
Valley Fever And Normal Donor Serum Samples Used In This Study	24
Blinded Test Patient Sample Set	25
Microarray Production And Processing	26
Statistical Classification Of Disease Groups	26
Statistical Classification Of Confounding Infections	27
Results	28
Valley Fever Immunosignature Is Distinct From That Of Other Infections	28
Valley Fever Immunosignature Is Distinct From That Of Uninfected Individuals	30
Creating A 96 Peptide VF Diagnostic Microarray	31
Performance Of A 96 Peptide VF-Diagnostic Microarray	35
Discussion	38
Acknowledgements	41
Grant acknowledgements	42
Supplementary Data	43

CHAPTER	Page
3. COMPARISON OF NON-NATURAL MIMOTOPE VERSUS EPITOPE PEPTIDES IN DIAGNOSING VALLEY FEVER.....	47
Abstract	47
Abbreviations	48
Introduction	48
Methods	52
Serum Samples Used In This Study	52
Microarray Production And Processing	54
Pre-Processing Of Data For Analysis.....	56
Statistical Analysis.....	56
GuiTope Analysis	57
Results	58
Comparing Classification Accuracy And Sensitivity Of Life Space Versus Random Peptides	58
Bioinformatic Rationale Underlying The Sensitivity Of Random (96) Vs. Life- Space (83) Epitope Peptides	61
Specificity And Robustness Of Random (96) Vs. Life-Space (83) VF Epitope Peptides	63
Discussion	73
Acknowledgements.....	78
Grant Acknowledgements	78

CHAPTER	Page
4. MULTI PATHOGEN PEPTIDE BASED SEROLOGICAL DIAGNOSTIC	109
Abstract	109
Keywords	110
Abbreviations	110
Introduction	110
Methods	113
Serum Samples And Rationale For Choosing Pathogens To Be Represented	113
Microarray Production And Processing	119
Data Analysis	120
Receiver Operating Characteristics (ROC) Curve Calculation	122
Results	122
Physical optimization of pathogen proteome peptide (PPP) array	122
Comparison 1: The Effect Of Temperature On Antibody-Peptide Association	123
Reducing Cross-Reactivity On Array By Reducing Peptide Density On Array Surface	127
Comparison 2: Slide Surface	129
Comparison 3: Time Of Incubation Of Sera	134
Comparison 4: Spacing Of Peptides Affecting Polyclonal Antibody Capture.	137
Comparison 5: Dilution Of Primary Patient Sera 1:5000 Patient Serum Dilution	139
Discussion	142

CHAPTER	Page
Grant Acknowledgements	149
Acknowledgements.....	149
Supplementary Figures And Tables	150
5. DE-CONVOLUTING ANTIBODY CROSS-REACTIVITY OBSERVED ON A	
PATHOGEN PROTEOME PEPTIDE MICROARRAY.....	158
Abstract	158
Abbreviations	159
Keywords	159
Introduction.....	160
Methods.....	163
Serum Samples And Monoclonal Antibodies Used In This Study.....	163
Microarray Production And Processing	164
Statistical Analysis And Software Used.....	166
Influenza PR8 Whole Virus ELISA Protocol	167
Results	168
Redundancy Observed Within Priority Pathogen Proteomes Represented On PPP Array.....	168
Redundancy Observed Within Priority Pathogen Peptides Represented On PPP Array.....	171
Redundancy Observed Within Peptides On The PPP Array And Pathogen Proteomes.....	173

CHAPTER	Page
Monoclonal Antibody Binding On The PPP Array	176
Simultaneous Detection Of Priority Pathogen And Common Exposure Pathogen Signature.....	178
Cross-Reactivity Observed On Pathogen Peptide Array From Evolutionarily Related Pathogen Exposures	183
Simulating An Artificial Infection Using Multiple Monoclonal Antibodies..	185
Influenza Antibody Reactivity Observed In Individuals Responding To Non- Influenza Virus Exposures.....	191
Defining The Umbrella Of Antibody Reactivity Observed On The Pathogen Array	198
Discussion	201
Grant Acknowledgement.....	206
Acknowledgement	206
Supplementary Information.....	207
6. CONCLUSION	209
Coccidioidomycosis.....	209
Development Of A Microarray Diagnostic That Exceeds Existing Diagnostic Standards	210
Bioinformatic Analysis Of Pathogen Proteomes Toward The Development Of A Multiplexed Life-Space Peptide Microarray Diagnostic	212

CHAPTER	Page
Designing A Multiplexed Pathogen Proteome Peptide Microarray – Future Directions	213
Cross-Reactivity Attributable To Common Exposures And Vaccinations.....	227
REFERENCES	256
APPENDIX	
APPENDIX I: <i>COCCIDIOIDES</i> SPHERULES IN SERA	231
INTERFERENCE IN MICROARRAYS – SUPPLEMENTAL FIGURES AND	
TABLES FOR CHAPTER 2	253
Hypothesis.....	260
Bibliography.....	262
APPENDIX II: SUPPLEMENTAL DATA FOR CHAPTER 3 – VALLEY FEVER	
EPITOPE PEPTIDES.....	264
Bibliography.....	287
APPENDIX III: SUPPLEMENTAL DATA FOR CHAPTER 4	
1.) F. Tularensis Vaccine Project: Overcoming ELISA Limitations Using The Pathogen Proteome Peptide (PPP) Array	289
2.) ASFV Vaccine Project: Mapping Humoral Response From Genetic Immunization Using The PPP Array.....	292
Immunization Protocol # AR000158	297
Immunization Protocol # AR000302	305

APPENDIX	Page
3.) IVTT Bead Protein Array–Rapid Screening Of Immunogenic/ Immunodominant Proteins	308
Sonication Printing Protocols	308
Slide 1: 400787	309
Slide 2: 400940	310
Slide 4: 400941	311
Acknowledgements.....	319
Bibliography.....	321
APPENDIX IV	323
INSTITUTIONAL REVIEW BOARD (IRB) APPROVAL.....	323
APPENDIX V	330
INSTITUTIONAL ANIMAL CARE & USE COMMITTEE.....	330
BIOGRAPHICAL SKETCH	339

LIST OF TABLES

Table	Page
Table 2- 1 Patient Sample Cohorts Per Infection Utilized In This Study	23
Table 2- 2 Diagnosis (IDCF) Of 55 Unique Patient Samples From The VF Training Cohort	24
Table 2- 3 Diagnosis (IDCF) Of 67 Blinded Samples From The VF Test Cohort.	25
Table 2- 4 Classification Results From Samples Shown In Figure 2- 1, Naïve Bayes Was Used To Simultaneously Classify The 108 Patients Into Their Respective Groups Using Hold Out (70% Train, 30% Test, 20 Iterations) Cross-Validation To Estimate Error.	28
Table 2- 5 Naïve Bayes Classification Results From The VF Training Cohort On The 10K Peptide Microarray Using The 96 Predictor Peptides. Holdout Splits All Data Randomly Into 70% Train/30% Predict. Results Are From 20 Iterations Of Random Holdouts.....	35
Table 2- 6 Naïve Bayes Classification Results From 96 Peptide VF Diagnostic Array. Top Panel: 96 Peptide Diagnostic-Array Data Was Tested For Performance On A Blinded Cohort Of False-Negative VF Patients. Middle Panel: Performance Using All Possible Patient Samples Including Test And Training Samples. Bottom Panel: Performance Using Only The Training Dataset.....	36
Supplementary Table 2- 1 Non-VF Infection Samples, ELISA Data From SeraCare	43
Table 3- 1 Naïve Bayes Classification Result On VF Test Dataset Using Random Vs Life Space Peptides.	60

Table	Page
Table 3- 2 Naïve Bayes Classification Results Using Igg And Igm Signals From VF 96 Random Predictor Peptides And 83 VF Epitope Peptides.....	63
Table 3- 3 Summary Of Guitope Matches Between 96-Random VF Predictor Peptides And 4 VF Antigens	69
Supplementary Table 3- 1 Sample Characteristics Of The Training Set For Valley Fever Study.	79
Supplementary Table 3- 2 Sample Characteristics Of The 67 Blinded Test Sera From 25 Patients.....	79
Supplementary Table 3- 3 Individual Patient Characteristics From The Un-Blinded Test Set.	80
Supplementary Table 3- 4 Summary Of Guitope Results With Inversion Weight =1 From Alignment Of 96-Random Peptides To 4 Immunodominant Antigens Of C.Immitis.....	81
Supplementary Table 3- 5 Summary Of Guitope Results With Inversion Weight =0 From Alignment Of 96-Random Peptides To 4 Immunodominant Antigens Of C.Immitis.....	98
Table 4- 1 Peptide Selection Strategy For PPP Array	114
Table 4- 2 Predicted & Empirical Epitopes (IEDB-Bepipred) [Accessed On: 30th November, 2011]	116
Table 4- 3 Number Of Peptides Per Priority Pathogen Proteome	117
Table 4- 4 Duplicate 5-Mers - 16-Mers Within The 4337 Peptides From The PPP Array And 10K Non-Natural Sequence Peptide Immunosignature Array.....	118

Table	Page
Table 4- 5 AUC Derived From ROC Summary Of Incubating Samples On Aminosilane Slides At Varying Temperatures, Time Of Primary Antibody Incubation Is Held Constant At 1 Hour.	125
Table 4- 6 ROC-AUC For Comparing Slide Surfaces Aminosilane Versus NSB-9	129
Table 4- 7 ROC-AUC Obtained For 2 Infections On NSB9 Slide Surface At Varying Temperatures.....	134
Table 4- 8 ROC-AUC During Varying Incubation Times On NSB-9 Surface	137
Table 4- 9 ROC-AUC After Combining NSB9 And NSB-27 (1:500) Data.....	139
Table 4-10 ROC-AUC Of Detection Of 2 Infections At Limiting Concentrations Of Antigen And Antibody.....	140
Supplementary Table 4- 1 Guitope Match Data (Score Cut=3)	155
Table 5- 1 ROC Summary Displaying Accuracy Of Diagnosing The Cognate Infection On Three Platforms.....	181
Table 5- 2 Summary Of The Worst AUC-ROC Changes Between Array Iterations, After The Addition Of Influenza Peptides In PPP(15), PPP (No. Of Pathogens Represented As Peptides On Array).	182
Table 5- 3 SVM (LOOCV) Results From PPP-15 Using The N-Mer Analysis For Classification.....	200
Supplementary Table 5- 1 Monoclonal And Polyclonal Antibodies Used On PPP Array	207

Table	Page
Table 6- 1 Unique 5-Mers And 9-Mers In-Common Between Pathogens Tested On The Andresen Assay	221
Table 6- 2 Five Mers In Common Between ASFV And Vaccinia Proteomes (Orange) And Several Herpes Viruses (Yellow).....	224
Table 6- 3 Amino Acid Frequencies In Proteomes Of Priority Pathogens And Common Pathogens	225
Table A1- 1 Summary Of Spherules-Like Objects Observed In VF Infected Individuals Sera When Incubated On Aminosilane Surface VF Diagnostic Sub-Arrays.....	258
Table A3- 1 Difference Between Immunization Groups And Naïve Sera Using PPP Array Data	291
Table A3- 2 Summary Of Statistical Differences Between Groups A, B And Control Group C Post-ASFV Challenge.....	304
Table A3- 3 T-Test P-Value From Samples On Day 70 Post-Immunization And Boost, Pre-Challenge As Captured Using ASFV And Vaccinia Peptides On PPP Array	306
Table A3- 4 Signal Captured From Slides Included In The Printing Protocol Comparison In Fluorescence Intensity Units (FIU).	315

LIST OF FIGURES

Figure	Page
Figure 2- 1 Hierarchical Clustering Of Informative Peptides Across Five Diseases.	29
Figure 2- 2 Hierarchical Clustering Of Valley Fever Immunosignature Apart From Uninfected Individuals.....	30
Figure 2- 3 Signal Intensity (Y-Axis) For 96 Peptides From The 10,000 Peptide Microarray That Distinguish Both VF And Influenza Vaccine Recipients.....	32
Figure 2- 4 Heat Map Showing Normalized Average Signals From The 96 Predictor Peptides As In Figure 2- 2, But Displaying The Cohort Separation.....	34
Figure 2- 5 Limits Of Detection Graphed From A Post-Hoc Power Calculation.....	37
Figure 3- 1 The Clinical Problem In Valley Fever Diagnosis.	50
Figure 3- 2 VF Patient Signal Average Intensity Data Per CF-Titer.....	59
Figure 3- 3 Sensitivity Of Assay - Number Of Unique N-Mers (2-6 Amino Acid Short Sequences) Between The 96-Random And 83-Lifespace Peptides In Common With The VF Pathogen Proteome (Panel A) And The Randomly Generated VF Proteome (Panel B).	62
Figure 3- 4 Cross-Reactivity Observed On Vf-Diagnostic Array Hypothetically Explained Using The Number Of Unique 5-Mers In Common (Y-Axis) Between Random (Blue Bars) And Life Space (Red Bars) Peptides And Pathogen Proteomes (X-Axis)....	67
Figure 3- 5 Specificity Of Assay - Number Of Unique N-Mers (2-6 Amino Acid Short Sequences) Between The 96-Random And 83-Lifespace Peptides In Common With The LVS Proteome (Panel A) And The Randomly Generated LVS Proteome (Panel B).....	68

Figure	Page
Figure 3- 6 Guitope Analysis Comparing 96-Random Peptide VF Predictors With Each Of The 4 VF Proteins Tiled For The 83 Life-Space Epitope Peptides.	71
Figure 3- 7 VF Predictor Random Peptides (96) Overlapping 83 Life-Space Peptides From Valley Fever.	72
Figure 3- 8 BLAST Alignment Map Depicting VF-Protein Coverage Of 96-Random Peptides Through Positive Hits From GuiTope.	73
Figure 4- 1 The Effect Of Incubation Temperature On Various Samples Tested On The Pathogen Array.	124
Figure 4-2 Estimating Cross-Reactivity - Histograms Displaying Signal Intensities From Arrays With Or Without Monoclonal Antibody Epitopes.	126
Figure 4- 3 Biotinylation For Comparing The Spot Morphology And Dynamic Range Of Signal From Three Slide Surfaces, Aminosilane (AS), NSB-9 And NSB-27.	128
Figure 4- 4 Box-Plots Showing Antibody Binding Distribution As Observed On NSB-9 Versus Aminosilane (AS) Slides.	131
Figure 4- 5 Histograms Displaying Cognate Peptide Reactivity On Aminosilane (AS) And NSB-9 Slides.	133
Figure 4-6 Cognate Pathogen Peptide Reactivity Is Enhanced At 16 Hour In Comparison To After 1 Hour Of Serum Incubation.	136
Figure 4- 7 ROC Curve AUC Summarizing Ability To Distinguish One Infection From Another On The PPP Array Under Longer Incubation.	138

Figure	Page
Figure 4- 8 Effect Of Incubation Time, Temperature And Slide Surface On Information Content Of Array.	141
Supplementary Figure 4- 1 Histograms Displaying Array Data For 6 Monoclonal Antibodies On NSB-9 Slides	150
Supplementary Figure 4- 2 Change In Signal Distribution And Cognate Versus Non-Cognate Reactivity Of p53Ab1 Monoclonal Incubated On NSB-9 Slides For 1, 16, 24 And 36 Hours Respectively.	151
Supplementary Figure 4- 3 Average Signal Intensity Observed For Various Infections On NSB-9 Slides At 16 Hour Incubation, 23°C And Serum Dilution Of 1:500	152
Supplementary Figure 4- 4 Structural (Anti-LPS, Anti-VEE) And Polyclonal Antibodies (FT03, Rco1, Rco2, Rco3, Rco4) On Array.	153
Supplementary Figure 4- 5 Capturing The Memory Immune Response From Exposure And Distinguishing Time Of Exposure – Vaccinia Vaccination.....	154
Figure 5- 1 BLAST Matrix Depicting Homology Between Pathogens Chosen To Be Represented On The Pathogen Proteome Peptide (PPP) Microarray.	170
Figure 5- 2 Pathogen Space Is Extremely Conserved On A 5-Mer Peptide Motif Level.	173
Figure 5- 3 Circular Connectogram Displaying 5-Mer Level Overlap Between Peptides Represented On The Pathogen Array And Their Respective Proteomes	176
Figure 5- 4 Monoclonal Antibody Binding Observed On PPP-14 Array (p53Ab1)	178

Figure	Page
Figure 5- 5 P-Value Score Chart For 1 WNV Infected Individual's Sera On 3 Different Array Platforms.....	179
Figure 5- 6 Cross-Reactivity Displayed On Three Versions Of PPP Arrays From One HSV-2 Infected Individual's Sera.....	184
Figure 5- 7 Median Signal Intensities On A Log10 Scale For 8 Monoclonal Antibody Epitopes (Blue Bars) Versus Signals From All Other Peptides On The Array (Green Bars) And PR8 Influenza Peptides (Red Bars). Error Bars Represent Standard Error, P-Value Cut-Off = 0.125.....	187
Figure 5- 8 Monoclonal Antibody Mix On Pathogen Arrays.....	190
Figure 5- 9 Influenza Reactivity Observed In Individuals With Non-Influenza Exposures.....	192
Figure 5- 10 WNV Patients Sera Processed At Three Dilutions On PPP-15.....	196
Figure 5- 11 VF Patient Sera Processed At Three Dilutions On PPP-14.....	197
Figure 6- 1 Schema For Designing A Multiplexed Pathogen Proteome Peptide Microarray.....	214
Figure 6- 2 Blast Matrix Depicting Proteome Level Overlap Between The Four Main Races Of Dengue Virus (Reference Proteomes) And WNV-I And II And JEV.....	215
Figure 6- 3 Blastmatrix Showing Torch Assay Pathogen Proteome Overlap.....	217
Figure 6- 4 Pathogen Proteome Level Overlap For Pathogens Represented In A Multiplexed 900 Peptide Microarray Showing Cross-Reactivity In Andresen Et Al (2009).....	220

Figure	Page
Figure 6- 5 Blast Matrix Depicting Proteome Level Overlap Between Herpes Viruses (Herpesviridae) And Other Pox-Viruses ASFV (Asfarviridae) And Vaccinia (Orthopoxviridae)	222
Figure 6- 6 Commonality On A 5-Mer Sequence Level Between Priority Pathogen Proteomes And Common Pathogen Proteomes Such As Herpes Viruses And Influenza Vaccine Proteomes (Highlighted In The Legend In Yellow).	229
Figure A1- 1 A Screenshot Of A Spherule-Like Object (Slide No. CNS00209) As Captured Using Genepix Pro On The VF Diagnostic Sub-Array (Slide Surface: Aminosilane).....	256
Figure A1- 2 A Screenshot Of A Spherule-Like Object (Slide No. CNS00209) As Captured Within Genepix On The VF Diagnostic Sub-Array (Slide Surface: Aminosilane).....	257
Figure A2-1 IgG Antibody Reactivity Captured On VF Epitope Peptides (83) From False-Negative CF-Titer=0 Patients Sera (N=54).Each Line On The Graph Represents Antibody Response From One VF Sample.....	267
Figure A2-2 IgM Antibody Reactivity Captured On VF Epitope Peptides (83) From False-Negative CF-Titer=0 Patients Sera (N=54) Each Line On The Graph Represents Antibody Response From One VF Sample.....	268
Figure A2-3 IgG Antibody Reactivity Captured On VF Epitope Peptides (83) From CF-Titer=1 Patients Sera (N=9). Each Line On The Graph Represents Antibody Response From One VF Sample.	269

Figure	Page
Figure A2-4 IgM Antibody Reactivity Captured On VF Epitope Peptides (83) From CF-Titer=1 Patients Sera (N=9). Each Line On The Graph Represents Antibody Response From One VF Sample.	270
Figure A2-5 IgG Antibody Reactivity Captured On VF Epitope Peptides (83) From CF-Titer=2 Patients Sera (N=15). Each Line On The Graph Represents Antibody Response From One VF Sample.	271
Figure A2-6 IgM Antibody Reactivity Captured On VF Epitope Peptides (83) From CF-Titer=2 Patients Sera (N=15). Each Line On The Graph Represents Antibody Response From One VF Sample.	272
Figure A2-7 IgG Antibody Reactivity Captured On VF Epitope Peptides (83) From CF-Titer=4 Patients Sera (N=8). Each Line On The Graph Represents Antibody Response From One VF Sample.	273
Figure A2-8 IgM Antibody Reactivity Captured On VF Epitope Peptides (83) From CF-Titer=4 Patients Sera (N=8). Each Line On The Graph Represents Antibody Response From One VF Sample.	274
Figure A2-9 IgG Antibody Reactivity Captured On VF Epitope Peptides (83) From CF-Titer=8 Patients Sera (N=4). Each Line On The Graph Represents Antibody Response From One VF Sample.	275
Figure A2-10 IgM Antibody Reactivity Captured On VF Epitope Peptides (83) From CF-Titer=8 Patients Sera (N=4). Each Line On The Graph Represents Antibody Response From One VF Sample.	276

Figure	Page
Figure A2-11 IgG Antibody Reactivity Captured On VF Epitope Peptides (83) From CF-Titer=16 Patients Sera (N=10). Each Line On The Graph Represents Antibody Response From One VF Sample.	277
Figure A2-12 IgM Antibody Reactivity Captured On VF Epitope Peptides (83) From CF-Titer=16 Patients Sera (N=10). Each Line On The Graph Represents Antibody Response From One VF Sample.	278
Figure A2-13 IgG Antibody Reactivity Captured On VF Epitope Peptides (83) From CF-Titer=32 Patients Sera (N=12). Each Line On The Graph Represents Antibody Response From One VF Sample.	279
Figure A2-14 IgM Antibody Reactivity Captured On VF Epitope Peptides (83) From CF-Titer=32 Patients Sera (N=12). Each Line On The Graph Represents Antibody Response From One VF Sample.	280
Figure A2-15 IgG Antibody Reactivity Captured On VF Epitope Peptides (83) From CF-Titer=64 Patients Sera (N=5). Each Line On The Graph Represents Antibody Response From One VF Sample.	281
Figure A2-16 IgM Antibody Reactivity Captured On VF Epitope Peptides (83) From CF-Titer=64 Patients Sera (N=5). Each Line On The Graph Represents Antibody Response From One VF Sample.	282
Figure A2-17 IgG Antibody Reactivity Captured On VF Epitope Peptides (83) From CF-Titer=128 Patients Sera (N=3). Each Line On The Graph Represents Antibody Response From One VF Sample.	283

Figure	Page
Figure A2-18 IgM Antibody Reactivity Captured On VF Epitope Peptides (83) From CF-Titer=128 Patients Sera (N=3). Each Line On The Graph Represents Antibody Response From One VF Sample.	284
Figure A2-19 IgG Antibody Reactivity Captured On VF Epitope Peptides (83) From CF-Titer=256 Patients Sera (N=2). Each Line On The Graph Represents Antibody Response From One VF Sample.	285
Figure A2-20 IgM Antibody Reactivity Captured On VF Epitope Peptides (83) From CF-Titer=256 Patients Sera (N=2). Each Line On The Graph Represents Antibody Response From One VF Sample.	286
Figure A3- 1 Box Plots Of Immune Response From Individual Rats Per Group (X-Axis) As Captured On 862 F. Tularensis (Schus4) Peptides Printed On An Array. The Raw (Un-Normalized) Fluorescence Intensity Units (FIU) Are Plotted On The Y-Axis On A Log Scale. The Line At The Center Of Every Box Represents The Median Signal Intensity For That Individual Rat.	290
Figure A3- 2 A Simultaneous Comparison Of Infectious (French Cohort) Versus Genetic-Immunization (UK Cohort) Antibody Responses As Captured By 299 ASFV Peptides On PPP Array.	294
Figure A3- 3 Average Signal Captured By PPP Array For 4 Groups Of ASFV Genetic Immunization Are Depicted With Every Animal's Antibody Response Represented Per Bar On The X-Axis.	296

Figure	Page
Figure A3- 4 Humoral Immune Response As Measured On PPP Array From Group A, B, C Pigs Sera Post-Challenge With ASFV	299
Figure A3- 5 Signal Intensities From ASFV Peptides Averaged Per ASFV Protein As Measured On The PPP Array From Group A, B And C Samples Post-ASFV Challenge.	300
Figure A3- 6 Average Signal Intensities In FIU (Y-Axis) From Various Stages (X-Axis) In Two Separate Immunization And Challenge Regimes.....	301
Figure A3- 7 Peptides Tiling Vp30 (ASFV127) An Immunodominant Antigen Of ASFV Displaying Individual (X-Axis) Responses From Sera On PPP Array.....	302
Figure A3- 8 Peptides Tiling Vp72 (ASFV113) An Immunodominant Antigen Of ASFV, Displaying Individual (X-Axis) Responses From Sera On PPP Array.....	303
Figure A3- 9 Signal Intensities Averaged Per ASFV Protein (N=12) Tested In The Form Of Peptides On The PPP Microarray.	307
Figure A3- 10 Plate Map For 0.5 mm Pitch Sonication Printing Protocol.	311
Figure A3- 11 Plate Map For 0.75 mm Pitch Sonication Printing Protocol.	312
Figure A3-12 Anti-GFP Antibody Reactivity Captured From Translated Proteins On IVTT Bead Protein Array.	314

PREFACE

This dissertation examines fundamental aspects of antibody behavior through the observation of their interaction with peptide targets. Historically, immunodiagnostics have fulfilled their role in healthcare by the measurement of the interaction between patient antibodies and select targets, whether auto-antigens, or viral, bacterial, or fungal antigens. The sensitivity and specificity of diagnostics is linked to the selection of ligand, and the quality of the measuring assay. The need for high sensitivity originates from the need to detect outbreaks, new zoonosis and animal-to-human disease transfer, epidemiology, and early detection of disease. The need for high specificity originates from the need to discriminate closely related pathogens, or detection of new disease in endemic regions, or areas of numerous commonly acquired infections. In this tome, there was a directed effort to cover a broad landscape of questions that directly address the performance of diagnostics for infectious disease, biochemically, informatically, and practically.

Chapter 2 demonstrates a diagnostic application of the Immunosignature non-natural sequence peptide microarray for diagnosing a single infection, Valley Fever (VF), *Coccidioidomycosis*. The introduction to this chapter explores the unmet need for a more sensitive diagnostic for Valley Fever false-negative individuals. The Valley Fever patient sera were kindly contributed by Dr. John Galgiani from the Valley Fever Center for Excellence at the University of Arizona. The work described here includes experimental data from 3 sets of non-natural Immunosignature microarrays, and compares the results. Experiments were done to assess whether or not Valley Fever could be distinguished from other fungal infections such as *Aspergillus fumigatus* and other confounding

community acquired pneumonias such as those cause by *Mycoplasma pneumoniae*, *Chlamydia pneumoniae*. Upon establishing a unique signature pattern for Valley fever, the sensitivity of this Immunosignaturing assay was tested using serum from patients obtained in the early stages of the infection in the form of independent training and test serum sample sets. A set of 96 predictor peptides were selected for their high sensitivity and tested independently on a smaller '*VF-diagnostic*' chip to verify sensitivity.

Chapter 3 evaluates the diagnostic accuracy of using natural antigen epitopes peptides versus 96 non-natural VF predictor peptides as diagnostics. These 96 non-natural predictor peptides were selected very early in the development of Immunosignatures. Although pathogen epitope proteins and never-born/non-natural proteins are bioinformatically compared in literature, this is the first study completing this comparison in a diagnostic context. From our data, the 96 non-natural VF predictor peptides showed higher accuracy at classifying all stages of VF infection over VF-epitope peptides.

Chapter 4 highlights the challenges involved when evolving a single pathogen diagnostic assay into a multiplexed immunodiagnostic. The assay was developed for simultaneous detection of 5 or more NIAID category A, B, C priority pathogens in fulfillment of a project supported by the Chemical Biological Technologies Directorate contract HDTRA-11-1-0010 from the Department of Defense Chemical and Biological Defense program through the Defense Threat Reduction Agency (DTRA) to Dr. Stephen Albert Johnston. My role in this undertaking was to evaluate the feasibility of selecting pathogen epitopes, both those known to bind empirically, and those predicted to bind from the IEDB (Immune Epitope DataBase). Based on our analysis I designed the

pathogen proteome peptide (PPP) microarray to represent immunodominant antigens for larger pathogen proteomes and complete proteomes for smaller viruses. I examined the behavior of serum from infected individuals on these peptides while dissecting the effects of temperature and time of incubation, concentration of primary, competitors, inter-peptide spacing on the array surface, peptide linkers, dual and single color scanning, and mathematical normalization methods. We developed an assay capable of distinguishing 4 priority pathogen infections apart with >90% AUC-ROC (Area under a receiver operator characteristics curve). Chapter 5 summarizes the bioinformatic efforts implemented to circumvent cross-reactivity observed on the multiplexed PPP pathogen epitope peptide microarray platform. We interpreted the cross-reactivity observed on the PPP array using an antibody *'Umbrella Approach'* for bioinformatically re-attributing observed cross-reactivity.

The first appendix covers the observation and characterization of globular VF spherule-like globular objects within infected individual's sera. Given the paucity of VF diagnostics, this observation might serve to enable diagnostics in this area. The presence of such spherule like circulating antigen-antibody complexes might pose significant interference on the peptide microarray's ability to capture antibodies bound to spherules as noted in other antigen based diagnostics. The second appendix includes data from VF epitope peptides for four immunodominant antigens showing binding of patient sera at various IDCF titers (incremental stages) of the infection. The third appendix summarizes the ASFV (Pirbright, UK) and *Francisella tularensis* (University of New Mexico) projects. These were applications requiring use of a more sensitive technology such as the PPP array as compared to standard ELISA assays to monitoring the antibody response

from various genetic immunization regimes. Serum samples for these two projects were contributed by Dr. Kathryn Sykes. My contribution to the Bead Protein Array project originally conceived and developed by Dr. Kathryn Sykes was to experimentally optimize this protein microarray system for screening of infectious or vaccinated sera using IVTT synthesized proteins on beads.

CHAPTER 1

INTRODUCTION

Project Overview

Through this work we explore the use of peptide microarray platforms towards diagnostic applications of infectious diseases. In the first phase, of this study we use a non-natural sequence peptide microarray platform for diagnosing a single, specific infection, Valley Fever caused by *Coccidioides*. In the second phase, in contrast we used a natural sequence peptide array as a multiplexed array platform capable of simultaneously discerning 5 or more infections. While most of the work presented in this dissertation has diagnostic applications, it answers several fundamental questions about antigen-antibody kinetics as observed in the context of an infectious response.

Peptide microarray as clinical diagnostics

Peptides are useful reagents for characterizing the humoral immune response to disease. Antibodies respond to a number of different types of antigens including linear and non-linear proteinaceous targets, polysaccharides and glycopeptides, phosphorylated proteins, and other biological molecules. Peptides can simulate the physico-chemical structure of many of these targets (mimotopes), creating a systematic one-stop-solution for probing antibody behavior. Technologies that rely on proteins as probes are varied [1]: bead based immunoassay (Luminex, Austin, TX), mass spectrometry (CIPHERGEN, Fremont, CA), surface plasmon resonance (Biacore, www.biacore.com), protein microarrays (Zeptosens-Witterswil, Switzerland; ProtoArray-Life Technologies), electro-

osmotic micro-fluidic LabChip (Calipertech, Hopkinton, MA), surface acoustic waves based micro-fluidic assays (Advalytix, Brunnthal, Germany), micro-cantilever measurement (Protiveris, Rockville, MD), but most widely used have been peptide microarrays: PEPperPRINT-Heidelberg, Germany; CombiMatrix-Mukilteo, WA; Immunosignaturing [2]. Microarrays enable thousands of peptides to be assayed simultaneously under identical assay processing conditions. Many groups have developed pathogen antigen based peptide microarrays diagnostics for specific infections such as Tuberculosis [3,4], *Echinococcus* spp. [5] and SARS [6,7]. The antibody response mapping strategy as outlined by these groups involves testing patient sera in comparison to normal donor sera. Using tiled regions of proteins, researchers have precisely identified small portions of proteins that correspond to the eliciting antigen [8]. Immunosignaturing is a novel microarray platform as compared to pathogen antigen based peptide microarrays because it uses non-natural peptides to capture antibody response [2,9,10]. This technology has led to fundamental breakthroughs in understanding antigen-antibody interactions that could potentially be used for medical diagnostics [11-13].

Advantages of using peptide microarrays

A significant advantage of using peptide microarrays is their ability to partition and measure separately, specific portions of an antibody response. The resolution of these responses captured on peptide microarrays can be traced down to the eliciting antigen fragments. In comparison, protein based ELISA's or protein microarrays merely allow

capturing a cumulative sum of antibodies against entire proteins. Unlike certain protein microarrays another advantage of using peptide microarrays is the minimal test sample preparation and lack of complex blocking steps required during sample processing. For example, in *Escherichia coli* based in-vitro translation and transcription (IVTT) protein microarrays, test sera is blocked using *E. coli* lysate to exclude false-positive reactivity to *E.coli* proteins within the IVTT protein mixture [14]. *E.coli* reside within the human gut microbiome comprising a 100 trillion microorganisms [15] classified under phyla: Bacteroidetes, Firmicutes and Actinobacteria [16]. Golby *et al.* [17] observed preliminary evidence for B-cell development in human fetal intestinal cells using immunohistochemistry studies. Additionally, recent evidence in mice suggests that bacteria within the gut microbiome might be capable of influencing B-cell development and immune response in the mouse intestine [18]. Given that the antibody response to *E. coli* residing in the intestine might be part of the primary immune response in humans, it would not be advisable to exclude this anti-*E.coli* protein lysate signature when attempting to capture pathogen specific antibody reactivity using microarrays. Peptide microarrays do not require biasing the observable infectious antibody response by including such high complexity sample preparation steps. Additional advantages of peptide microarrays are their ability to tile continuous fragments of proteins to characterize monoclonal antibody reactivity with higher resolution than is possible with protein microarrays. Peptides are easier and less expensive to produce in comparison to proteins through IVTT. Considering these significant advantages, it would be prudent to

apply peptide microarrays to diagnose and distill the complex immune response observed in chronic infectious diseases such as Valley fever.

Project I: Valley Fever Immunosignaturing diagnostic

Coccidioidomycosis (Valley Fever) is caused by a dimorphic fungus that grows in the southwestern desert regions of United States and Central and South Americas. The two genotypically variant strains are *C. immitis* found in California and *C. posadasii* found outside California. The disease is caused by inhalation of the spores called Arthroconidia and manifests initially with pneumonia-like symptoms due to the mode of entry being lungs. The disease is most prevalent in the states of Arizona, California, Nevada and New Mexico and infects more than an estimated 150,000 [19] people in the United States every year.

Symptomatically, Valley Fever (VF) infection is very difficult to diagnose in the early stages as several of its symptoms are confounded with those of most community acquired pneumonias (CAP) such as tuberculosis. Approximately 60% [20] of Valley Fever cases are from the state of Arizona and therefore the Arizona Department of Health Services (ADHS) initiated an enhanced surveillance scheme for Valley Fever. ADHS conducted an interview based survey of 493 patients out of the 4,832 total patients diagnosed with Valley Fever in 2007 as part of their enhanced surveillance initiative [20]. They outlined several reasons for delays in the diagnosis of Valley Fever. Patients wait for 44 days on an average before seeking care. Another reason for delay was also lack of uniform awareness about the disease and treatment modalities among both physicians as

well as patients. From the physician's perspective this might be due to the commonality of symptoms elicited by Valley Fever in comparison with other community acquired pneumonias. On an average Valley Fever patients visited physicians about 3 times before they were even tested for Valley Fever. If patients are made aware of the possibility of being infected due to living in an endemic region, they would perhaps not wait so long before seeking medical care and would even request being tested for Valley Fever. Valley Fever alone is known to account for \$86 million in hospital charges in Arizona in the year 2007 [20].

As per the CDC Summary of Notifiable Diseases in 2011 [21], 22,634 total cases of coccidioidomycosis were reported. Partly this number is much smaller than the estimated 150,000, as, in Arizona, one third [20] of the physicians were not aware that Valley Fever is a reportable disease and this might be the case with physicians from other non-endemic locations as well [22]. Also, a majority of the cases that are reported belong to the 40% in whom the infection does not self-resolve, thereby obscuring data from the remaining 60% people exposed. As per the CDC, 30-60% [23] of people living in regions endemic for Valley Fever will have been exposed to it. The total population of the 4 main states endemic for Valley Fever, namely: Arizona, California, New Mexico and Nevada obtained from US Census Bureau figures is approximately 49.4 million [24]. Just 30% of this value, 14.8 million people, as per CDC estimates would be exposed to Valley Fever in these endemic states.

Current diagnostics available for this disease primarily use antibody based indirect methodologies such as immunodiffusion, whereby, the patients' serum is tested for

the presence of IgM and IgG antibodies to major Coccidioidal antigens CF and TP. The problem with this technique is false negatives: approximately 5% [25] of patients [both immuno-compromised and immuno-competent] suffering from Valley Fever do not show detectable levels or even presence of antibody in their sera. A good prognosis in Coccidioidomycosis is when a person elicits a cell mediated immune response against the infection [26,27]. Sixty percent of the patients, in whom the infection is contained within the lungs or resolves by itself, show almost non-detectable antibody levels (by ELISA or Immunodiffusion) to Coccidioidal antigens. But Coccidiodes may only be contained in these patients' lungs instead of being completely destroyed by their immune system and so the infection might recur when the patient is later in an immunocompromised state [26]. An antibody mediated (humoral) response is usually seen in individuals in whom the infection does not resolve on its own and instead disseminates.

An alternative to this is direct detection via culturing the organism in the laboratory from the patients' body fluids. However, this involves the potential risk of exposing the technicians to the infectious form of this fungal pathogen. Since Valley Fever is primarily a lung infection, a chest x-ray showing either a cavity or a patch of infection in the lung is followed by a nasopharyngeal wash or surgical computed tomogram [CT] guided lung biopsy to retrieve a sample for culturing and Hematoxylin-Eosin staining. Both culturing and CT guided biopsies are technically cumbersome procedures. In an effort to avoid these invasive and potentially risky procedures, we propose utilizing the peptide microarray platform to ascertain a specific signature pattern for the early detection of Valley fever separating it from other CAPs such as tuberculosis.

This would help detect the infection in the 60% of people in whom the primary infection resolves without showing detectable antibody levels in their serum, but might latently recur. If patients knew they were exposed, they could make informed decisions with their physicians about clinical procedures requiring suppression of the immune system.

The current alternative commercial diagnostic efforts include using nucleic acid amplification of Coccidioidal DNA from sputum samples through Polymerase Chain Reaction [28], microarray based whole genome level Comparative Genomic Hybridization (aCGH) technology [29] and utilizing the BacT/ALERT[®] [30] automated microbial detection media system. All these technologies do not detect early infection and have also not been proven to detect latent infection. The immunosignature, non-natural peptide microarray technology [9] might surpass both these limitations, paving the way towards accurate and early diagnosis of Valley Fever.

The scope of my dissertation is to ascertain the humoral immune response pattern that is specific for Coccidioidomycosis from IgG and IgM antibody interaction in VF patient sera with randomly generated (non-natural, Chapter 2) and epitope (from Coccidioides, Chapter 3) antigen peptides spotted on a peptide microarray platform. Experiments designed to examine presence and absence of classes of Coccidioides specific immunoglobulins were conducted in order to completely characterize the spectrum of patient sera we would be likely to encounter in a clinical setting. Chapter 3 compares the diagnostic performance of non-natural sequence (random-space) VF-predictor peptides with VF-antigen epitope peptides (life-space) to evaluate the feasibility of using either life versus random space diagnostic peptide reagents. Several efforts to

chemically characterize and classify random (never-born proteins) apart from natural protein sequences have been conducted *in-silico* [31,32]. A side by side comparison of non-natural versus life-space epitopes within a diagnostic context has not been previously reported. Through data from this work, a bioinformatic modulation to the Smith-Waterman [33] local sequence-alignment algorithm termed ‘di-peptide inversion’ was suggested and implemented within GuiTope [34], an alignment program from our lab. This significantly improved GuiTope’s accuracy at finding alignments between natural VF pathogen proteins and the non-natural sequence antibody capturing VF-predictor peptides from the immunosignaturing platform. Platform optimization expertise obtained through this project was applied to the second project involving creation of a multiplexed peptide microarray platform for simultaneous detection of multiple priority pathogen infections.

Cross-reactivity observed in peptide microarrays

Antigen-antibody cross-reactivity is a salient feature of all immunodiagnostics and peptide microarrays are no exception to this rule [35]. Unlike single pathogen diagnostic peptide microarrays distinguishing infectious sera from uninfected sera, Felger *et al.* [5] tested their *Echinococcus* specific peptide microarray platform against other symptomatically confounding nematode infections. The peptide array was developed to discriminate between *Echinococcus* species: *multilocularis* and *granulosus*. 45 peptides from 6 proteins of the pathogens showed 94% specificity and 57% sensitivity, but overall these peptides were not effective at differentiating between the two species. Andresen et

al. [36] tested a 900 peptide microarray for simultaneous distinction of viral infections from phylogenetically related Herpes & Hepatitis C virus genotypes. CMV and EBV patient sera showed appropriate reactivity on their assay but Hepatitis C virus infected sera showed broad cross-reactivity.

Another cross-reactive result obtained when using peptide microarrays was by Maeurer *et al.* [3] on their 7446 peptide microarray representing 12-mer overlapping 15-mer (total length) peptides from 61 *Mycobacterium tuberculosis* proteins. The authors observed 3 patterns of patient serum IgG reactivity to peptides on the array including a set of 89, TB-specific peptides, capable of distinguishing TB-positive from TB-negative individuals. Additionally, they observed 24 TB-sensitive peptides exclusively reacting with TB positive patient sera but not with normal TB sero-negative sera. And, a set of 13 peptides from *M. tuberculosis* exclusively recognized by only normal TB-negative (Quantiferon assay negative) individuals' sera but are not recognized by TB positive patients sera. When performing a BLAST search of these 13 peptides for possible matches with the human proteome, several potential matches were identified due to sequence level similarities. A working hypothesis is that the innate overlap between the host (human) and pathogen proteomes create natural self (host)-reactive targets that react to identical sequences found in pathogens. Whether this could be interpreted as low level auto-immunity or these antibody reactivities are due to mimotopes from other environmental non-pathogenic Mycobacteria as originally proposed by the authors, is speculative in the absence of previous immune exposure history from these patients. Obtaining orthogonally characterized sera with detailed annotation regarding previous

vaccinations/infection histories would have benefitted such a study by helping resolve cross-reactivity observed to *M. tuberculosis* peptides from uninfected individuals.

Lo *et al.* [6] attempted to circumvent potential cross-reactivity observed on peptide microarrays between phylogenetically related pathogens by selecting 27 peptides that were specific only to the SARS-CoV (Severe Acute Respiratory Syndrome-Coronavirus) and not to other Coronaviruses or the human and mouse proteomes on a sequence level (BLAST analysis). This array was only tested against SARS infected versus not infected patients and not against serum from other closely related Coronaviruses to prove the specificity of their SARS specific peptides and justify using informatics intervention during peptide selection. Such an approach, of making single pathogen specific diagnostics using peptide microarrays is typically adopted to circumvent possible cross-reactivity on these assays. Due to high cross-reactivity observed in peptide microarray data, none of these groups have attempted multiplexing the diagnosis of more than one infection on the same chip/ microarray platform.

Multiplexed diagnostics for human pathogens and bio-threat agents

Serum based multiplexed diagnostics are implemented using technologies such as multiplexed ELISA's, protein and peptide microarrays and microsphere immunoassay (MIA). A commercial example of a multiplexed ELISA is the ToRCH screen for measuring antibody reactivity in pregnant mothers against 7 vertically transmitted infections [37]. The infections tested are *Toxoplasma gondii*, Rubella virus, Cytomegalovirus (CMV), Herpes simplex virus (HSV) type 1 and 2, Varicella zoster

virus (VZV), *Chlamydia trachomatis* with variable IgG sensitivity per pathogen ranging from 46% (HSV2) to 97% (VZV) and specificity ranging from 88% (*T. gondii*) to 100% (VZV, Rubella, CMV).

Apart from clinical diagnostic applications, multiplexed diagnostics are also needed for biothreat agents. Biothreat surveillance is important not only from a national perspective but also more pertinent to armed forces personnel being deployed in unsafe territories. Microbial biothreat pathogen lists from various regulatory organizations help prioritize exposure to pathogens based on their weapon potential and the severity of symptoms they are capable of causing in their hosts. The National Institute of Allergy and Infectious Diseases (NIAID) category A, B, C priority pathogen list [38] includes primarily deadly encephalitis viruses and pathogens with a high weaponization potential such as *Bacillus anthracis* in category A. Category B includes pathogens acquired or transmitted via food or water and Category C includes pathogens causing newly emergent infectious diseases. Over time these might get re-classified depending on their weaponization potential or change in virulence to increase severity of symptoms. Other priority pathogen lists are from U.S. Department of Health and Human Services (HHS) and U.S. Department of Agriculture (USDA) [39]. Some priority pathogens from the NIAID list overlap with the HHS and USDA lists, but the USDA list primarily has zoonotic pathogens potentially capable of infecting humans such as the African Swine Fever Virus (ASFV) virus [40]. The preliminary evidence for this indication came from a pyro-sequencing study where Loh *et al.* [40] found ASFV-like sequences in human serum from individuals having an acute febrile illness (AFI) in the Middle East and in

multiple sewage samples from Barcelona, Spain. Although the source of the sewage samples could not be identified specifically as being from human or animal origin, the geographic distance between these two observations was alarming enough to add ASFV to the HHS & USDA priority pathogen lists.

The CDC recently developed a Luminex based microsphere immunoassay (MIA) simultaneously distinguishing 13 viruses listed as biothreat agents from viral families of, Bunyaviridae (LaCrosse encephalitis-LAC), Togaviridae (Eastern equine encephalitis-EEE, Western equine encephalitis-WEE, Venezuelan equine encephalitis-VEE, Chikungunya-CHIK, Mayaro-MAY, Ross river virus-RR) and Flaviviridae (West Nile virus-WNV, Japanese encephalitis virus-JEV, Dengue-DEN, Yellow fever virus-YFV, St. Louis encephalitis-SLE, Powassan-POW) [41]. Using the LogitBoost algorithm their cross-validated average error rate was 8.3%. In their assay, Luminex Microplex (Luminex Corporation, Austin, TX) carboxylated microspheres are coated with commercially available anti-virus monoclonal antibodies. Viruses are generated by either inoculating suckling mouse brains or expressed in-vitro using recombinant vectors in monkey kidney fibroblast-like COS-1 cells. The viruses are then incubated with the monoclonal anti-viral antibody coated microspheres to allow capturing and surface presentation and generate a sandwich ELISA once incubated with the patient sera. The drawback on this assay is its requirement of unstable reagents with a shelf-life of 6 months the handling of which needs to be monitored due to them being biothreat agents. These drawbacks hinder the deployability of this assay to local reference laboratories, requiring that samples be shipped to CDC for evaluation, delaying diagnosis. Peptide

microarrays on the other hand are more stable, they can be stored at room temperature [42] and have a shelf-life after printing can be >1 year [43,44] making them easily deployable to even local reference laboratories, utilize a fraction of the sample used in MIA's (1:500 vs. 1:20) and represent only short sequences of biothreat agent proteomes, assay processing not needing supervision. The detection limit of technologies such as Luminex assays is 1-10 pg/ml [45].

Alternative biothreat detection technologies such as multiplexed PCR's and assays using B-cells as sensors (CANARY) [46] fall under the category of direct detection of pathogen instead of detecting the immune response raised by them in hosts. The LLMDA – Lawrence Livermore Microbial Detection Array [47,48], PathChip [49], GreeneChip [50] and ViroChip [51] are examples of multiplexed PCR's. The LLMDA contains 388,000 probes containing 38,000 viral sequences from ~2200 viral species and 3500 bacteria sequences representing approximately 900 different bacterial species. The PathChip contains approximately 170K probes and is capable of recognizing all known viral pathogens. The diagnostic accuracy of this assay from testing 290 pediatric nasal wash samples was 85.9% for Rhinoviruses or Enteroviruses and for 98.6% Parainfluenza virus 2.

An antigen detection B-cell based sensor named CANARY- cellular analysis and notification of antigen risks and yields [46] for rapid identification of pathogens can detect as little as 50 CFU/50 μ L of *Yersinia pestis*, 1000 CFU of *Bacillus anthracis* in 1 ml of extraction medium, 500 CFU/50 μ L of *Escherichia coli* (O157:H7) in contaminated lettuce (25 g), 500 PFU/50 μ L of Vaccinia virus and 5×10^5 PFU/50 μ L of Venezuelan

encephalitis virus (VEE) virus. While the shelf-life of reagents required for CANARY is low at room temperature (RT), 2 days; prepared cells can be refrigerated for up to 2 weeks and frozen for longer time periods. An alternative to antigen-antibody detection based assays would be sequencing the complementarity determining region (CDR) of antibodies within an infected individual's serum to decode the antigen/pathogen they were raised against [52]. This technology however is cumbersome and not yet easily deployable in local laboratories.

Cross-reactive components of the humoral antibody response to an infection

The humoral antibody response in humans when responding to an infection/exposure could be classified into the primary and secondary adaptive immune response. The primary response comprises of natural antibodies, circulating antibodies generated through memory responses against prior exposures/ vaccinations. The secondary adaptive immune response is the component of humoral immunity generated specifically as an adaption to the new exposure. Understanding the antibody subcomponents is critical to creating antibody based diagnostics so as to *a priori* circumvent cross-reactivity by intelligent design of the assay. Slifka *et al.* [53] monitored the antibody response from 45 individuals for 26 years, collecting 630 serum samples total. They measured antibody responses to 8 pathogens, 6 being part of vaccinations e.g. Measles, Mumps, Rubella-MMR vaccine, Vaccinia virus (smallpox vaccine), Diphtheria (*Corynebacterium diphtheriae*) and the tetanus toxoid (*Clostridium tetani*). The annual percent change using longitudinal mixed-effects model was determined to derive the

antibody-half life (in years). Tetanus toxin and Diphtheria toxin had short half-lives (11 & 19 years respectively). The half-lives of the remaining exposures ranged from 50 years for Varicella zoster virus to 11,552 years for Epstein Barr virus (EBV). They concluded that most childhood prophylactic vaccine exposures left behind circulating antibodies that could be detected throughout the life of these individuals tested with negligible change in the concentration over time. In addition to these vaccinations, Palese *et al.* [54] demonstrated through longitudinal characterization of the influenza antibodies within 40 individual's sera monitored for 20 years obtained through the Framingham Heart Study that the neutralizing antibody titers against several influenza virus strains increased over time. Apart from influenza they measured CMV antibodies and noted negligible change in anti-CMV titers within exposed individuals.

The population prevalence estimates between 1999-2004 (age: 6-49 years) of CMV in United States is 50.9%, with sero-positivity in certain counties such as Los Angeles being higher at 69.7%.; and that among certain ethnic minorities such as Mexican American individuals residing in LA being 79.7% [55]. Palese *et al.* chose to measure the antibody reactivity to CMV due to the antigenic stability of this virus as compared to influenza and its higher prevalence within the general population. Other pathogens showing notable sero-prevalence within the population are Varicella (96%), Rubella (91.2%), Mumps (90%), Measles (95.9%), HSV-2 (17.3%), HSV-1 (58.1%), Hepatitis A virus (35.9%), *Toxoplasma gondii* (11%) [55]. Given the high prevalence of these exposures and their ability to leave behind a memory response with circulating antibodies observed throughout an individual's lifetime, developing a sensitive diagnostic

capable of distinguishing all known human pathogens simultaneously becomes challenging. Sensitive technologies such as peptide microarrays are capable of measuring these interfering memory antibody responses, leading to interference observed with the signature of a given infection. Such an effort would require the use of data analysis techniques allowing for discerning more than one exposure simultaneously so as to distinguish the inseparable matrix of prior exposure related antibody reactivity versus the most current exposure and compensate for cross-reactivity observed on these platforms.

Project II: Multiplexed priority pathogen proteome peptide array

This work is aligned with a DTRA (Defense Threat Reduction Agency) funded project (Grant# HDTRA1-11-1-0010) which involves development of a scalable technology so as to monitor the exposure of military personnel to NIAID Category A, B, C Priority biothreat pathogens. The first task of this proposed work involves generation of a 100K random peptide silicon chip, the proprietary technology for which could later be used if needed to create a 1 million peptide feature chip so as to represent all known human pathogen proteomes. The second milestone required the production and evaluation of a 10K peptide prototype pathogen proteome array capable of distinguishing between five or more infectious bio-threat agents simultaneously in a multiplexed assay. This work required testing the feasibility of such a system, designing peptide candidates to be tested on the microarray, thermodynamically and physically optimizing array configuration and testing the platform, bioinformatically assessing the expected versus actually observed peptide antigen-antibody cross-reactivity from sera for evolutionarily

related and unrelated bio-threat agents. The pathogens selected to be represented on the array were based on infectious serum availability. Their epitope selection strategy and thermodynamic considerations while optimizing the assay to reduce cross-reactivity are explained in greater detail in Chapter 4. An analysis pipeline specific to the multiplexed pathogen proteome peptide array was created by combining eight statistical metrics. A novel aspect of this work was observing a reduction in assay accuracy after adding influenza peptides along-side priority pathogen peptides. The addition of Influenza peptides required a change in the data-analysis strategy adopted previously and is detailed in Chapter 5. The antibody cross-reactivity observed after including influenza peptides required mapping the ‘umbrellas of antibody reactivity’ down to an n-mer (peptide sub-sequence) level in an attempt to circumvent cross-reactivity and detect the cognate infection.

CHAPTER 2

APPLICATION OF IMMUNOSIGNATURES TO DIAGNOSIS OF VALLEY FEVER.

Abstract

Background

Valley Fever (VF, Coccidioidomycosis) infection is difficult to diagnose based on symptoms in part because of the similarity to community-acquired pneumonias (CAP). Confirmatory diagnostics detect IgM and IgG antibodies against Coccidioidal antigens via Immunodiffusion (ID). However, the false negative rate using ID can be 50-70% and 5% of symptomatic patients never show detectable antibody levels at all. Here we test the capability of the immunosignature diagnostic to resolve the false negative diagnostic problem for VF. Immunosignatures are developed from arrays of non-natural-sequence peptides. Blood antibodies bind to the arrays to create disease specific signatures.

Methods

A 10,000 peptide array was used to determine if VF infection produced signatures distinct from 3 other infections. A similar array was used to distinguish VF infection from non-infection in a training/test set format. The signature peptides from the 10,000 peptide array were used to design a smaller VF-specific array of 96 select peptides. The performance of the 10,000 peptide array and the 96 peptide array were compared to the ID diagnostic standard.

Results

The 10,000 peptide array classified the VF samples from the other 3 infections with 98% accuracy. The array was also able to classify all the VF, ID negative patients versus non-infected controls with 100% sensitivity in a blinded test set. The sensitivity of ID on the test set was 28%. In comparison the 96 peptide array performed with 82% sensitivity on the same sample sets.

Conclusion

The immunosignature diagnostic can be used to simultaneously distinguish VF infections from a fungal and two other bacterial infections. The same array can diagnose with 100% sensitivity the clinically important ID negative patients. A smaller 96 peptide array was less specific in diagnosing the ID negative patients. We conclude that by training using a clinically confounding sample set a robust immunosignature diagnostic could be developed to be used in combination, or possibly in lieu of, the existing diagnostics.

Abbreviations

BSL, Biosafety level; CAP, community acquired pneumonia; CF, Complement Fixation; CNS, Central Nervous System; CT, Computed Tomography; EIA, Enzyme Immunoassay; ID, Immunodiffusion; IDCF, Complement fixation antibodies detected by Immunodiffusion; IDTP, Tube precipitin antibodies detected by Immunodiffusion; KNN, K-nearest neighbors; LVS, Live Vaccine Strain; subsp, Sub-species; LDA, Linear Discriminate Analysis; LOOCV, Leave One Out Cross Validation; NPV, Negative

predictive value; PPV, Positive predictive value; TP, Tube Precipitation; TB, Tuberculosis; VF, Valley Fever.

Introduction

Coccidioidomycosis, commonly known as Valley Fever (VF), is caused by a fungus *Coccidioides immitis* (California strain) or *C. posadasii* found in the arid soil of the southwestern desert regions of United States and South America. Human disease is caused by inhalation of the arthroconidia (spores) of the fungus, and presents primarily with flu-like symptoms or, progressively, pneumonia. VF affects an estimated 150,000 [19] people in US every year, primarily in the states of Arizona [56], California [57], Nevada, New Mexico and Utah. A major problem in the management of the disease is the failure of detection (sensitivity) in 30% of the infected individuals. We have tested whether a new diagnostic technology, immunosignatures, could address this problem.

Sixty percent [26] of the VF exposed individuals are either asymptomatic or have mild symptoms with the infection usually being self-limiting. The remaining 40% [58] of exposed individuals demonstrate symptoms such as skin rash and respiratory ailment lasting from months to years. In 5-10% [26,59] of these, infection disseminates, affecting other organs, skin, bones and nervous system. Individuals from non-Caucasian ethnicities [19] such as African Americans, Filipino and Asians and 65 years or older, pregnant women and patients with immunocompromised immune systems are more susceptible to VF and particularly the disseminated form of the disease. As per Arizona Department of Health Services (ADHS), VF patients visit physicians on average three times before they

are tested for VF, more so if patients visiting AZ from non-endemic regions are diagnosed by physicians unacquainted with diseases of the American Southwest [60]. VF alone is known to account for \$86 million in hospital charges in Arizona in the year 2007 [60], and an unestimated amount in states outside AZ.

The confirmatory diagnostic test for VF is an immunodiffusion (ID) assay detecting antibodies against antigens within fungal coccidioidin causing complement fixation (CF) and tube precipitation (TP). Coccidioidin is a culture filtrate of the mycelial form of *C. immitis*, the heat treated portion of which is used to detect IgM antibodies, and the untreated portion is used to detect IgG antibodies [61]. The sensitivity of IDCF is 77% and IDTP is between 75-91% [62]. An alternative is to culture the organism from body fluids or tissue, but a concern is infection of technicians [63]. Although, culture is a preliminary diagnostic for pneumonias, the sensitivity of this approach for VF ranges from 23-100% depending on clinical status [64]. The recovery rate of this pathogen through culture ranges from 0.4% from blood to 8.3% from respiratory tract specimens [65]. As noted the most clinically pressing issue is the low sensitivity of these diagnostics as primary tests.

We propose utilizing the immunosignature diagnostic technology [11] to address some or all the limitations of current diagnosis of VF, particularly as a diagnosis for patients misclassified at the first test. The immunosignature technology utilizes a high-density array of non-life-space peptides to provide mimics of epitopes, for even discontinuous epitopes or non-protein antigens. In this report the arrays consist of 10,000 peptides whose sequences were chosen from random sequence space. The peptides are

20 amino acids long with 17 variable positions and 3 constant at the attachment end. As opposed to single antigen ELISA-based assays, the disease-specific signature signal in an immunosignature comes from multiple peptides that form a distinct, disease-specific pattern of antibody binding. Most antibody based immunological tests examine the presence of new antibodies in infected individuals.

An immunosignature can actually display both, the presence of new antibodies relative to infection or chronic disease, but also any suppression of antibodies (measured as loss of signal) that were commonly present in healthy controls reflecting memory responses to vaccinations and common pathogen exposures. An immunosignature, unlike many genetic or immunological tests, is both sample sparing and robust to sample handling [66]. Because the sensitivity of an immunosignature is higher than that of ELISA-based serological tests [10,11], and disease discrimination is possible on the same array across multiple infectious diseases, we asked whether the platform was suited to be used as a VF, disease-specific diagnostic. VF diagnosis frequently results in false negatives, resulting in late recognition of the disease [67-69], adversely affecting patient outcomes. We therefore proposed a series of tests to characterize whether an immunosignature assay performs better than existing diagnostics for detecting VF. We postulate this assay would detect VF earlier and with a greater sensitivity and at lower cost than conventional methods. Here we report testing this possibility. The ability of immunosignatures to distinguish VF from 3 other infections was tested. The same array was used to test the ability to discern ID negative patients from non-infected controls. The effect of reducing the number of peptides to a smaller array was also evaluated.

Methods

Serum samples used in this study

All patient sera used in this study are listed in Table 2- 1.

Table 2- 1 Patient sample cohorts per infection utilized in this study

No.	Infection	No. of patients	No. of samples
Confounding infection pilot study			
1	Aspergillus	20	20
2	Chlamydia	20	20
3	Mycoplasma	19	19
4	Normal	31	31
5	VF-Training set	18	18
Valley fever patient sera with non-VF controls			
1	VF-Training set (U of A)	35	55
2	VF-Test set (U of A)	25	67
3	Normal individuals (ASU)	41	41
4	Influenza vaccinees (2006-2007-seasonal vaccine) (ASU)	7	7

Confounding infection samples

For the experiment testing different infections, patient sera representing 19 *Aspergillus fumigatus*, 19 *Mycoplasma pneumoniae* and 19 *Chlamydia pneumoniae* were processed alongside 18 VF and 31 normal sera on the 10,000 peptide microarray. The *A. fumigatus*, *M. pneumoniae* and *C. pneumoniae* samples were acquired from SeraCare Life Sciences (Gaithersburg, MD) and were tested by commercial ELISA tests for presence of antibodies to respective infections by SeraCare (*Supplementary Table 2- 1*).

Valley Fever and normal donor serum samples used in this study

A training cohort of 55 samples and a blinded test set of 67 samples were obtained as de-identified human patient sera from John Galgiani at the University of Arizona (IRB# FWA00004218). Non-disease sera included 7 influenza vaccine (2006-2007) recipient sera ‘pre-vaccine’ and ‘post-vaccine’ plus 41 locally obtained healthy donor samples (ASU IRB 0905004024) which were used to ensure specificity. Following submission of our classification results to J. Galgiani, the test set was unblinded and revealed to contain 25 patients with two or more serum samples collected longitudinally per patient during subsequent clinic visits. For each patient in the test cohort the initial sample was measured as having a zero-titer (negative) on IDCF but sero-converted at a later date as the infection progressed. All samples were serologically characterized by J. Galgiani’s laboratory for IDCF and IDTP titers. *Table 2- 2* and *Table 2- 3* describe the patients CF titer distribution in training and test cohorts respectively.

Table 2- 2 *Diagnosis (IDCF) of 55 unique patient samples from the VF training cohort*

CF Titer	# Samples
0	6
1	4
2	8
4	5
8	3
16	8
32	11
64	5
128	3
256	2

Table 2- 3 Diagnosis (IDCF) of 67 blinded samples from the VF test cohort.

CF Titer	# Samples (# patients)
0	48 (25)
1	5 (4)
2	7 (7)
4	3 (3)
8	1 (1)
16	2 (2)
32	1 (1)

Blinded test patient sample set

The test sample set includes 25 patients with two or more serum samples per individual, for a total of 67 samples. 24 of these symptomatic patients had an IDCF titer of zero and were given a negative diagnosis for VF after their first clinic visit. All 24 patients returned to the clinic for a follow-up appointment between 7 and 27 days and blood samples were drawn for the second time at which point 12 of them were still sero-negative on the IDCF test. Of the 12 IDCF negative patients only 6 returned for the third follow up visit due to continued symptoms and 6 others returned either for monitoring of increasing CF titers or re-testing due to a positive IDTP result. The time interval for the third visit ranged between 4 and 159 days after the second visit. Four of these patients' samples were drawn again between 96 and 147 days at which time a verified IDCF titer was observed in 2 patients who were given a positive VF diagnosis. One symptomatic patient returned for a fifth visit and remained negative on both the IDCF and IDTP tests 113 days later despite being symptomatic for Valley Fever.

Microarray production and processing

The 10,000 (10K) non-natural sequence peptide immunosignature array and the 96 peptide ‘VF diagnostic’ arrays were produced and processed as described in Legutki and Stafford *et al.* [2,11]. Briefly, the peptides are spotted onto standard slides using a piezo-electric printer. The average spot diameter is $\sim 140\mu\text{m}$. The slides are washed with buffer and the serum (diluted 500-fold in buffer) is applied to the array for 1hr. It is then washed with buffer and the antibody binding pattern determined by incubation with a secondary to human IgG antibody. The 16-bit $10\mu\text{m}$ TIFF images from the Agilent ‘C’ scanner were aligned using GenePix 6.0 software (Axon Instruments, Union City, CA) and the data files imported into GeneSpring 7.3.1 (Agilent, Santa Clara, CA) and R [70] for further analysis. Each training patient sample was processed in triplicate on the 10K array. The 10K array data was median-normalized per chip and per feature. Any array with a Pearson Correlation Coefficient less than 0.80 across technical replicates was re-processed. Patient samples were excluded from further analyses if they consistently produced extremely high background and/or consistently failed to provide reproducible results across technical replicates, suggesting serum degradation.

Statistical classification of disease groups

The statistical classification of disease groups was done using Naïve Bayes from the R ‘klaR’ package [71] combined with the Leave one out cross validation (LOOCV) and Holdout algorithm as implemented in the R package ‘DMwR’ [72]. Testing the classifier was done using a data-holdout experiment where training and test datasets are

combined and 70% of randomly chosen data is used to train and predict on the remaining 30% dataset. This procedure is repeated 20-times to ensure every sample was predicted more than once by training on multiple combinations of other samples.. The evaluation of diagnostic metrics such as sensitivity, specificity, positive predictive value (PPV), negative predictive value (NPV) and accuracy of the CF-Titer test based on its performance on our specific patient sample set are reported alongside for comparison purposes.

Statistical classification of confounding infections

To assess if the random peptide microarray could specifically distinguish multiple confounding infections, samples were processed on the 10K random peptide array under similar assay conditions as before. Six different slide batches were used to process these sera and ComBat normalization was applied to median normalized data to eliminate differences between samples due to batch effects. [73,74] 243 random peptides capable of distinguishing between the five classes namely, VF, *Aspergillus*, *Mycoplasma*, *Chlamydia* and Normal were selected using Fisher's exact association test as implemented in GeneSpring GX 7.3.1. Since a physically separate training and test dataset were missing for this analysis, the stringent holdout cross-validation as implemented in R package 'DMwR' was applied to the training dataset as described previously [72].

Results

Valley Fever immunosignature is distinct from that of other infections

Our first question was whether VF infection would produce an immunosignature that was distinguishable from other infections. The concern was that a general inflammatory response to infection may dominate the signature. To test this issue we used sera from individuals infected with *A. fumigatus*, *M. pneumoniae* and *C. pneumoniae*. *Figure 2- 1* and *Table 2- 4* show the results from an experiment where disease cohorts were tested for observable signature differences, and cross-validated using the 70/30 train/test hold out approach described in Methods.

Table 2- 4 Classification results from samples shown in **Figure 2- 1**

Naïve Bayes was used to simultaneously classify the 108 patients into their respective groups using hold out (70% train, 30% test, 20 iterations) cross-validation to estimate error.

Infection	Sensitivity	Specificity	PPV	NPV	Accuracy
Aspergillus	92%	98%	93%	98%	97%
Chlamydia	95%	99%	97%	99%	98%
Mycoplasma	98%	98%	87%	100%	97%
VF	88%	99%	97%	98%	98%

Figure 2- 1 shows the relative intensities of 243 peptides found by Fisher's exact test with the grouping of the individual cohorts shown on the X-axis. Each disease cohort groups together in the heatmap. A quantitative assessment of the classification using the Naïve Bayes algorithm is presented in *Table 2- 4*. The accuracy of simultaneous

classification was 97% for *Aspergillus* and *Mycoplasma* and 98% for *Chlamydia* and VF. These results support the conclusion that a VF specific signature can be distinguished from other potentially confounding infections.

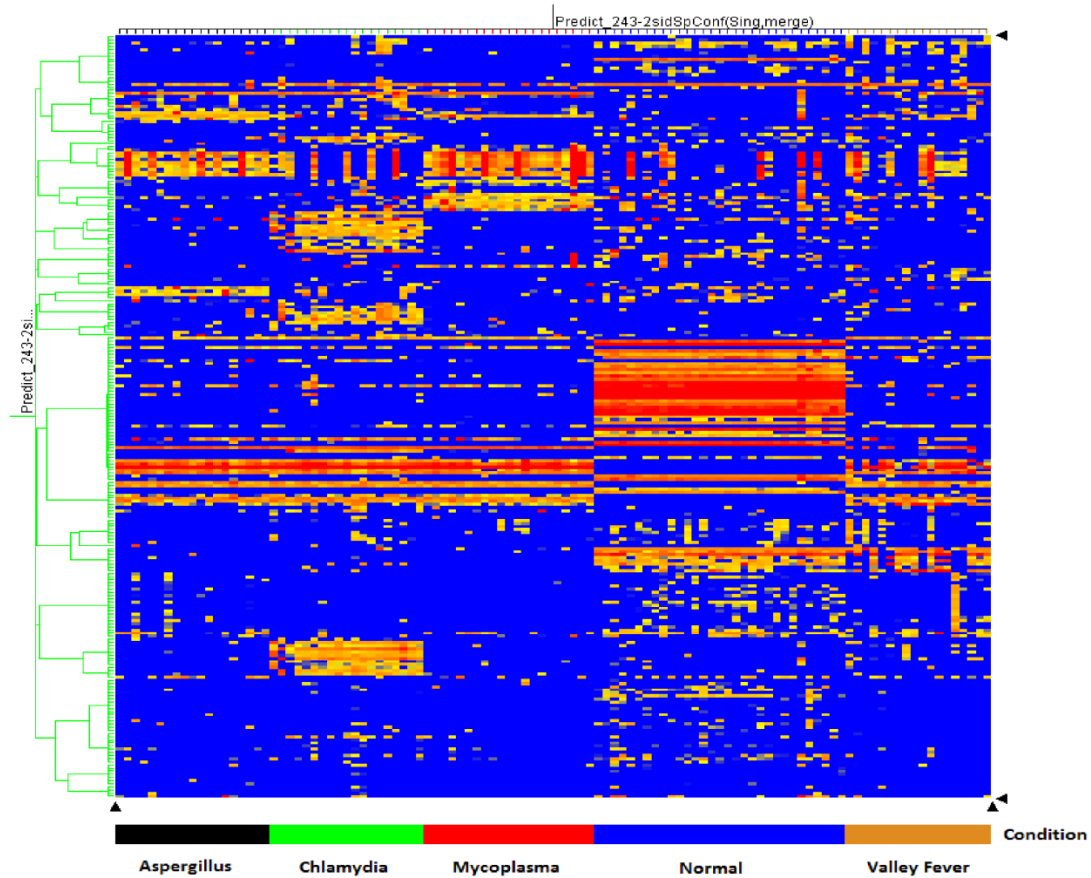


Figure 2- 1 Hierarchical clustering of informative peptides across five diseases.

Peptides (Y-axis) are colored by intensity with blue corresponding to low intensity, red to high intensity. Patients (X-axis) are grouped by their corresponding peptide values with *Aspergillus* (black), *Mycoplasma* (red), *Chlamydia* (green), Normal (blue) and Valley Fever (brown) grouping by cohort as computed by GeneSpring 7.3.1 (Agilent, Santa Clara, CA). Peptides were selected by Fisher's exact test.

Valley Fever immunosignature is distinct from that of uninfected individuals

We examined antibody signature responses of 45 out of the 55 total VF clinical samples shown in *Table 2- 2* on the 10K peptide microarray and identified 1586 peptides from a 1-way ANOVA (5% FWER-family wise error correction) with a threshold of $p < 1 \times 10^{-14}$ indicating significance between the 45 VF training samples and 34 non-disease controls and 7 flu-vaccine recipients both pre-vaccine and 21 days post-vaccine. The influenza signature was included to exclude a potential common confounding signal. This signature is presented as a heatmap in *Figure 2- 2*.

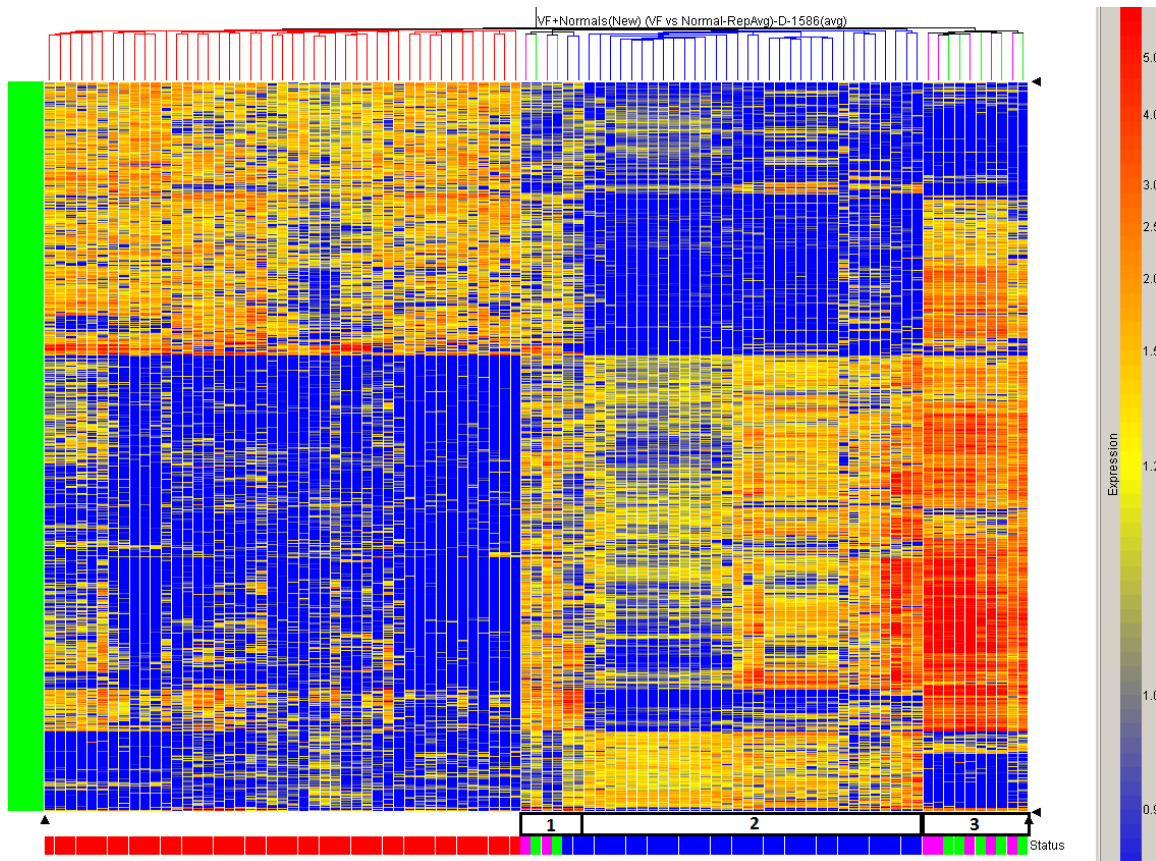


Figure 2- 2 Hierarchical clustering of Valley Fever Immunosignature apart from uninfected individuals.

1586 peptides from a 1-way ANOVA between VF and uninfected individuals are plotted on the Y-axis. Coloring is based on signal intensities obtained from relative binding on the 10K array with blue representing low relative intensity and red representing high signal intensity. Each column represents one individual's Immunosignature with VF patients (red) and uninfected individuals (blue) including influenza pre-vaccine (green) and post-vaccine sera (magenta).

There are three distinct clusters within groups of non-VF normals as highlighted in Figure 2-2 above the status color legend. The first and third clusters within non-VF individuals include influenza vaccine recipient sera showing mild overlapping VF signature. This may be due to these samples being obtained from endemic donors. Note that the differences between non-VF and VF samples include reactivity that is higher in non-VF than the VF samples. Using 70% of the sample to define a classification immunosignature and then testing the classifier on the 30% withheld and averaging the performance of repeating this 20 times, the infected from non-infected samples are classified with 100% accuracy.

Creating a 96 peptide VF diagnostic microarray

Under some circumstances it may be useful to use the 10K array as a discovery platform for informative peptides and then create a smaller, diagnostic-specific array. To test this idea we selected 96 peptides from the 1586 peptide signature described above and using pattern matching algorithms within GeneSpring GX. We used 96 peptides as this is the number easily handled on standard microtiter plates. 48 peptides were chosen

based on the criteria of capturing consistently high antibody signal across ID titers in the VF samples and low antibody signal in the flu vaccine samples. The other 48 were chosen based on the criteria of consistently low antibody signal in the VF samples but high in the flu vaccine samples. The patterns of performance are depicted in *Figure 2- 3* in a line-plot showing the values for each of the 96 peptides across patients (X-axis) whose signals were averaged by their CF titer. The Y-axis shows the median normalized signal intensities represented on a logarithmic scale.

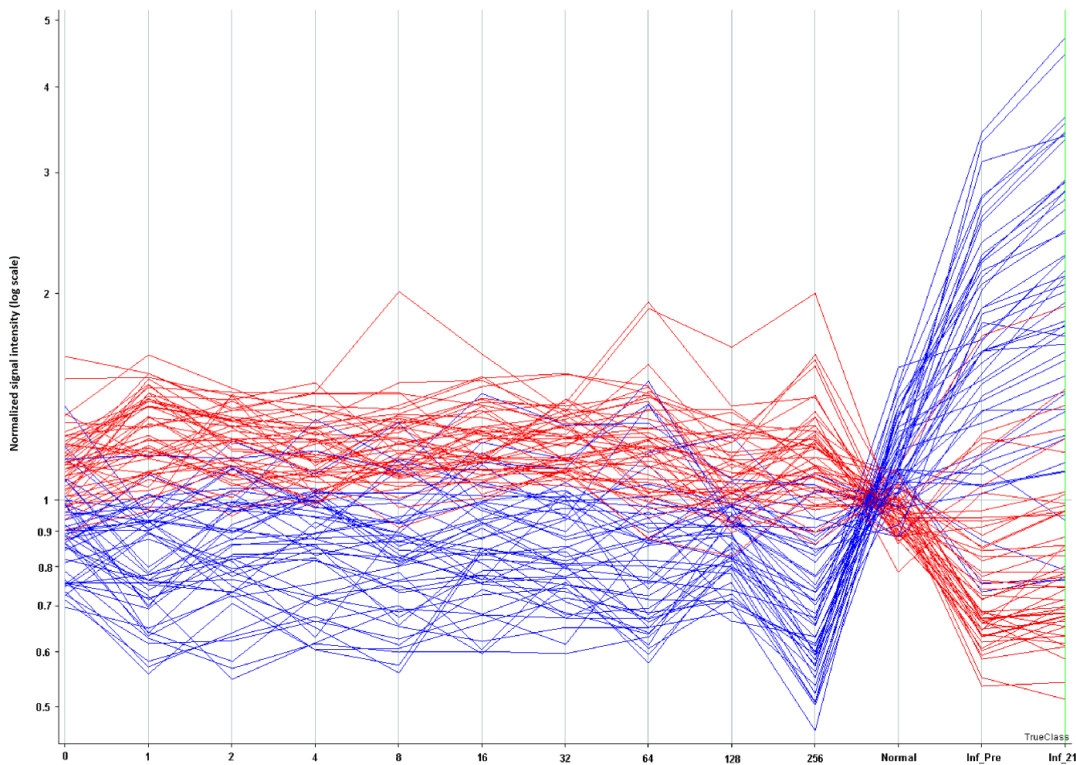


Figure 2- 3 Signal intensity (y-axis) for 96 peptides from the 10,000 peptide microarray that distinguish both VF and influenza vaccine recipients.

X-axis indicates signal response averaged across patients for each CF-titer. Far right are signals averaged for the flu vaccine recipients and normal donors. These data

originate from the full 10,000 peptide array. 48 peptides that capture high antibody binding in VF patients and low signals in normal/influenza vaccine recipients are colored in red. 48 peptides showing higher signals in normal/ influenza vaccine recipients and low signals for VF patients are colored in blue. Consistency is seen across the Valley Fever patients, and a reversal in signal is seen for non-VF patients.

To test the robustness of these signature peptides, we performed a permuted T-test by randomly reassigning the patient identifiers on the samples. The best p-value then obtainable was $p < 2.8 \times 10^{-3}$, 9 orders of magnitude larger than when patients were correctly labeled. It is therefore, unlikely, that the selected peptides were obtained by random chance. *Figure 2- 4* shows a heatmap representation of these same 96 peptides, averaged per CF-titer or flu vaccine status. Hierarchical clustering was used to cluster patient groups (X-axis, individual columns) and peptides (Y-axis, individual rows), with colors within cells representing high (red) to low (blue) intensities from the microarray. The horizontal red bar represents VF patients signal intensities (averaged by CF-Titer), blue bar represents the averaged signals from seven influenza vaccine recipients, cyan represents the averaged vaccine recipient's signature response 3 days prior to receiving the vaccine and yellow indicates the 34 averaged normal donor signatures. *Table 2- 5* lists the performance of pairwise comparisons using 70% training/30% test, averaged over 20 reiterations. The best performance was in distinguishing VF infection from non-infection (100% sensitivity, 97% specificity) and the worst was VF infection versus flu vaccines (100% sensitivity, 82% specificity). Based on this performance in the context of the 10K array, these 96 predictor peptides were re-synthesized (Sigma GenoSys, St.

Louis, MO) and printed on a smaller array to test the performance of the VF focused array.

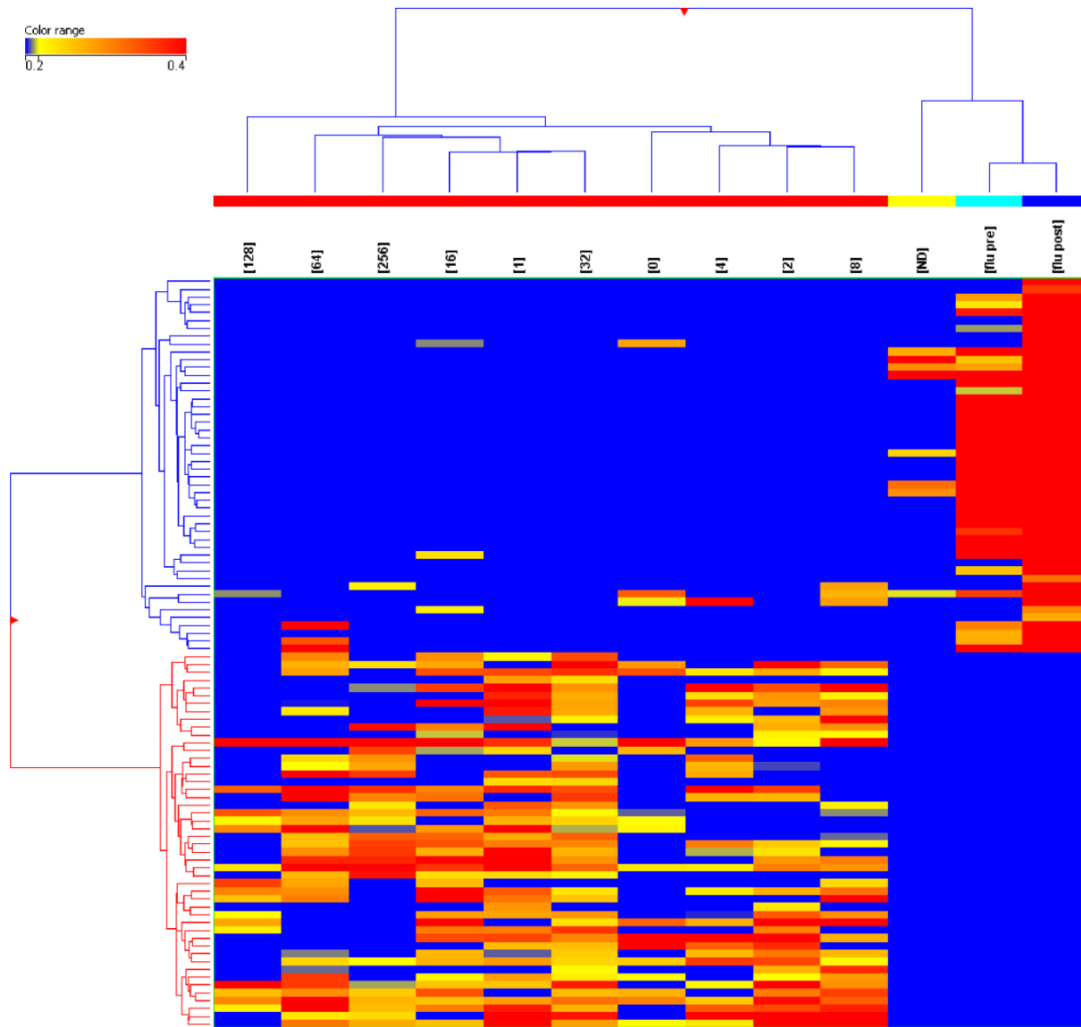


Figure 2- 4 Heat map showing normalized average signals from the 96 predictor peptides as in Figure 2- 2, but displaying the cohort separation.

Data averaged per CF titer and patient group for 45 VF patients (Red bars), 34 healthy controls (yellow bar), 7 pre-2006 influenza vaccine recipients (cyan bar) and 21-day post

vaccine (dark blue bar) (x axis). T-test identified 96 peptides (y-axis) highly significant for distinguishing VF and healthy controls.

Table 2- 5 Naïve Bayes classification results from the VF training cohort on the 10K peptide microarray using the 96 predictor peptides. Holdout splits all data randomly into 70% train/30% predict. Results are from 20 iterations of random holdouts.

Dataset used: Training (Holdout expt.)	Sensitivity	Specificity	PPV	NPV	Accuracy
VF, Normal	100%	97%	97%	100%	98%
VF, Influenza Vaccine	100%	91%	99%	100%	99%
VF, Normal, Influenza Vaccine	100%	96%	96%	100%	98%
0 (CF-Titer), Influenza Vaccine	100%	82%	76%	100%	88%
LOOCV, noHoldOut (all data)	100%	92%	92%	100%	96%
For comparison:					
CF-Titer (IDCF results)	87%	100%	100%	50%	88%

Performance of a 96 peptide VF-diagnostic microarray

The diagnostic capability of the VF-diagnostic sub-array was tested using a smaller set of training and non-VF control samples. Upon verification, the complete training and blinded test samples (67 blinded samples, 13 non-VF controls) were processed on the VF-diagnostic 96 peptide sub-array under similar conditions as the 10K array. *Table 2- 6* shows the resulting classification performance. Of particular note is the performance against the CF Titer=0 samples. While the VF diagnostic peptide set clearly had higher sensitivity compared to the ID assay, there was a substantial drop in the

specificity compared to the ID assay and the performance of those peptides in the 10K array.

Table 2- 6 Naïve Bayes classification results from 96 peptide VF diagnostic array. *Top Panel: 96 peptide diagnostic-array data was tested for performance on a blinded cohort of false-negative VF patients. Middle Panel: Performance using all possible patient samples including test and training samples. Bottom Panel: Performance using only the training dataset.*

Dataset used: Test	Sensitivity	Specificity	PPV	NPV	Accuracy
CF-Titer (IDCF results)	28%	100%	100%	13%	35%
CF-Titer = 0	100%	43%	92%	100%	93%
All data (0 & other titers)	99%	43%	94%	75%	93%
Dataset used: Training & Test Holdout 20 iterations	Sensitivity	Specificity	PPV	NPV	Accuracy
CF Titer (IDCF results)	52%	100%	100%	19%	57%
CF-Titer = 0	91%	85%	96%	70%	90%
All data (0 & other titers)	82%	92%	99%	37%	83%
Dataset used: Training LOOCV	Sensitivity	Specificity	PPV	NPV	Accuracy
CF-Titer (IDCF results)	87%	100%	100%	50%	88%
CF-Titer = 0	100%	67%	75%	100%	83%
All data (0 & other titers)	100%	67%	96%	100%	96%

To examine the difference in performance of the different arrays, we examined the detection limits for each peptide in the context of the actual fold change values as measured from patient samples. *Figure 2- 5* is a graph combining real fold-change values for every peptide (vertical bars) plotted against the detection limit (delta, represented by the black curve) and the p-value obtained from a t-test between the VF vs. normal cohorts

(red circles). The smaller the delta (black curve), the more sensitive the peptide is to a signal and, consequently, the smaller the fold change needed to exceed this limit. Of note are Panels B and C which compare the performance differences between 96 VF-diagnostic peptides within the context of the 10,000 peptide arrays and the same peptides that were resynthesized and independently printed on the VF-diagnostic arrays. This comparison demonstrates the higher performance of the 96 peptides in the context of the 10K array.

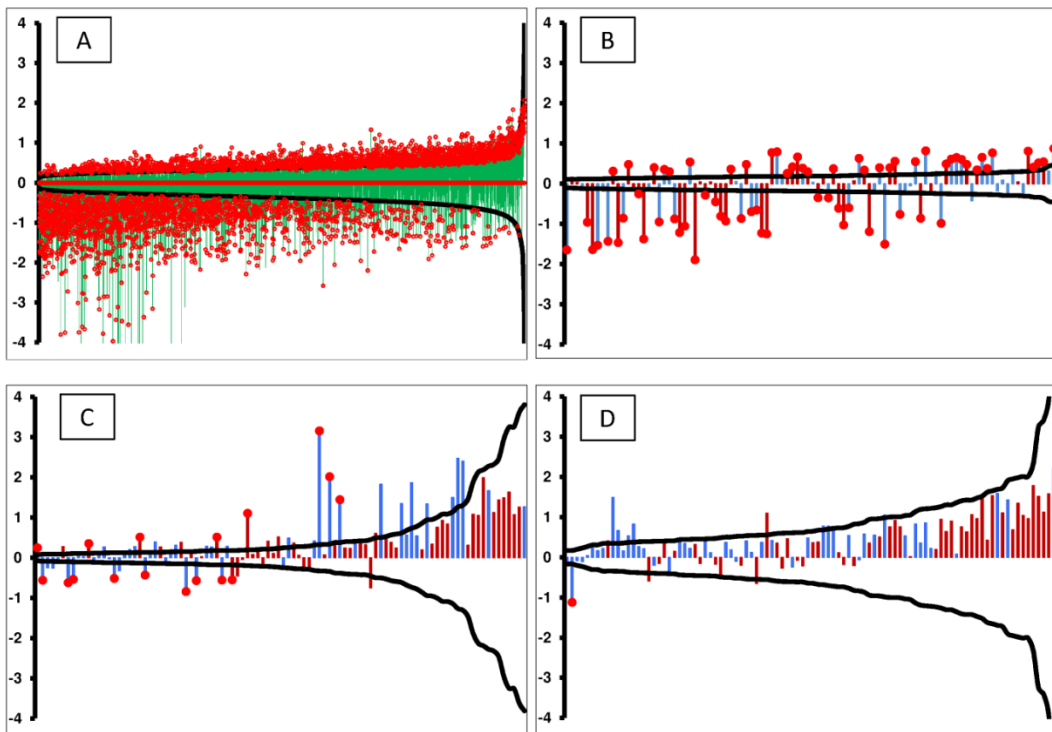


Figure 2- 5 Limits of detection graphed from a post-hoc power calculation.

The black curve in each figure represents the \pm delta (minimum detectable fold-change) calculated from the statistical precision of each peptide independently. The probes along the X-axis are sorted by the calculated power, thus forming a smooth curve. Delta was

calculated using $\alpha=1/\text{Number of peptides/microarray}$, $\beta=0.20$ and $N = \text{number of patients per group}$. The vertical bars (Y axis) represent the \log_2 ratio between healthy and VF-infected patients with red bars indicating a peptide selected to predict VF, and blue bars representing peptides selected for detection of non-VF condition. The red circles on top of certain bars specify statistically significant fold changes at $p\text{-value}<0.01$. Panel A: 10,440 random peptides (Training dataset) using VF and healthy controls. Panel B: 96 VF predictor peptides (Training dataset) within the 10K microarray. Panel C: 96 resynthesized VF predictor peptides (Training dataset) 'VF-diagnostic' assay. Panel D: 96 VF predictor peptides (Test dataset) 'VF-diagnostic' assay.

Discussion

Our objectives in this study were to determine if the immunosignature diagnostic had the potential to address the clinical problem of detecting infection in IDCF-titer=0 patients, and if so what was the best array format. We first demonstrated that VF infection as assayed on the 10K array has a distinct immunosignature relative to 2 bacterial and one other fungal infection. We then showed using a 70% training/30% test format that the 10K array could accurately discriminate VF infection samples from non-VF infection and flu vaccinees. 1586 peptides were statistically significantly different between the classes. A portion of the signature was from peptides that had less reactivity in the VF infection samples than the non-infection controls. 96 peptides from the 1586 that had good signature performance in the context of the 10K array were resynthesized

and used to create a smaller VF diagnostic subarray. When tested against the VF infection and control samples this array demonstrated increased sensitivity (100%) than the conventional IDCF assay, but poorer specificity. Individual statistical analysis of the 96 peptides demonstrated that all performed better in the context of the 10K array than the subarray format.

We had previously published studies demonstrating that influenza virus infection in mice [75] and the flu vaccine in humans [11] could be distinguished from normal controls by immunosignatures. Here we extend this list showing that the immunosignatures of two different species of bacteria and two fungi are distinct. Only 283 peptides of the 10K array were required to simultaneously distinguish the 4 infections with >97% accuracy. Development of the immunosignature diagnostic for clinical application will require further validation testing against other common agents of community acquired pneumonias and infections causing flu-like symptoms.

As noted, for VF a clinically important issue is the people that report with symptoms caused by VF infection but are not detected as sero-positive by the standard immunological tests, the CF titer=0 patients. Using the 10K immunosignature array we demonstrated that there were 1586 peptides that were reproducibly different between VF infection samples and non-VF samples. The non-VF samples included ones that had received the flu vaccine as an effort to exclude flu infection signatures. Noteworthy is that a large portion of this signature was composed of peptides that had lower signal in the VF-infection sample than the non-infection. We have noted this phenomenon before [2,11,13]. This type of reactivity would not be easily detected in standard ELISA-like

assays. We pose that this may be due to the infection causing suppression or elimination of B-cells producing antibodies that are normally present in most people.

A reasonable strategy for developing immunosignatures would be to use the large 10K array as a discovery format and then produce subarrays with smaller number of peptides for the clinical diagnostic. The advantages of the smaller arrays would be that they may be less expensive to manufacture since fewer peptides would be required, the peptides could be of higher quality and they may be simpler to read. To test this approach we chose 96 peptides from the 1586 10K signature and pattern matching analysis between disease and non-disease groups. 48 were chosen which were consistently high in VF infection samples but low in flu vaccine samples and 48 with the converse signature. From a practical perspective, 96 is convenient as it is the basic unit used in peptide synthesis and spotting the arrays. The peptides were selected based on their consistent signal over all titers, including the CF=0, of the standard ID assay. We did not determine if signatures that distinguish the titers could be selected to monitor VF progression. The implication is that the antibody reactivity that these peptides measure is independent of that measured in the ID assay.

This VF diagnostic sub array was tested in a blinded test against the VF infection and non-infection samples. The infection samples include the CF titer=0 samples. While this subarray was significantly more sensitive than the IDCF assay, it was also less specific. This increase in sensitivity but loss of specificity was evident in the CF titer=0 samples. The implication is that this subarray at least would need to be used in combination with the standard ID to obtain maximum specificity and sensitivity.

Interestingly, the sub-array performed less well than the 10K array. This may in part be due to the selection criteria for the 96 peptides which were against the flu vaccine samples. Peptides selected against a wider assortment of non-VF infection samples could perform better. It may also be that the additional peptides on the 10K array distribute the antibody response to infection in a finer resolution allowing high sensitivity and specificity. The 10K format, as demonstrated here for 3 other infections, may have the advantage of being used to discriminate multiple infections on the same platform.

We have demonstrated that the immunosignature platform has clinical diagnostic potential relative to VF infection. It can address the clinical problem of the CF titer=0 infections, either on the 10K format or the sub-array format in combination with the standard ID assay. There are ~50M people in the VF endemic region, with an estimated 30% being exposed over time to the infectious agent. However, since most people have little if any symptoms, it is unlikely a diagnostic would be used generally to screen for VF infection. There is an existing standard antifungal treatment (Fluconazole) and a new one in development (Nikkomyacin). An improved diagnostic could at least identify symptomatic patients more accurately for having VF infections and may allow more effective use of treatments.

Acknowledgements

The authors wish to thank Dr. John Galgiani for providing IDCF characterized Valley Fever patient samples from the Valley Fever Center for Excellence and for advice on the diagnostic constraints in this infection. We thank John Lainsou for contact printing

of experimental peptide microarrays. We would also like to thank Elizabeth Lambert, Mara Gardner, John Lainson and Bart Legutki for processing patient serum samples on the 10K (v1) random peptide arrays as per stipulated protocol and experimental layout. We thank Neal Woodbury for critical suggestions to the manuscript. The arrays described are available through the Peptide Array Core at www.peptidearraycore.com

Grant acknowledgements

This work was partially supported by Startup funds from the Arizona State Technology Research Infrastructure Fund to SAJ. This work was supported by the Chemical Biological Technologies Directorate contracts HDTRA-11-1-0010 from the Department of Defense Chemical and Biological Defense program through the Defense Threat Reduction Agency (DTRA) to SAJ.

Supplementary Data:

Supplementary Table 2- 1 Non-VF infection samples, ELISA data from SeraCare

Name of assay: Platelia for Aspergillus spp. IgG from Bio-Rad (Hercules, CA)

No.	Patient No.	Infection	ELISA (AU/ml)
1	2016079638	Aspergillus	61.9
2	2016088190	Aspergillus	35.8
3	2016173268	Aspergillus	>80
4	2016187069	Aspergillus	18.1
5	2016191891	Aspergillus	>80
6	2016200731	Aspergillus	>80
7	2016231777	Aspergillus	21
8	2016244297	Aspergillus	24.8
9	2016245083	Aspergillus	23.9
10	2016293410	Aspergillus	>80
11	2016330923	Aspergillus	18.1
12	2016332606	Aspergillus	24.1
13	2016362872	Aspergillus	57.3
14	2016393395	Aspergillus	21.3
15	2016397247	Aspergillus	44.7
16	2016397812	Aspergillus	>80
17	2016451743	Aspergillus	38
18	2016454148	Aspergillus	60.3
19	2016479167	Aspergillus	80
20	2016203861	Aspergillus	22.9

Name of assay: ANI labsystems for Mycoplasma pneumoniae IgG (Vantaa, Finland)

No.	Patient No.	Infection	ELISA (AU/L)
1	86	Mycoplasma	57
2	131	Mycoplasma	47
3	1596	Mycoplasma	50
4	3356	Mycoplasma	96
5	5659	Mycoplasma	95
6	2011444020	Mycoplasma	91

7	2016061010	Mycoplasma	115
8	2016062204	Mycoplasma	68
9	2016065663	Mycoplasma	209
10	2016065745	Mycoplasma	71
11	2016065862	Mycoplasma	131
12	2016080956	Mycoplasma	108
13	2016084956	Mycoplasma	153
14	2016085828	Mycoplasma	84
15	2016086204	Mycoplasma	99
16	2016088339	Mycoplasma	179
17	2016088435	Mycoplasma	111
18	2016090988	Mycoplasma	141
19	2016091115	Mycoplasma	309
20	2016092572	Mycoplasma	79

No.	Patient No.	Infection	ELISA (S/CO)	Name of assay
1	9245819	Chlamydia	5.456	Trinity Biotech EIA (Ireland)
2	9245824	Chlamydia	4.186	Trinity Biotech EIA
3	9245825	Chlamydia	4.211	Trinity Biotech EIA
4	9245826	Chlamydia	5.873	Trinity Biotech EIA
5	9245827	Chlamydia	6.434	Trinity Biotech EIA
6	9245829	Chlamydia	4.868	Trinity Biotech EIA
7	9245830	Chlamydia	5.579	Trinity Biotech EIA
8	9245833	Chlamydia	1.3	Trinity Biotech EIA
9	2013298347	Chlamydia	43 (UA/L)	NovaLisa from NovaTec for <i>Chlamydia pneumoniae</i> IgG (Germany)
10	2013352672	Chlamydia	42 (UA/L)	NovaLisa from NovaTec for <i>Chlamydia pneumoniae</i> IgG
11	2016328813	Chlamydia	46 (UA/L)	NovaLisa from NovaTec for <i>Chlamydia</i>

				<i>pneumoniae</i> IgG
12	2016343255	Chlamydia	41 (UA/L)	NovaLisa from NovaTec for <i>Chlamydia pneumoniae</i> IgG
13	BM200809	Chlamydia	2.077	Trinity Biotech EIA
14	BM201051	Chlamydia	2.048	Trinity Biotech EIA
15	BM201105	Chlamydia	1.815	Trinity Biotech EIA
16	BM201340	Chlamydia	3.168	Trinity Biotech EIA
17	BM202017	Chlamydia	1.815	Trinity Biotech EIA
18	BM202083	Chlamydia	2.851	Trinity Biotech EIA
19	BM205162	Chlamydia	1.124	Trinity Biotech EIA
20	BM205163	Chlamydia	1.192	Trinity Biotech EIA

Name of assay: Complement fixation antibodies detected using Immunodiffusion (IDCF) measured by Dr. John Galgiani's lab

No.	Patient No.	Infection	CF-Titer/ IDCF
1	VF0-1077	Valley fever	0
2	VF0-1176	Valley fever	0
3	VF1-1153	Valley fever	1
4	VF1-142	Valley fever	1
5	VF1-178	Valley fever	1
6	VF1-432	Valley fever	1
7	VF2-1304	Valley fever	2
8	VF2-1344	Valley fever	2
9	VF2-1346	Valley fever	2
10	VF2-2	Valley fever	2
11	VF16-1	Valley fever	16
12	VF16-1142	Valley fever	16
13	VF16-399	Valley fever	16
14	VF32-1280	Valley fever	32
15	VF64-262	Valley fever	64
16	VF64-556	Valley fever	64

17	VF128-1012	Valley fever	128
18	VF256-793	Valley fever	256

CHAPTER 3

COMPARISON OF NON-NATURAL MIMOTOPE VERSUS EPITOPE PEPTIDES IN DIAGNOSING VALLEY FEVER

Abstract

Peptide-based diagnostics are not in widespread use not because of poor sensitivity but because of diminished specificity. Numerous reports suggest that protein-based rather than peptide-based detection is more specific. We examined two different approaches to peptide-based diagnostics using Valley Fever (VF) as the model. Although the pathogen was discovered more than a century ago, a sensitive diagnostic is not available. We present a case study where two different approaches were used: the first, a standard overlapping VF-epitope peptide array representing immunodominant *Coccidioides* antigens. Second, a set of random sequence peptides that function as mimotopes and partial epitopes was used. Such a comparison within a diagnostic context has not been previously reported. My results indicate that non-natural (random) sequence peptides show higher accuracy at classifying all stages of VF infection over VF-epitope peptides in a microarray format. The epitope peptide array did provide better performance than the standard immunodiffusion array, but when directly compared to the random sequence peptides, reported lower overall accuracy. This study hints at novel aspects associated with antibody recognition on an amino acid level and suggests methods for improving the accuracy of peptide microarray based diagnostic immunoassays not previously considered.

Abbreviations

CAP, Community Acquired Pneumonias; CF, Complement Fixation; CT, Computed Tomography; CNS, Central Nervous System; EIA, Enzyme Immunoassay; FPR, False Positive Rate; ID, Immunodiffusion; IDCF, Complement fixation antibodies detected by Immunodiffusion; IDTP, Tube precipitin antibodies detected by Immunodiffusion; LDA, Linear Discriminate Analysis; KNN, K-nearest neighbors; LOOCV, Leave One Out Cross Validation; LVS, Live Vaccine Strain; NPV, Negative Predictive Value; PPV, Positive Predictive Value; TP, Tube Precipitation; TB, Tuberculosis; VF, Valley Fever.

Introduction

Superficial fungal infections affecting nails and skin afflict approximately 1.7 billion people worldwide and this number is much higher as compared to the 1.5 million people per year mortality due to invasive fungal infections [76]. Valley Fever (VF) is caused by a dimorphic fungus, *Coccidioides*, prevalent in the southwestern Sonoran desert region of the United States and in certain areas of South America. The pathogen is known to cause both superficial as well as invasive disease in infected individuals. Diagnosis and treatment of VF is surrounded by several delays, due to diagnostic challenges as well as clinical inadequacies. Figure 3- 1 is a flowchart describing the clinical insufficiencies hindering early diagnosis of VF infection as highlighted by an Arizona Department of Health Services (ADHS) survey [20]. Additionally, the diagnostic delays involve very low recovery rates of this pathogen, 0.4% [n=5,026] from blood and 8.3% [n=10,372] from respiratory tract specimens [3.2% overall i.e. from blood,

respiratory tract, urinary tract, bone marrow, cerebrospinal fluid, other sterile and non-sterile body sites; n=55,788] as ascertained from a retrospective analysis of fungal culture specimens submitted to a lab in Phoenix (endemic for VF) by Sussland *et al.* [77]. The sensitivity of serum based assays such as Enzyme Immunoassay (EIA) is 83-87%, that of complement fixation and tube-precipitation antibodies detected by Immunodiffusion (IDCF, IDTP) is 71-73% and that of complement fixation by itself is low between 56-75% [78,79]. We demonstrated in our previous study [80] that Immunosignatures [2,10-12] using non-natural sequence peptide microarray technology could be successfully applied to resolve the diagnostic challenges surrounding VF serum based diagnosis. The random peptide ‘VF-diagnostic’ microarray platform accurately classified 63 longitudinal samples from 25 symptomatic yet clinically false-negative (IDCF=0 titer) patients as having valley fever. The confirmatory assay, IDCF’s sensitivity on this specific training and initially blinded test dataset used in the previous assay was 52% and specificity 100%. Despite being a difficult sample set, the non-natural sequence peptide microarray out-performed IDCF with an overall cross-validated (holdout) sensitivity of 82% and specificity of 92%. In this work we sought to test an alternative diagnostic approach using epitope peptides representing immunodominant VF antigens. This article compares the diagnostic performance of non-natural (random) sequence predictor peptides for VF and that from VF-epitope (life-space) peptides representing four immunodominant VF antigens. In doing so, it evaluates a central hypothesis of whether randomly generated; non-natural sequence predictor peptides from Immunosignatures are more or less

effective at accurately capturing all stages of VF infection with more sensitivity and specificity than pathogen antigen peptides in a similar microarray.

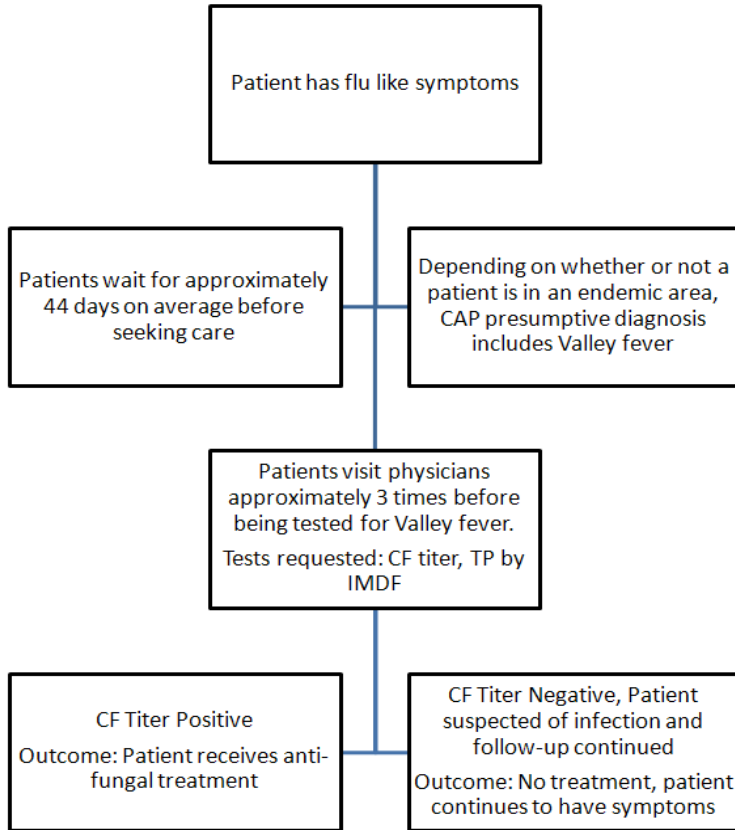


Figure 3- 1 The clinical problem in Valley fever diagnosis.

A diagnostic peptide microarray composed of 96 random peptides was created as part of a prior study [80] to enable sensitive diagnosis of VF in patients that were initially characterized as false-negatives by the IDCF titer gold-standard diagnostic assay. Briefly, a well characterized VF patient serum sample training set was tested on a 10,000 random peptide microarray to select the 96 VF predictor peptides for the smaller sub-array. These 96 random peptides were selected for specificity in discriminating VF patient samples from both non-VF disease and healthy controls in the training set.

Influenza vaccinee sera were included as a confounding infection. Encouraged by higher sensitivity obtained on this smaller sub-array for predominantly false negative samples (IDCF=0), we sought to test whether using antigen epitope peptides from *C. immitis* might deliver an equally sensitive and perhaps more specific diagnostic than that obtained by using non-natural (random-sequence) predictor peptides. To this effect, we chose to represent four immunodominant VF antigens that are potential vaccine candidates in the form of six amino acid overlapping peptides. These antigens are chitinase-F (CF) [81], Antigen-2 [82], Expression Library Immunization-Antigen1 (ELI-Ag1) [83] and *Coccidioides immitis* specific antigen (CSA) [84] from *Coccidioides immitis* (strain-RS). The CF antigen is considered the main immune stimulating antigen as measured by the IDCF assay [61]. IDCF detects antibodies to several protein antigens present within an untreated (by heat), autolyzed, mycelial culture filtrate. In this study, a side by side comparison of the diagnostic capability of these 96 VF specific non-natural peptides was made with 83 antigen epitope peptides representing four VF immunodominant antigens. Additional bioinformatic analyses were conducted to ascertain the reasons underlying high sensitivity and specificity of the 96 non-natural VF predictor peptides.

When classifying non-natural proteins versus natural antigen proteins, one of the several metrics used for classification is the amino acid frequency of sequences being compared [31]. Within these groups of characteristic metrics, a di-peptide frequency pattern is typically used to automatically annotate proteomes by classifying protein sequences and informatically attributing function based on di-peptide complexity [85]. In order to ascertain why the 96 non-natural peptides function as VF predictors, a di-peptide

and short-sequence (2-mer to 6-mer) composition analysis is performed. For the purpose of this study, instead of the di-peptide frequency, the total possible di-peptides in common between 96-random and 83-life space epitope peptides versus VF proteome is calculated. Additionally we use an amino acid sequence similarity based alignment program named GuiTope [34] to compare the 96 non-natural VF predictor peptides to the four VF protein antigens in an effort to de-convolute the mechanism enabling randomly generated non-natural sequence peptide predictors to sensitively detect VF. GuiTope is a program that aligns non-natural sequence peptides to natural sequence proteins based on sequence level amino acid physico-chemical and structural similarity in an effort to map back to the original antigen from observed antibody binding on a microarray. It includes the novel feature of aligning sequences by taking into consideration di-peptide inversions within random peptides which was a phenomenon first observed while analyzing the data presented in this article and led to statistically significant improvement in GuiTope's epitope discovery accuracy.

Methods

Serum samples used in this study

A training and blinded test serum sample set were collected under the University of Arizona's IRB# FWA00004218 and received by The Center for Innovations in Medicine at Arizona State University under their IRB# 0905004024 allowing unfettered data analysis of this material. Most patients sample within the training and blinded test set were initially characterized as being false negative on the CF-titer (IDCF) assay.

Supplementary Table 3- 1 describes the CF titer distribution in the samples from the training cohort. A training sample set consisting of 55 longitudinal samples from 35 VF symptomatic individuals including some 0 CF-titer early time point sera from 6 individuals that later sero-converted was acquired from the University of Arizona. The accuracy of diagnosis using IDCF for the training set sera was 88%, with sensitivity = 87%, specificity = 100%, PPV (Positive predictive value) = 100% and NPV (Negative predictive value) = 50%. Supplementary Table 3- 2 describes the CF titer distribution in the samples from the initially blinded test cohort. A blinded test sample set was acquired containing 67 serum samples of which 48 which were later revealed to be sero-negative on IDCF. These test group sera were from 25 patients with two or more serum samples per individual collected longitudinally during their disease progression. Supplementary Table 3- 3 summarizes the individual sample characteristics of patients sera included within the test set. The accuracy of diagnosis using IDCF for the test set sera was 35%, with sensitivity = 28%, specificity = 100%, PPV = 13% and NPV = 35%. The overall accuracy of both training and test dataset samples using IDCF for diagnosis was 57% (sensitivity= 52%, specificity= 100%, PPV= 19% and NPV= 57%).

For the exploratory non-natural feature selection training portion of the experiment, 45 out of the total 55 training sera were processed to ensure adequate representation of all CF-titers (progressive stages of infection) on a 10,000 random peptide Immunosignature microarray. Additionally, blood samples were processed from 48 otherwise healthy male and female individuals of various ages along with 7 influenza vaccinee's who supplied blood 3 days prior ('pre') to receiving the 2006/2007 influenza

vaccine and 21 days later ('post'), and the data from their antibody reactivity's to the 10,000 peptides were classified as 'non-disease' for training purposes. 96-random VF predictor peptides were selected out of 10K peptides from this exploratory assay as explained in the prior publication [80].

All VF training and blinded test samples were processed on the smaller diagnostic array containing the selected 96-random and 83-life space epitope peptides in triplicate. Thirteen non-disease samples, including sera from healthy volunteers as well as influenza vaccinee samples were processed on the smaller diagnostic array. To measure the specificity of the smaller diagnostic array, we processed 10 *Fransicella tularensis* (LVS-Live Vaccine Strain) vaccinated individuals sera obtained from Dr. Anders Sjöstedt's lab from Umeå University. This serum was part of a time course study and the samples selected for processing were the ones that were collected 28-30 days post receiving the LVS vaccine.

Microarray production and processing

The 96 random peptides as well as 83 life space peptides were synthesized by Sigma (St.Louis, MO) and printed as described in Legutki *et al.* [11] Every 17 amino acid peptide was designed to have an N-terminal CSG linker and printed on aminosilane-coated glass slides which were activated with sulfo-SMCC (Pierce, Rockland, MD). All peptides were printed in triplicate next to each other in a two array printings per slide format. Arrays were printed using a Nanoprint 60 (ArrayIt, Santa Clara, CA) at 60%

relative humidity at 23°C. Patient serum from training and test sets were processed on this smaller microarray in duplicate.

Microarray slides were pre-washed with a solution containing 7.33% acetonitrile, 33% isopropanol and 0.55% TFA to remove any unbound peptides. Slides were blocked in 1X PBS, 3% BSA, 0.05% Tween 20, 0.014% β -mercaptohexanol for 1hr at 25°C. Sera samples were diluted 1:500 in the Incubation buffer containing 3% BSA, 1X PBS, 0.05% Tween 20, and allowed to bind to the microarray for 1 hour at 37°C in 100 μ l total volume per array on a Tecan 4800 Pro Hybridization Station (Tecan, Salzburg, Austria). Slides were washed in-between primary and secondary antibody incubation steps for 30 seconds with 1X tris-buffered saline (TBS), 0.05% Tween 20 pH 7.2. Patient IgG antibodies were detected using 5nM, DyLight-549 conjugated Goat anti-Human, IgG Fc (γ) fragment specific secondary antibody and 5nM, Dylight-649 conjugated Goat anti-Human, IgM (5 μ) fragment specific antibody from Jackson ImmunoResearch Laboratories, Inc., West Grove, PA diluted in the incubation buffer. These slides were scanned using the Agilent 'C' Scanner (Agilent Technologies, Santa Clara, CA) at 532 nm and 647 nm excitation wavelengths under 100% PMT and 100% laser power with a 10 μ m image resolution. Both red and green channel TIFF images were simultaneously aligned per individual array, using the GenePix software (Axon Instruments, Union City, CA) and the data files imported into GeneSpring 7.3.1 (Agilent, Santa Clara, CA) for further analysis.

Pre-processing of data for analysis

Data are collected in the form of .gpr files. Each .gpr file contains the peptide name and the foreground intensity for each measured peptide for both IgG (green, 545nm channel) and IgM (red, 647nm channel). Data were loaded into GeneSpring GX 7.3.1 for analysis. Since the diagnostic array included two color data, a Lowess normalization was completed in GeneSpring whereby the ratio between the signal and control channels was used for classification. Any array with a Pearson Correlation Coefficient less than 0.80 across technical replicates was re-processed. Upon reprocessing if the Pearson correlation between replicates did not improve, that patient's sample was excluded from further analysis.

Statistical analysis

Classification was performed using the Naïve Bayes algorithm as implemented in the klaR [71] package in R. Due to the unbalanced nature of this dataset, the holdout algorithm was used to balance the groups, from the R package DMwR as published in the book, Data Mining with R [72]. This helped overcome in-accurate estimation of specificity due to lesser non-disease samples. The holdout experiment was done by combining the training and test dataset and is a more rigorous cross-validation technique whereby 70% of randomly selected total data was used for training and prediction was made on the remaining 30% data. This was done for 20 iterations so as to predict the class of every sample more than once and get a better assessment of diagnostic metrics such as sensitivity, specificity, negative predictive value (NPV), positive predictive value

(PPV) and accuracy. The results for both standard train and test (without cross-validation) and holdout are included side-by-side for every comparison.

GuiTope analysis

Previous work done by Halperin *et al.* [34] showed an unusual property of antibody recognition of near-epitope sequences. Two amino acids in a row could be swapped in position with no decrease in the apparent binding affinity. This occurred often enough in a broad analysis of monoclonals and polyclonals on Immunosignature random peptide microarrays, and phage display datasets from MimoDB [86] that Halperin and colleagues embedded an allowance for this in a program for analysis of peptide alignments called GuiTope [34]. The current article is the first report displaying the use of this program for finding mimotopes within non-natural peptides through antibody binding observed from VF patient sera.

The protein sequences of the four immunodominant VF antigens were uploaded as a .fasta format file into the Protein section of GuiTope. The 96 non-natural space peptide sequences were uploaded into the peptide input section. In the library section, the original 10K random peptide library was uploaded from which the 96-random peptides were selected as VF predictors. These 96 selected random peptides were excluded from the library section. This was done so as to calculate the false-positive rate (FPR) by calculating the score for an equal number of library peptides as the selected VF-predictors (96) for multiple iterations (1000) and assessing the probability of finding another peptide in the library that had a higher similarity to the four VF proteins, above

that calculated for the 96-selected. The default amino acid distance matrix, Grantham 1974 [87] was used but the amino acid frequencies of the query proteins and query 96-random peptides were pasted into the appropriate sections under the Generate Matrix tab. Under the parameters tab, the inversion weight was set to 1 or 0 to either include or exclude the di-peptide inversion modulation to the Smith-Waterman maximal gapless local alignment algorithm [33]. A new distance matrix was generated after taking into consideration the amino acid frequencies for the query protein and peptide. The sampling iterations under the ‘Graphical output’ tab was set to 1000, which is the number of times 96 other peptides would be selected at random from the 10K library to compare scores for the selected 96-peptides and generate the FPR.

Results

Comparing classification accuracy and sensitivity of life space versus random peptides

A comparison between pathogen epitope peptides and non-natural sequence peptides within a peptide microarray diagnostic had not been previously reported in the literature. We examined the signature response captured by 83 valley fever antigen epitope peptides and compared that to the antibody response captured by 96 non-natural VF-diagnostic peptides as depicted in Figure 3- 2.

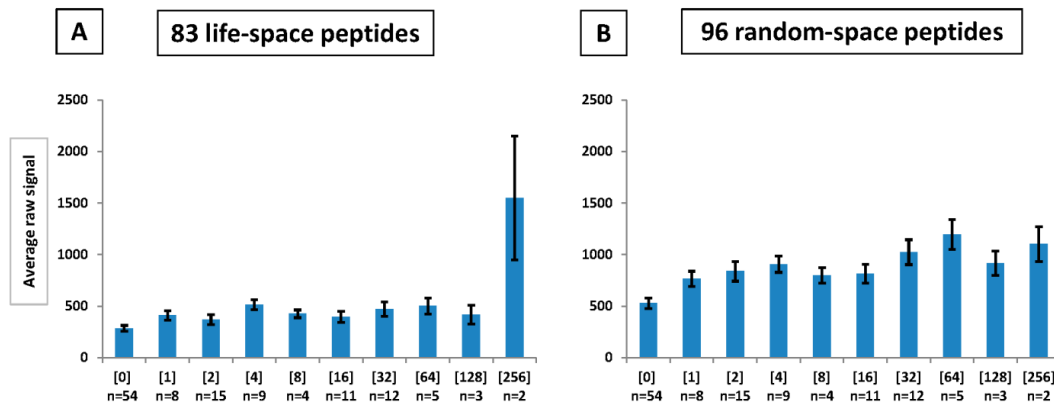


Figure 3- 2 VF patient signal average intensity data per CF-titer.

The Y-axis displays the average raw (non-normalized) signal in fluorescence intensity units (FIU) captured by 83 VF antigen life-space peptides in Panel A and 96 non-natural (random) peptides in panel B. Error bar depict standard error. The X-axis displays signal intensities as averaged by CF-titer (IDCF) with ‘n’ reflecting the number of patients in the training and test groups combined per CF-titer.

IgG antibody averaged signals in panel A captured by tiled VF-antigen peptides do not show incremental correlation with increasing CF-titer until the CF-titer reaches 1:256. At every CF-titer, except 1:256, the 96-random peptides capture higher amount of antibodies on average as compared to the life-space peptides. The 96-random VF predictor peptides might thus have more potential for accurately measuring symptomatic yet false-negative patient sera mis-classified by the IDCF test. Table 3- 1 summarizes the Naïve Bayes classification result from false negative (CF-titer=0) patients within the VF dataset and compares the performance of the 83 life-space peptides versus 96-random peptides.

Table 3- 1 Naïve Bayes classification result on VF test dataset using random vs life space peptides.

IgG	Peptides	Sensitivity	Specificity	PPV	NPV	Accuracy
0 (CF-Titer)	Random (96)	100%	43%	92%	100%	93%
	Life space (83)	96%	71%	96%	71%	93%

IgM	Peptides	Sensitivity	Specificity	PPV	NPV	Accuracy
0 (CF-Titer)	Random (96)	94%	43%	92%	50%	87%
	Life space (83)	88%	57%	93%	40%	84%

Holdout exp (70- 30), 20 iterations

IgG	Peptides	Sensitivity	Specificity	PPV	NPV	Accuracy
0 (CF-Titer)	Random (96)	91%	85%	96%	70%	90%
	Life space (83)	86%	71%	93%	52%	83%

IgM	Peptides	Sensitivity	Specificity	PPV	NPV	Accuracy
0 (CF-Titer)	Random (96)	99%	58%	86%	96%	88%
	Life space (83)	80%	68%	91%	46%	78%

The random peptides are more sensitive at diagnosing valley fever than the life space peptides. The top half of this table represents the IgG (green-channel) and IgM (red-channel) sensitivity from generating a Naïve Bayes model by training on the training

dataset and testing on a physically separate test dataset. The bottom half of the table represents a more rigorous assessment of these metrics by performing the holdout cross-validation for 20 iterations and using 70% randomly selected training samples to train and predict the remaining 30% of data. The results presented are averaged for multiple predictions per sample for all 20 iterations. The resulting values are more accurate estimates to be expected from this assay when testing with additional clinical samples in the future. Random peptides detect false-negative symptomatic patient sera more accurately as compared to life space epitope peptides. As might be expected early in an infectious response the IgM responses offer higher sensitivity (98.96%, random peptides).

Bioinformatic rationale underlying the sensitivity of random (96) vs. life-space (83) epitope peptides

A linear B-cell antibody epitope ranges from 4-12 amino acids in length as previously delineated through peptide microarray analysis [88]. Sun *et al.* [89] determined from 161 Protein Data Bank (PDB) antigen-antibody pair structures that in conformational epitopes, antibody paratopes associate with antigens in short non-contiguous segments, 2-5 amino acids in length. The reasons underlying higher sensitivity and specificity of random predictor peptides in comparison to pathogen epitope peptides could be bioinformatically ascertained by comparing the level of short sequence overlap between the two groups of predictor peptides and the VF proteome. Figure 3- 3 depicts the number of unique n-mers between the 96-random and 83-lifespace

peptides in common with the VF pathogen proteome (panel A) and the randomly generated VF proteome (panel B).

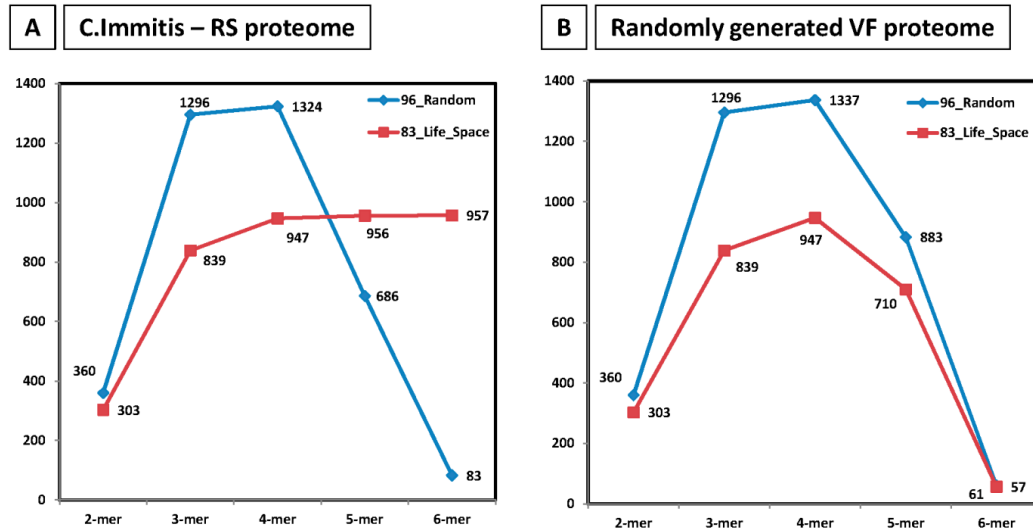


Figure 3- 3 Sensitivity of assay - Number of unique n-mers (2-6 amino acid short sequences) between the 96-random and 83-lifespace peptides in common with the VF pathogen proteome (panel A) and the randomly generated VF proteome (panel B).

The Y-axis shows the number of 2-6 mers in common between groups of peptides and pathogen proteomes as a continuous line graph with n-mer groups displayed on the X-axis.

The bioinformatically *in-silico* generated artificial VF proteome uses amino acid alphabets in an unbiased random manner to match the number and length per protein within the natural *Coccidioides immitis* strain-RS proteome. The total possible combinations of di-peptides using 20 amino acids is 400 and the 96-random peptides represent 360 out of those 400 possibilities. The 83 life-space peptides only represent 303 out of the 400 possible di-peptide combinations. The number of overlapping 6-mers in

common between the life-space peptides and the natural VF-proteome increase but this extent of overlap is not by random chance as depicted by the artificially generated VF proteome. The number of 6-mers identical between the 96-random peptides and both the natural and artificially generated VF-proteome is low and show the true randomness of these 96 VF-predictor non-natural peptides.

Specificity and robustness of random (96) vs. life-space (83) VF epitope peptides

In an effort to assess the specificity of this assay, we statistically classified all CF-titer (non-zero) VF patient sera to test whether the peptide microarray could distinguish all progressing stages of VF infection apart from uninfected sera (normal donors, influenza vaccinees). Additionally, we processed sera from *Francisella tularensis* (LVS) vaccinated individuals 28-30 days post-vaccine. When *Francisella tularensis* infects the lungs, symptoms resemble those of respiratory distress similar to those observed in VF [90]. To measure specificity against a confounding exposure, the 10 LVS samples were randomly split between the training and the test samples (5 per group). Separate classifications were done for 2 groups (VF vs. non-VF – Part A, without LVS sera) or 3 groups (VF vs. non-VF vs. LVS – Part B) (Table 3- 2). The assay performance metrics for IDCF are included for side-by-side comparison in Part A.

Table 3- 2 Naïve Bayes classification results using IgG and IgM signals from VF 96 random predictor peptides and 83 VF epitope peptides

A.) Groups: VF, Normals (No LVS)						
IgG	Peptides	Sensitivity	Specificity	PPV	NPV	Accuracy
All (CF-Titer)	Random (96)	99%	43%	94%	75%	93%
	Life space	96%	50%	94%	57%	91%

	(83)					
IgM	Peptides	Sensitivity	Specificity	PPV	NPV	Accuracy
All (CF-Titer)	Random (96)	99%	25%	92%	67%	91%
	Life space (83)	90%	50%	94%	36%	85%
CF-Titer	IDCF results	28%	100%	100%	13%	35%
Holdout experiment (70-30), 20 iterations						
IgG	Peptides	Sensitivity	Specificity	PPV	NPV	Accuracy
All (CF-Titer)	Random (96)	82%	92%	99%	37%	83%
	Life space (83)	79%	73%	96%	30%	78%
IgM	Peptides	Sensitivity	Specificity	PPV	NPV	Accuracy
All (CF-Titer)	Random (96)	93%	74%	97%	55%	91%
	Life space (83)	84%	68%	96%	34%	82%
CF-Titer	IDCF results	52%	100%	100%	19%	57%

B.) Groups: VF, LVS, Normals						
IgG	Peptides	Sensitivity	Specificity	PPV	NPV	Accuracy
All (CF-Titer)	Random (96)	99%	50%	92%	86%	91%
	Life space (83)	96%	62%	93%	73%	90%
IgM	Peptides	Sensitivity	Specificity	PPV	NPV	Accuracy
All (CF-Titer)	Random (96)	99%	46%	90%	86%	90%
	Life space (83)	87%	54%	91%	44%	81%
Holdout experiment (70-30), 20 iterations						
IgG	Peptides	Sensitivity	Specificity	PPV	NPV	Accuracy
All (CF-Titer)	Random (96)	79%	87%	97%	44%	80%
	Life space (83)	91%	73%	94%	62%	87%
IgM	Peptides	Sensitivity	Specificity	PPV	NPV	Accuracy
All (CF-Titer)	Random (96)	93%	70%	93%	67%	89%
	Life space (83)	83%	75%	94%	48%	81%

A - Model classifying between 2 groups VF and Non-VF (Normal)

B - Model classifying between 3 groups VF, Non-VF and LVS

Holdout experiment - combine training and test set data, Train on randomly selected 70% data and test on remaining 30% (20 iterations)

Naïve Bayes (no holdout) yielded 99% sensitivity using both IgG and IgM signals from 96-random predictor peptides when including the LVS samples (*Table 3- 2, Part B*). In comparison, the 83 life-space epitope VF peptides showed 96% sensitivity when using IgG signals and 87% when using IgM signals. The holdout experiment was performed so as to reduce biased estimates of specificity due to comparatively lower number of non-disease patient sera tested on this assay in comparison to VF patient sera. The specificity at distinguishing VF apart from normal by non-natural 96-random VF predictor peptides through the holdout analysis for IgG is 92% (*Table 3- 2, Part A*) in comparison to 73% (*Table 3- 2, Part A*) from 83 VF life-space epitope peptides. This was unexpected given our original hypothesis of expecting higher specificity from VF life-space epitope peptides as compared to non-natural sequence peptides (96-Random). When testing the classification (holdout) of these same VF and normal samples in the context of LVS, the specificity of non-natural peptides capturing IgG reactivity within this assay dropped from 92% (*Table 3- 2, Part A*) to 87% (*Table 3- 2, Part B*) merely because the platform was not originally trained or designed to distinguish between these specific disease groups. This 87% specificity though is still higher than that demonstrated by life-space

VF epitope peptides (73%). The sensitivity (91%) and accuracy (87%) of life-space peptides was higher than non-natural peptides when including the LVS group (Table 3- 2, Part B).

As often seen in assays involving antigen-antibody interactions [3,5], some peptide-level cross-reactivity was observed from the LVS vaccinees towards some random and life-space peptides selected to distinguish Valley Fever from influenza and healthy controls. The cross-reactivity of these VF predictor peptides to antibodies from individuals exposed to LVS might be partially explained due to the number of overlapping 5-mers between them and the pathogen proteomes tested in this analysis (Figure 3- 4).

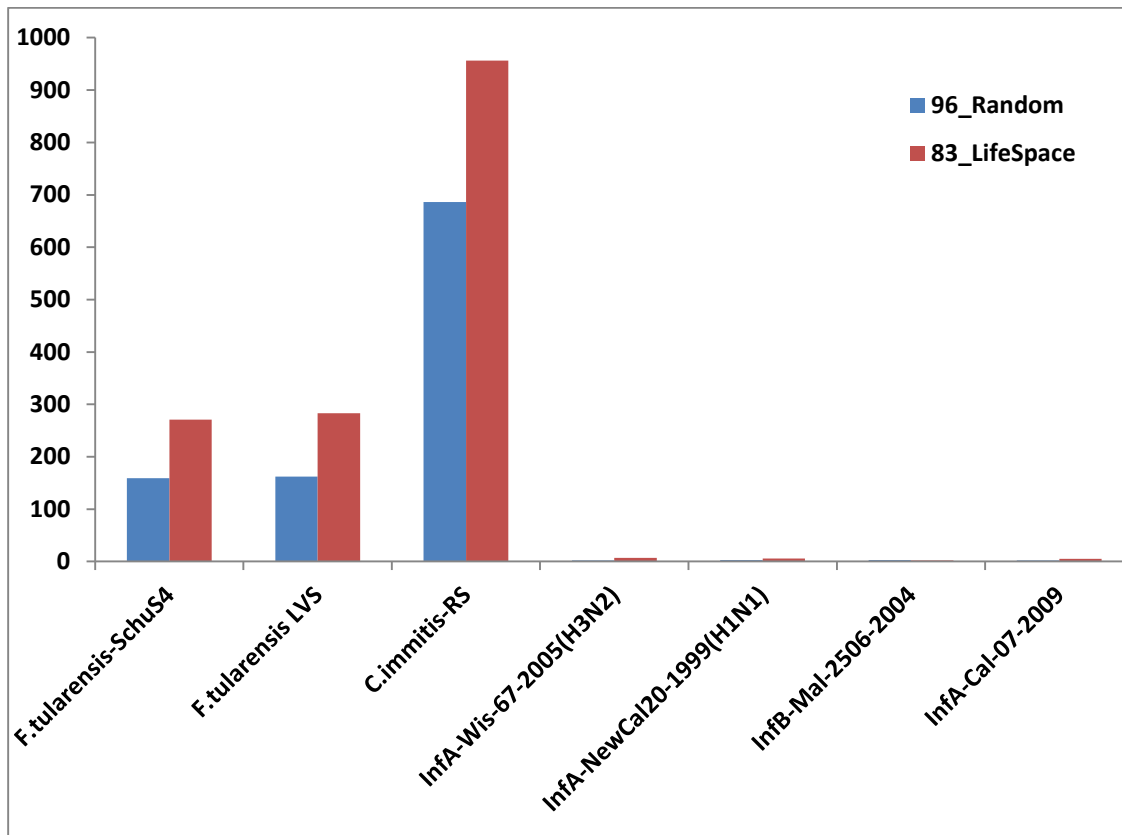


Figure 3- 4 Cross-reactivity observed on VF-diagnostic array hypothetically explained using the number of unique 5-mers in common (Y-axis) between random (blue bars) and life space (red bars) peptides and pathogen proteomes (X-axis).

Influenza/A/Wisconsin and New Caledonia and Influenza/B/Malaysia strains were included in the 2006-2007 seasonal Influenza vaccine. The extent of identical overlapping 5-mers between the Valley Fever proteome and both the random and life-space peptides is much higher compared to Influenza or *Francisella* proteomes. The extent of overlap may also be partially affected by the significantly different size of these pathogen proteomes, with *C. immitis* having 10,440 proteins and *F. tularensis str. SchuS4* having 1,556 proteins and *F. tularensis str. LVS* having 1,754 proteins while only 12

proteins represent the Influenza proteomes. The 96-random peptides performed with higher specificity in being able to distinguish VF from non-VF patients and LVS vaccinees as compared to VF epitope peptides (life-space). Figure 3- 5 shows the number of unique n-mers (2-6 amino acids) between the 96-random and 83-lifespace peptides in common with the LVS proteome (panel A) and the randomly generated LVS proteome (panel B).

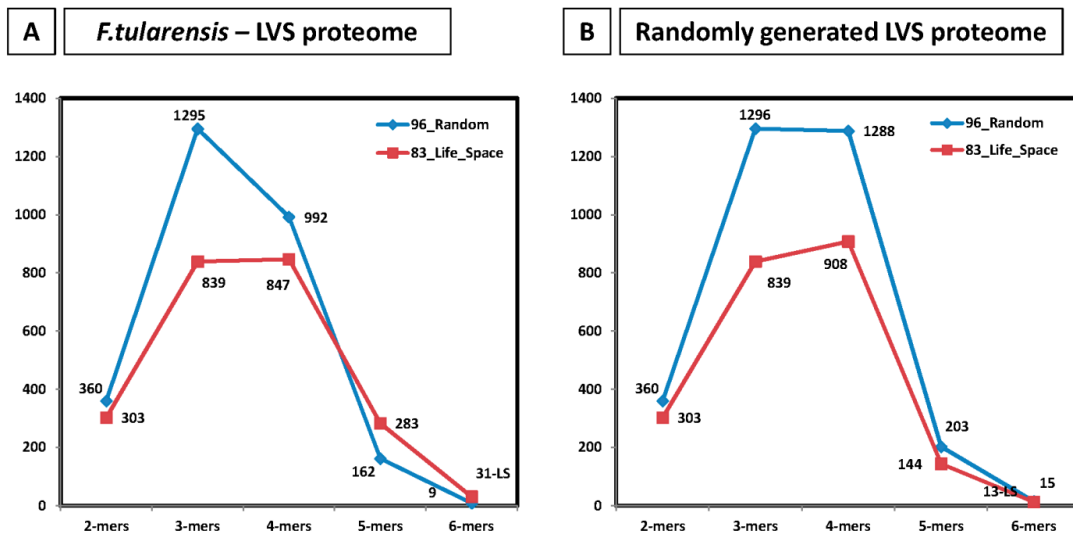


Figure 3- 5 Specificity of assay - Number of unique n-mers (2-6 amino acid short sequences) between the 96-random and 83-lifespace peptides in common with the LVS proteome (panel A) and the randomly generated LVS proteome (panel B).

The Y-axis shows the number of 2-6 mers in common between groups of peptides and pathogen proteomes as a continuous line graph with n-mer groups displayed on the X-axis.

The extent of 5-mer and 6-mer overlap between random peptides and the LVS proteome whose signature they were not designed to capture is low as compared to that

observed between the two peptide groups and VF proteome in Figure 3, Panel A. This explains why the specificity of non-natural (96-Random) peptides at distinguishing a previously un-trained on exposure (LVS) was higher than that of VF epitope peptides (life-space).

Bioinformatic rationale underlying the specificity of random (96) vs. life-space (83) epitope peptides

A comparison between the 96-random peptides and the 4 immunodominant VF antigens was done using GuiTope. Using the protein BLAST program [91] very few alignments were found between the VF proteins and 96-random peptides. Table 3- 3 and Figure 3- 6 summarize the positive matches between 96-random peptides and 4 VF antigen proteins.

Table 3- 3 Summary of GuiTope matches between 96-Random VF predictor peptides and 4 VF antigens

Score cutoff: 6.56 Moving Average: 15
 Sampling Iterations: 1000 Subtracting Mean Lib Scores? Checked

Part A.) Inversions = 1

Name	Rank	Max Score	Max Score Position (amino acid)	FPR	Length (aa)	No. of Guitope Matches
CF-CIMG_02795	1	7.32	249	0	427	82
CSA-CIMG_01181	2	6.64	40	0	146	46
Eli-Ag1-CIMG_10032	3	6.34	159	0	224	62
AG2-CIMG_09696	4	5.44	145	0.001	194	43

Part B.) Inversions = 0

Name	Rank	Max Score	Max Score Position (amino acid)	FPR	Length (aa)	No. of Guitope Matches
CF-CIMG_02795	1	6.37	362	0	427	51
CSA-CIMG_01181	2	6.33	60	0	146	23
Eli-Ag1-CIMG_10032	3	4.68	210	0.0013	224	39
AG2-CIMG_09696	4	4.55	74	0.0015	194	16

The number of positive hits obtained when using the di-peptide inversion modulation in addition to the Smith-Waterman [33] positional search algorithm is higher than those obtained without including di-peptide inversions. The individual peptide positive hits per protein are summarized in Supplementary Table 3- 4 with inversions and Supplementary Table 3- 5 without inversions.

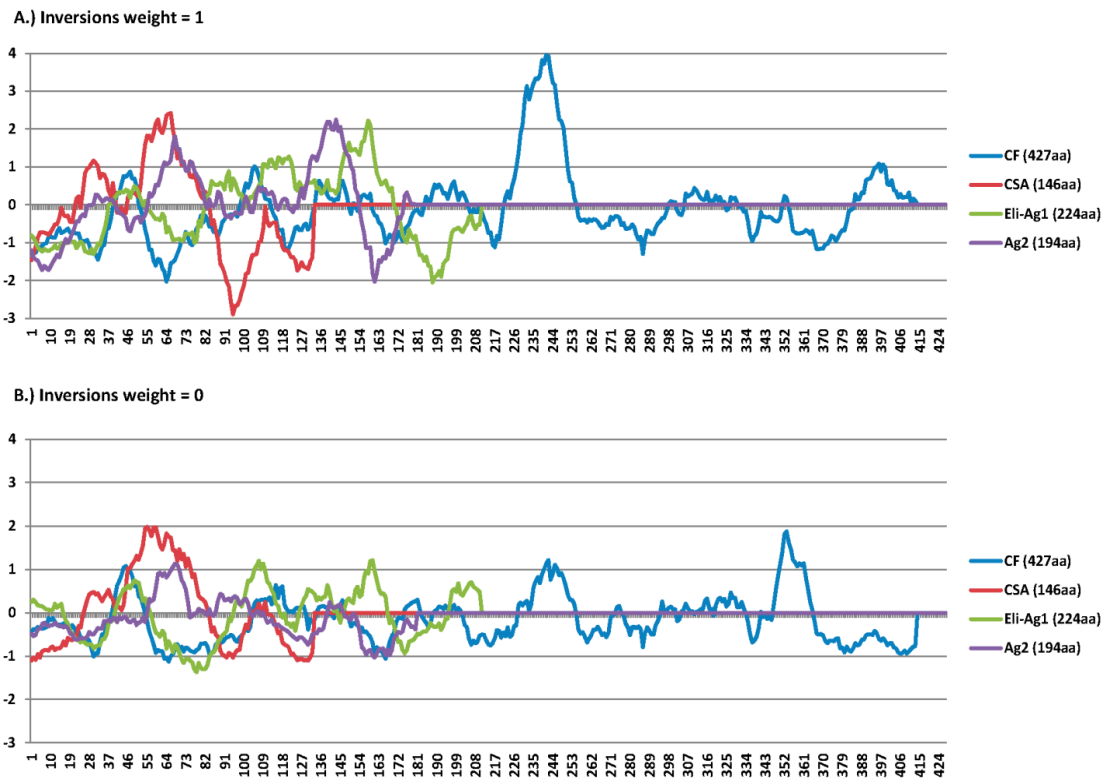


Figure 3- 6 GuiTope analysis comparing 96-random peptide VF predictors with each of the 4 VF proteins tiled for the 83 life-space epitope peptides.

The X-axis shows amino acid position on the protein and Y-axis shows the GuiTope score calculated after library subtraction. Panel A shows the score distribution per amino acid residue when Inversion weight is set to a maximum value of 1 and Panel B shows the detection rate when the di-peptide inversion algorithm is not used to find peptide vs. protein matches for the same dataset (inversion weight=0).

When inspecting the raw signal data averaged per peptide (83 life-space) per CF-titer (Figure 3- 7), as expected, earlier in the infection (CF-titer=0), the IgM antibody response is much higher than the IgG antibody level.

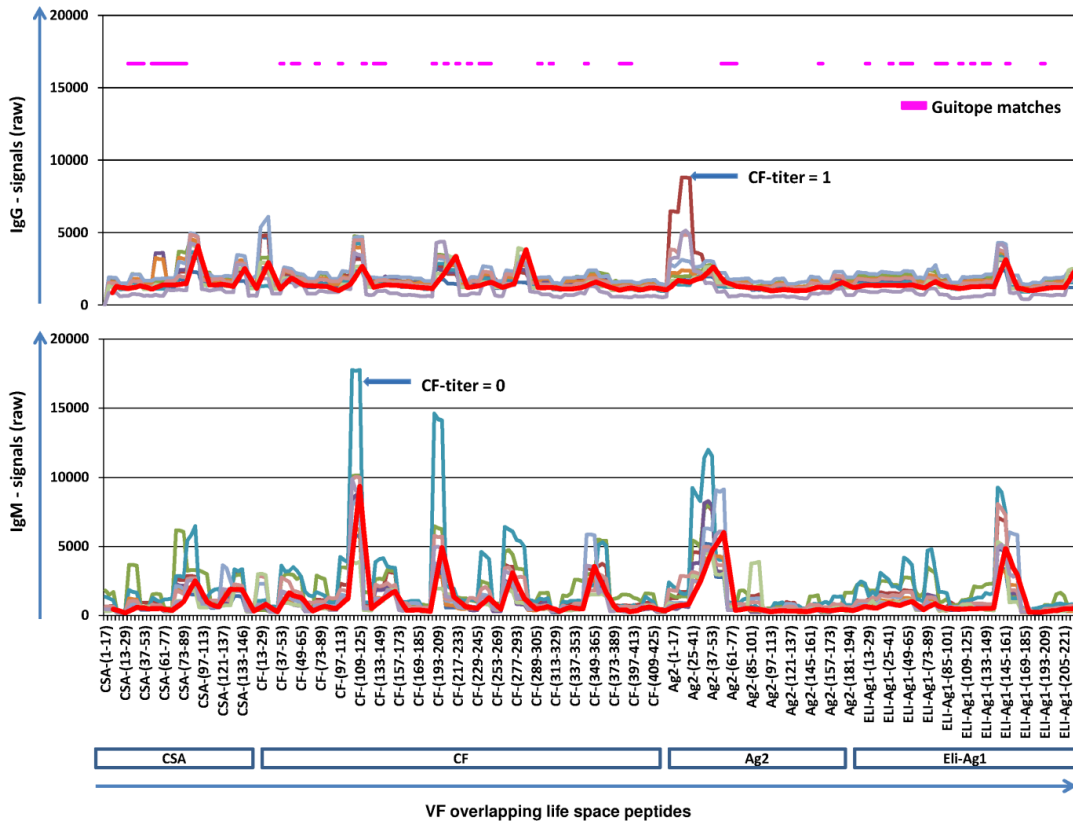


Figure 3- 7 VF predictor random peptides (96) overlapping 83 life-space peptides from Valley fever.

The un-normalized IgG and IgM antibody signals (X-axis) from VF patients as captured by the 83 life-space peptides (Y-axis) are displayed. Patient signals are averaged based on the individual patient's CF-titer (cyan= 0-titer, brown = IDCF-titer 1 etc.) per life-space peptide. The red line is a moving average representing the trend observed in these data. The pink line displays the overall coverage of Guitope matches between 96-random peptides and 4 VF protein antigens.

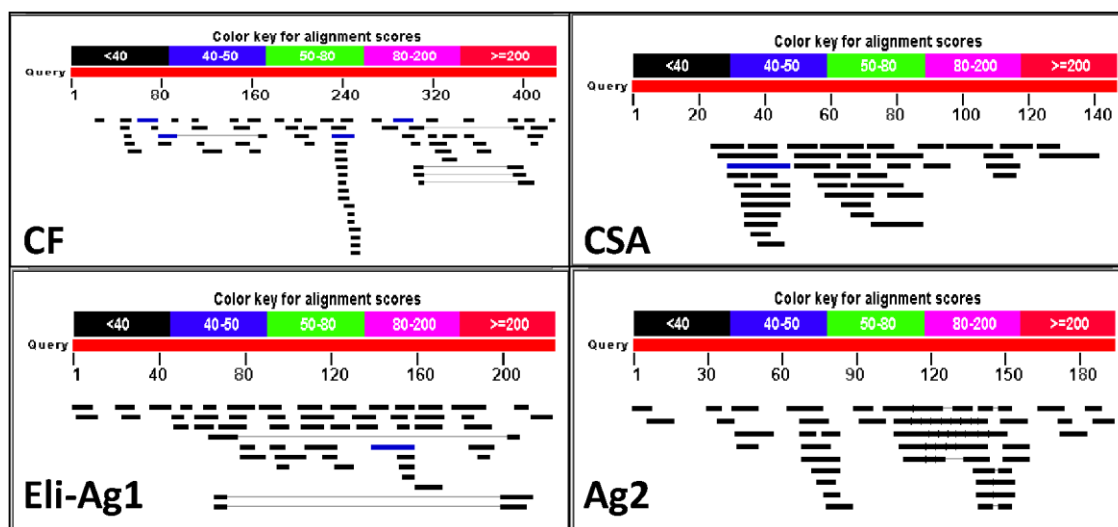


Figure 3- 8 BLAST alignment map depicting VF-protein coverage of 96-random peptides through positive hits from GuiTope.

Figure 3- 8 shows the BLAST alignment map per antigen depicting positive GuiTope hits between 96-random peptides and matching short protein sequences on the 4 VF antigens. Some regions have multiple positive hits with several different peptides within the 96-random VF predictor peptides. These bioinformatics analysis might begin to explain why non-natural sequence peptides are capable of capturing disease specific antibody reactivity.

Discussion

We generated a sub-array for testing the diagnostic performance of 96-random non-natural sequence VF predictor peptides versus 83 life-space epitope peptides from VF. The 96-random peptides selected for this comparison were previously empirically tested to be good predictors for capturing VF specific antibody reactivity [80]. The current comparison is presented to ascertain whether non-natural peptides or life-space

peptides would be most useful in distinguishing infections such as Valley Fever in a microarray diagnostic format. We tested VF patient sera for IgG and IgM antibody against VF. As expected for a chronic infection, we observed higher IgM antibody early in patients that were sero-negative on the gold-standard IDCF assay. We then tested this array's ability to distinguish VF patient sera (including false-negatives; IDCF=0) from normal using 55 sera with various CF-titers from an orthogonally characterized training set and 63 sera from an initially blinded test set. VF patients were distinguished from non-VF individuals using either the 96-random or 83 life-space epitope peptides by Naïve Bayes. The sensitivity of these two groups of peptides was assessed using 0-titer samples and comparing against non-VF sera. The specificity of diagnosing every stage of the infection was assessed by using incremental CF-titer samples suggestive of progression versus non-VF sera. In both comparisons, random peptides performed more accurately compared to life-space epitope peptides. The higher accuracy obtained might be partially attributable to the 96-random peptides having a higher diversity of di-peptides as compared to 83 life-space peptides. More diversity of di-peptides within random peptides could translate to more combinations of di-peptide antibody contact points presented by random peptides. A comparison of the 96-random VF predictor peptides versus the four life-space VF antigens using GuiTope explains why these 96 non-natural sequence peptides perform with higher accuracy when distinguishing VF. Using di-peptide inversions there are 233 unique short-sequence matches (129 matches without inversions) between the 96 random VF predictor peptides and VF antigens allowing

random peptides to compete for antibodies originally generated against VF epitope peptides.

Cross-reactivity is an inherent problem observed in antigen-antibody assays with VF specific assays not being an exception to this rule [92]. Kuberski *et al.* [93] recommended using the cross-reactivity observed on a *Histoplasma* antigen assay from VF infected individuals samples for VF diagnosis. By comparing a previously un-trained on exposure capable of presenting confounding symptoms, we assessed the specificity and robustness of both non-natural and epitope peptides. Since the random peptides were not originally trained to distinguish between VF and LVS, as expected the specificity dropped from 92% (without LVS group) to 87% (with LVS, Naïve Bayes, holdout, *Table 3- 2 - Part A and B*). This highlights an important problem in the biomarker field whereby during the initial training phase of assay development, if the diagnostic system is not trained *a priori* to rule out similar confounding infections, the sensitivity of the assay might not be easily affected but the specificity will change significantly. Ideally, for testing the specificity of such an assay one would compare clinically confounding infections that cause similar symptoms or are presented by pathogens that operate under similar mechanisms of pathogenicity (e.g. invasive mycoses). Additional appropriate confounding infections for training and feature selection would be Community Acquired Pneumonias (CAP) such as tuberculosis (TB), and invasive mycoses such as *Blastomyces*, *Histoplasma* and *Cryptococcus*.

A CF-Titer of 1:2 or 1:4 suggests a better prognosis, whereas a titer of 1:16 or greater (up to 1:256) is indicative of disseminated disease. Several patient case histories

of zero CF-Titer or a titer not suggestive of dissemination i.e. under 1:16 have been documented to show meningeal dissemination [67]. Approximately 1% of patient samples post-dissemination are false negative on the IDCF assay [94]. While this is not an alarming statistic, it is nevertheless important when the dissemination is meningeal. Early detection is crucial to better prognosis for patients with meningeal VF [95]. The blinded test set also included a CSF sample that was false negative on the CF-titer assay but was accurately diagnosed as being sero-positive for VF on the random peptide sub-array. Thus, the immunosignature technology, due to its higher positive predictive value (PPV), may be able to assess disease progression, especially in cases of meningeal dissemination despite a negative IDCF (confirmatory test) result.

From a survey of 39,500 infected valley fever patient sera Smith *et al.* [96] determined that within the first week, complement fixation antibodies measured by the IDCF assay were detected in approximately 10% of patients and were significantly reduced a month later. This is correlated by the measurably lower amount of antibody captured by the life-space epitope peptides (as measured by average intensity) as compared to random peptides (Figure 3-2, panel A). Pappagianis *et al.* (2011) recently demonstrated *in-vitro* that early treatment with anti-fungal agents like Fluconazole, results in reduced or absent production of the chitinase antigen in Coccidioidal cultures [97]. They thereby correlated early intervention with anti-fungals such as Fluconazole in some patients causing a reduction in IDCF detectable levels of IgG antibodies predominantly to the chitinase antigen. This, in their opinion, results in delaying patient diagnosis and therefore they recommend that primary pulmonary infections not be treated

with the antifungal before being tested and monitored for Valley Fever. A similar trend in the reduction of galactomannan antigenemia in invasive Aspergillosis post anti-fungal intervention with Fluconazole was not mis-construed as being detrimental due to reduced diagnosis on assay [98]. In fact, a decrease in antigenemia correlated with survival and an increase despite anti-fungal intervention correlated with morbidity in infected individuals. These problems in diagnosis are typically observed in single correlates of infection. Technologies such as immunosignatures may surpass limitations posed by such single correlates for diagnosis due to being strengthened by multiple predictors while assessing infection.

The 96 non-natural peptides have a higher number of 5-mer sequence overlap with the VF proteome (686 identical 5-mers in common) as compared to the *F. tularensis* (LVS) proteome (162 identical 5-mers in common). As per Lund *et al.*, 85% of antibody structures characterized in the Protein Data Bank (PDB) database are associated with 5-mers epitope sequences [99]. Figure 3-7 and Figure 3-8 partially explain the 96 non-natural peptides ability to capture VF-specific antibodies through their coverage of 83 VF-epitopes and the 4 immunodominant VF-antigens they represent, respectively. Current methods of diagnosis are quite coarse and rely on single markers such as CF titer. Graybill and colleagues [100] noted that CF titer did not change significantly during treatment, where patient symptoms had greatly improved. With a larger panel of sensors (peptides), a more complete picture of the status of the humoral immune response can be observed, without the risk of relying on the abundance or antibody response to a single antigen. High information-content technologies like Immunosignatures can enable more

subtle modulation of antifungal interventions, relieving the patient of the burden of side effects. This work presents encouraging evidence suggesting that non-natural sequence peptides might serve as more accurate molecular beacons for VF diagnosis than life-space pathogen epitopes.

Acknowledgements

The authors wish to thank Dr. John Galgiani for providing us the well-characterized IDCF tested Valley Fever patient serum set from the Valley Fever Center for Excellence. We thank John Lainson for contact printing of the peptide microarrays used in this work. We would also like to thank Elizabeth Lambert, Mara Gardner, John Lainson and Dr. Bart Legutki for processing patient serum samples on the 10K (v1) random peptide arrays as per stipulated protocol and experimental layout. We are grateful to Dr. Anders Sjöstedt, Umeå University for having kindly contributed the *Fransicella tularensis* (LVS) vaccine recipient samples. We would like to thank Josh Richer for developing a python script that calculates n-mers in common among several .fasta format files.

Grant acknowledgements

This work was partially supported by Startup funds from the Arizona State Technology Research Infrastructure Fund to SAJ. This work was also supported by the Chemical Biological Technologies Directorate contracts HDTRA-11-1-0010 from the Department of Defense Chemical and Biological Defense program through the Defense Threat Reduction Agency (DTRA) to SAJ.

Supplementary Tables:

Supplementary Table 3- 1 Sample characteristics of the training set for Valley fever study.

IDCF	# Samples
0	6
1	4
2	8
4	5
8	3
16	8
32	11
64	5
128	3
256	2

Note: 55 sera from 35 patients within the training dataset. The IDCF titer and number of patients with that titer are shown in columns 1 and 2.

Supplementary Table 3- 2 Sample characteristics of the 67 blinded test sera from 25 patients.

IDCF	# Samples
0	48
1	5
2	7
4	3
8	1
16	2
32	1

Note: These samples were initially blinded by the clinic.

Supplementary Table 3- 3 Individual patient characteristics from the un-blinded test set.

Tube #	Patient #	CF titer	TP titer	Date diff.	False Negative CF results	# Blood draws
1	109	0	0	0	1	1
2	109	2	0	25		2
3	109	0	0	26 CSF	1	CSF
4	116	0	0	0	1	1
5	116	4	0	7		2
7	123	4	0	0		1
8	123	0	0	27	1	2
9	138	0	0	0	1	1
11	138	1	0	44		2
12	162	0	0	0	1	1
14	162	16	1	71		2
15	184	0	0	0	1	1
16	184	2	0	18		2
18	188	0	0	0	1	1
19	188	0	1	24	1	2
20	188	0	0	84	1	3
21	216	0	0	0	1	1
23	216	2	0	12		2
25	232	0	0	84	1	1
26	232	0	0	42	1	2
27	232	0	1	10	1	3
28	236	0	0	0	1	1
30	236	2	0	41		2
31	251	0	0	0	1	1
32	251	0	0	41	1	2
33	251	0	0	90	1	3
35	251	16	0	96		4
36	288	0	0	0	1	1
37	288	1	0	44		2
38	288	0	0	159	1	3
40	290	0	0	0	1	1
41	290	0	1	23	1	2
42	290	0	0	88	1	3
43	363	0	0	0	1	1
44	363	2	0	8		2
45	383	0	0	0	1	1
46	383	0	0	85	1	2
47	383	1	0	14		3

49	391	0	0	0	1	1
50	391	0	1	18	1	2
51	401	0	0	0	1	1
52	401	0	0	30	1	2
54	401	0	1	4		3
55	407	0	0	0	1	1
56	407	32	0	71		2
57	412	0	0	0	1	1
58	412	1	0	49		2
60	412	1	0	94		3
61	413	0	0	0	1	1
62	413	0	1	10	1	2
63	437	0	0	0	1	1
65	437	4	0	45		2
66	437	2	0	80		3
67	437	0	0	98	1	4
68	472	0	0	0	1	1
70	472	2	0	18		2
71	473	0	0	0	1	1
73	473	0	1	7	1	2
74	487	0	0	0	1	1
75	487	0	0	40	1	2
76	487	0	1	49	1	3
77	487	0	1	147	1	4
79	487	0	0	113	1	5
80	503	0	0	0	1	1
81	503	0	0	20	1	2
82	503	0	0	36	1	3
84	503	8	0	113		4

Note: False negative CF-titer results are coded as 1 for each sample tested. The accession numbers of these patients were left out of this table to de-identify them further for this work.

Supplementary Table 3- 4 Summary of GuiTope results with inversion weight =1 from alignment of 96-random peptides to 4 immunodominant antigens of C.immitis

Library subtracted, moving average=15

Match data for score cut 6.56 for protein :
CF-CIMG_02795

***** FORWARD PEPTIDES *****

No.	SEQUENCE	SCORE	ALIGN LENGTH	PRO POS	PEP POS	PRO WINDOW	PEP WINDOW
1	RVMFEGFQ GKGPNYLQ VGSC	6.757	5	14	15	LvqaS	LqvgS
2	MQWHSNY MMKRPYNP ELGSC	6.671	9	23	8	Mpn sy pPE	Mmk rpy nPE
3	QVDWTRWR KPKNEMAW KGSC	6.903	11	45	2	VnWaiygrgh N	VdWtrwrkpk N
4	GFMLFGGN PLEYAWYA HGSC	6.872	9	45	10	vn wA iYgrG	ley Aw YahG
5	RTMNTALW IPLTWALW GSC	7.893	5	47	14	WAiyG	WAlwG
6	LYTSEQMTF YGGRDDEIG SC	8.235	7	49	9	iY Gr ghn	fY Gr dd
7	NRKNKGHA YRDGHNIQL GSC	7.386	8	50	9	YgrGHNpQ	YrdGHNiQ
8	RIIRWSPGQ DAKFQDQN GSC	7.943	12	52	4	RghnpQDI K adq	RwspgQDa K fqd
9	MAIQGMNI YTWFTDRI MGSC	10.485	18	61	2	AdQfthIlyaF anir sg	AiQgmnIytw Ftdrim gs
10	MTRRWKTF PHEIEDRIKG SC	7.065	6	73	14	nir sg	drik gs
11	YDVMLSQP NPVSWMRF PGSC	7.599	17	79	2	eVyLSdtwad tdkhyPG	dVmLSqnp vswmrfPG
12	YFWLDVNY DEWTAVVD	7.804	12	79	5	eVylsdtwAdt D	dVnydewtAv vD

	QGSC						
13	TKRIHKWPQ DAYRIRRG SC	7.76	6	91	5	khYPgD	hkWPqD
14	TMIHMQRV KPRKLTNY VGSC	7.4	4	104	15	NvyG	NyvG
15	MRPRHAMP NIKEYMLSP GSC	9.201	6	109	10	IKqmyL	IKeymL
16	PNPWLEWM HMLLWNNQ DGSC	8.2050 01	13	109	5	ikqMylLkkN Nrn	lewMhmLlw NNqd
17	EFTWMLNK NNEMHRHP PGSC	8.319	7	113	4	ylLkKNN	wmLnKNN
18	WFNERKRA QLYEVGEFT GSC	7.787	17	118	3	NnRnlktLlsi GgwTyS	NeRkraQlye vGefTgS
19	HMRAMNPF KPHTNIGRW GSC	7.5320 01	5	135	6	pnFKt	npFKp
20	ARWKKKSH FHRGKKKM FGSC	8.7289 99	8	142	7	SteegrKK	ShfhrgrKK
21	HRGKKAPD FQVGYLKA DGSC	10.442	15	145	1	egrKKfaDtsl klmK	hrgrKKapDfq vgyLk
22	RKFKKRRH WHFPKFPK WGSC	8.31	13	147	1	RKkfadtslkl mK	RKfkrrhwhf pK
23	FDMLFKDS YIWGMTIMF GSC	7.937	12	157	4	LmKDlGfdG idI	LfKDsyiwG mtI
24	HEGLEGDQ TIYQFMIEY GSC	6.9889 99	10	159	1	kdlGfdgidI	heglegdqtI
25	KGDFGAEW GRWRKWVT KGSC	7.392	4	162	2	GfdG	GdfG
26	VTGTEGQW DGYPLWHL FGSC	7.423	5	169	8	dweYP	wdgYP

27	DQWMTMR VKFRDWWQ LIGSC	7.391	9	181	12	DfVILlkaC	DwVqLigsC
28	YSWDAINW RGKAYPVE TGSC	7.844	11	191	4	eAldaysakhP	dAinwrgkayP
29	KARWNGRN MTAPVYWR NGSC	7.75	7	198	1	akh pNGk	kar wNGr
30	YANRGNGK KVHWLLFY QGSC	8.9990 01	13	198	2	AkhpNGKK flti	AnrgNGKKv hwll
31	MYYFPDTG GQPDGSMW NGSC	7.591	12	207	1	lltiaspaG pqn	myyfpdtgG q pd
32	FNLGWKVQ GKLDMSAP KGSC	8.642	8	208	11	LtiasPaG	LdmsaPkG
33	KQKLPHWY RRLDRPVTV GSC	8.394	12	221	1	KlKLaemdk yLD	KqKLphwyrr LD
34	TRQLAPYFD WHNYSIAIG SC	8.6259 99	13	231	7	ldf Wnlmayd fsg	yfd Whnysiai gs
35	DKFHYYMY MLYGINDKI GSC	10.083	19	232	1	DfwnlmaYdf sGswDKvsg	DkfhwymYm lyGinDKigs
36	EVERGDMN WLTISVNNA GSC	8.4070 01	5	232	6	Df wn L	D mnw L
37	WAEKPKIK NWLGRQKL GGSC	7	11	234	9	wn Lmaydfs GS	nw LgrqklgG S
38	GFNQWFSID NWLHTAQW GSC	8.596	10	234	10	wn Lmaydf sg	nw Lhta qws
39	YKMDWSIA FQIMHFDVS GSC	11.234	11	234	9	wnlMayDfS GS	fqiMhfDvSG S
40	RPPIRLRDV LNDHYEVR GSC	7.092	10	235	10	nlmaYdfsGS	lndhYevrGS
41	RLCKNKTFC	8.001	8	237	12	may dfsGS	fya qweGS

	WGFYAQWE GSC						
42	HGPDWTIHP FPGLWVFD GSC	7.614	7	237	13	may dfsg	lwv fdgs
43	IALFDPTKW PEHHQYFA GSC	7.919	9	237	1	mAy dfsgs W	iAl fd ptkW
44	VYEMWYNT SANIDQDHR GSC	6.8819 99	10	237	4	MaYdfSgsw D	MwYntSani D
45	MFDYSPWW EMYSYGV LPGSC	8.917	11	239	2	y Df SgsWdk vS	fd ySpwWem yS
46	NTAEADWG TESTWSMH RGSC	8.568	9	242	11	Sg sw dkvsg	St ws mhrgs
47	HHRTHRPK DGHVQWM HVGSC	7.391	6	245	14	WdkV sg	WmhV gs
48	IHKTEHWIS TNADDWRA GSC	8.196	6	245	14	w dkvsg	d wrags
49	QDLLDYHLS DFVLFAHM GSC	9.332	11	246	2	DkvsgHmSn vf	DlldyHlS dfv
50	VKGKLSNV PSWFNHFHS GSC	9.226	8	248	1	VsGhmSNV	VkGklSNV
51	LSVISGMHS EWPVLWLF GSC	9.548	8	248	4	vSG hm Snv	iSG mh Sew
52	YSGHRHNV PEIDMRQQF GSC	8.232	8	248	1	vSGHmsNV	ySGHrhNV
53	KYIGEHPVF ESTEYRQGG SC	6.672	5	255	8	VFpST	VFeST
54	MYDAATNF FMDSKGV RKGSC	8.877	8	267	9	FssdKaVk	FmdsKgVr
55	TPTDHIRSA AARHKYLIG	7.499	15	275	4	Dylkagvpan KivlG	DhIrsaarhK yliG

	SC						
56	QKAPNKFE HNVINAHN WGSC	7.8569 99	5	282	3	paNKi	apNKf
57	KLVLQWAV HMRKWNA MDGSC	9.563	18	285	1	KiVLgmply gRafastDG	KiVLqwavh mRkwnamD G
58	MTFHGYMV RGSRGDIID GSC	9.089	11	293	5	ygrafaStdgI	gymvrgSrgdI
59	SLDGVAR WPGGYGEG HGSC	8.418	14	299	1	StDGigtSfn GvgG	SIDGvarSwp GgyG
60	GEDDTMQR SYNWyQTN VGSC	6.584	8	301	4	DgigtSfN	DtmqrSyN
61	YMEAHKTY NKQISRGVS GSC	7.036	5	310	15	vvgGS	gvsGS
62	ISVETQWVP LHDTGWDQ GSC	8.628	11	314	2	SwEngvwdy kD	SvEtqwvplh D
63	YAENGAWD VRVYSSAN QGSC	9.904	8	316	3	ENGvWDyk	ENGaWDvr
64	TNATWHYY SINLMYQAQ GSC	6.6629 99	15	317	2	NgvWdYkd mpqqgaq	NatWhYysinl myqa
65	PKMRDRIQ WTPVFTELQ GSC	8.318	15	322	3	ykDmpQqga qvTELe	mrDriQwtpvf TELq
66	DRQQLEGTL VERFERLW GSC	6.8520 01	14	328	6	qGaqVtelEdi aaS	eGtlVerfErlw gS
67	KKQSAWGL WVAELNYM HGSC	7.268	13	329	7	GaqVtELedi aaS	GlwVaELny mhgS
68	KYSNQKIW ASYDSAPSR GSC	7.739	9	347	4	NkryliSYD	NqkiwaSYD
69	NGKDNV SIDYLHTRLGIG SC	7.956	8	348	3	Krylisyd	Kdnvsidy

70	DTFWQFEK YPEYNMHM DGSC	7.546	12	355	1	DTvkiagKka EY	DTfwqfeKyp EY
71	TEYSLTPEK VEYYAWEG GSC	8.248	13	359	5	iagkKaEYitk nG	ltpeKvEYya weG
72	KSITDRGQK TWWEWRR NGSC	6.934	4	376	11	mW we	wW ew
73	YLSTSMEQE QEQVHGNW GSC	7.346	15	385	4	TgnEslvgtV vnglG	TsmEqeqeqV hgnwG
74	RWFVGS MN GQNPVGTFS GSC	8.828	9	386	8	g neslVGTv	ng qnpVGTf
75	GRWLGE PN VQAGPTFFP GSC	7.641	12	390	3	lvGtv v nglGg T	wlGep nv qaG pT
76	VKPVDFMG RYGQLHNF EGSC	8.166	14	395	4	VnglGgtGkL eqrE	VdfmGryGq LhnfE
77	TLAPWQGL KIWERQVPN GSC	7.757	9	401	6	tG k leqren	qG l kiwer q
78	SYKQYHIGR HIDLESLEG SC	7.2020 01	14	403	6	kleqren e lSyp eS	higrh id leSleg S
79	DSNKNEEN QTDRSQYDS GSC	8.612	15	406	3	q renElsypeS vYDn	nk ne EnqtdrS qYDs
80	IHQFEVTRQ QHEYS PFDG SC	7.888	7	406	8	qrenEIS	rqqhEyS
81	RKGNVPRT ARLFSVEW WGSC	7.753	5	422	2	K ngmP	K gnvP
82	PVENKGR TS THGFILWHG SC	6.841	6	422	4	kn GmpS	nk GrtS

Match data for score cut 6.56 for protein :
CSA-CIMG_01181

***** FORWARD PEPTIDES *****

No.	SEQUENCE	SCORE	ALIGN LENGTH	PRO POS	PEP POS	PRO WINDOW	PEP WINDOW
1	KYIGEHPVFES TEYRQGGSC	7.01 6	5	15	7	vpFtS	pvFeS
2	RWFVGSMMNG QNPVGTFSGS C	7.23 6	5	15	13	VpftS	VgtfS
3	PKMRDRIQWT PVFTELQGSC	7.18 2	4	15	11	vpFT	pvFT
4	VYEMWYNTS ANIDQDHRS C	6.84 9	10	25	8	sttdlsyDth	tsanidqDhr
5	QDLLDYHLSD FVLFAMGSC	7.37 5	18	27	1	tDLsydthyD dpslAlsG	qDLldyhlsDf vlfAhmG
6	NSWNQEYTD HVYHGMFG SC	8.20 9	19	30	2	SydthYdDps lalsgvtcs	SwnqeYtDhv vyhgmfgsc
7	SYKQYHIGRHI DLESLEGSC	7.20 4	6	30	1	SYdthy	SYkqyh
8	ISVETQWVPL HDTGWDQGS C	7.23 7	8	32	12	DThyDdpS	DTgwDqgS
9	ETNRWHRNR QGYLAHSTGS C	8.09 100 1	15	34	6	Hyddpslalsg vtcs	Hrnrgyлахst gsc
10	TNATWHYYSI NLMYQAQGS C	6.96 3	15	34	6	HYddpsLals gvtcs	HYysinLmyq aqgsc
11	YDVMLSQPNP VSWMRFPGSC	6.83 8	11	35	1	YDdpslalsg V	YDvmlsqnp V
12	TRQLAPYFDW HNYSIAIGSC	10.2 67	10	35	10	yddpSlAlsG	whnySiAigs
13	NRKNKGHAY RDGHNIQLGS C	7.15 8	9	36	11	DdpslaLsg	DghniqLgs
14	MYYFPDTGGQ PDGSMWNGS C	6.70 9	8	37	12	DpSlalsg	DgSmwngs
15	YKMDWSIAFQ IMHFDVSGSC	6.94 2	6	37	4	DpSlAl	DwSiAf

16	LSVISGMHSE WPVLWLFSGC	8.89 1	8	39	1	slalSGvt	lsviSGmh
17	RTMNTALWIIP LTWALWFGSC	7.19 4	5	40	15	lalsg	alwgs
18	VQERMHNRT WKRFGGSMG SC	8.32 7	6	43	15	sgvtcs	gsmgsc
19	FDMLFKDSYI WGMTIMFGSC	8.20 500 1	9	48	7	sdgdnGMit	dsyiwGMti
20	EVERGDMNW LTISVNNAGSC	9.78 8	14	50	5	GDngmiTkg yNtAG	GDmnlTisv NnAG
21	GEDDTMQRSY NWYQTNVGS C	6.96 9	11	50	1	GdngmitkgY N	GeddtmqrsY N
22	SKTRSLSHAH QMPASWFGSC	7	11	56	3	TkgyntAgei P	TrslshAhqmP
23	HMRAMNPFKP HTNIGRWGSC	6.57 3	9	57	9	KgyntaGei	KphtniGrw
24	GFNQWFSIDN WLHTAQWGS C	7.61 5	13	58	1	GyNtageIpN ypH	GfNqwfsIdN wlH
25	MFDYSPWWE MYSYGVLPGS C	7.03 1	15	59	4	YntagEipnY phvgG	YspwwEmys YgvlpG
26	RVMFEGFQGK GPNYLQVGSC	9.44 5	10	63	9	GeiPNYphV G	GkgPNYlqV G
27	RKFKKRRHW HFPKFPKWGS C	6.69 6	9	64	10	eiPnyPhvG	hfPkfPkwG
28	MQWHSNYM MKRPYNPELG SC	9.48 9	7	66	12	PnyPhvG	PynPelG
29	RKGNVPRTAR LFSVEWWGSC	10.6 53	16	67	4	NyPhvggaFt VETWnS	NvPrtarlFsV EwWgS
30	DTFWQFEKYP EYNMHMDGS C	7.33	7	67	12	nypHvgG	ynmHmdG
31	GRWLGEPNVQ AGPTFFPGSC	7.32 2	9	69	7	PhVggafTv	PnVqagpTf
32	YSWDAINWR GKAYPVETGS C	8.88 6	8	72	10	GgAftVET	GkAypVET

33	YAENGAWDV RVYSSANQGS C	12.3 19	16	73	5	GAftVetwnS pNcGkC	GAwdVrvys SaNqGsC
34	QKAPNKFEHN VINAHNWGSC	6.58 3	14	75	7	FtvewNspN cGkC	FehnviNahN wGsC
35	IHKTEHWISTN ADDWRAGSC	7.16 8	7	78	5	EtWnSpN	EhWiStN
36	YFWLDVNYD EWTAVVDQG SC	7.32 2	11	78	10	EtwnspncGk C	EwtavvdqGs C
37	TMIHMQRVKP RKLTYVVGSC	8.17 9	8	87	9	KeyKvTyn	KprKlTny
38	HRGKKAPDFQ VGYLKADGSC	6.64 1	8	89	9	ykVtYnak	fqVgYlka
39	NRAKHRHWL FPDKDHNLS C	9.50 7	14	96	6	kti f taiDHsn sg	rhwl f pdkDH nlgs
40	INRHGDWNQH FQIPKHPGSC	7.67 9	9	107	8	NsgFnIaKk	NqhFqIpKh
41	ARWKKKSHF HRGKKKMFGS C	6.95 4	10	108	7	SgFniaKKs M	ShFhrgKKk M
42	MYDAATNFF MDSKGVRKGS C	7.23 7	7	110	7	fniakks	nffmdsk
43	MAIQGMNIYT WFTDRIMGSC	6.73 6	10	112	1	iAksMdvIT	mAiqgMniyT
44	KSITDRGQKT WWEWRRNGS C	7.21 099 9	5	120	3	ITngr	iTdrng
45	LYTSEQMTFY GGRDDEIGSC	7.82	7	123	12	GRaeElG	GRddEiG
46	DRQQLEGTLV ERFERLWGSC	10.1 22	18	124	2	Rae l Grikvt yEevasS	Rqq l eGtlverf Erlwgs

Match data for score cut 6.56 for protein :
Eli-Ag1-CIMG_10032

***** FORWARD PEPTIDES *****

No.	SEQUENCE	SCORE	ALIGN LENGT H	PRO POS	PEP POS	PRO WINDOW	PEP WINDOW
-----	----------	-------	---------------------	------------	------------	---------------	---------------

1	QDLLDYHLS DFVLF AHM GSC	11.818	10	1	6	mHLSgiVfaf	yHLSdFVlfa
2	FDMLFKDS YIWGMTIMF GSC	6.879	10	3	10	lsGivfaFsS	iwGmtimFgS
3	YKKMYFRR WQPTARLS RGSC	7.137	9	21	6	FRlvdPppR	FRrwqPtaR
4	YFWLDVNY DEWTAVVD QGSC	7.189	5	21	2	FrLvd	FwLdv
5	YSGHRHNV PEIDMRQQF GSC	6.567	9	24	11	vDppprgfS	iDmrqqfgS
6	VQERMHNR TWKRFGGS MGSC	6.562	10	37	8	trfpcgGqSM	rtwkrfGgSM
7	PVENKGRTS THGFILWHG SC	7.219	6	47	4	sKsRTS	nKgRTS
8	SKTRSLSHA HQMPASWF GSC	11.149	7	48	1	ksrtSvS	sktrSIS
9	TEYSLTPEK VEYYAWEG GSC	6.562	6	51	1	TsvSLT	TeySLT
10	YKMDWSIA FQIMHFDVS GSC	7.267	11	58	3	lempIAlemg H	mdwsIAfqim H
11	ISQQMVLH MRYAPELL GGSC	6.902	9	58	7	LeMpiAIEm	LhMryApEI
12	MAIQGMNI YTWFTDRI MGSC	7.9699 99	6	62	1	iAlemg	mAiqgm
13	LSVISGMHS EWPVLWLF GSC	9.5919 99	14	64	4	lemgHdqtaV qvLl	isgmHsewpV lwLf
14	HEGLEGDQ TIYQFMIEY GSC	12.15	13	69	7	DQTavQvlla lGS	DQTiyQfmie yGS
15	DKFHYWMY	6.665	13	73	7	vqvLlalgshp	mymLygindk

	MLYGINDKI GSC					GS	iGS
16	HHRTHRPK DGHVQWM HVGSC	8.1079 99	8	74	12	qv llalGS	qv wmhvGS
17	TRQLAPYFD WHNYSIAIG SC	7.772	5	77	15	lAIGS	iAiGS
18	ETNRWHRN RQGYLAHS TGSC	8.791	7	79	13	Lgsh hp GS	Lah st GS
19	VKGKLSNV PSWFNHFHS GSC	6.671	12	79	5	LgshPgs nf ni t	LsnvPsw fn hf h
20	ASNSHHRPP KLHNFYPH GSC	7.209	4	82	16	hp GS	ph GS
21	KARWNGRN MTAPVYWR NGSC	9.49	10	88	8	NiTlvptfRq	NmTapvywR n
22	PKMRDRIQ WTPVFTELQ GSC	7.3809 99	8	92	11	vp tfqvG	pv ftelqG
23	QRSWFSGK EPKFQRIWK GSC	7.645	9	93	10	Pt Fr qvlgG	Pk Fq riwkG
24	RVMFEGFQ GKGPNYLQ VGSC	6.898	7	93	12	PtfrQVG	PnylQVG
25	FNLGWKVQ GKLDMSAP KGSC	7.7529 99	15	95	5	fr qv GlgDfcl PsvS	wk qv GklDm saPkgS
26	WAEKPKIK NWLGRQKL GGSC	8.1849 99	6	96	13	RQ vl gG	RQ kl gG
27	VYEMWYNT SANIDQDHR GSC	6.736	11	106	8	pSvslDeqrlG	tSaniDqdhrG
28	YLSTSMEQE QEQVHGNW GSC	9.074	16	107	3	SvSlde qr lgV kpvG	StSme qe qeq VhgnwG
29	NGKDNVSID YLHTRLGIG	7.101	11	107	7	SvsldeqRLG v	SidylhtRLGi

	SC						
30	NSWNQEYT DHVVYHGM FGSC	7.049	15	109	2	Sldeqrlgvkp vdGM	Swnqeytdhvv yhGM
31	VKPVDFMG RYGQLHNF EGSC	10.087	7	117	1	VKPVDgM	VKPVDfM
32	EVERGDMN WLTISVNNA GSC	11.996	12	121	5	dgMNatlqv VtN	gdMNwltisV nN
33	INRHGDWN QHFQIPKHP GSC	8.169	9	121	5	dgmNatlQv	gdwNqhfQi
34	RTMNTALW IPLTWALW GSC	9.139	9	123	3	MNatlQqvvt	MNtaLwiip
35	MYYFPDTG GQPDGSMW NGSC	10.358	11	131	7	TnGdPnGgl yN	TgGqPdGsm wN
36	NRKNKGHA YRDGHNIQL GSC	7.036	10	133	11	gdpNggLyn C	dghNiqLgSC
37	LYTSEQMTF YGGRDDEIG SC	6.6410 01	9	139	1	LYncadiTF	LYtseqmTF
38	YSWDAINW RGKAYPVE TGSC	7.2769 99	20	140	1	YncadItfsste ytvpsSC	YswdaInwrg kaypvetgSC
39	ISVETQWVP LHDTGWDQ GSC	7.56	8	149	2	StteytVP	SvetqwVP
40	KYIGEHPVF ESTEYRQGG SC	8.7830 01	9	151	12	TEYtvpsSC	TEYrqggSC
41	MRPRHAMP NIKEYMLSP GSC	7.238	6	152	12	EYtvps	EYmlsp
42	RPPIRLRDV LNDHYEVR GSC	7.327	8	152	13	eYtVpsSC	hYeVrgSC
43	KGDFGAEW GRWRKWVT KGSC	7.754	7	153	14	ytvpsSC	wvtkgSC

44	KQKLPHWY RRLDRPVTV GSC	7.34	6	154	15	tvpsSC	vtvgSC
45	RLCKNKTFC WGFYAQWE GSC	7.1720 01	5	159	3	CKNgT	CKNkT
46	RKGNVPRT ARLFSVEW WGSC	12.072	14	160	2	KngtgvTAtp FSgE	KgnvprTArI FSvE
47	LANVLYRE QTRPNATER GSC	6.604	13	160	7	kngTgvtATp fsg	reqTrpnATer gs
48	EFTWMLNK NNEMHRHP PGSC	7.471	13	160	7	kngtgvTatPfs g	nknmemhrhP pgs
49	HGPDWTIHP FPGLWVFD GSC	7.806	11	162	2	GtgvTatPFs G	GpdwTihPFp G
50	YDVMLSQP NPVSWMRF PGSC	7.291	4	169	16	pfsg	fpgs
51	GRWLGEPN VQAGPTFFP GSC	7.291	4	169	16	pfsg	fpgs
52	DSNKNEEN QTDRSQYDS GSC	7.795	16	177	4	rNanesTpng QpqrGn	kNeenqTdrs QydsGs
53	YAENGAWD VRVYSSAN QGSC	7.3279 99	6	182	13	StpNgg	SsaNgg
54	YMEAHKTY NKQISRGVS GSC	11.146	13	183	7	TpNgQpqR GnSGS	TyNkQisRG vSGS
55	RWFVGSMN GQNPVGTFS GSC	9.7984 99	12	185	8	NGQpqrGns gsg	NGQnpvGtfs gs
56	KSITDRGQK TWEWRR NGSC	7.435	5	189	15	qRgnS	rRngS
57	TLAPWQGL KIWERQVPN GSC	6.768	6	189	14	QrgNsg	QvpNgs
58	HMRAMNPF	6.626	5	190	15	rgnsg	grwgs

	KPHTNIGRW GSC						
59	MFDYSPWW EMYSYGV LPGSC	7.046	15	200	3	niaghle tatw GVLg	dyspwwE mysyGV Lp
60	GFNQWFSID NWLHTAQW GSC	9.9959 99	12	200	7	nlaghLe TAt WG	sldnwLh TAq WG
61	NTAEADWG TESTWSMH RGSC	7.695	7	206	9	etaTWg v	tesTWsm
62	GFMLFGGN PLEYAWYA HGSC	7.391	10	214	1	GaivvGG v L	GfmlfGG npl

Match data for score cut 6.56 for protein :
AG2-CIMG_09696

***** FORWARD PEPTIDES *****

No.	SEQUENCE	SCORE	ALIGN LENGT H	PRO POS	PEP POS	PRO WINDOW	PEP WINDOW
1	MQWHSNY MMKRPYNP ELGSC	8.671	8	1	1	MQfshali	MQwhsnym
2	RTMNTALW IPLTWALW GSC	6.791	11	7	9	llaLvaA glaS	iipLtwAl wgs
3	KGDFGAEW GRWRKWVT KGSC	6.622	6	31	4	FvealG	FgaewG
4	HEGLEGDQ TIYQFMIEY GSC	8.102	7	35	3	lgndgcT	glegdqT
5	MAIQGMNI YTWFTDRI MGSC	7.222	11	41	10	TrlTDfk chcs	TwfTDrim gs c
6	INRHGDWN QHFQIPKHP GSC	6.8359 99	16	42	3	RltDfkc Hesk PelPG	RhgDwnq Hf qiPkhPG
7	YKMDWSIA FQIMHFDVS	7.175	9	43	12	ltdfkch cs	mhfDvsg sc

	GSC						
8	EVERGDMN WLTISVNNA GSC	7.333	15	63	1	ve Eacpldaris vs N	ev Ergdmnwl is vN
9	RKGNVPRT ARLFSVEW WGSC	8.4790 01	12	68	6	PldARisvsni v	PrtARlfsve w
10	TPTDHIRSA AARHKYLIG SC	7.951	7	68	2	PI Dari S	PtD hir S
11	QDLLDYHLS DFVLFAHM GSC	7.8309 99	12	69	2	l darisvSniVv	d lldyhlSdfVl
12	YFWLDVNY DEWTAVVD QGSC	8.695	16	69	4	LDarisvsniV VDQcS	LDvnydewta VVDQgS
13	YKKMYFRR WQPTARLS RGSC	6.596	4	71	13	ARiS	ARIS
14	HRGKKAPD FQVGYLKA DGSC	7.04	12	73	9	isVsnivvDq c s	fqVgylkaDg s c
15	TNATWHYY SINLMYQAQ GSC	7.318	8	75	8	v S nivvdQ	y S inlmyQ
16	DTFWQFEK YPEYNMHM DGSC	8.8300 01	8	77	13	NivvDq cs	NmhmDg sc
17	HGPDWTIHP FPGLWVFD GSC	7.701	7	78	14	iVvDq cs	wVfDg sc
18	YDVMLSQP NPVSWMRF PGSC	7.545	11	79	1	v d qcSkagv p	y d vmlSqpn p v
19	YSGHRHNV PEIDMRQQF GSC	6.96	4	88	8	V P ie	V P ei
20	PKMRDRIQ WTPVFTELQ GSC	6.6939 99	8	90	7	IeipPVdT	IqwtPVfT
21	IALFDPTKW PEHHQYFA GSC	7.6719 99	11	92	1	IppvDtTaaP E	IalfDpTkwp E

22	GRWLGEPN VQAGPTFFP GSC	7.902	12	102	6	EPsetAePTa eP	EPnvqAgPTf fP
23	LANVLYRE QTRPNATER GSC	7.252	9	112	8	EpTeep ta E	EqTrp nat E
24	TEYSLTPEK VEYYAWEG GSC	7.158	14	114	1	TEepta pta E ptA	TEysl tp ekvE yyA
25	KYIGEHPVF ESTEYRQGG SC	8.0820 01	13	131	5	he PteEpTav ptG	eh PvfEsTeyr qG
26	ISVETQWVP LHDTGWDQ GSC	6.588	11	134	4	tee ptav ptgt	et qwvpl hd tg
27	KARWNGRN MTAPVYWR NGSC	7.157	9	138	10	TA v ptgtgG	TA p vywrnG
28	MYYFPDTG GQPDGSMW NGSC	6.643	6	140	4	v P tgtG	f P dtgG
29	SLDGVAR WPGGYGEG HGSC	10.264	15	140	5	V p tgtgGG v p t G tGS	Var s w p GG y g e G hGS
30	RWFVGS MN GQNPVGTFS GSC	11.723	15	140	4	V p tgtG g v p t g t g s	V g s m n G q n p v g t f s g
31	VTGTEGQW DGYPLWHL FGSC	7.705	17	143	2	g t g g G v pt G t g s f vt G	t g t e G q w d G y pl w h l f G
32	YSWDAINW RGKAYPVE TGSC	6.97	10	145	10	G g v P t g T G S	G k a y P v e T G S
33	ETNRWHRN RQGYLAHS TGSC	6.922	9	146	11	G g v pt g T G S	G y l a h s T G S
34	MYYFPDTG GQPDGSMW NGSC	6.643	6	148	4	v P tgtG	f P dtgG
35	LYTSEQMTF YGGRDDEIG SC	7.173	11	150	3	T g t g s f vt G R	T s e q m t f y g G R
36	NTAEADWG	7.82	11	150	8	t g t g s f vt g r	g t e s t w s m h r g

	TESTWSMH RGSC						
37	KQKLPHWY RRLDRPVTV GSC	6.976	4	156	15	tvtG	vtvG
38	IHKTEHWIS TNADDWRA GSC	7.934	11	164	9	STpAefpgA GS	STnAddwrA GS
39	YAENGAWD VRVYSSAN QGSC	7.23	6	172	5	agsnVR	gawdVR
40	MTFHGYMV RGSRGDIID GSC	7.785	11	173	5	GsnVRaSvG gI	GymVRgSrG dI
41	YMEAHKTY NKQISRGVS GSC	6.9819 99	5	177	14	RasvG	RgvsG
42	ISQQMVLH MRYAPELL GGSC	6.93	7	183	11	iAaaLLG	yApeLLG
43	KKQSAWGL WVAELNYM HGSC	7.933	9	186	5	AllglaAyL	AwglwvAeL

Supplementary Table 3- 5 Summary of GuiTope results with inversion weight =0 from alignment of 96-random peptides to 4 immunodominant antigens of *C.immitis*

Library subtracted, moving average=15

Match data for score cut 6.56 for protein :

CF-CIMG_02795

***** FORWARD PEPTIDES *****

No.	SEQUENCE	SCORE	ALIGN LENGTH	PRO POS	PEP POS	PRO WINDOW	PEP WINDOW
1	ARWKKKSH FHRGKKKM FGSC	6.67	7	144	10	eeGrKKf	hrGkKKm
2	KARWNGRN MTAPVYWR	7.437	19	363	1	KAeyitkNg mgggmWwe	KArwngrN mtapvyWrn

	NGSC					sS	gS
3	HMRAMNPF KPHTNIGRW GSC	6.584	10	122	8	IKtllsIGgW	fKphtnIGrW
4	KQKLPHWY RRLDRPVTV GSC	8.394	12	221	1	KIKLaemdk yLD	KqKLphwyr rLD
5	KSITDRGQK TWWEWRRN GSC	6.762	3	377	11	WWE	WWE
6	QVDWTRWR KPKNEMAW KGSC	6.903	11	45	2	VnWaiygrg hN	VdWtrwrkp kN
7	NRKNKGHA YRDGHNIQL GSC	7.386	8	50	9	YgrGHNPqQ	YrdGHNiQ
8	HHRTHRPKD GHVQWMHV GSC	6.709	7	52	3	RgHnPqD	RtHrPkD
9	VKGKLSNVP SWFNHFHSG SC	9.226	8	248	1	VsGhmSNV	VkGkISNV
10	MTRRWKTFP HEIEDRIKGS C	6.9	13	137	5	fKTpasteEg RkK	wKTfpheiEd RiK
11	MRPRHAMP NIKEYMLSP GSC	8.294 999	12	201	8	PNgKkflTi aS	PNiKeymLs pgS
12	TPTDHRSAA ARHKYLIGS C	7.499	15	275	4	Dylkagvpan KivlG	DhIrsaaarhK yliG
13	KYSNQKIWA SYDSAPSRG SC	7.739	9	347	4	NkryliSYD	NqkiwaSYD
14	YMEAHKTY NKQISRGVS GSC	6.956	10	276	1	YikAgvpaN K	YmeAhktyN K
15	HRGKKAPDF QVGYLKAD GSC	7.162	4	361	3	GKKA	GKKA
16	RTMNTALWI IPLTWALWG SC	7.893	5	47	14	WAiyG	WAlwG

17	DQWMTMRV KFRDWWQLI GSC	7.391	9	181	12	DfVILkaC	DwVqLigsC
18	KKQSAWGL WVAELNYM HGSC	7.268	13	329	7	GaqVtELedi aaS	GlwVaELny mhgS
19	DKFHYWMY MLYGINDKI GSC	7.278	13	62	1	DqFthilYafa nI	DkFhywmY mlygI
20	QDLLDYHLS DFVLFAHMG SC	7.948	6	180	9	nDFVLI	sDFVLf
21	KLVLQWAV HMRKWNA MDGSC	9.563	18	285	1	KiVLgmply gRafastDG	KIVLqwavh mRkwnamD G
22	YANRGNGK KVHWLLFY QGSC	8.999 001	13	198	2	AkhpNGKK fIti	AnrgNGKK vhwll
23	MYYFPDTGG QPDGSMWN GSC	7.566	10	309	9	GvggGSwe NG	GqpdGSmw NG
24	MFDYSPWW EMYSYGVLP GSC	8.917	11	239	2	yDfSgsWdk vS	fDySpwWe myS
25	HEGLEGDQT IYQFMIEYGS C	6.562	5	12	8	QTlvQ	QTiyQ
26	GEDDTMQRS YNWYQTNV GSC	6.584	8	301	4	DgigtSfN	DtmqrSyN
27	FDMLFKDSY IWGMTIMFG SC	7.937	12	157	4	LmKDlGfdG idI	LfKDsyiwG mtI
28	DTFWQFEKY PEYNMHMD GSC	7.546	12	355	1	DTvkiagKk aEY	DTfwqfeKy pEY
29	PNPWLEWM HMLLWNNQ DGSC	8.205 001	13	109	5	ikqMylLkk NNrn	lewMhmLlw NNqd
30	YAENGAWD VRVYSSANQ GSC	9.904	8	316	3	ENGvWDy k	ENGaWDvr
31	DRQQLEGTL	6.852	14	328	6	qGaqVtelEd	eGtlVerfErl

	VERFERLWG SC	001				iaaS	wgS
32	YKMDWSIAF QIMHFDVSG SC	11.23 4	11	234	9	wnlMayDfS GS	fqiMhfDvS GS
33	LSVISGMHS EWPVLWLF GSC	9.047	12	18	2	SsmSsMpns yPV	SviSgMhse wPV
34	GFMLFGGNP LEYAWYAH GSC	6.872	9	45	10	vnwAiYgrG	leyAwYahG
35	SLDGVARSW PGGYGEGHG SC	8.418	14	299	1	StDGigtSfn GvgG	SIDGvarSw pGgyG
36	KYIGEHPVF ESTEYRQGG SC	6.672	5	255	8	VFpST	VFeST
37	YDVMLSQPN PVSWMRFPG SC	7.599	17	79	2	eVyLSdtwa dtdkhyPG	dVmLSqnpn vswmrPG
38	SYKQYHIGR HIDLESLEGS C	6.564	13	2	4	rflIGalltLqt L	qyhIGrhidLe sL
39	YSWDAINW RGKAYPVET GSC	7.599 999	11	352	1	iSyDtvkiaG K	ySwDainwr GK
40	WFNERKRA QLYEVGEFT GSC	7.787	17	118	3	NnRnlktLlsi GgwTyS	NeRkraqLye vGefTgS
41	VKPVD FMG RYGQLHNFE GSC	8.166	14	395	4	VnglGgtGk LeqrE	VdfmGryGq LhnfE
42	NGKDNVSID YLHTRLGIG SC	7.931	8	122	11	LkTILsIG	LhTrLgIG
43	YSGHRHNVP EIDMRQQFG SC	8.232	8	248	1	vSGHmsNV	ySGHrhNV
44	EFTWMLNK NNEMHRHPP GSC	8.319	7	113	4	ylLkKNN	wmLnKNN
45	RVMFEGFQG KGPNYLQVG	6.755	10	359	7	iaGKkaeYit	fqGKgpnYl q

	SC						
46	RWFGSMN GQNPVGTFS GSC	7.354	4	241	16	FSGS	FSGS
47	PKMRDRIQW TPVFTELQG SC	8.318	15	322	3	ykDmpQqga qvTELe	mrDriQwtpv fTELq
48	ISVETQWVP LHDTGWDQ GSC	7.241	13	152	4	dTslklmkDl GfD	eTqwvplhDt GwD
49	TEYSLTPEK VEYYAWEG GSC	8.248	13	359	5	iagkKaEYit knG	ltpeKvEYya weG
50	TRQLAPYFD WHNYSIAIG SC	6.944	7	230	7	YIDfwNI	YfDwhNy
51	VYEMWYNT SANIDQDHR GSC	6.881 999	10	237	4	MaYdfSgsw D	MwYntSani D

Match data for score cut 6.56 for protein :
CSA-CIMG_01181

***** FORWARD PEPTIDES *****

No	SEQUENCE	SCORE	ALIGN LENGT H	PRO POS	PEP POS	PRO WINDOW	PEP WINDOW
1	RKFKKRRHW HFPKFPKWG SC	6.696	9	64	10	eiPnyPhvG	hfPkfPkwG
2	ARWKKKSHF HRGKKKMFG SC	6.954	10	108	7	SgFniaKKs M	ShFhrgKKk M
3	RKGNVPRTA RLFSVEWWG SC	10.65 3	16	67	4	NyPhvggaFt VEtWnS	NvPrtarlFsV EwWgS
4	SKTRSLSHAH QMPASWFGS C	7	11	56	3	TkgyntAgei P	TrslshAhqm P
5	RTMNTALWII PLTWALWGS C	7.192	10	11	6	AavfvPfTsA	AlwiiPITwA

6	QKAPNKFEH NVINAHNWG SC	6.583	14	75	7	FtvewNspN cGkC	FehnviNahN wGsC
7	MYDAATNFF MDSKGVKRG SC	6.77	8	93	2	YnAkTiFl	YdAaTnFf
8	IHKTEHWIST NADDWRAGS C	7.168	7	78	5	EtWnSpN	EhWiStN
9	EVERGDMN WLTISVNNA GSC	9.788	14	50	5	GDngmiTkg yNtAG	GDmnwlTis vNnAG
10	MGDYSPWWE MYSYGVLP SC	7.031	15	59	4	YntagEipnY phvgG	YspwwEmy sYgvlpG
11	LYTSEQMTF YGGRDDEIGS C	7.82	7	123	12	GRaeElG	GRddEiG
12	GEDDTMQRS YNWYQTNV GSC	6.969	11	50	1	Gdngmitkg YN	GeddtmqsY N
13	YAENGAWD VRVYSSANQ GSC	12.31 9	16	73	5	GAftVetwn SpNcGkC	GAwdVrvys SaNqGsC
14	GFNQWFSIDN WLHTAQWGS C	7.615	13	58	1	GyNtagelpN ypH	GfNqwfslD NwlH
15	NSWNQEYTD HVYHGMFG SC	6.918	8	30	2	SydhYdD	SwnqeYtD
16	YKMDWSIAF QIMHFDVSGS C	6.942	6	37	4	DpSlAl	DwSiAf
17	MAIQGMNIY TWFTDRIMG SC	6.736	10	112	1	iAkksMdvIT	mAiqgMniy T
18	YSWDAINWR GKAYPVETG SC	8.886	8	72	10	GgAftVET	GkAypVET
19	MQWHSNYM MKRPYNPEL GSC	8.238	10	52	6	NgMitkgYN t	NyMmkrpY Np
20	RVMFEGFQG	9.445	10	63	9	GeiPNYphV	GkgPNYlqV

	KGPNYLQVGS SC					G	G
21	INRHGDWNQ HFQIPKHPGS C	7.679	9	107	8	NsgFnIaKk	NqhFqIpKh
22	ISVETQWVPL HDTGWDQGS C	7.237	8	32	12	DThyDdpS	DTgwDqgS
23	TRQLAPYFD WHNYSIAIGS C	6.68	8	35	10	yddpSIaI	whnySiAi

Match data for score cut 6.56 for protein :
Eli-Ag1-CIMG_10032

***** FORWARD PEPTIDES *****

No	SEQUENCE	SCORE	ALIGN LENGTH	PRO POS	PEP POS	PRO WINDOW	PEP WINDOW
1	KARWNGRN MTAPVYWRN GSC	7.759	10	161	5	NGTgvTAtpf	NGrnmTApvy
2	RKGNVPRTA RLFSVEWWG SC	7.586	14	160	2	KngtgvTAtp FSgE	KgnvprTArI FSvE
3	KSITDRGQKT WWEWRRNG SC	6.694	4	54	2	SITD	SiTD
4	KGDFGAEWG RWRKWVTK GSC	6.640 999	13	208	6	AtWGvlgai VvgG	AeWGrwrk wVtkG
5	SKTRSLSHAH QMPASWFGS C	8.974	6	15	5	SLStAH	SLShAH
6	YMEAHKTYN KQISRGVSGS C	11.14 6	13	183	7	TpNgQpqR GnSGS	TyNkQisRG vSGS
7	RLCKNKTFC WGFYAQWE GSC	7.172 001	5	159	3	CKNgT	CKNkT
8	PVENKGRST HGFILWHGSC	7.219	6	47	4	sKsRTS	nKgRTS

9	RTMNTALWII PLTWALWGS C	8.551	17	198	2	TsNiAghleta TWgvlG	TmNtAlwiip ITWalwG
10	DKFHYWMY MLYGINDKIG SC	6.665	13	73	7	vqvLlalgshp GS	mymLygind kiGS
11	QDLLDYHLS DFVLF AHMG SC	8.154	8	1	6	mHLSgiVf	yHLSdfVl
12	YLSTSMEQE QEQVHGNW GSC	7.191	6	190	14	rGNsGS	hGNwGS
13	EVERGDMN WLTISVNNA GSC	7.045	16	97	1	qVglGDfclp svSlde	eVerGDmn wltiSvnn
14	WAEKPKIKN WLGRQKLG SC	6.622	7	110	11	LdeQrLG	LgrQkLG
15	YKKMYFRR WQPTARLSR GSC	7.137	9	21	6	FRlvdPppR	FRrwqPtaR
16	MYYFPDTGG QPDGSMWNG SC	10.35 8	11	131	7	TnGdPnGgl yN	TgGqPdGs mwN
17	MFDYSPWWE MYSYGVLP SC	7.046	15	200	3	niaghEtatw GVLg	dyspwwEmy syGVLp
18	LYTSEQMTF YGGRDDEIGS C	6.641 001	9	139	1	LYncadiTF	LYtseqmTF
19	HEGLEGDQTI YQFMIEYGSC	12.15	13	69	7	DQTavQvll alGS	DQTiyQfmi eyGS
20	FDMLFKDSYI WGMTIMFGS C	6.879	10	3	10	lsGivfaFsS	iwGmtimFg S
21	NTAEADWGT ESTWSMHRG SC	6.794 999	15	143	5	ADitfsSTtey tvpS	ADwgteST wsmhrGS
22	HGPDWTIHPF PGLWVFDGS C	7.806	11	162	2	GtgvTatPFs G	GpdwTihPF pG
23	GFNQWFSIDN WLHTAQWGS	9.995 999	12	200	7	nIaghLeTAt WG	sIdnwLhTA qWG

	C						
24	NSWNQEYTD HVYHGMFG SC	6.658	7	148	2	SsttEYT	SwnqEYT
25	YKMDWSIAF QIMHFDVSGS C	7.267	11	58	3	lempIAlemg H	mdwsIAfqi mH
26	LSVISGMHSE WPVLWLFGS C	7.292	7	75	13	VllalGS	VLwlfGS
27	GFMLFGGNP LEYAWYAHG SC	7.391	10	214	1	GaivvGGva L	GfmlfGGnp L
28	KYIGEHPVFE STEYRQGGSC	8.783 001	9	151	12	TEYtvpsSC	TEYrqggSC
29	VKPVDfMGR YQQLHNFEG SC	10.08 7	7	117	1	VKPVDgM	VKPVDfM
30	NGKDNVSID YLHTRLGIGS C	7.101	11	107	7	SvsldeqRLG v	SidylhtRLGi
31	ISQQMVLHM RYAPELLGGS C	6.902	9	58	7	LeMpiAlEm	LhMryApEl
32	TLAPWQGLKI WERQVPNGS C	6.643	15	119	4	PvdGmnatlq vVtNG	PwqGlkiwer qVpNG
33	RVMFEGFQG KGPNYLQVG SC	6.898	7	93	12	PtfrQVG	PnylQVG
34	RPPIRLRDVL NDHYEVRGS C	7.327	8	152	13	eYtVpsSC	hYeVrgSC
35	INRHGDWNQ HFQIPKHPGS C	8.047	9	77	11	lalgsHPGS	fqipkHPGS
36	ISVETQWVPL HDTGWDQGS C	6.771	13	14	1	ISlsTahfrLv Dp	ISveTqwvp LhDt
37	TEYSLTPEKV EYYAWEGGS C	6.562	6	51	1	TsvSLT	TeySLT
38	TRQLAPYFD	7.772	5	77	15	lAlGS	iAiGS

	WHNYSIAIGS C						
39	VYEMWYNTS ANIDQDHRG SC	6.736	11	106	8	pSvslDeqrl G	tSaniDqdhr G

Match data for score cut 6.56 for protein :
AG2-CIMG_09696

***** FORWARD PEPTIDES *****

No	SEQ	SCORE	ALIGN LENGT H	PRO POS	PEP POS	PRO WINDOW	PEP WINDOW
1	ETNRWHRNR QGYLAHSTG SC	6.922	9	146	11	GgvptgTGS	GylahsTGS
2	RTMNTALWII PLTWALWGS C	6.791	11	7	9	llaLvaAglaS	iIpLtwAlwg S
3	KKQSAWGL WVAELNYM HGSC	7.236 001	9	12	5	AaGLasAqL	AwGLwvAe L
4	IHKTEHWIST NADDWRAGS C	7.934	11	164	9	STpAefpgA GS	STnAddwrA GS
5	QDLLDYHLS DFVLF AHMG SC	6.597	6	69	4	LDariS	LDyhlS
6	EVERGDMN WLTISVNNA GSC	7.257	5	73	12	ISVsN	ISVnN
7	YKKMYFRR WQPTARLSR GSC	6.596	4	71	13	ARiS	ARIS
8	SLDGVARSW PGGYGEGHG SC	10.26 4	15	140	5	VptgtgGGv ptGtGS	VarswpGGy geGhGS
9	IALFDPTKWP EHHQYFAGS C	7.671 999	11	92	1	IppvDtTaaP E	IalfDpTkwp P E
10	GRWLGEPNV QAGPTFFPGS	7.902	12	102	6	EPsetAePTa eP	EPnvqAgPT ffP

	C						
11	YSWDAINWR GKAYPVETG SC	6.97	10	145	10	GggvPtgTG S	GkayPveTG S
12	MTFHGYMVR GSRGDIIDGS C	7.785	11	173	5	GsnVRaSv GgI	GymVRgSr GdI
13	ISQQMVLHM RYAPELLGGS C	6.93	7	183	11	iAaaLLG	yApeLLG
14	INRHGDWNQ HFQIPKHPGS C	6.835 999	16	42	3	RltDfkcHcs kPelPG	RhgDwnqHf qiPkhPG
15	PKMRDRIQW TPVFTELQGS C	6.693 999	8	90	7	IeipPVdT	IqwtPVfT
16	YFWLDVNYD EWTAVVDQG SC	8.695	16	69	4	LDarisvsniV VDQcS	LDvnydewta VVDQgS

CHAPTER 4

MULTI PATHOGEN PEPTIDE BASED SEROLOGICAL DIAGNOSTIC

Abstract

Pathogen detection is vital for successful detection of sudden outbreaks with diffuse symptoms. It is important to detect pathogens with high specificity. While DNA detection conforms to the requirement of high specificity, sufficient pathogen must remain in the patient to ensure positive signals. Host-based immunological detection should overcome this limitation, as well as provide information on the hosts' health status, unlike pathogen based PCR. To enable the broadest possible panel of immunological tests that are highly accurate, such that a new outbreak (SARS) or an intentional bio-threat release could be rapidly located, one requires a larger, more complex detection panel, such as one representing all NIAID priority pathogens. While a peptide microarray tiling all possible pathogen proteins may seem like a promising platform for such a detection panel, we tested the concept and found non-obvious problems that appeared, and possible solutions. We developed a pathogen peptide microarray using tiled peptides. Results suggest a profound lack of specificity, but illuminated several possible sources for cross-reactivity. We modified a number of assay conditions to minimize cross-reactivity and provide a comparison study of six different pathogen exposures. We eventually improved our assay from <50% specificity to simultaneous detection accuracy with >90% AUC-ROC on a 4K peptide microarray. The array is composed of peptides from fourteen priority pathogens. The basic platform could be further developed as a surveillance tool or as an epidemiological probe for

monitoring outbreaks, but more importantly, several fundamental biochemical conditions were optimized specifically for multiplexed host-based immune detection.

Keywords

Multiplexed, peptide microarray, multi-pathogen, specificity, peptide cross-reactivity, epitope, diagnostic assay, immunosignature, antibody.

Abbreviations

BLAST, Basic local alignment search tool; Cytomegalovirus, CMV; Epstein Barr virus, EBV; Hepatitis C virus, HCV; HSV1, Herpes simplex virus 1; HSV2, Herpes simplex virus 2; Human Immunodeficiency virus, HIV; ROC-AUC, Receiver operator characteristics – area under the curve; Severe acute respiratory syndrome, SARS; ToRCH, *Toxoplasma gondii*+*Rubella*+CMV+HSV1 & HSV2.

Introduction

Peptide microarray-based diagnostics have been used for diseases such as tuberculosis [3,4], *Echinococcus* spp. [5] and SARS [6,7]. The antibody response mapping strategy as outlined through these research efforts involve testing patient sera relative to normal donor sera. List *et al* [5] diverged from this accepted methodology and tested their *Echinococcus* specific peptide microarray platform against other symptomatically confounding nematode infections. Due to the relatively high cross-reactivity observed in peptide epitope arrays, none of these groups have attempted multiplexing the diagnosis of more than one infection from unrelated pathogens on the

same microarray. The goal of the present project was to test the feasibility of creating a functional multiplexed pathogen proteome peptide epitope array.

Cross-reactivity is a generic feature of any antigen-antibody detection system [101,102]. Polyreactivity is a feature of certain viral infections such as Hepatitis viruses, HIV and Epstein Barr virus (EBV) [103]. Ulrich *et al.* [92] attempted to use *Yersinia pestis* protein microarrays to distinguish infections of *Y. pestis* as well as seven other species of gram-negative bacteria vs. *Bacillus anthracis*. The authors acknowledged detection of cross-reacting antibodies to *Y. pestis* proteins from these unrelated pathogen exposures but rather than see this as a lack of specificity, instead used it as a fingerprint for detecting those unrelated infections. They attributed this cross-reactivity to sequence-level similarities between different unrelated bacterial proteins.

Following the success of creating multiplexed ToRCH [104] protein assays that use crude whole pathogen protein extracts from five vertically transmitted pathogens, namely, *Toxoplasma gondii*, Rubella, Cytomegalovirus and Herpes simplex virus 1 and 2, Andresen *et al.* [36] created a peptide microarray containing 900 peptides for distinguishing Hepatitis C virus, EBV, Cytomegalovirus (CMV), Herpes simplex virus 1 (HSV1) and HSV2. Individual patients infected with CMV and EBV showed reactivity to their cognate peptides but the authors noted broad cross-reactivity from HSV1 and HSV2 infected patients making it impossible to serologically discriminate between these viruses using antibody-binding data from multiplexed peptide arrays. From this work we expected to observe inconsistent patterns of antibody binding per patient and infection on our multiplexed array.

Similarly confounding results were obtained by List *et al.* [5], when they attempted to discriminate between *Echinococcus* species: *multilocularis* and *granulosus* using 45 peptides from 6 proteins of the pathogens. One of the best performing peptides out of 45 selected had 94% specificity and 57% sensitivity at detecting Echinococcosis apart from other nematode infections, but was ineffective at differentiating between the two species. Maeurer *et al.* [3] on their 7446 peptide microarray representing 61 *Mycobacterium tuberculosis* proteins found positive antibody reactivities from TB negative (Quantiferon assay negative) individuals' sera. Whether this could be interpreted as cross-reactivity attributable to non-pathogenic *Mycobacterium* species or to autoimmunity is speculative in the absence of immune histories from these patients. Auto-immunity has been documented to be a side effect from several common infections such as measles, mumps and chicken pox [103]. Chow *et al.* [6] attempted to circumvent this issue by selecting 27 peptides that were restricted to the SARS-CoV (Severe Acute Respiratory Syndrome-Coronavirus) but without any portion of other Coronaviruses or human or mouse proteomes. This array was only tested against SARS infected versus uninfected patients, not against serum from other closely related Coronaviruses but it implied that informatics should be used to filter peptide selection.

In our study we developed a multiplexed pathogen peptide array representing 14 priority pathogens such that either the complete proteomes of small viruses or a few immunodominant antigens for large bacteria and viruses were tiled contiguously. Surprisingly there was a pronounced lack of specificity in initial assays. In order to reduce cross-reactivity, we subsequently optimized physical assay conditions to capture

specific reactivity from infected sera and reduce signals from non-targets. First, we examined the effect of the surface density of the peptides by changing the spacing of the linker that attaches peptide to the glass slide. Next, we examined detecting antibody concentrations, then the temperature of incubation and finally we tested a number of competitors for the primary sera incubation step. The literature for antigen-antibody thermodynamics [105] and protein and peptide microarray optimization [3,5,6,8,36], suggests that incubating serum samples longer (as in an ELISA) might allow the system to approach equilibrium and better discriminate antibody affinities. The patient serum samples we used to train this system are characterized using alternative immunoassays (ELISA or immunodiffusion) representing exposures to *Coccidioides spp.* (Valley Fever-VF), *Fransicella tularensis* - attenuated live vaccine strain (LVS), Vaccinia (small pox), African Swine Fever Virus (ASFV, a non-human pathogen), *Plasmodium* (Malaria) and West Nile Virus (WNV).

Methods

Serum samples and rationale for choosing pathogens to be represented

Human patient serum samples from five Vaccinia vaccine recipients and five non-disease individuals were collected under the ASU IRB 0905004024, “Blood Collection for Immunological Studies”. *Fransicella tularensis subsp. holarctica* live vaccine strain (LVS) vaccinated individuals’ sera from 11 individuals were received from Dr. Anders Sjöstedt’s laboratory at Umeå University, Sweden under the same IRB approval. Samples used were 28-30 days post-vaccination. VF infected patient sera was received

from Dr. John Galgiani at the University of Arizona (IRB# FWA00004218, 122 samples). Two *Plasmodium* and 6 WNV infected sera was obtained from SeraCare Life Sciences (Milford, MA). Four ASFV infected porcine sera with 2 uninfected control pig sera were obtained from Dr. Linda Dixon at The Pirbright Institute, UK under the USDA import license # 111099 by Dr. Kathryn Sykes. The choice of pathogens to be represented on the assay was based on serum sample availability for testing NIAID Category A, B and C priority pathogens [38]. The majority of pathogens chosen were small encephalitis viruses along with other priority pathogens with larger proteomes. Table 4- 1 displays the distribution of peptides per pathogen on the pathogen proteome peptide (PPP) array.

Table 4- 1 Peptide selection strategy for PPP array

Type of Pathogen	Pathogen Name (NIAID Priority Pathogens list category)	Number of Proteins in Proteome	Proteins Selected	Number of Peptides	% Coverage (Proteome)
Viruses	Japanese encephalitis virus (B)	13	all	203	100%
	Equine encephalitis virus (B)	2	all	223	100%
	Venezuelan encephalitis virus (B)	2	all	215	100%
	Machupo Virus (A)	4	all	181	100%
	Junin Virus (A)	4	all	199	100%
	Guanarito Virus (A)	4	all	204	100%
	Lassa Virus (A)	4	all	205	100%
	West Nile Virus I	13 + 13	all	194 + 120	100%

	+ II (B)				
	African Swine Fever Virus (USDA Veterinary services select agent)	188	12 [106- 108]	299	6.38%
	Vaccinia Virus – Western Reserve (A)	223	32 [109- 111]	567	14.34%
Bacteria	<i>Francisella</i> <i>tularensis</i> SCHU <i>S4</i> (A)	1604	45 [112,113]	862	2.80%
	<i>Bacillus anthracis</i> (A)	5715	1 [114-116]	44	0.05%
Protist	<i>Plasmodium vivax</i> (Infections observed in deployed populations)	5051	17 [117]	708	0.31%
Fungi	<i>Coccidioides</i> <i>immitis</i> (C)	10454	4 [81- 83,118,119]	83	0.03%

Three approaches were considered for selecting the epitopes to be represented on the array. The first approach utilized the Immune Epitope Database's (IEDB) collection of empirically mapped epitopes that yielded 4,124 total B-cell epitopes representing the 14 priority pathogens. The distribution of these epitopes was severely skewed for some pathogens. The second approach relied on utilizing information from the six [120-123], B-cell linear epitope prediction algorithms provided through IEDB. Each one of these algorithms gives weight to a certain characteristic of the peptide sequence, e.g. the Chou & Fasman Beta turn prediction algorithm, predicts whether a portion of the protein could have a trans-membrane domain due to presence of beta-turns in their structure. The Bepipred algorithm includes propensity scaling of the amino acids based on their

probability of occurring in an antigenic site in addition to a Hidden Markov model (HMM) approach to systematically identifying cryptic sites. This resulted in ~24,000 peptide epitopes predicted from the 11 out of 14 pathogen proteomes under consideration. A summary of both these approaches is depicted in Table 4- 2.

Table 4- 2 Predicted & Empirical epitopes (IEDB-Bepipred) [Accessed on: 30th

November, 2011]

Organism	# Predicted Epitopes (Bepipred)	# Epitopes in IEDB database	Total proteins in Proteome
<i>Bacillus anthracis</i>	18486	3174	5289
<i>Francisella tularensis</i> (SchuS4)	4365	797	1604
ASFV	723	128	128
Junin virus	98	4	4
Machupo virus	96	4	4
Guanarito virus	98	4	4
Lassa fever virus	86	4	4
West Nile virus I & II	137	2	10 + 10
JEV	70	1	10
VEE	136	3	2
EEE	137	3	2
Total	24432	4124	7071

The third approach involved tiling the whole proteome of the pathogen into contiguous 17-mers. This is easily achievable for several of the encephalitis viruses having smaller proteomes, containing at most 2-10 proteins in their proteome. Bacteria and fungi have much larger proteomes and would result in more 17-mer peptides than the physical limit allowed on this platform. As summarized in Table 4-3 the 14 pathogen proteomes under consideration have 12,744 total proteins and would amount in 344,316

contiguous 17-mer peptides. Our current piezo printed array can accommodate only 20,000 peptides per slide.

Table 4- 3 Number of peptides per priority pathogen proteome

Organism	Total proteins in Proteome	Amino acids total	# of contiguous non-overlapping 17-mers
<i>Bacillus anthracis</i>	5289	1460522	85913
<i>Francisella tularensis</i> (SchuS4)	1604	497951	29291
Vaccinia virus	223	57833	3402
<i>Plasmodium vivax</i> (Sal-I)	5390	3748088	220476
ASFV (Georgia 2007/1)	188	55884	3287
Junin virus	4	3353	197
Machupo virus	4	3363	198
Guanarito virus	4	3332	196
Lassa fever virus	4	3377	199
West Nile virus I & II	10 + 10	WNV-I: 3433 + WNV-II: 3430	202 + 202
JEV	10	3432	202
VEE	2	3748	221
EEE	2	5612	330
Total	12744	5853358	344316

We therefore chose to represent complete viral proteomes for small viruses and partial proteomes for larger pathogens representing tiled empirically classified immunodominant proteins (Table 4- 1). We hypothesized that including only immunodominant antigens would be sufficient to help distinguish that infection from others on the array. The peptides were filtered so as not to include any duplicate 16 or 17-mers. Any duplication in a sequence between amino acid lengths 5 through 15 was

noted so as to map possible binding events observed due to short peptide sequence identity (Table 4- 4). The n-mer level overlap observed when using natural sequence epitopes is much higher than that observed by chance in a randomly generated peptide library containing the same number of peptides and in comparison to two separate randomly generated, non-natural sequence 10K Immunosignature peptide libraries (Table 4- 4). The peptides were then printed onto glass slides and all assay conditions such as time and temperature of serum sample incubation, slide surface, blocking buffer were systematically optimized to reduce cross-reactivity.

Table 4- 4 Duplicate 5-mers – 16-mers within the 4337 peptides from the PPP array and 10K non-natural sequence peptide Immunosignature array

n-mer size	# n-mers observed more than once in pathogen peptides	#n-mer observed more than once in random sequence peptides	10K(v2)	10K(v1)
16-mer	211	2	2	0
15-mer	345	5	16	0
14-mer	522	8	141	0
13-mer	763	13	378	5
12-mer	1061	19	635	12
11-mer	1435	27	908	32
10-mer	1903	37	1123	45
9-mer	2482	62	1389	61
8-mer	3467	358	1659	114
7-mer	4673	694	2167	584
6-mer	6737	1819	5143	3912
5-mer	9171	3143	9530	8309

Microarray production and processing

An N-terminal CRH (cysteine-arginine-histidine) linker sequence was added to the 17mer pathogen peptides. A total of 4337 peptides were purchased from Sigma Genosys (St. Louis, MO). Array printing was performed at AMI (Applied Microarrays, Tempe, AZ) using non-contact piezo printing. Slides were either Schott Nexterion (Gena, Germany) aminosilane-coated slides which provide ~1nm spacing between covalently-attached peptides, or Postech NSB slides (Seoul, Korea). The NSB slides were either NSB-9 (3nm spacing between peptides) or NSB-27 (6nm spacing between peptides). All slide surfaces were coated with sulfo-SMCC linker (Pierce, Rockland, MD) and peptides were conjugated to the surface using maleimide conjugation chemistry at 70% humidity. Identical arrays were printed on the top and bottom half of each slide, and each peptide was printed twice within an array.

Microarray slides were pre-washed with a solution containing 7.33% acetonitrile, 33% isopropanol and 0.55% TFA to remove unbound peptide. Slides were blocked in 1X PBS, 3% BSA, 0.05% Tween 20, 0.014% β -mercaptohexanol for 1hr at 25°C. Sera samples were diluted 1:500 or 1:5000 in Incubation buffer containing 3% BSA, 1X PBS, 0.05% Tween 20, and allowed to bind to the microarray for varying time points including 1 or 16 hour at either 23°C or 37°C in 200 μ l total volume per array. A Tecan 4800 Pro Hybridization Station (Tecan, Salzburg, Austria) was used for array incubation and primary sera was detected using Alexa Fluor-647 conjugated Goat anti-Human, IgG Fc (γ) fragment specific secondary antibody from Jackson ImmunoResearch (West Grove, PA). The slides were scanned using Agilent C scanner (Santa Clara, CA) at 635nm

excitation wavelength with 100% PMT and high laser power at 10 μm image resolution. The 16-bit TIFF images were aligned using GenePix 6.0 software (Axon Instruments, Union City, CA) and the data files imported into GeneSpring 7.3.1 (Agilent, Santa Clara, CA) and Matlab (version R2012a, MathWorks, Natick, MA) for further analysis. Every patient's serum sample was processed in duplicate and since every peptide was printed twice within a sub-array, it gave 4 measurements from the same peptide upon combining both technical replicates. Any sample with a Pearson Correlation Coefficient less than 0.85 across technical replicates was re-processed. Upon meeting the quality criteria, all technical replicates for a given individual patient were averaged for further data analysis.

Data analysis

Median spot signal intensities were imported into Matlab (Natick, MA) for further analysis. Spots flagged as bad based on visual inspection were treated as missing data, and values of replicate spots were averaged. The global median background intensity was subtracted from each slide. The background subtracted median spot signals are referred to as the peptide signals in subsequent analysis. Analysis of patient data used eight statistical metrics for scoring pathogen peptides, average signal, T-test, and Pearson's Correlation were the most predictive. Each pathogen on the array is not represented by equal numbers of peptides. The proportion of peptides per array and per pathogen was noted for each assessment.

Analysis methods:

- 1) Average signal method: the arithmetic mean signal intensity of the peptides belonging to each pathogen is used to generate a rank order, without incorporating standard deviation or number of peptides/pathogen.
- 2) T-test p-value method: the p-value from a one-sided t-test between the signal intensities of the peptides belonging to each pathogen compared to the rest of the peptides on the array, assuming variance is unequal.
- 3) Pearson Correlation method: correlation is calculated between a vector containing the signal intensities for a patient and a binary vector composed of 1's (representing a signal within the cognate pathogen) and 0's (everywhere else).
- 4) Signal – log(P-value) method: The mean signal for each patient's peptides multiplied by the negative of the log₁₀ p-value across the patient vs. all other peptides on the array.
- 5) Signal to noise method: The average peptide signal for each pathogen group is divided by the standard deviation of the peptide signal across those groups.
- 6) Median Signal method: A nonparametric rank based on the median of the signal of peptides within a pathogen. Highest rank is the designated call.
- 7) Mean ranks method: Per sample, peptides are ranked by signal intensity and the mean of the rank is calculated per pathogen.
- 8) Wilcoxon Mann Whitnet Rank sum method: Non-parametric version of T-test across patient peptides and all other peptides on the array.

In the NSB-9 and NSB-27 combined analysis, the geometric mean of the average signal or t-test p-value were used, while the arithmetic mean of the Pearson correlations from each platform were used.

Receiver Operating Characteristics (ROC) curve calculation

Receiver Operating Characteristics (ROC) [124] curves were calculated using the ‘perfcurve’ function in Matlab. A ROC curve is a plot of the True Positive Rate (TPR) against the False Positive Rate (FPR). The area under the ROC curve (AUC) represents the probability that a positive example (in this case the score for the correct pathogen) has a higher score than a negative example (in this case the score for another pathogen).

Results

Physical optimization of pathogen proteome peptide (PPP) array

Basic peptide microarray assay conditions such as the blocking and incubation buffer and the concentration of the secondary antibody were previously optimized for other peptide microarray assays[11]. These were the starting conditions and provided extremely low specificity when testing multiple infectious sera. The temperature and incubation time had been optimized for Immunosignature arrays, so these conditions may not be optimal for the analysis of antibody binding to cognate linear epitopes [105]. The first condition tested was the effect of temperature.

Comparison 1: The effect of temperature on antibody-peptide association

The Aminosilane slide surface was used and temperature of incubating serum sample or monoclonal antibody was varied (23°C vs. 37°C). The primary sera incubation time was held constant at 1 hour with 1:500 serum dilution or 5nM monoclonal antibody concentration processed. Figure 4- 1 represents the average signal intensities of peptides per pathogen group of proteins from Aminosilane slides at the end of one hour incubation. Serum samples from one LVS vaccinee, one VF patient, one Normal donor and monoclonal antibody p53Ab1 were tested. Red bars represent data from slides processed at 37°C and blue bars from slides processed at 23°C. The monoclonal antibody against human P53 protein (p53Ab1) identified its cognate epitope, a peptide containing the 5-mer 'RHSVV' and some other peptides containing the same 5-mer. LVS and VF exposed polyclonal sera had more non-specific binding to other pathogen peptides as compared to cognate pathogen peptides FTT or VF (highlighted with red boxes). The LVS serum is showing higher reactivity to Lassa, Guanarito and Machupo virus peptides as compared to FTT, cognate peptides. The VF infected individual's serum is showing higher reactivity to FTT, Junin and Lassa virus peptides alongwith showing reactivity to VF cognate antigen peptides.

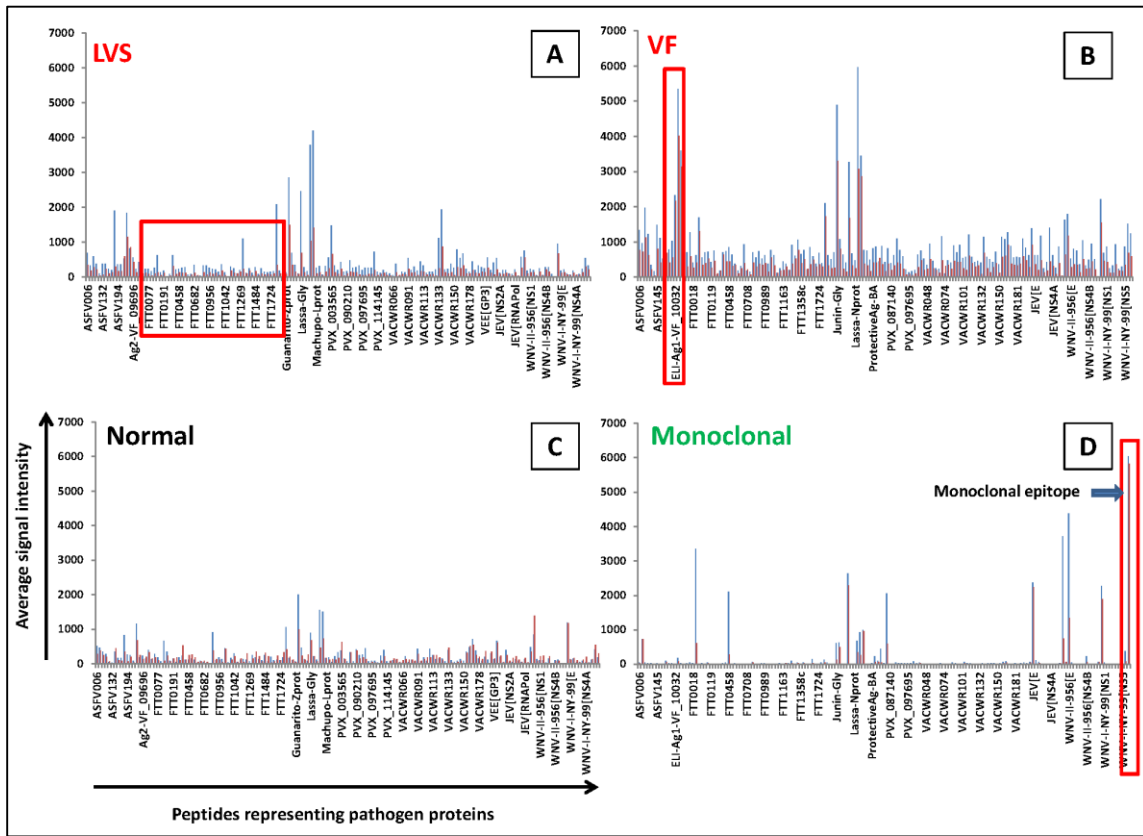


Figure 4- 1 The effect of incubation temperature on various samples tested on the pathogen array.

The average signal intensities for peptides per pathogen proteins are represented using bar graphs with red bars representing signals from slides processed at 37°C and blue bars from slides processed at 23°C. Panel A shows the antibody reactivity from a *F. tularensis* LVS vaccinated individual on the PPP array with FTT peptide (cognate) signals highlighted in the red box. Panel B shows the antibody response from a VF infected individual with a red box highlighting VF specific peptide signals (cognate). Panel C shows the antibody reactivity from a Normal individual's serum sample. Panel D

shows a monoclonal antibody (p53Ab1) binding its epitope peptide containing sequence 'RHSVV' (red box) and few other peptides, containing the epitope sub-sequence.

We observed statistically significant discrimination between cognate and non-cognate peptide groups at 23°C, so further analysis was conducted at this temperature.

Table 4- 5 summarizes the AUC obtained from this analysis.

Table 4- 5 AUC derived from ROC summary of incubating samples on Aminosilane slides at varying temperatures, time of primary antibody incubation is held constant at 1 hour.

Surface: Aminosilane, Primary antibody incubated for 1 hour at 37°C

Infection (No. of patients)	Mean Signal	T-test p-value	Pearson Correlation
Valley fever (1)	0.98	0.98	0.98
LVS (1)	0.13	0.03	0.03
p53Ab1 (1)	1.00	1.00	1.00

Surface: Aminosilane, Primary antibody incubated for 1 hour at 23°C

Infection (No. of patients)	Mean Signal	T-test p-value	Pearson Correlation
Valley fever (1)	0.98	0.98	0.98
LVS (1)	0.25	0.02	0.03
p53Ab1 (1)	1.00	1.00	1.00

In an effort to estimate cross-reactivity, well-characterized monoclonal antibodies (anti-FLAG and anti-p53Ab1) were processed on aminosilane arrays with and without the epitope peptides for the monoclonals being tested. Figure 4-2 shows the signal intensities from binding observed on arrays at the end of 1 hour of primary incubation at 23°C. Even in the absence of the epitope peptide, the monoclonal antibodies bound

pathogen peptides that either naturally contained the partial monoclonal epitope or a mimotope of their cognate site. The monoclonal antibodies show reduced binding to the non-cognate peptides when the epitope peptide was present suggesting higher affinity for the cognate sequence.

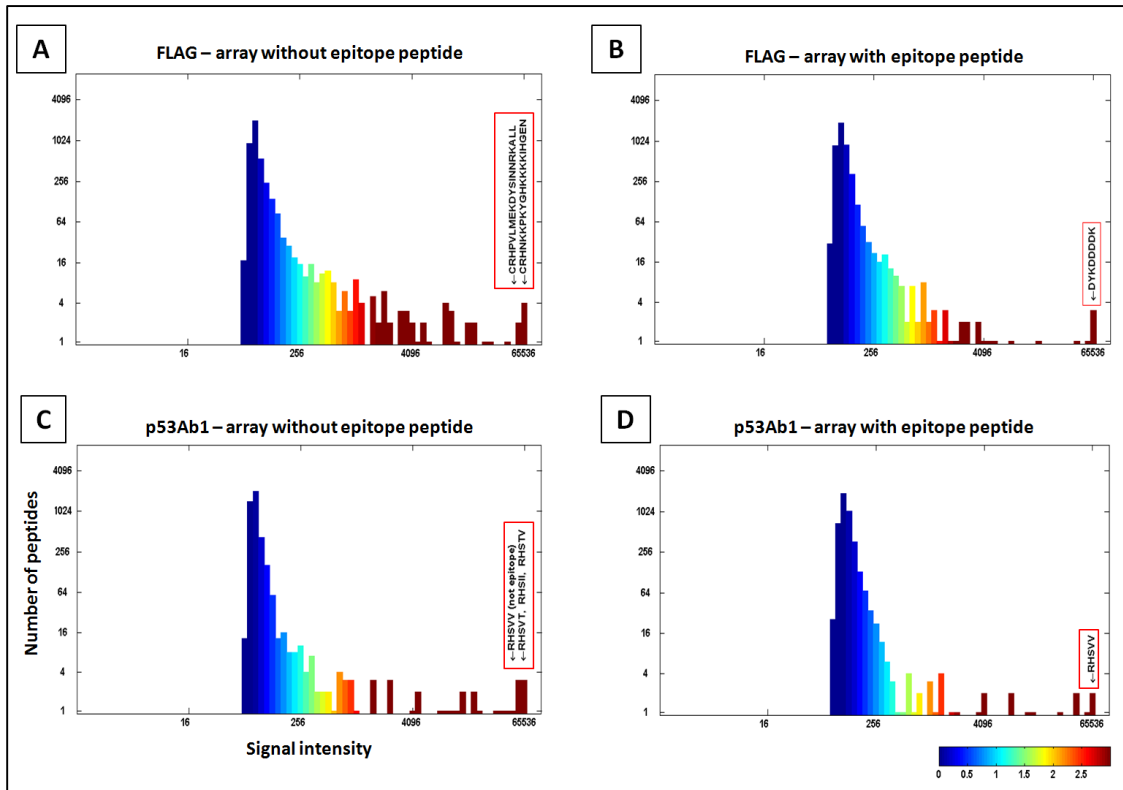


Figure 4-2 Estimating cross-reactivity - Histograms displaying signal intensities from arrays with or without monoclonal antibody epitopes.

The Y-axis shows the number of peptides at a given signal intensity displayed on the X-axis in all four panels. Panels A and B display the binding of the FLAG tag monoclonal antibody on arrays without and with cognate epitope peptides respectively. Panels C and D display the binding of p53Ab1 monoclonal antibody on PPP arrays without and with

cognate epitope peptides respectively. Panels A and C show data from arrays without the monoclonal antibody epitope and panels B and D show data from arrays containing the monoclonal epitope.

Reducing cross-reactivity on array by reducing peptide density on array surface

To reduce non-cognate peptide binding due to high peptide density on the surface, we tested NanoSurface Biosciences [125] NSB-9 and NSB-27 slide surfaces. The primary amine groups on these surfaces are spaced 3nm and 6nm apart, respectively, as compared to aminosilane slides where space between amine groups is approximately 1nm. In order to determine spot morphology on these alternate slide surfaces as compared to Aminosilane, peptides were biotinylated using NHS ester-coupled biotin from Thermo Scientific (Rockford, IL). This approach was designed to be used to semi-quantitatively assess the quality of spotting within various slide print batches of a given Immunosignature array [126]. Free amine groups on the peptides were bound with biotin, and Alexafluor 647-conjugated streptavidin bound only biotinylated sites (Figure 4- 3). The NSB-9 slides show lower dynamic range of signal intensity of peptide compared to aminosilane, due to the higher distance between peptides than AS. The higher distance of primary amine groups on NSB-27 slides contributed to lower dynamic range of signal than both NSB-9 and AS slides. The spot morphology of NSB-27 slides was not optimal and hence for the initial comparison with Aminosilane only NSB-9 slides were used.

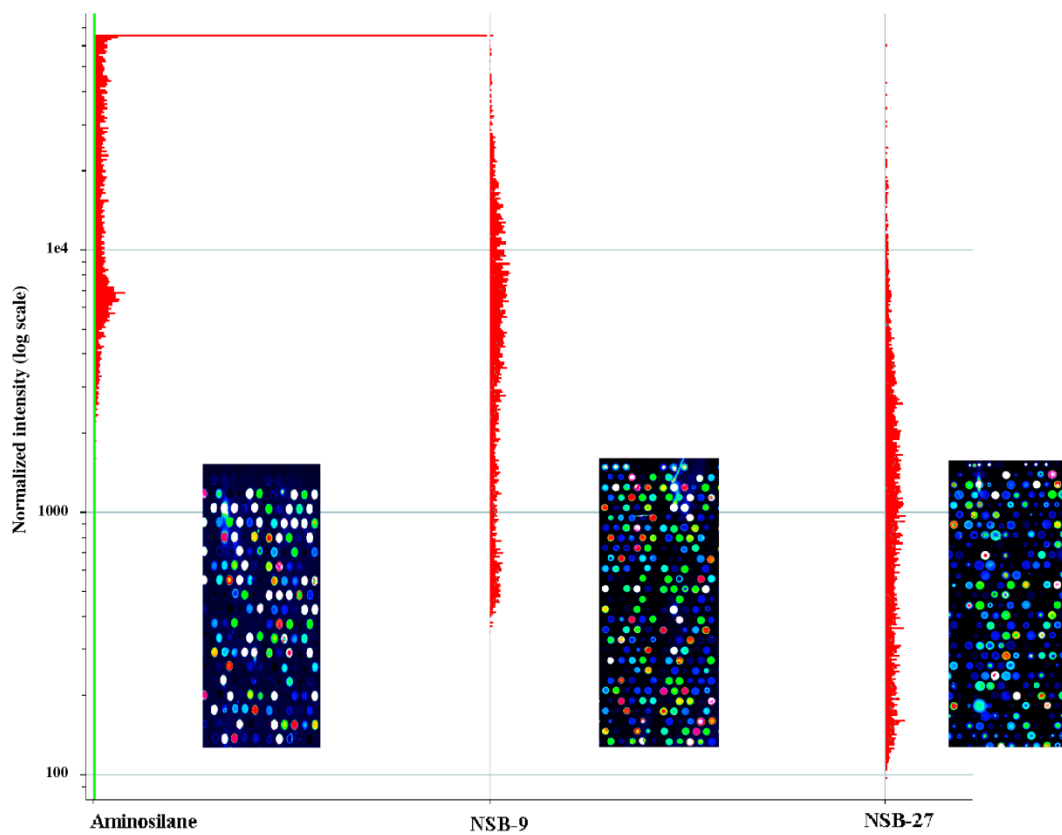


Figure 4- 3 Biotinylation for comparing the spot morphology and dynamic range of signal from three slide surfaces, Aminosilane (AS), NSB-9 and NSB-27.

The histograms display the binding of streptavidin conjugated Alexafluor 647 on the three different slide surfaces. The images inset are screen shots of the three surfaces showing spot morphology.

Six monoclonal antibodies were processed for estimating binding specificity on NSB-9 slides for 1 hour at 23°C: anti-FLAG, anti-V5, anti-cMyc, anti-p53Ab1, anti-p53ab8 and anti-Leu Enkephalin. All antibodies other than anti-Leu-Enkephalin bound their cognate epitopes along with other peptides that partially contained the epitope sub-sequence or mimics of it. (Supplementary Figure 4- 1)

Comparison 2: Slide surface

A comparison was made between Aminosilane vs. NSB-9 slides to decide which slide surface to use for printed PPP arrays to test polyclonal infectious sera. The primary serum incubation time was held constant at 1 hour and 23°C and 1:500 dilution of primary.

The samples processed for the previous comparison were now processed on NSB-9 slide surface. Table 4- 6 summarizes the results from comparing three samples on both Aminosilane and NSB-9 slides. A moderate improvement in ROC-AUC for detecting the LVS sample is observed on NSB-9 slides as compared to Aminosilane. This observation would need to be tested with additional samples for the two infection groups to be confirmed.

Table 4- 6 ROC-AUC for comparing slide surfaces Aminosilane versus NSB-9

Surface: Aminosilane, Primary antibody incubated for 1 hour at 23°C

Infection (No. of patients)	Mean Signal	T-test p-value	Pearson Correlation
Valley fever (1)	0.98	0.98	0.98
LVS (1)	0.19	0.02	0.04
p53Ab1 (1)	1.00	1.00	1.00

Surface: NSB-9, Primary antibody incubated for 1 hour at 23°C

Infection (No. of patients)	Mean Signal	T-test p-value	Pearson Correlation
Valley fever (1)	0.98	0.15	0.96
LVS (1)	0.47	0.13	0.09
p53Ab1 (1)	1.00	0.55	1.00

Note: The normal sample from the previous comparison was excluded when recalculating the ROC-AUC for the previous set of AS slides and while calculating it for NSB-9 slides as a more relevant comparison would be between infectious groups.

In addition to the samples processed to match those used in comparison 1, the anti-FLAG tag antibody was processed under identical conditions for this comparison. Figure 4- 4 summarizes the box-plots from antibody binding distribution as observed on NSB-9 and Aminosilane slides. The top left panel showing anti-FLAG epitope specific monoclonal antibody reactivity show lesser non-cognate peptide reactivity on NSB-9 slides as compared to on AS. The top right panel, showing anti-P53Ab1 antibody binding, displays higher cognate epitope binding observed on NSB-9 slides as compared to on AS. However, both bottom panels showing polyclonal exposure specific response from VF infected and LVS vaccinated individuals' sera does not show significantly higher cognate pathogen peptide binding than that observed on other non-cognate pathogen peptides. The LVS sample processed on NSB-9 slides shows higher median binding of both cognate as well as non-cognate groups of pathogen peptides than that observed on AS slides. The VF sample tested shows moderately higher binding to cognate peptides as compared to non-cognate peptides on AS slides.

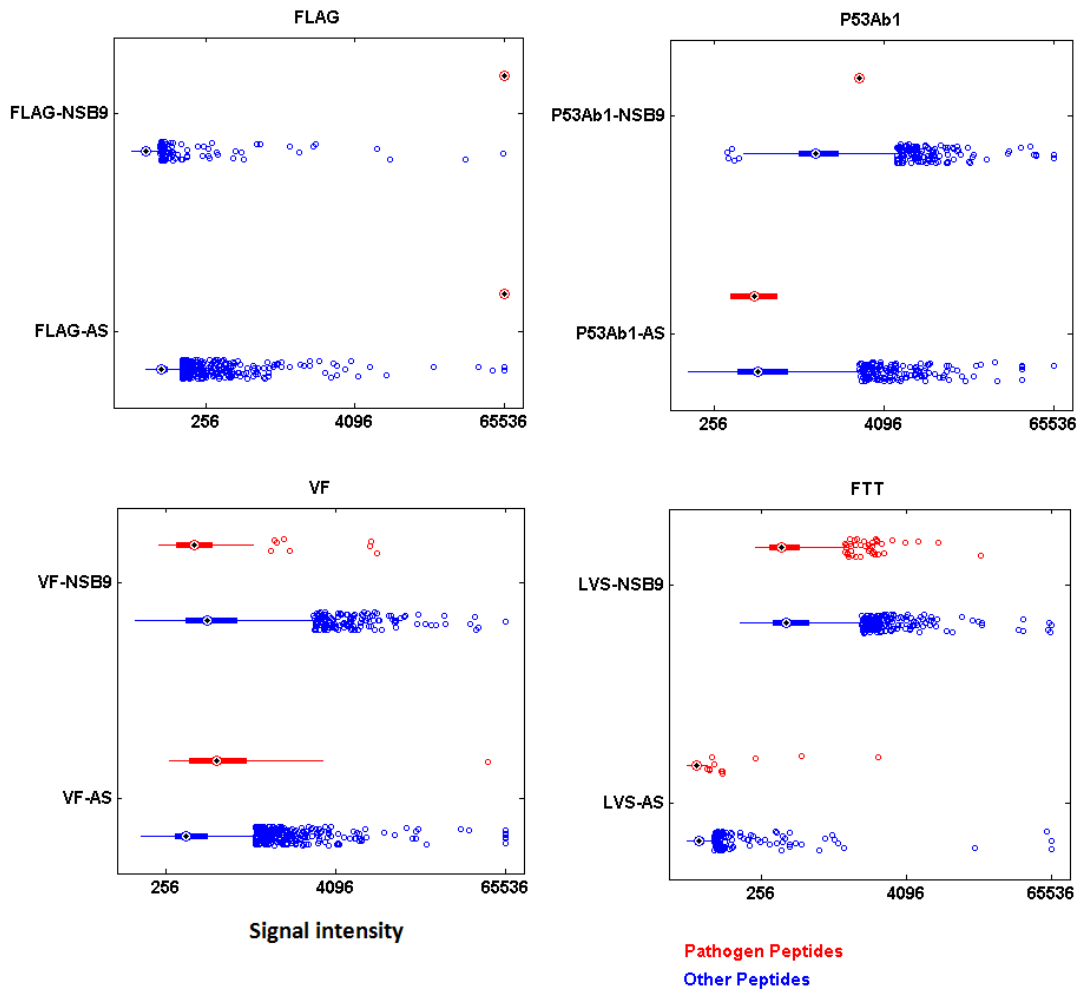


Figure 4- 4 Box-plots showing antibody binding distribution as observed on NSB-9 versus Aminosilane (AS) slides.

The top two panels show the binding observed on the array using two monoclonal antibodies, anti-FLAG tag and anti-P53Ab1. The bottom two panels show the antibody binding distribution to cognate pathogen versus non-cognate peptides for one exposed individual each from VF and *F. Tularensis* (LVS). The antibody binding distribution of peptides is plotted along the X-axis, while the Y-axis is discontinuous and compares

signal intensity data from NSB-9 versus AS for every sample processed. The antibody binding distribution from cognate pathogen peptides or monoclonal antibody epitope peptides are plotted as a separate distribution and highlighted in red next to the antibody binding observed from the remaining peptides on the array (blue dots).

Additional sera from both these infectious groups would need to be processed to evaluate this antagonistic observation per infection. However, given that the monoclonal antibodies show better specificity on NSB-9 slides, they were used for all further comparisons. Figure 4- 5 supplements this observation by showing the exact position of cognate peptides (highlighted in black) within the overall antibody binding distribution observed on AS and NSB-9 slides for the same samples. The LVS sample (top right panel) shows a significant change with higher cognate reactivity distribution on NSB-9 slides as compared to AS.

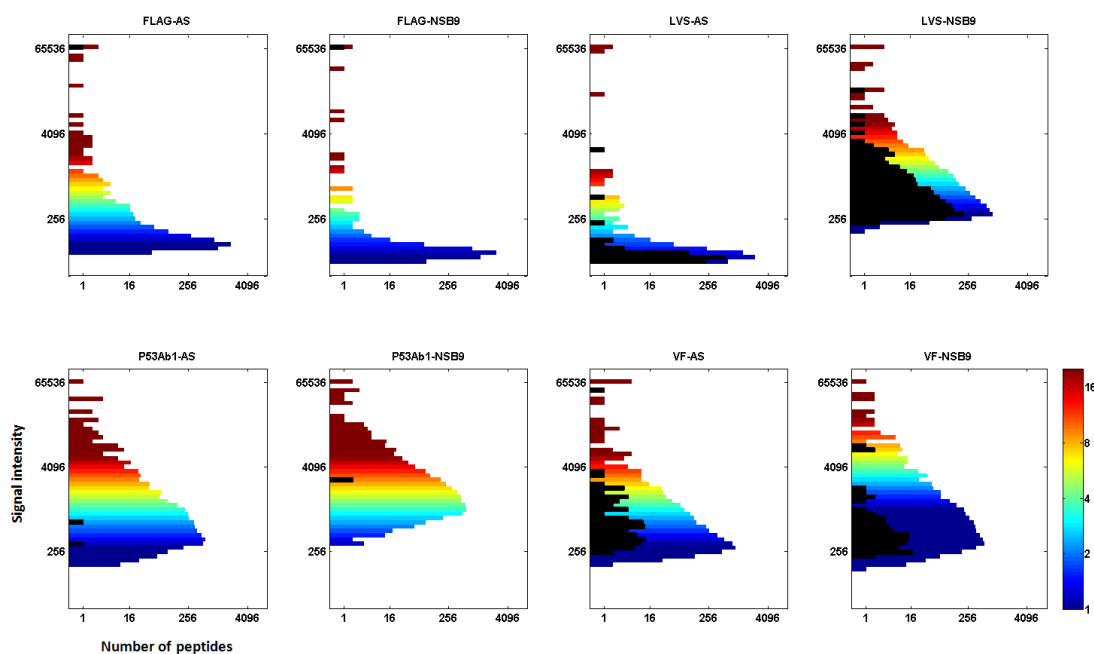


Figure 4- 5 Histograms displaying cognate peptide reactivity on Aminosilane (AS) and NSB-9 slides.

The X axis shows the number of peptides sorted based on signal intensities depicted on the Y-axis. The coloring is based on an arbitrary scale in Matlab. The cognate peptides for two monoclonal antibodies and one sample each of LVS and VF are highlighted in black.

Three VF infected individuals and three *F. tularensis* (LVS) vaccinee sera were used to verify the previous observation of improvement in LVS cognate reactivity on NSB-9 slides. The 37°C comparison is included to ensure the 23°C criterion established previously for AS is also valid for NSB-9 slides. Table 4- 7 summarizes the ROC-AUC of distinguishing VF vs. LVS on NSB9 slides at varying temperatures.

Table 4- 7 ROC-AUC obtained for 2 infections on NSB9 slide surface at varying temperatures

Time of incubation held constant at 1 hour, temperature 23°C vs. 37°C

Surface: NSB9, Primary incubated for 1 hour, 37°C

Infection (No. of patients)	Mean Signal	T-test value	p-	Pearson Correlation
VF(3)	0.90	0.10		0.66
F. tularensis(3)	0.21	0.36		0.24

Surface: NSB9, Primary incubated for 1 hour, 23°C

Infection (No. of patients)	Mean Signal	T-test value	p-	Pearson Correlation
VF(3)	0.85	0.10		0.73
F. tularensis(3)	0.23	0.24		0.25

The NSB-9 (Table 4- 7) slides show moderate improvement in detecting *F.tularensis (LVS)* exposure as compared to aminosilane slides (Table 4-5). Following this methodical analysis, we then tested the effect of incubation time of sera on the PPP array.

Comparison 3: Time of Incubation of sera.

Single antigen ELISA's, show high specificity at capturing appropriate antibody reactivity. Longer times of incubation were tested to mimic ELISA like binding conditions (overnight incubation). Supplementary Figure 4- 2 demonstrates the change in binding over varying incubation times of a monoclonal antibody against TP53 to its cognate epitope peptide on the array. Binding to a number of non-cognate peptides containing the identical 'RHSVV' recognition sequence of this monoclonal or other

mimics such as 'RHSV1' or 'RHSV2' at the end of 1 hour of incubation is higher than that observed at the end of 36 hours. It appears that by 16 hours the monoclonal antibody binding its cognate epitope peptide starts tending towards equilibrium. At 24 and 36 hour time points, the antibody likely degrades as observed through progressively lower signals for one of the two epitope peptides on the array. Additionally, three VF infected and LVS vaccinated patient sera were used as before to compare incubation of the antibody for 1 hour versus 16 hours (factors held constant: slide surface-NSB-9, 23°C, 1:500 serum dilution)

Figure 4-6 displays histograms for one LVS and VF exposed individual each out of the three tested per group, showing data from all peptides on NSB-9 slides colored by an arbitrary scale in Matlab. The cognate pathogen peptides FTT or VF are highlighted in black. Incubating the primary antibody for a longer duration of 16 hours increases the overall binding observed on the assay (cognate and non-cognate). Higher cognate pathogen peptide reactivity is observed at 16 hour serum incubations for all six sera as depicted by data in Table 4-8.

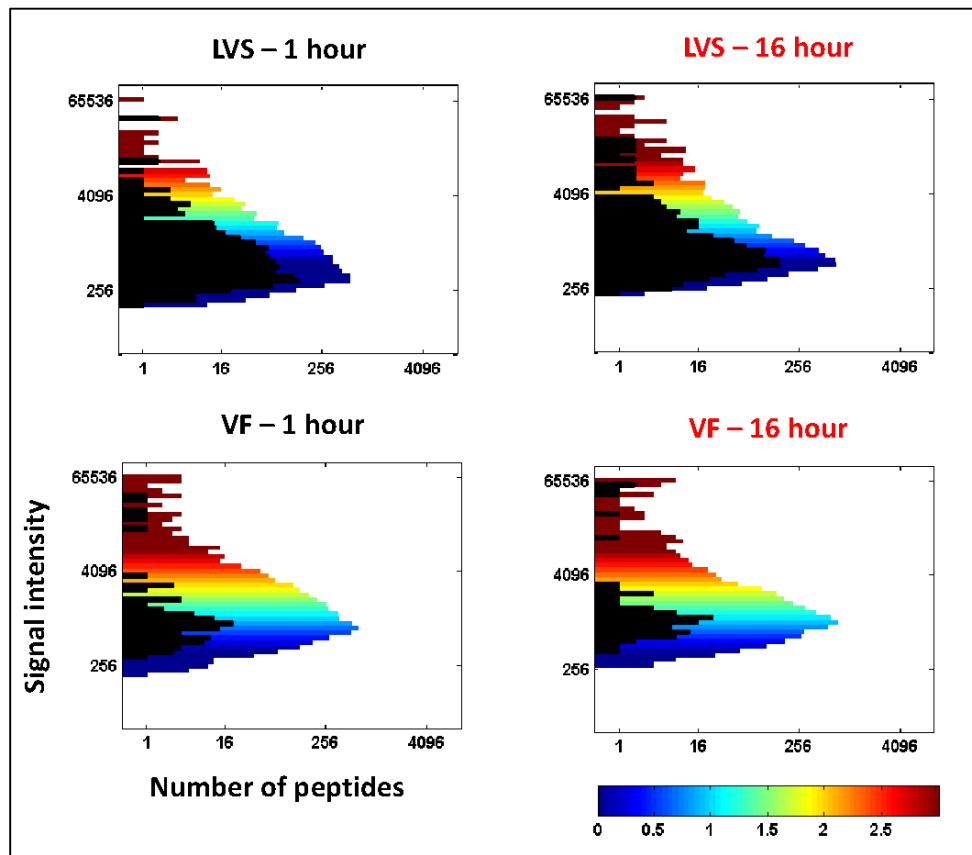


Figure 4-6 Cognate pathogen peptide reactivity is enhanced at 16 hour in comparison to after 1 hour of serum incubation.

Histograms displaying raw signal intensities on the Y-axis and number of peptides on the X-axis sorted based on signal intensity. The top panel displays one LVS and bottom panel displays one VF exposed individuals sera binding the PPP array after 1 hour and 16 hour (red) respectively in paired panels next to each other. The distribution of cognate pathogen peptides (VF or LVS) is highlighted in black.

Table 4- 8 ROC-AUC during varying incubation times on NSB-9 surface

Surface: NSB9, Primary incubated for 1 hour, 23°C (reproduced for comparison from Table 4-4)

Infection (No. of patients)	Mean Signal	T-test p-value	Pearson Correlation
VF (3)	0.85	0.10	0.73
<i>F. tularensis</i> (3)	0.23	0.24	0.25

Surface: NSB9, Primary incubated for 16 hour, 23°C

Infection (No. of patients)	Mean Signal	T-test p-value	Pearson Correlation
VF (3)	0.89	0.16	0.84
<i>F. tularensis</i> (3)	0.28	0.21	0.35

From observing this moderate improvement in cognate peptide binding at 23°C after 16 hours of incubation, we continued to process additional infectious sera on the PPP array under these conditions.

Comparison 4: Spacing of peptides affecting polyclonal antibody capture.

We tested the concentration of deposited peptide on the surface and the effect it had on antigen presentation and the specificity of antibody association on the array. To do this we used NSB-9 and NSB-27 slides along with serum incubation conditions optimized in the previous comparison. The incubation time for infectious sera was held constant at 16 hours, 23°C with 1:500 serum dilution.

Figure 4- 7 summarizes the ROC-AUC of detecting 6 different infections apart on both NSB-9 and NSB-27 slide surfaces at longer incubation times (16 hour) and 23°C.

NSB-9 slides showed greater detection accuracy for VF and Malaria samples as compared to NSB-27. *F tularensis* (LVS) samples however were detected with greater accuracy using NSB-27 slides.

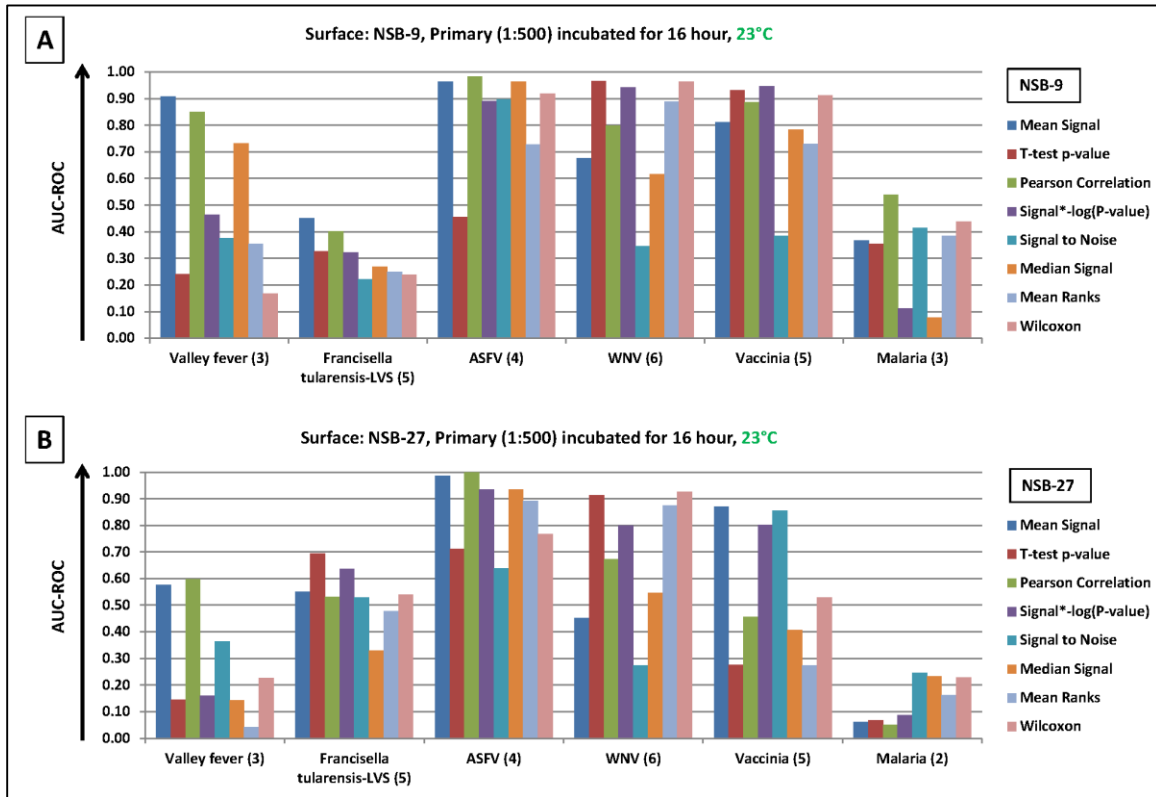


Figure 4- 7 ROC curve AUC summarizing ability to distinguish one infection from another on the PPP array under longer incubation

The NSB-27 slides showed inconsistent spot morphology and poorer replicate correlations due to the interaction between printing conditions (volume and peptide concentration held constant throughout) and the 6nm distant primary amines. We expected this higher distance between individual peptides to improve specificity on the assay. This higher spacing likely affected its reproducibility; therefore, NSB-27 slides

were excluded from further analysis except to test limiting conditions of antigen presentation and antibody dilution in the next comparison. A score combination approach which combined the scores for the eight statistical metrics obtained from NSB-9 (1:500) and NSB-27 (1:500) slides was also tested, but did not yield significantly higher accuracy as depicted in Table 4- 9 as compared to results in Figure 4- 7, panel A. This approach of combining multiple observations is typically utilized when analyzing Surface Plasmon Resonance (SPR) data. The NSB-9 and NSB-27 data were treated as replicates when completing this analysis.

Table 4- 9 ROC-AUC after combining NSB9 and NSB-27 (1:500) data

Infection (No. of patients)	Mean Signal	T-test p-value	Pearson Correlation
Valley fever(3)	0.82	0.14	0.84
Francisella tularensis-LVS (3)	0.38	0.31	0.35
ASFV (4)	0.97	0.60	1.00
WNV (5)	0.51	0.99	0.77
Vaccinia (5)	0.89	0.42	0.85
Malaria (2)	0.05	0.04	0.02

Comparison 5: Dilution of primary patient sera 1:5000 patient serum dilution

In order to test the robustness of this system and estimate physical conditions under which it would fail to detect the appropriate pathogen infection, the assay was processed under limiting conditions of peptide antigen and antibody from infected/exposed sera. Doing this exercise gives us an estimate of likely assay conditions or sample related problems (degradation) to be tested in the event of failure. We used NSB-27 slides to test limiting conditions of antigen presentation for this assay and diluted

the serum 10 fold higher than is recommended for use on piezo-printed peptide glass microarray based Immunosignature platforms [11]. Table 4-10 summarizes the ROC-AUC of distinguishing VF from LVS under these limiting conditions. Processing patient sera under these conditions did not significantly reduce the detection ability of this assay using the pathogen mean signal metric as can be observed from comparing Figure 4- 7, Panel B and Table 4-10. The p-value score and Pearson Correlation scores however were significantly lower as compared to those observed from NSB-27 slides processed at 1:500 serum dilution (Figure 4- 7, Panel B).

Table 4-10 ROC-AUC of detection of 2 infections at limiting concentrations of antigen and antibody

Surface: NSB27, Primary (1:5000) incubated for 16 hour, 23°C

Infection (# patients)	Mean Signal	T-test p-value	Pearson Correlation
VF (3)	0.63	0.13	0.15
F. tularensis(3)	0.51	0.55	0.76

In summary, the information content obtained from such a multiplexed assay is dependent on several thermodynamic parameters and physical assay conditions tested above. Figure 4- 8 demonstrates this concept by displaying the average signal intensities of peptides per pathogen groups of proteins between aminosilane (top panel) and NSB-9 and NSB-27 slides (bottom panel). One VF infected individuals' serum is visualized under different thermodynamic conditions. Kinetic factors being tested here are amount of antigen presented on the surface (AS-dense, NSB9 and NSB27-less dense),

temperature (23°C vs. 37°C) and time of incubation of primary antibody (1 hour vs. 16 hours). Longer incubation times on the NSB9 surface at 23°C (blue bars, panel B) showed highest resolution of cognate VF peptide reactivity (highlighted with red box). The graph shows data for one Valley Fever-infected individual but is representative of the effect of optimizing these parameters for all infections studied in this work.

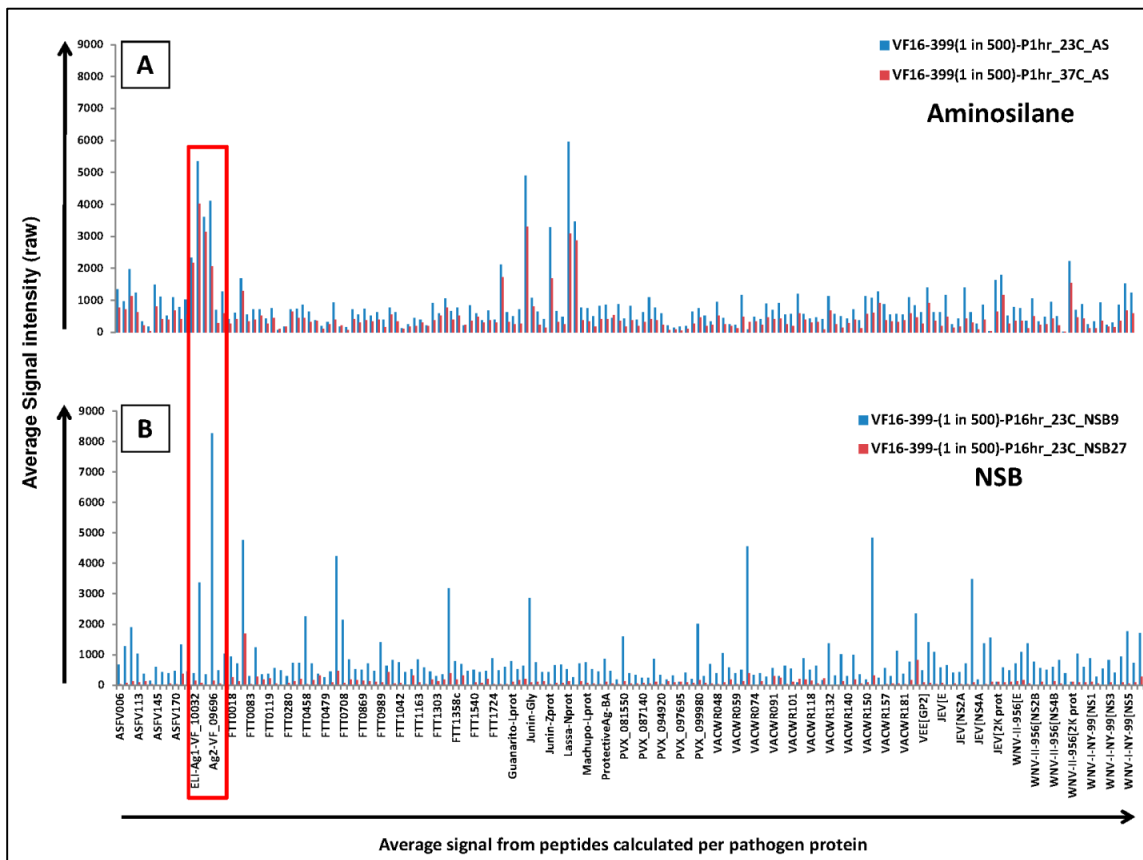


Figure 4- 8 Effect of incubation time, temperature and slide surface on information content of array.

Each bar represents the signal from peptides composing a given pathogen protein. Signal intensities to VF peptides averaged as proteins highlighted using a red box. Panel A

depicts the signal intensities as captured by pathogen peptides on the entire PPP microarray printed on Aminosilane slides. Panel B depicts the signal intensities as captured by pathogen peptides on the entire PPP microarray printed on NSB-9 and NSB-27 slides. Blue bars represent one VF infected individual's serum sample processed on Aminosilane or NSB-9 slide at 23°C. The red bars in Panel A represent this same VF infected individual's serum sample binding PPP peptides at 37°C on Aminosilane slide surface. The red bars in Panel B represent this VF patient's serum binding PPP array printed on NSB-27 slides.

Discussion

We have demonstrated that biochemical parameters associated with peptides spotted onto a glass microarray can be optimized to reduce the cross-reactivity observed in a multiplexed microarray. A peptide array representing epitope peptides from 14 priority pathogens was created and examined for accuracy of simultaneously distinguishing multiple exposures. Three bioinformatic peptide selection strategies were explored but empirical evidence from other research groups [3,6,36] suggested it was ambiguous whether using bioinformatic selection would be beneficial only when testing single pathogen and not as useful when simultaneously detecting multiple pathogen exposures. The hypothesis tested in this work was whether antigens previously shown to be immunoreactive would be sufficient to identify the infection among the pathogens represented on the peptide array. To this effect we represented complete proteomes for smaller viruses and partial proteomes for larger pathogens. The proteins tiled as peptides

for larger pathogens were immunodominant antigens from protein microarray experiments and those listed as B-cell epitopes in IEDB. We used well -characterized monoclonal antibodies and ELISA or immunodiffusion characterized infectious sera to assess cross-reactivity on our multiplexed platform.

Likely parameters that should affect antibody binding such as temperature, peptide spacing, and duration of incubation, were tested and optimized. The selected parameters (23°C, 16 hour incubation, NSB-9 slide surface) were empirically determined based on improvement in the accuracy of simultaneous detection. Additionally, eight statistical analyses were tested for their ability to distinguish infections. The three most predictive analytical methods were average signal from groups of pathogen peptides, p-value across pathogens (groups of peptide) and Pearson's Correlation score (within and across pathogen peptide groups). Four out of the six infections/exposures tested resolved on one of these three statistical metrics with >90% ROC-AUC. While no statistical method worked best for all infections, these four could be detected with greater than 80% ROC-AUC on the Pearson's Correlation score metric. Different infections resolved to a varying extent using the eight metrics tested. VF, *Fransicella* (LVS) and ASFV resolved on the Mean signal pathogen scoring scale while WNV and Vaccinia resolved best on the P-value scale. Malaria did not resolve well on any of the eight metrics tested.

Temperature, longer patient serum incubation times and concentration of antigen presented on the surface had a significant impact on the information content obtained from the assay. Prior work on antigen-antibody interactions using surface plasmon

resonance (SPR) demonstrates a reduction in the association and dissociation rate constants during antibody affinity maturation [127]. A longer incubation time should allow the binding to overcome mass transport limitations and approach equilibrium so that the binding observed better correlates with affinity [128]. The immune response to an infection/exposure has an initial natural antibody component and a latter adaptive (specific to the infection) component [129]. These natural antibodies are poly-reactive and often not high-affinity unlike those generated later in the infection post affinity maturation [103]. Longer incubations result in dissociation from non-cognate peptides and support association of slow on-rate or mass-action limited high affinity antibodies with cognate peptides.

The statistical method by which different infections were detected may rely on the extent of peptide diversity required to accurately capture a given infection in the presence of other pathogen peptides. The P-value scale tends to resolve infections such as WNV, whose complete proteome is represented on the array in the form of 17-mer peptides. The probability of detecting the infection (e.g. WNV) improves with comprehensively mapping the entire proteome. Exposures such as Vaccinia vaccination resolved on the P-value scale suggesting that perhaps a minimum amount of proteome coverage is required (14.3% of Vaccinia proteome represented) for accurate detection. *Francisella tularensis* (LVS) vaccine (2.8% of proteome represented), VF (0.03%) and Malaria (0.31%) did not resolve on the P-value scale. Additional testing using patient samples for pathogen proteomes completely represented on the array would be required to verify this trend.

ASFV and VF resolved on the average signal scale. ASFV is a porcine infection with the potential for infecting humans [40]. The sera tested for ASFV was of swine origin and had overall higher reactivity as compared to human infection/exposure sera. Supplementary Figure 4- 3 displays the average signal intensity observed per individual per infection. VF is a chronic infection and one of the largest pathogen proteomes represented on the assay. The antibody response observed in all patients from VF infection is higher than other human infections or exposures tested on the platform, except one *Vaccinia vaccinee* as observed in Supplementary Figure 4- 3. The Pearson Correlation score for WNV, *Vaccinia*, VF and ASFV is high suggesting more cognate pathogen peptides are responsible for the higher signal intensities on the array, which in turn influences the Pearson's Correlation score.

LVS and Malaria resolved with low accuracy on the average signal scale. The Pearson correlation score was also low for these infections suggesting more cross-reactivity observed to non-cognate peptides on the assay for LVS and Malaria. One possible explanation might be low proteome representation on the array, 2.8% and 0.31% respectively, and also certain peculiarities of these infections. *Francisella* is a gram-negative bacteria and the majority of the host immune response is directed to the lipopolysaccharide (LPS) surrounding this pathogen [130] rather than to specific linear stretches of pathogen proteins. Using a commercial antibody against *Francisella* LPS and one against VEE we observed very little binding on the assay. Supplementary Figure 4- 4 demonstrates this, where only a handful of peptides show high reactivity for anti-LPS antibody or anti-VEE antibody. None of these peptides showing high antibody

binding are cognate peptides belonging to FTT or VEE peptide groups. Peptides belonging to the pathogen being compared are highlighted with arrows on the histogram and are marked in red. Additionally, histograms of polyclonal sera generated by immunizing naïve special pathogen free mice with peptides are also depicted (FT03, Rco1, Rco2, Rco3 and Rco4). Three out of five polyclonal sera recognized the cognate peptides used for immunization accurately with high signal intensity. Two of these immunized peptides were not recognized but other peptides representing partial mimotopes (Supplementary Table 4-1) had higher signal intensities on the array than the cognate peptides demonstrating the possibility of generating cross-reactive antibodies even on immunizing with a 20-amino acid peptide.

Plasmodium infected erythrocytes produce surface antigens to which IgG response is observed in infected individuals [131]. Additionally, pathogen specific antibody (IgG and IgM) may remain bound to circulating antigens [132-135] and the sample used to assess this reactivity on our assay is serum without the infected RBC's. No additional pre-treatment to dissociate circulating immune-complexes from sera were applied in our protocol. It is likely that for infections like malaria, that produce circulating immune complexes, pre-treatment of plasma from blood collected in anti-coagulant tubes and treated with heat to dissociate circulating antigen and RBC bound antibodies might be necessary before separating the plasma for detecting anti-Plasmodium antibodies [136]. From these data, to best ensure capturing cognate pathogen reactivity it would be optimal, to represent the complete pathogen proteome in

the form of peptides. For representing larger pathogens this would mean generating an array containing up to 1 million peptides.

The platform could be optimized to distinguish current versus prior exposure consistently based on measuring a quantitative increase in the immune response captured over time of exposure. From studying the Vaccinia vaccination response on our array, we could predict more recent exposure versus vaccination received 4 years ago. Supplementary Figure 4- 5 demonstrates a proportionate increase in the response captured between current versus prior vaccination recipients. Plots demonstrate the P-value score on X-axis and pathogen ranking based on the score on Y-axis for individual vaccinees. The two most recently vaccinated individuals show higher P-value score than the remaining three vaccinees. This concept needs to be validated with additional samples and tested for consistency in different infections and on different print-batches of arrays.

Additionally, optimizing the platform to distinguish closely related pathogens, such as various strains of Influenza or various Flaviviruses might prove beneficial. The second leading cause of death in the world, 5.7 million deaths/year, are attributed to cerebrovascular disease [137]. Viral meningitis with estimated 434,000 hospitalizations (1988-1999)[138] is known to cause cerebrovascular complications [139]. Viral encephalitic meningitis infections such as those due to most NIAID priority pathogens do not have FDA approved diagnostics available that could readily be used in local laboratories for early detection of exposure. Due to the severity of meningeal symptoms typically a spinal-tap procedure is performed for acquiring cerebrospinal fluid (CSF).

This CSF is then used for PCR-based direct detection of the pathogen. To avoid these invasive procedures we recommend utilizing a pathogen proteome based peptide microarray, which would yield the infecting pathogen using as little as 1 μ l of blood [66]. Given that most encephalitis viral proteomes are small (2-12 proteins in proteome), it would be possible to represent all known encephalitis viruses on a higher density peptide array.

Cross-reactivity on peptide microarray platforms such as the one presented is predominantly linear under the conditions optimized and easy to re-attribute to the original antigen. Natural pathogen proteome specific peptide space is fairly conserved and redundant [140]. The cross-reactivity observed from monoclonal antibody binding can be re-attributed to either the partial epitope or a linear mimotope similar to the cognate epitope. Similar analysis can be attempted on polyclonal patient sera to deconvolute and re-attribute cross-reactivity to the cognate antigen responsible for infection/exposure. Although epitope-based peptide microarrays are of great utility, they also require physical optimization and rigorous bioinformatic analysis to reattribute cross-reactivity. Based on the decreased monoclonal cross-reactivity when the epitope peptide is present on the array, we would expect including proteomes for commonly exposed pathogens might absorb antibodies from prior exposures to them and thus reduce non-cognate binding. Given that complete medical histories and prior exposures for the patients tested are generally unknown, adding more pathogens might help comprehensively map the antibody response for individuals.

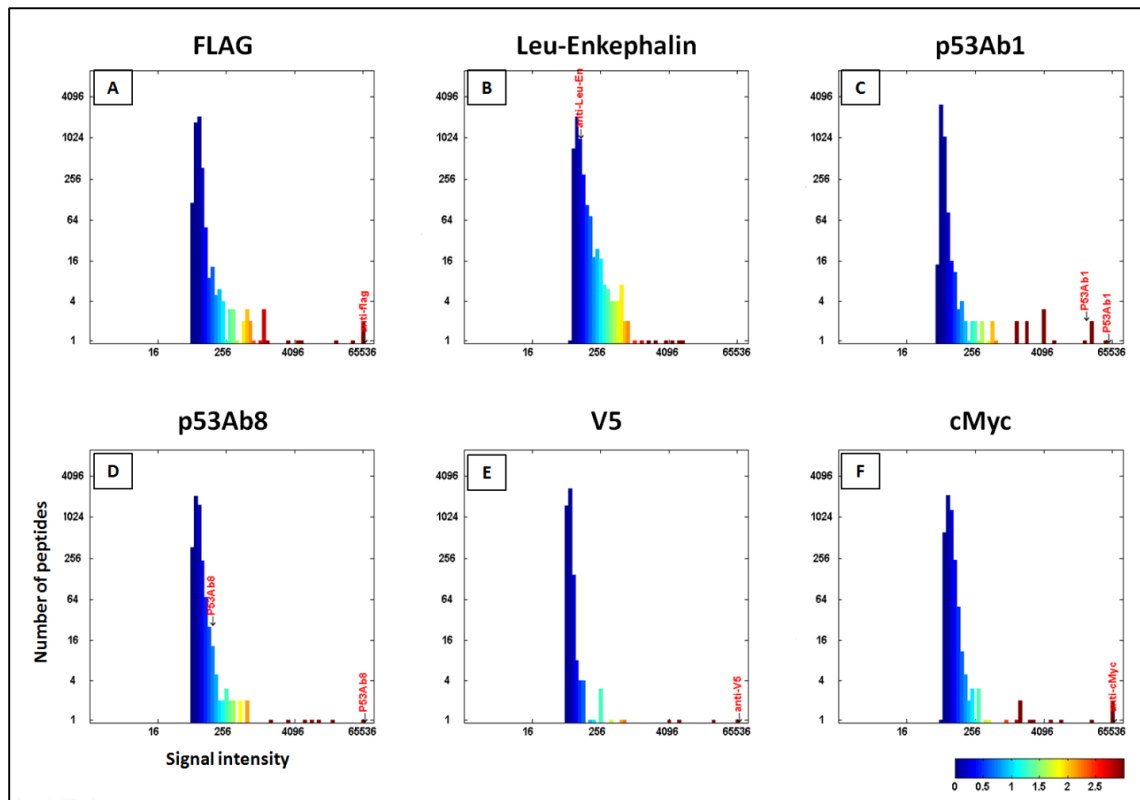
Grant Acknowledgements

This work was supported by the Chemical Biological Technologies Directorate contract HDTRA-11-1-0010 from the Department of Defense Chemical and Biological Defense program through the Defense Threat Reduction Agency (DTRA) to SAJ.

Acknowledgements

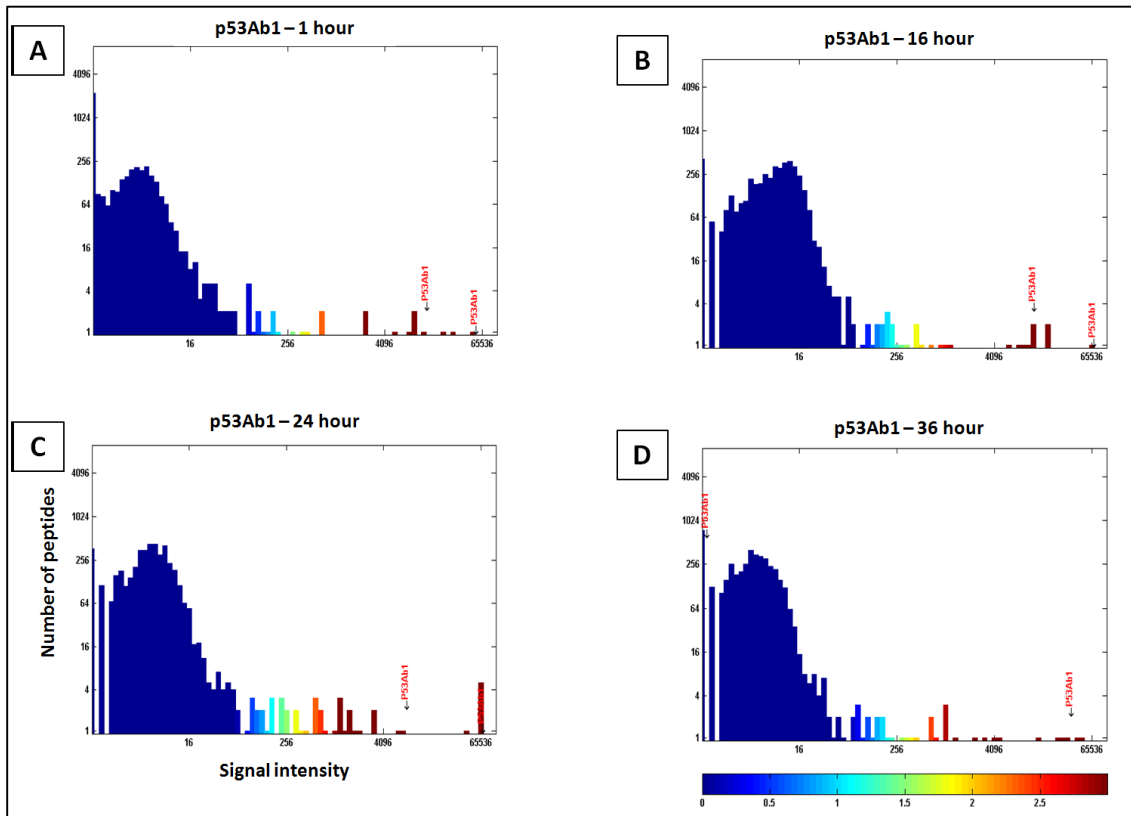
The authors wish to thank Kevin Brown for writing programs to query the IEDB algorithms for B-cell epitope prediction. We are grateful to Lawrence Livermore National Laboratory for providing us with infected patient sera for West Nile virus and Malaria originally acquired from SeraCare.

Supplementary Figures and Tables:



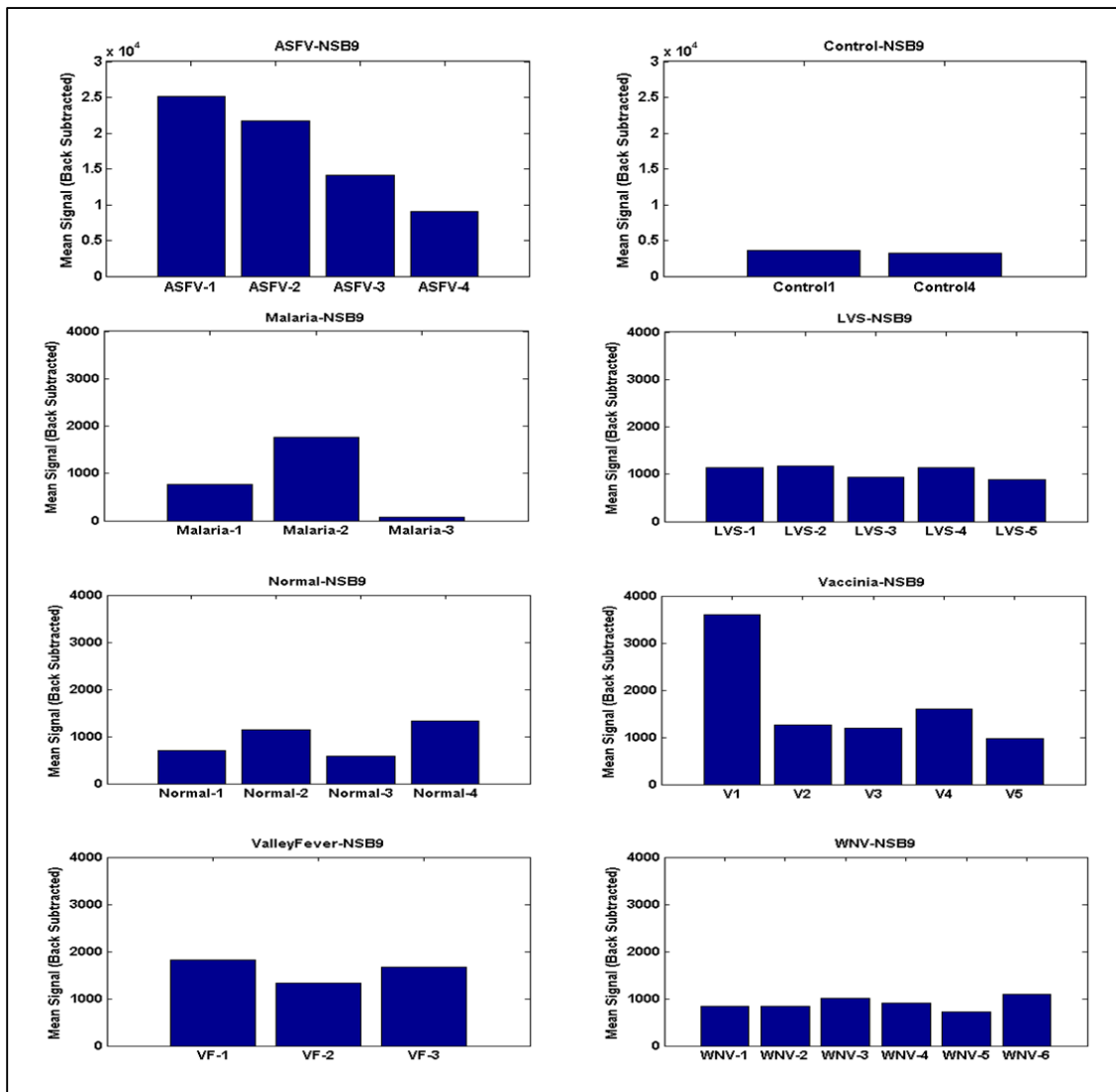
Supplementary Figure 4- 1 Histograms displaying array data for 6 monoclonal antibodies on NSB-9 slides

The X-axis demonstrates the signal intensity obtained from the assay and Y-axis represents the number of peptides displaying a given signal intensity. Every plot represents one monoclonal antibody's reactivity as observed on the pathogen array.



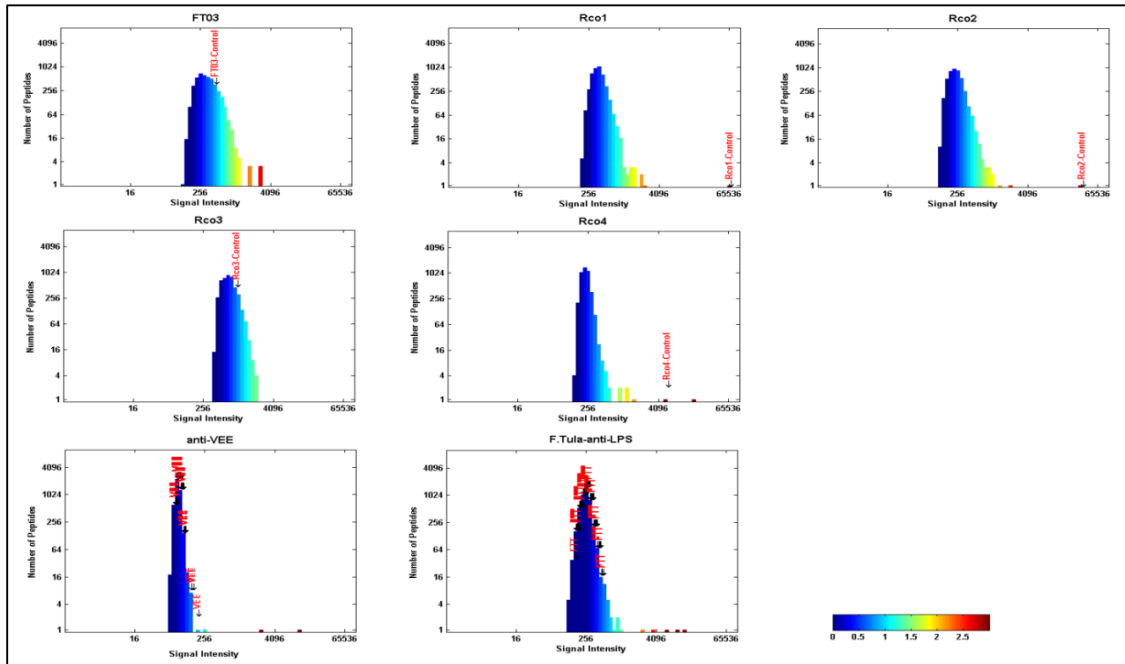
Supplementary Figure 4- 2 Change in signal distribution and cognate versus non-cognate reactivity of p53Ab1 monoclonal incubated on NSB-9 slides for 1, 16, 24 and 36 hours respectively.

The X-axis demonstrates the signal intensity obtained from the assay and Y-axis represents the number of peptides displaying a given signal intensity. Every plot displays the reactivity of p53Ab1 monoclonal antibody on the array under incremental times of incubation. The signal intensity of its cognate epitope is depicted on the histogram using an arrow to demarcate its position within the histogram of peptide signal intensities.



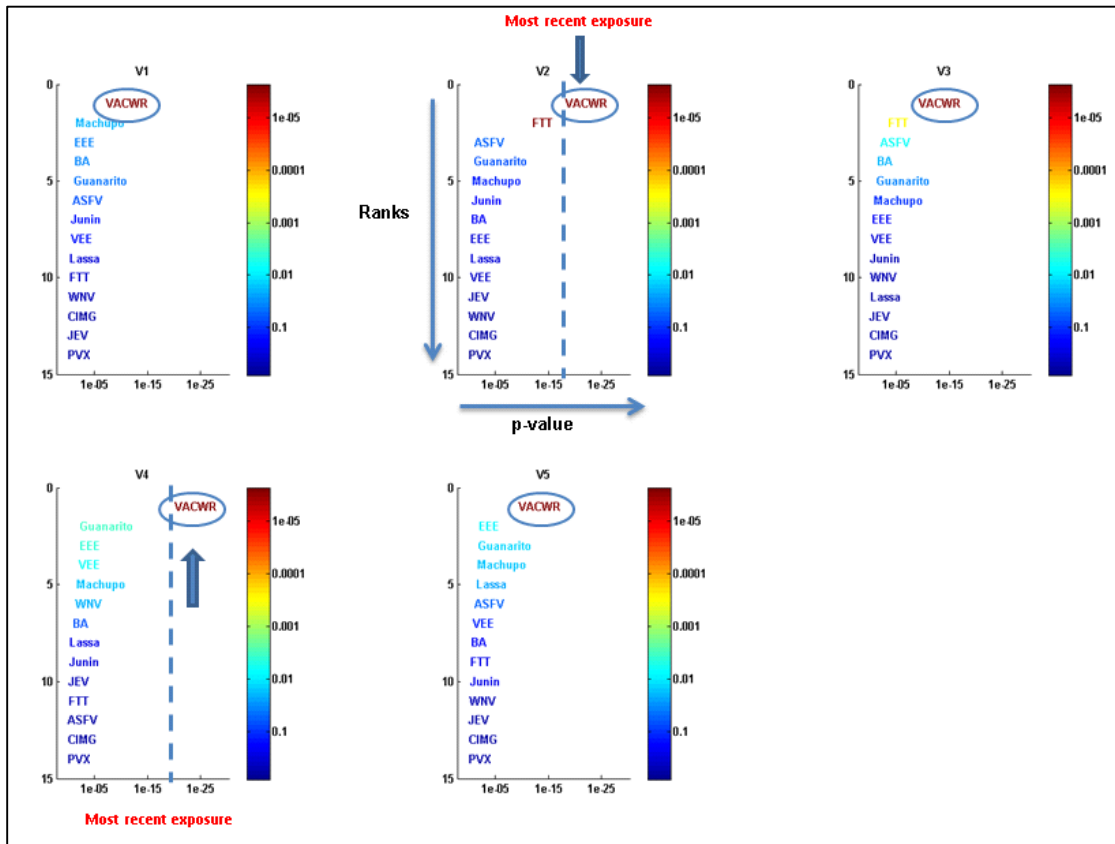
Supplementary Figure 4- 3 Average signal intensity observed for various infections on NSB-9 slides at 16 hour incubation, 23°C and serum dilution of 1:500

The X-axis represents number of patients tested per infection group and Y-axis displays average signal intensities. The Y-axis for ASFV control (un-infected) and infected groups is different as compared to that for human infections merely to display all data.



Supplementary Figure 4- 4 Structural (anti-LPS, anti-VEE) and polyclonal antibodies (FT03, Rco1, Rco2, Rco3, Rco4) on array.

The X-axis represents signal intensities observed on array, Y-axis represents the number of peptides displaying a given signal intensity. The position of cognate epitopes is highlighted in red on the histogram.



Supplementary Figure 4- 5 Capturing the memory immune response from exposure and distinguishing time of exposure – Vaccinia vaccination

The X-axis depicts the p-value score for the cognate group of pathogen peptides (VACWR - Vaccinia) versus all other groups of pathogen peptides on the array. The Y-axis displays the ranks of pathogen groups basis p-values from top to bottom. The graph is colored on an arbitrary scale correlating to the range of p-values. The P-value score is calculated basis how significantly a group of pathogen peptides contributes to signal intensities observed on the array.

Supplementary Table 4-1 Guitope match data (score cut=3)

KANWFDKTFNQMTQVWGSC

FT03

***** FORWARD PEPTIDES *****

SEQ	SCORE	ALIGN LENGTH	PRO POS	PEP POS	PRO WINDOW	PEP WINDOW	UniqueID
CRHNIEASQLA EVRSYCYHA	5.5 21	10	11	8	nQmtq VwgsC	sQlaeV rsyC	JEV[E](341-357)
CSGEQKLISEE DLEQKLISE	4.3 6	2	19	1	sc	cs	anti-cMyc (9E10)
MMIFRNDFEW LKIHKTRGSC	6.1 76	8	13	13	mtqvw GSC	ihktrGS C	FT04- Control
CRHDTLKNLQ QDLHQYFKGK	4.4 89	6	7	6	fKtfnQ	lKnlqQ	PVX_09768 0(1000-1016)
CRHMSQAIAA VSQDRCKNIT	3.9 29	4	12	3	qMtQ	hMsQ	FTT0083(103-119)
CRHKAEECTC NNGSCSLKTS	6.1 19	3	18	13	GSC	GSC	ASFV132(45-61)

TIPAHNIFWILYFSIGTGSC

Rco3

***** FORWARD PEPTIDES *****

SEQ	SCORE	ALIGN LENGTH	PRO POS	PEP POS	PRO WINDOW	PEP WINDOW	UniqueID
CRHILLASKHD LMKQKCLKG	4.3 14	5	10	4	ILyfS	ILlaS	Lassa- Lprot(352-368)
CSGKWDEPGN NVYGCIKQMY	4.3 6	2	19	1	sc	cs	CF- VF_02795- (97-113)
CRHPTHRHLK GEACPLPHKL	3.4 54	3	3	4	PaH	PtH	Machupo- Gly(456-472)
CRHWKAVEKS VAMKHLTSFK	4.7 54	4	11	16	Lyfs	Ltsf	JEV[C](69-85)
CRHIPHTIAGP KSKHNRREG	3.7 3	2	5	15	HN	HN	JEV[NS1](1037-1053)
CRHGRGEQQI NHHWHKSGSS	4.0 01	3	5	9	hni	qin	WNV-I-NY- 99[E](677-693);WNV-

							II-956[E](673-689)
CRHKKADITSK VNHVKEKTS	3.9 73	3	5	13	hni	nhv	PVX_09770 0(783-799)
CRHGHPVSRG TAKLRWLVER	4.6 01	4	14	8	SiGT	SrGT	WNV-I-NY-99[NS5](2580-2596);WNV-II-956[NS5](2577-2593)
CRHLLWGGFP WVSLGYSQTE	5.4 42	5	12	11	yfSiG	wvSiG	FTT0614(137-153)
CRHALTFKAC DHIMKSGDLK	4.0 62	5	15	13	Igtgs	Imksg	VACWR148 (222-238)
CRHVRHTHSK HKYHCICPMK	3.1 07	3	17	7	TgS	ThS	EEE[GP2](69-85)
CRHYSSTWHQ DANHPYRTWN	5.4 55	3	4	12	Ahn	Anh	WNV-II-956[NS5](2815-2831)
CRHPHFVQHS YTVQCKCRST	3.3 82	4	17	12	TgsC	TvqC	PVX_00099 5(341-357)
CSGYGGFLYG GFLYGGFLAA	4.3 6	2	19	1	sc	cs	anti-Leu- Enkaphalin clone 1193/220
CRHERSHPEIW HHLSTLIQ	5.4 5	6	9	10	wilyfS	iwhhLS	Machupo- Lprot(422- 438)
CRHMDEYVQE LKGLIRKHIP	3.6 36	7	10	14	ilyfSIg	lirkhIp	Machupo- Lprot(1-17)
CSGYGGFYGG FYGGFYGGFA	4.3 6	2	19	1	sc	cs	Peptide 9449
CRHVERCYLQ ALSVCNKVKG	3.6 22	2	11	8	ly	yl	Junin- Lprot(322- 338)
CRHIHAMTPER VQRLKASRP	3.5 82	2	4	5	ah	ha	VEE[GP2](1599-1615)
CRHTQEKFEM GWKAWGKSIL	4.3 48	4	13	8	FsiG	FemG	JEV[NS1](901-917)
EFWDKEWHTR ADWPVWDGS	6.1 19	3	18	18	GSC	GSC	Rco2- Control

C							
CRHGVMVEGV FHTLWHTTKG	3.3 92	4	5	12	Hnif	Htlw	WNV-I-NY-99[NS3](1544-1560);WNV-II-956[NS3](1540-1556)
CRHSESHSPQE VCEKYCSWG	4.9 75	5	12	16	YfSiG	YcSwG	ASFV006(127-143)
CRHPSEDLEY SWLNLAHH	5.0 76	4	2	16	ipAH	laAH	Lassa-Lprot(1538-1554)
CRHILGFYHLK HKPPKKKCK	4.7 48	4	12	7	yfsi	fyhl	ASFV194(19-35)
CRHYGRCTRT RHSKRSSRSV	3.6 98	3	18	5	GsC	GrC	JEV[preM(219);M(220)](205-221)
CRHVAKAEEA KKEADNAKVA	3.1 48	3	4	14	AhN	AdN	PVX_097680(647-663)
CRHSLMHWDL ETQAPKNSIN	6.5 08	6	1	12	TipahN	TqapkN	FTT1775(477-493)
CRHKGCTLKIE GEYAYGWLRL	3.6 48	2	9	18	Wi	Wl	FTT0191(137-153)
CRHTALHFLN AMSKVRKDIQ	3.2 06	3	11	6	LyF	LhF	JEV[RNAPo1](3208-3224)
CRHCHQGINN KLTAHEVKLQ	5.2 43	6	2	12	ipAHni	ltAHev	Lassa-Lprot(221-237)
CRHEIDRIYKTI KQYHESRK	3.9 97	5	11	8	IYfsI	iYktI	VACWR130(222-238)

Table displaying alignment matches of high signal intensity peptides with immunized cognate peptides (FT03, Rco3) using alignment program GuiTope [34]. Setting a low cut-off score = 3, so as to capture discontinuous and short epitope matches.

CHAPTER 5

DE-CONVOLUTING ANTIBODY CROSS-REACTIVITY OBSERVED ON A PATHOGEN PROTEOME PEPTIDE MICROARRAY

Abstract

Multiplexed proteomic microarray platforms have been unsuccessful at distinguishing infections apart due to antigen-antibody cross-reactivity on the assay. Given the specificity of antigen antibody interactions and diagnostic success of single pathogen based ELISA assays, using epitope peptide microarrays might appear to be a logical transition. Previous studies have failed to address cross-reactivity observed on multiplexed pathogen proteome based microarrays. We developed a multiplexed, pathogen proteome peptide (PPP) microarray designed to distinguish four priority pathogens apart. Despite optimizing microarray processing conditions on the PPP array to reduce cross-reactivity, we observed non-obvious antibody binding between unrelated pathogen peptides. We investigated the underlying factors that impact specificity and report several biochemical and computational aspects that affect and, if resolved, could enhance the accuracy of multiplexed epitope microarrays. A confounding aspect in mapping infection is observing cross-reactivity on the array from identical 5-7 amino acid long sequences in common between unrelated pathogen peptides. Secondly, the presence of common pathogen epitopes, such as Influenza virus, reduces the specificity of the remaining non-influenza pathogen peptides on a multiplexed assay. The primary goal of this work is to assess the limitations of the PPP array while simultaneously distinguishing

priority pathogen and common pathogen exposures. Third, to circumvent cross-reactivity we developed an alternative data analysis strategy which uses a pattern of common short-sequence motifs in the cross-reactive response to accurately detect an infection. We utilized peptide sequence identity on a 2-mer to 7-mer repetitive epitope level to analyze data and discern groups of peptide n-mer motifs that we refer to as an ‘*umbrella of antibody reactivity*’. We classified the original infection/exposure by reading a *pattern* of antibody reactivity after averaging the signal intensity for these individual n-mer umbrellas. In doing so, we attempt to mathematically re-appropriate antibody cross-reactivity observed on the platform to the actual pathogen causing the infection. This approach could be applied to historical peptide microarray data, likely considered unusable due to cross-reactivity, thus rescuing a number of important research projects.

Abbreviations

ASFV, African Swine Fever Virus; BLAST, Basic local alignment search tool; CMG, Comparative microbial genomics; FIU, Fluorescence intensity units; HIV, Human Immunodeficiency Virus; HCV, Hepatitis C Virus; JEV, Japanese Encephalitis Virus; NIAID, National Institute of Allergy and Infectious Diseases; PPP, Pathogen proteome peptide; WNV, West Nile Virus.

Keywords

Multiplexed, peptide microarray, multi-pathogen, specificity, peptide cross-reactivity, epitope, diagnostic assay, immunosignature, antibody.

Introduction

Pathogen protein sequences are extremely conserved. While it may not be immediately apparent on the protein level, it definitely is on an n-mer (short-peptide) level [140]. A B-cell antibody epitope ranges from 4-12 amino acids in length [88]. Mapping this level of n-mer commonality is crucial to understand cross-reactive observations when developing immunoassays. Previous work done by our group [141] explored the feasibility of using a life space peptide array representing epitopes for 14 NIAID category A, B, C priority pathogens to distinguish those infections on a single multiplexed platform. From six infectious sera tested on that platform, four infections were distinguished with >90% AUC-ROC (area under a receiver-operator characteristics curve) simultaneously. These four groups of infectious sera were from exposures to, *Coccidioides* spp. (Valley Fever), African Swine Fever Virus (ASFV), West Nile Virus (WNV) and Vaccinia, the smallpox vaccine. The platform failed to correctly distinguish Malaria and *Francisella tularensis* LVS-live vaccine strain sera. In this paper, we examine the effect of a change in chemical diversity of the platform on the interaction and local competition between antibodies and peptides on the microarray. This work addresses the peptide-antibody cross-reactivity observed on a multiplexed assay using bioinformatic solutions to eliminate confounding effects of cross reactivity on pathogen identification.

The humoral antibody response to an infection consists of multiple components including but not limited to natural antibodies, highly neutralizing antibodies specific to the infection or exposure, poly-reactive antibodies and cross-reactive antibodies [129].

The persistent presence of cross-reactive antibodies has been documented through numerous studies in infections such as Influenza, Dengue, HIV, HCV and Malaria [142]. The advent of advanced indirect (antibody based) pathogen surveillance assays, has resulted in discovering pre-existing reactivity to Influenza virus strains such as the swine-origin H1N1 [143] and Japanese encephalitis virus (JEV) [144] in previously unexposed populations. Cross-reactivity is an inherent feature of all antigen-antibody reactions partly due to plausible conformational and structural reasons highlighted in literature [101]. In some instances cross-reactivity is beneficial, due to offering cross-protection for example, neutralization of the pandemic swine (2009 H1N1) and avian (1997, H5N1) origin influenza viruses due to a memory response from seasonal influenza vaccine strains [145-147]. When developing a single pathogen based diagnostic serological assay, explaining cross-reactivity captured on the assay from other unrelated pathogens is difficult. Ulrich *et al* [92] encountered this problem while developing a *Yersinia pestis* (gram-negative) specific proteome protein microarray. They observed cross-reactivity on *Y.pestis* proteins from rabbit sera experimentally infected with seven other genetically unrelated gram-negative bacteria and *Bacillus anthracis* a gram-positive. They used the signature pattern of cross-reactivity from other infections observed on their *Y. pestis* protein microarray to distinguish the cross-reactive pattern per pathogen.

Cross-reactions are observed on serology based assays within genetically related strains of a given virus, for example, within Dengue strains 1, 2, 3 and 4 and also within viruses belonging to the same family, Flaviviridae- between Dengue and JEV [148,149]. Cross-reactivity has been documented on multiplexed diagnostic assays such as the

ToRCH assay that simultaneously measures antibodies from five vertically transmitted pathogens. The assay sensitivity when measuring antibodies against genetically distinct *Toxoplasma gondii* and Rubella versus Herpesviruses: Cytomegalovirus (CMV), Herpes Simplex virus 1 (HSV-1) and HSV-2 using ToRCH is variable per infection ranging from 46-97% and specificity between 88-100% [37]. Cross-reactivity in antigen-antibody diagnostics could be explained as being observed due to short n-mer identity on a 5-mer to 11-mer amino acid level between unrelated pathogen proteomes. Based on this rationale, Kanduc and Kobinger *et al.* map the redundancy between pathogens and the human (host) proteome, for developing better pathogen targeted vaccines that could potentially generate lesser self-reactive antibodies [140,150,151].

In this study, we tested how incrementally adding common exposure pathogen peptides on the PPP array affected its ability to discern priority infection antibody response. The original platform contained 12 pathogen epitopes (PPP-12) from either immunodominant antigens for larger pathogens or complete proteomes for smaller viruses. To test the effect of change in chemical diversity, we made two incremental sets of arrays, one in which we added ASFV and Vaccinia peptides (PPP-14) and another in which we added Influenza peptides (PPP-15). ASFV and Vaccinia viruses are both double stranded DNA viruses closely related to Herpes viruses. These pathogen peptide groups were added due to recent availability of sera and to measure the effect of adding peptides that are potentially capable of capturing Herpes virus cross-reactivity. The addition of ASFV and Vaccinia peptides did not have a detrimental effect on the PPP array's ability to distinguish multiple infections. By adding influenza peptides, we

evaluate the effect of including a common exposure yet priority pathogen on the array. Due to the frequency of human exposures to various influenza strains [152], we expected to observe a distinct separation of memory influenza specific antibody response and priority pathogen reactivity, leading to more specific priority pathogen detection. The addition of influenza peptides on the array however, reduced the assay's ability to distinguish priority pathogen infections. The most parsimonious explanation for this observation might be that the influenza peptides likely competed for antibody reactivity to other priority pathogen peptides. This competition reduced the pathogen specific response apparent on arrays without influenza peptides. This observed cross-reactivity to influenza peptides from all infectious sera led us to developing an improved bioinformatics approach to mathematically reattribute cross-reactivity. While doing so we used the cross-reactivity observed due to the addition of influenza peptides on the multiplexed assay to distinguish priority pathogen infections apart.

Methods

Serum samples and monoclonal antibodies used in this study

Human patient serum samples from Influenza and Vaccinia vaccine recipients and healthy non-disease individuals were collected under the ASU IRB 0905004024, "Blood Collection for Immunological Studies". *Fransicella tularensis subsp. holarctica* live vaccine strain (LVS) vaccinated individuals' sera was received from Dr. Anders Sjöstedt's laboratory at Umeå University, Sweden. They are part of a time course study; samples used were 28-30 days post-receiving the LVS vaccine. Valley fever infected

patient sera was received from Dr. John Galgiani at the University of Arizona (IRB# FWA00004218). *Plasmodium vivax* and West Nile virus infected sera was obtained from SeraCare Life Sciences (Milford, MA). All monoclonal antibodies used in this publication are listed in *Supplementary Table 5- 1*.

Microarray production and processing

Pathogen proteome peptide microarrays were produced as described in Chapter 4. Briefly, peptides were obtained from Sigma Genosys (St.Louis, MO) and printed on NSB-9 aminosilane slides from NSB Postech (Los Alamitos, CA). All slide surfaces were coated with sulfo-SMCC linker (Pierce, Rockford, IL) and peptides were conjugated to the surface using maleimide conjugation chemistry. Each peptide was printed twice on a two-up array by Applied Microarrays Inc. (Tempe, AZ) using piezo electric printing.

The following pathogen peptides were represented on the PPP array:

- a.) **PPP-12:** Array representing 12 pathogens (3546 peptides) - *Francisella tularensis* [Tularemia-LVS], *Coccidioides immitis* [Valley fever], West Nile virus (WNV) [strain: I & II], Japanese encephalitis virus (JEV), *Plasmodium vivax* [Malaria], Venezuelan Equine Encephalitis, Eastern Equine Encephalitis, *Bacillus anthracis*, Machupo virus, Junin virus, Guanarito virus, Lassa virus and monoclonal antibody epitope peptide controls.
- b.) **PPP-14:** Array representing 14 pathogens (4337 peptides) - PPP(12) peptides + African swine fever virus [ASFV] and Vaccinia [strain: Western Reserve] peptides.

c.) **PPP-15:** Array representing 15 pathogens (4693 peptides) - PPP(14) + 283 Influenza PR8 (H1N1) peptides

Microarray slides were pre-washed with a solution containing 7.33% acetonitrile, 33% isopropanol and 0.55% TFA to remove unbound peptides. Slides were blocked in 1X PBS, 3% BSA, 0.05% Tween 20, 0.014% β -mercaptohexanol for 1hr at 25°C. Sera samples were diluted 1:500 in the Incubation buffer containing 3% BSA, 1X PBS, 0.05% Tween 20, and allowed to bind to the microarray for 16 hours at 23°C in 100 μ l total volume per pathogen peptide array. The optimum thermodynamic parameters chosen for processing these pathogen arrays were based on empirical data from our previous work [141]. A Tecan 4800 Pro Hybridization Station (Tecan, Salzburg, Austria) was used for array incubation and primary sera was detected using Alexa Fluor-647 conjugated Goat anti-Human, IgG Fc (γ) fragment specific secondary antibody from Jackson ImmunoResearch (West Grove, PA).

The slides were scanned using Agilent C scanner (Santa Clara, CA) at 635 nm excitation wavelength with 100% PMT and laser power at 10 μ m image resolution. The 16-bit TIFF images were aligned using GenePix 6.0 software (Axon Instruments, Union City, CA) and the data files imported into GeneSpring 7.3.1 (Agilent, Santa Clara, CA) and Matlab (Natick, MA) for further analysis. Every patient's serum sample was processed in duplicate and since every peptide was printed twice within a sub-array, it gave 4 measurements from the same peptide upon combining both technical replicates. Any array with a Pearson Correlation Coefficient less than 0.85 across technical

replicates was re-processed. Upon meeting the quality criteria, all technical replicates for a given individual patient were averaged for further data analysis.

Statistical analysis and software used

The arrays were initially analyzed using Matlab (Natick, MA) code written from our previous work [141]. Short sub-sequence n-mer analysis was performed using a regular expression search program published in Richer *et al.* [153]. The algorithm was designed to find short identical sub-sequences in common within the peptides represented on a microarray. From a peptide sequence library, the algorithm divides all peptides into all possible subsequences within user input length ranges, 2-19 amino acids for a 20-mer peptide length array. The signal intensity associated with each one of these peptide subsequences is extracted from the original peptide sequence they belong to and averaged together per sub-sequence, provided there are at least 2 replicates per sub-sequence fulfilling signal intensity criteria. These list of subsequences with signal intensities associated with them are ranked and sorted based on their signal intensity and subsequences below user input signal intensity cut-off (<500 FIU-Fluorescence intensity units) are excluded. This list of significant sub-sequences, are obtained per individual sample and the number of n-mers in common per infection and per individual are estimated using a custom python script. The mathematical pattern containing this information is used to classify the sample into an infectious group using leave one out cross-validated (LOOCV), Support Vector Machine (SVM) algorithm from the e1071 library in R. The number of n-mer sub-sequences in common between individual serum

samples or individual pathogens was calculated using a custom python script. Using these numbers the Connectograms in Figures 2 and 3 are constructed using Circos online [154]. The pathogen proteome BLAST matrices are generated using CMG-biotools [155].

Influenza PR8 whole virus ELISA protocol

Nunc Maxisorp microtiter ELISA plates were coated by incubating overnight at 4°C with purified UV-inactivated Influenza H1N1 A/PR/8/34 (PR8) virus commercially available through Advanced Biotechnologies Inc. (Cat. No.: 10-2/3-500, Lot: 8J0006) at 100 ng/well. Additional plates were coated with 5% non-fat milk in TBST (19.98mM Tris, 136mMNaCl, pH 7.4 with 0.05% Tween 20) as control for background binding and the same serum samples were processed on them simultaneously. The non-specific absorbance obtained from these plates was then subtracted from that obtained from PR8 coated plates. As a positive control for secondary binding, 1:500 diluted pooled naïve mouse (C57BL6J) and uninfected pooled human sera was applied in 2 wells each, per plate. All control sera and antigens were diluted in the carbonate/bicarbonate buffer (15mM Na₂CO₃, 35mM NaHCO₃). As a secondary antibody negative control, 3 wells per plate were coated overnight with the antigen and blocked to be detected directly with the anti-human secondary antibody and three with the anti-mouse secondary antibody per plate. These absorbance values were then averaged and subtracted from their respective human or mouse sera wells as background absorbance due to secondary antibody. All plates were washed between steps three times each using TBST. The plates were then blocked with 5% non-fat milk and incubated for 1 hour at 37°C. For the assay, serum

samples were serially twofold diluted in PBST and incubated on the plates for 1 hour at 37°C starting at 1:50 dilution up to 1:800. The bound serum antibodies were detected using the appropriate species specific secondary antibodies diluted 1:1000 in PBST. Anti-mouse IgG (H+L)-HRP conjugated (Bethyl Laboratories, Montgomery, TX; Cat. No.:A90-216P) for mouse sera and anti-human IgG (H+L)-HRP conjugated (Vector laboratories, Burlingame, CA; Cat. No. PI-3000) for human sera, were incubated for 1 hour at 37°C. Bound secondary antibody was detected by adding 100 µL of the substrate for HRP, ABTS (KPL, Gaithersburg, MD) and incubating for 30 minutes at 37°C. This colorimetric reaction was stopped using SDS (1%, 50 µL per well) and absorbance's were read using the SpectraMax 190 absorbance microplate reader (Molecular Devices, Sunnyvale, CA) at 405nm.

Results

Redundancy observed within priority pathogen proteomes represented on PPP array

We first sought to quantitatively measure the degree of sequence redundancy present in the pathogen proteomes. *Figure 5-1* is a BLAST (Basic local alignment search tool) matrix generated using the CMG-biotools [155] proteome comparison workbench. The figure represents 289 comparisons (17X17) of pathogen proteomes represented on the PPP array. Every cell of this BLAST matrix represents a summary of BLAST queries with a 50% homology restriction applied to between 2 (EEE and VEE proteomes) and 10,454 proteins (*Coccidioides immitis* proteome) summarizing the results of

approximately 543 million BLAST searches between 23,311 total proteins. The epitope peptides used as positive control on the assay are intentionally included in this analysis to display no overlap at a stringent restriction of 50% identity in at least 50% alignment match of the two proteins being compared. As is expected Flaviviruses, WNV strains I and II and JEV are 76.9% homologous represented by bright green cells in the matrix. The Arenaviruses (Junin, Machupo, Lassa and Guanarito) are homologous amongst themselves as are the equine encephalitis viruses (EEE and VEE). The last row of this matrix depicts homology within the proteome and larger proteome pathogens such as *Bacillus anthracis* (Sterne) have up to 258 redundant homologous proteins within their proteome. In summary, on a proteome level, there is not much apparent homology between phylogenetically distant priority pathogens, at least under these criteria.

A BLAST hit within this program is considered homologous (green) if at least 50% of the two protein sequences are aligned and 50% of the amino acids within the alignment are identical. The last row at the bottom of this matrix depicts homology within a given pathogen proteome under the strict homology criteria (gray to red scale).

Redundancy observed within priority pathogen peptides represented on PPP array

Homology calculated between full length proteins would be insufficient to explain the observed cross reactivity between evolutionarily distant priority pathogen proteomes. Therefore, we explored sequence identity on a finer scale, examining sequence motifs in the range of common epitope lengths. The numbers of identical 5 to 10-mers in common between pathogen proteomes represented on the pathogen array and common pathogens such as Herpes and Influenza were calculated using a Python script from a suite of programs published in Richer *et al.* [153]. The overlap between pathogens based on shared sequence motifs is illustrated as a connectogram in *Figure 5- 2*.

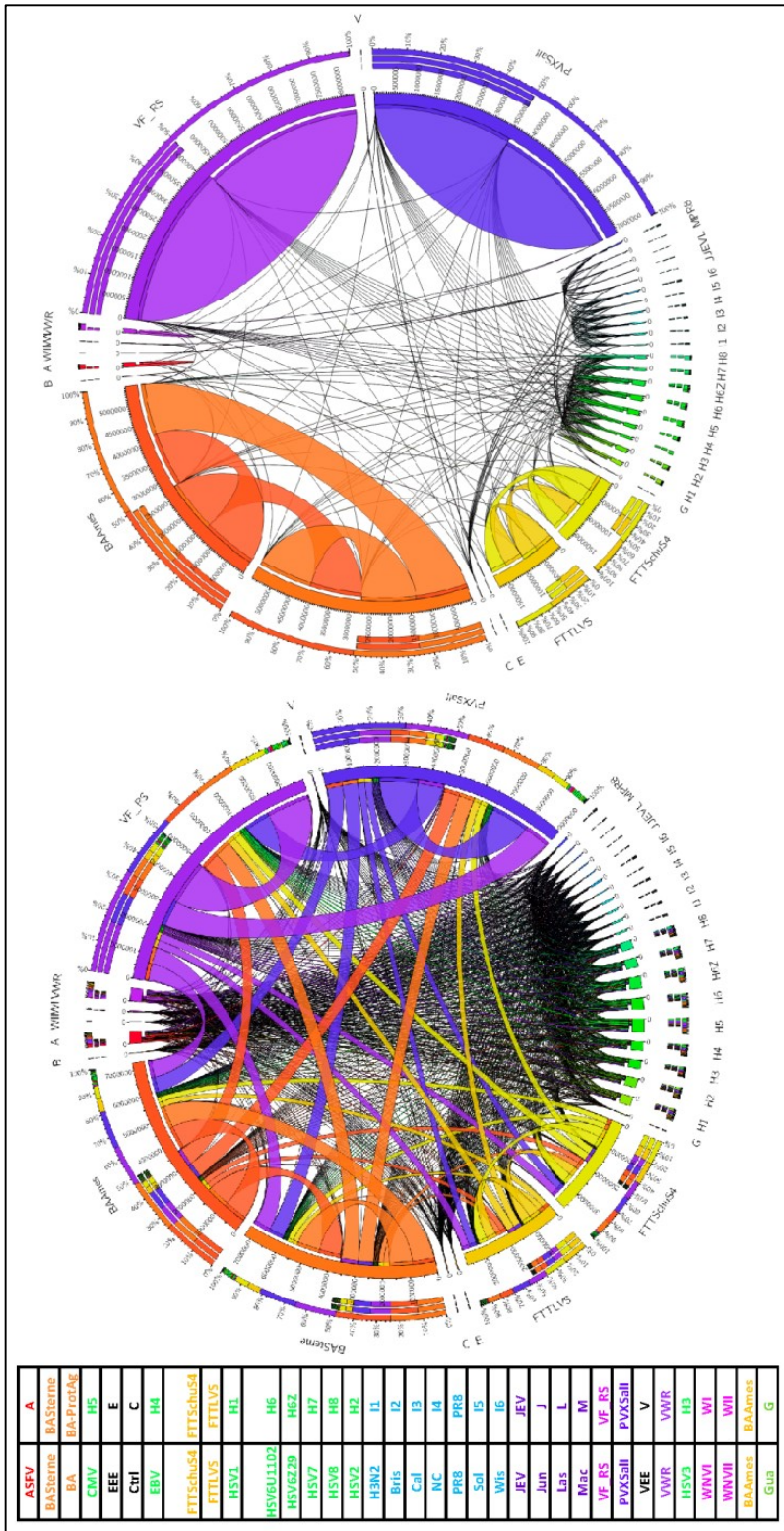


Figure 5- 2 Pathogen space is extremely conserved on a 5-mer peptide motif level.

Every pathogen has a unique color and the size of the ribbon is proportional to the level of overlap between those pathogens on either a 5 amino acid sequence (5-mer) or 10 amino acid sequence (10-mer) levels. The extent of overlap appears to diminish as epitope length increases with 10-mers having the least overlap suggesting short sequence motifs might be responsible for driving cross-reactivity. The code for designations on the circle is given in a table on the left.

Redundancy observed within peptides on the PPP array and pathogen proteomes

Having established that a number of identical short motifs are conserved between unrelated pathogens, we sought to characterize the motifs present on the PPP array. The implication from this analysis would be to *a priori* expect cross-reactivity to non-cognate pathogen peptides due to identical n-mers in common between the infecting pathogens proteome and several other pathogen peptides on the array. The peptides were selected for inclusion on the PPP so as not to represent any duplicate 16 & 17-mers. Any duplication in sequence between amino acid lengths 5 through 15 was noted so as to map possible cross-reactive binding between unrelated pathogen peptides. Distribution of common 5-mers between pathogen proteomes and peptides on the PPP is presented in *Figure 5- 3* as a connectogram. The size of the ribbon between two groups is correlated to the extent of overlap between those groups. A distinct pattern of common motifs radiates outward from each pathogen. This analysis indicates that multiple 5-mers are commonly present between complete pathogen proteomes and unrelated pathogen peptides on the array. As depicted in *Figure 5- 3*, it may be possible using this

information to predict *a priori* cross reactivity between Valley Fever (*Coccidioides immitis*) infected individual's serum antibodies to *Francisella tularensis* and *Plasmodium vivax* peptides on the PPP array. Taken together this suggests that the unique pattern of potentially cross-reactive n-mers may be used to identify the priority pathogen exposure.

Figure 5- 3 Circular connectogram displaying 5-mer level overlap between peptides represented on the pathogen array and their respective proteomes

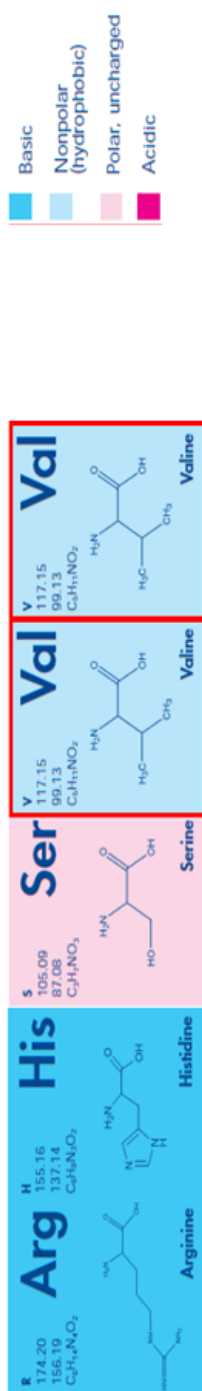
Every pathogen has a unique color and the size of the ribbon is proportional to the level of overlap between those pathogens peptides and other pathogen proteomes on a 5 amino acid sequence (5-mer). The code for designations on the circle is given in a table on the left.

Monoclonal antibody binding on the PPP array

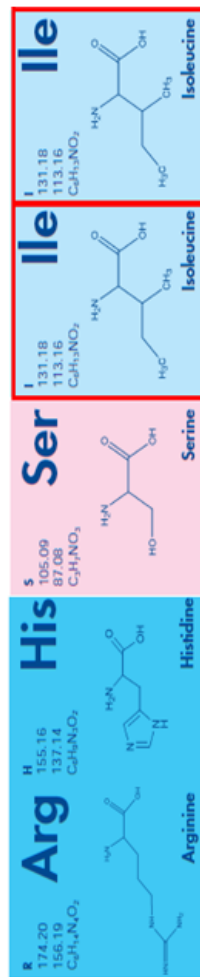
The sequence analysis indicates that common short motifs might be responsible for antibody cross-reactivity observed on the PPP array. To test this hypothesis, we tested the binding of individual well characterized monoclonal antibodies on the platform. These monoclonals bound specifically to their cognate linear epitope peptide along with other peptides having amino acid sequence similarities as demonstrated in *Figure 5- 4*. As listed in the top panel of *Figure 5- 4*, the p53Ab1 monoclonal antibody recognizes the linear peptide sequence ‘RHSVV’ with high affinity (estimated $K_D < 100\text{pM}$) [2]. Additionally, on the array, it binds other unrelated peptides that either have the exact 5-mer epitope or have a structural analog of it such as, ‘RHSII’ and ‘RHSVI’ as listed in table. This group of antibody reactivity could thus be classified as one ‘*umbrella of reactivity*’ due to one antibody binding all these related peptides and will be referred to as such, throughout the Chapter. This result was verified with 4 other monoclonal antibodies namely, p53Ab8, cMyc, FLAG, V5-tag and support the hypothesis that the presence of short motifs in unrelated pathogen peptides might drive cross-reactivity.

Peptide Annotation	Med_Sig_5nM	Peptide Sequence	Alignment around consensus sequence
PF33Ab1 (pAb240) original	13569	CSGSGSRHSVNSGSRHSV	C S G S G S G R H S V V S G S G R H S V
PF33Ab1 repetitive epitope	53158	CSGRHSVVRHSVGRHSVVR	C S G R H S V V R H S V V G R H S V R
Lassa-Gly(111-127)	39393	CRHSIINHFKFNLSDAHKKN	111 - C R H S I I N H K F C N L S D A H K K N - 127
Machupo-Lprot(1689-1715)	27445	CRHSTVKEPKPVLNNQNF	1689 - C R H S T V K E P Q K P L V L N N Q N F - 1715
MNV-4-NY-99(gp1)[541-557]	25619	CRHSVALGSGEGALHQAALA	541 - C R H S V I A L G S Q E G A L H Q A L A - 557
Machupo-Lprot(2116-2132)	23718	CRHSVSMHLQIWPYLKATS	2116 - C R H S V S M L H Q L W P Y L K A T S - 2132
MNV-4I-956(gp1)[537-553]	19689	CRHSVALGSGEGALHQAALA	537 - C R H S V V A L G S Q E G A L H Q A L A - 553
JEV(gp1)[545-561]	18543	CRHSVALGSGEGGLHQAALA	545 - C R H S V V A L G S Q E G L H Q A L A - 561

CSGRHSVVRHSVNSGSRHSVVR [FIU: 53158, Original epitope repeated]



CRHSIINHFKFNLSDAHKKN [FIU: 39393, Lassa-Gly(111-127)]



Amino acid images reproduced from BACHEM's Periodic Chart of Amino Acids

Figure 5- 4 Monoclonal antibody binding observed on PPP-14 array (p53Ab1)

The top panel lists the median signal intensity obtained for peptides binding the monoclonal antibody p53Ab1 alongside their sequence. The alignment of consensus sequence within these peptides is depicted in the last column. The bottom panel shows the amino acid structure and properties of a mimotope peptide within Lassa virus that has an analog of p53Ab1's original recognition sequence 'RHSVV'.

Simultaneous detection of priority pathogen and common exposure pathogen signature

Within a population, individuals are always exposed to common pathogens that may confound diagnosis of a priority pathogen through manifesting similar symptoms or increased lethality during co-infection [156]. For this reason, we sought to test the multiplexed PPP array's ability to distinguish more than one infection/exposure in the same individual's serum sample. The hypothesis was that the array would be capable of simultaneous detection of common pathogen signature (e.g. Influenza, Herpes) and priority pathogen signature. To test this concept we added 283 peptides representing 100% of the Influenza-A/PuertoRico/8/1934 (H1N1) proteome. Given the high frequency of influenza exposures in human populations [157] and maintenance of long term memory responses to various influenza strains [54], we expected to be able to separate influenza and priority pathogen reactivity on the array simultaneously. Adding influenza peptides to the existing 14 pathogen peptides (PPP-14) reduced the specificity of the PPP array to distinguish between pathogens.

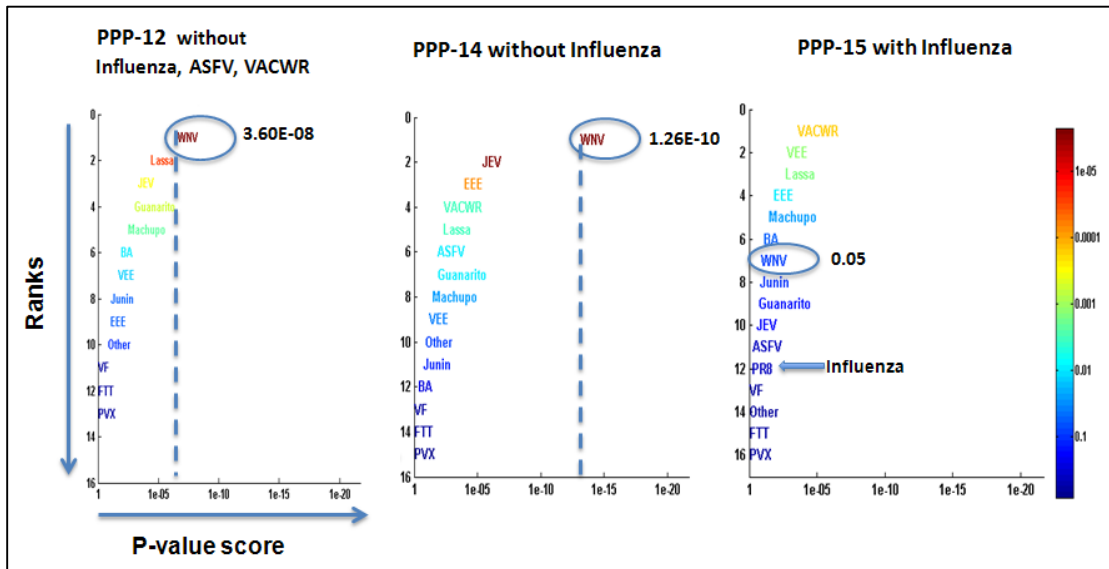


Figure 5- 5 P-value score chart for 1 WNV infected individual's sera on 3 different array platforms.

The X-axis depicts the P-value score for group of pathogen peptides versus all other peptides on the array and the Y-axis displays the ranks of these pathogens based on the P-value score. The group labeled 'Other' represents signals from antibody binding to internal control monoclonal antibody epitopes peptides. The p-value cut-off for PPP-12 is 0.0003 and that for PPP-14 and PPP-15 is 0.0002. The p-values of WNV group of peptides calculated on all 3 arrays are displayed within the graph.

The addition of influenza peptides altered antibody binding to cognate infection pathogen peptides for all infections being tested. This can be observed in *Figure 5- 5* showing p-value score based pathogen rank plots. The 3 panels of *Figure 5- 5* show change in antibody binding for one WNV virus infected individual on 3 different arrays, merely representing the trend observed in this dataset for all infectious samples tested.

The first panel shows this WNV infected individual's antibody binding as observed on an array representing peptides for 12 priority pathogens, not including Influenza, ASFV and Vaccinia. The p-value score of WNV group of peptides is 3.60×10^{-8} , statistically significantly higher as compared to the p-value score of the remaining pathogen groups of peptides. The p-value score of Lassa (0.00014) and JEV (0.00012), other encephalitis viruses are above the p-value score cut-off = 0.0003 for this platform, displaying cross-reactivity on the assay. These p-values however are much lower as compared to that of WNV showing a clear separation of WNV specific antibody reactivity. Panel 2 shows this same individuals' antibody binding profile on an array that included ASFV and Vaccinia, but not influenza peptides. The addition of Vaccinia and ASFV peptides capable of capturing other poxvirus (such as Herpes) related antibody response, appears to improve the assay's capability of detecting the priority pathogen antibody response. The p-value score of WNV group of peptides is 1.26×10^{-10} , and while cross-reactivity to JEV (9.25×10^{-5}) is retained and above p-value cut-off 0.0002, the p-value of WNV is significantly lower than that of JEV. Panel 3 displays how the change in antibody binding on the array after the addition of influenza peptides diminishes the platform's ability to distinguish the WNV signature. The p-value score of WNV group of peptides is 0.05, with Vaccinia (VACWR) group of peptides being ranked highest at p-value 0.0005 below cut-off 0.0002. Using existing analysis techniques that involved ranking groups of pathogen peptides through eight statistical metrics did not resolve any of the priority pathogen signature responses including WNV on arrays containing influenza peptides. A summary of results from all three versions of arrays is depicted in *Table 5- 1* and all the

scoring metric transitions between these three array versions are summarized in *Table 5-*

2. This observation warranted a bioinformatic intervention to re-appropriate cross-reactivity observed on the assay regardless of change in the platforms' chemical diversity.

Table 5- 1 ROC summary displaying accuracy of diagnosing the cognate infection on three platforms

Infection (No. of patients) PPP (12 pathogens, no ASFV,VA CWR,PR8)	Mean Sig.	T-test p-val.	Signal *- log(P-val)	Signal to Noise	Median Signal	Mean Ranks	Wilcoxon	Pearson Correlation
Valley fever (6)	0.94	0.24	0.41	0.43	0.77	0.38	0.20	0.80
WNV (5)	0.58	0.95	0.86	0.44	0.63	0.87	0.95	0.69
Malaria (3)	0.52	0.04	0.06	0.20	0.36	0.14	0.17	0.23
LVS-Francisella tularensis (5)	0.37	0.48	0.41	0.15	0.23	0.37	0.47	0.57

Infection (No. of patients) PPP (14 pathogens, added ASFV, VACWR)	Mean Sig.	T-test p-val.	Signal *- log(P-val)	Signal to Noise	Median Signal	Mean Ranks	Wilcoxon	Pearson Correlation
Valley fever (3)	0.91	0.24	0.46	0.38	0.73	0.35	0.17	0.85
ASFV (4)	0.96	0.46	0.89	0.90	0.96	0.73	0.92	0.98

WNV (6)	0.68	0.97	0.94	0.34	0.62	0.89	0.96	0.80
Vaccinia (5)	0.81	0.93	0.95	0.39	0.78	0.73	0.91	0.89
Malaria (3)	0.37	0.35	0.11	0.41	0.08	0.38	0.44	0.54
LVS-Francisella tularensis (5)	0.45	0.33	0.32	0.22	0.27	0.25	0.24	0.40

Infection (No. of patients) PPP (15 pathogens, added PR8, ASFV, VACWR)	Mean Sig.	T-test p-val.	Signal *-log(P-val.)	Signal to Noise	Median Signal	Mean Ranks	Wilcoxon	Pearson Correlation
Valley fever (3)	0.90	0.19	0.30	0.20	0.18	0.30	0.31	0.92
ASFV (4)	0.99	0.64	0.96	0.69	0.98	0.94	0.84	0.99
WNV (6)	0.57	0.59	0.61	0.47	0.61	0.49	0.38	0.57
Vaccinia (5)	0.89	0.36	0.56	0.67	0.88	0.63	0.44	0.80
Malaria (3)	0.43	0.18	0.17	0.17	0.39	0.29	0.35	0.38
LVS-Francisella tularensis (3)	0.29	0.58	0.46	0.25	0.19	0.49	0.46	0.54
Influenza(5)	0.84	0.96	0.97	0.33	0.66	0.96	0.97	0.99

Table 5- 2 Summary of the worst AUC-ROC changes between array iterations, after the addition of Influenza peptides in PPP (15), PPP (no. of pathogens represented as peptides on array).

Infection (no. of patients)	PPP (12)	PPP (14)	PPP (15)	Statistical metric
------------------------------------	-----------------	-----------------	-----------------	---------------------------

Valley fever (3)	0.94	0.91	0.90	Mean Signal
WNV (6)	0.95	0.97	0.59	T-test p-value
Vaccinia (5)	NA*	0.93	0.36	T-test p-value
Francisella tularensis (LVS) (6)	0.37	0.45	0.29	Mean Signal
Malaria (3)	0.23	0.54	0.38	Pearson Correlation

Cross-reactivity observed on pathogen peptide array from evolutionarily related pathogen exposures

Cross-reactivity is not limited to the inclusion of influenza peptides. Two out of the five tested Vaccinia vaccinees showed reactivity to both ASFV and Vaccinia peptides. Given that both these pathogens are double stranded DNA viruses and belong to evolutionarily related viral families, Asfarviridae and Poxviridae, one might expect significant commonality in peptide motifs. Cross-reactivity is also observed between Herpes virus infected individuals (human sera) and ASFV/Vaccinia peptides as demonstrated in *Figure 5-6*.

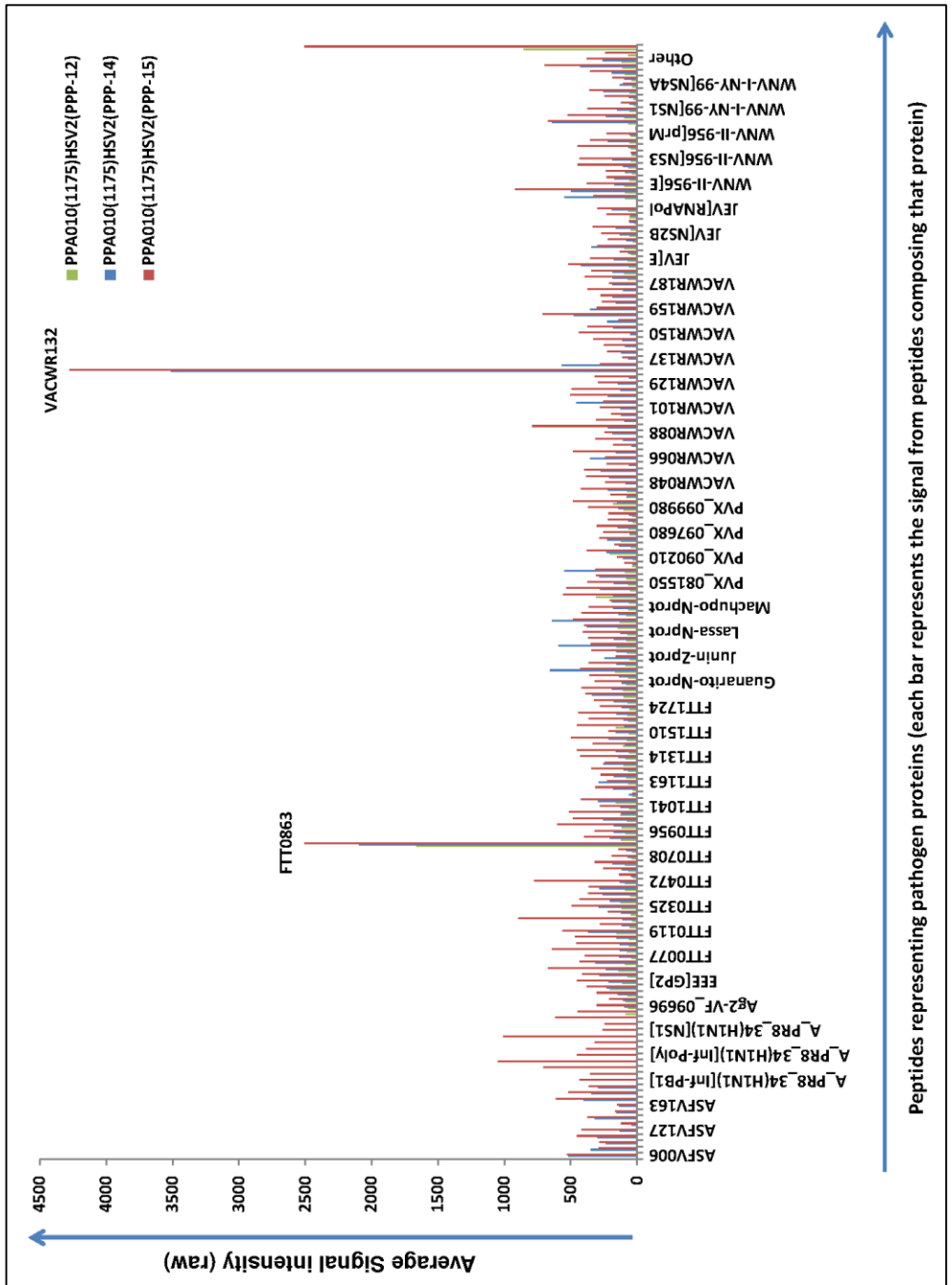


Figure 5- 6 Cross-reactivity displayed on three versions of PPP arrays from one HSV-2 infected individual's sera.

The Y-axis shows the scale of non-normalized signal intensity from averaging signal of peptides per pathogen protein (X-axis). The green bars display signal from peptides averaged per protein from the 12 pathogen peptide array. Blue bars represent signal from the 14 pathogen peptide array and Red bars represent signal intensities from the 15 pathogen peptide array containing influenza peptides.

ASFV is a swine infection and has currently not been documented as being transmitted to humans. Though ASFV-like genetic sequences have been isolated from febrile patient's sera in the Middle East and several sewage sources [40]. It is highly unlikely the sera we tested represents past exposure to ASFV. Therefore the reactivity on ASFV peptides is almost assuredly due to cross-reactivity. The prior exposure and vaccination history of both Vaccinia vaccines and herpes virus infected sera is unavailable. It is therefore, not possible to exclude prior Vaccinia vaccination in Herpes infected sera or Herpes exposure in Vaccinia vaccines. To test whether antibody cross-reactivity between related pathogens poses a significant diagnostic problem, we tested four Herpes virus infected patient sera on the arrays which do not have herpes virus peptides represented. We observed cross-reactivity to ASFV and Vaccinia peptides (*Figure 5-6*) which was expected given that they are both dsDNA viruses like Herpes [40].

Simulating an artificial infection using multiple monoclonal antibodies

In order to de-convolute cross-reactivity observed from infected sera on PPP-15 arrays containing influenza peptides a mix of monoclonal antibodies was processed on all

three versions and array signals obtained. The monoclonal antibody mix experiment was done to mimic a polyclonal infection specific immune response, except where the linear epitope peptides expected to capture those antibodies were known *a priori*. The experiment included eight pre-characterized linear epitope binding monoclonal antibodies as listed in *Supplementary Table 5- 1*. In addition to the eight monoclonals, three influenza polyclonals against immunodominant antigens hemagglutinin (HA), neuraminidase (NA) and nucleoprotein (NP) were added in samples denoted as ‘with Influenza (INF)’ to study the effect of having a memory influenza antibody component within non-influenza infectious sera. **Figure 5- 7** illustrates the median signal intensity for three peptide groups on three array versions with or without the influenza antibody component.

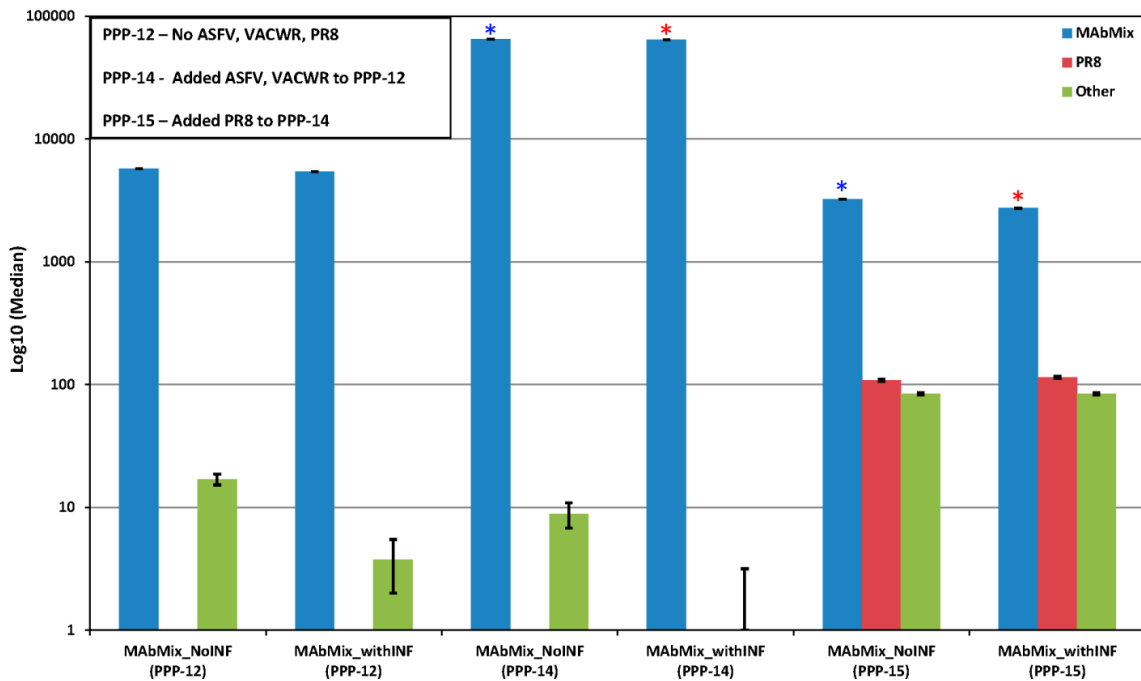


Figure 5- 7 Median signal intensities on a log₁₀ scale for 8 monoclonal antibody epitopes (blue bars) versus signals from all other peptides on the array (green bars) and PR8 influenza peptides (red bars). Error bars represent standard error, P-value cut-off = 0.125.

* Significant between arrays with and without influenza peptides for monoclonal antibody mix experiment without an influenza antibody component on a one-tailed, paired t-test (p-value=0.02)

* Significant between arrays with and without influenza peptides for monoclonal antibody mix experiment with an influenza antibody component on a one-tailed, paired t-test (p-value=0.02)

The blue bars represent the binding observed on the eight linear monoclonal antibody epitope peptides. Signals from all the remaining peptides on the array are represented by

green bars and influenza PR8 peptides on PPP-15 array containing them are represented by red bars.

The remaining peptides (non-monoclonal pathogen epitopes) on the array (green bars) have 19%, 3-mers in common with the immunogens used to generate the 8 monoclonal antibodies. These 3-mers might represent potential antibody contact points which explains the cross-reactivity observed on some non-monoclonal epitope peptides on each version of the array (green-bars). This number of n-mers in common between the remaining peptides and monoclonal antibody immunogens reduces as expected to 1.8% in common when searching for 4-mers. Despite the addition of influenza polyclonal antibodies within the monoclonal antibody mix, a clear bifurcation of influenza specific and monoclonal specific antibody responses can be measured on PPP-15 array. A surprising observation, during this analysis was the binding observed on influenza peptides from monoclonal antibodies despite no influenza polyclonals added with the monoclonal antibody mix (PPP-15, MAbMix_NoINF). This as well could be partially explained by the number of 3-mers in common between influenza peptides and monoclonal antibody immunogens (22%). Additionally, the amount of antibody reactivity captured from monoclonal antibodies on PPP-15 was statistically significantly lower as compared to that observed on PPP-14. This observable change in median signal intensities corresponds to a significant change in antibody binding distribution on the three array versions as observed from the antibody binding histograms of this data in *Figure 5-8*. The peptides for each monoclonal antibody are highlighted using arrows

demarcating their position within the histograms. This suggests cross-reactivity occurs on a short n-mer amino acid level to partial epitopes within unrelated peptides.

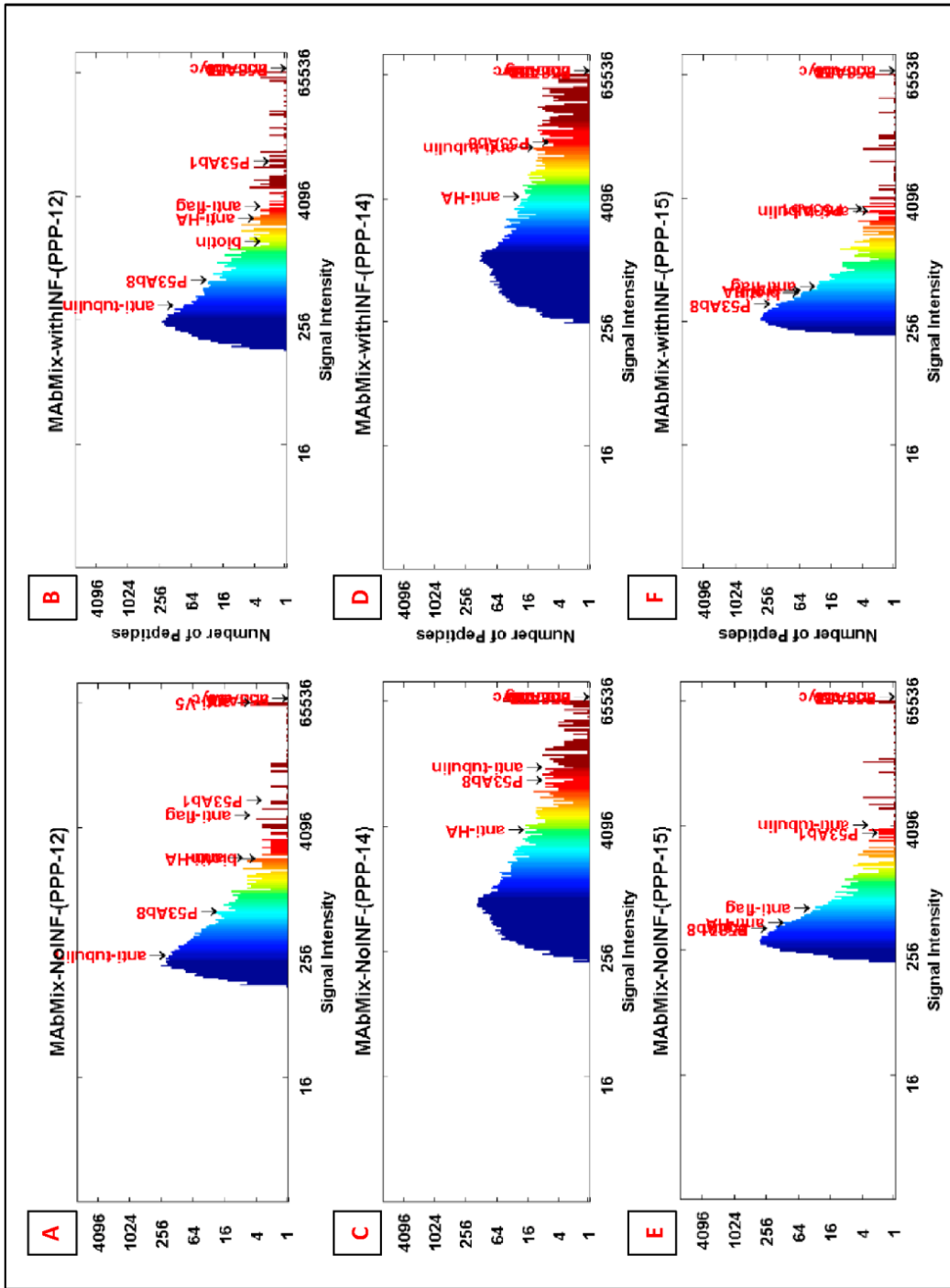


Figure 5- 8 Monoclonal antibody mix on pathogen arrays.

Histograms showing the distribution of signal intensities due to monoclonal antibodies binding peptides on three PPP arrays. The Y-axis shows the number of peptides at a given signal intensity (red=high signal, blue=low signal) whose range is displayed on the X-axis. The positions within these histograms showing cognate monoclonal antibody binding epitope peptides, is highlighted with arrows. (PPP-12 has 12 pathogen peptides excluding Influenza, ASFV and Vaccinia peptides; PPP-14 has 14 pathogen peptides excluding influenza peptides; PPP-15 has 15 pathogen peptides including influenza).

Influenza antibody reactivity observed in individuals responding to non-influenza virus exposures

Due to a high level of homology among all influenza virus proteomes, representing the Influenza PR8 proteome in the form of peptides, inadvertently also represents multiple human vaccine strains. *Figure 5- 9* summarizes the analysis performed to de-convolute influenza peptide related cross-reactivity observed on the PPP array.

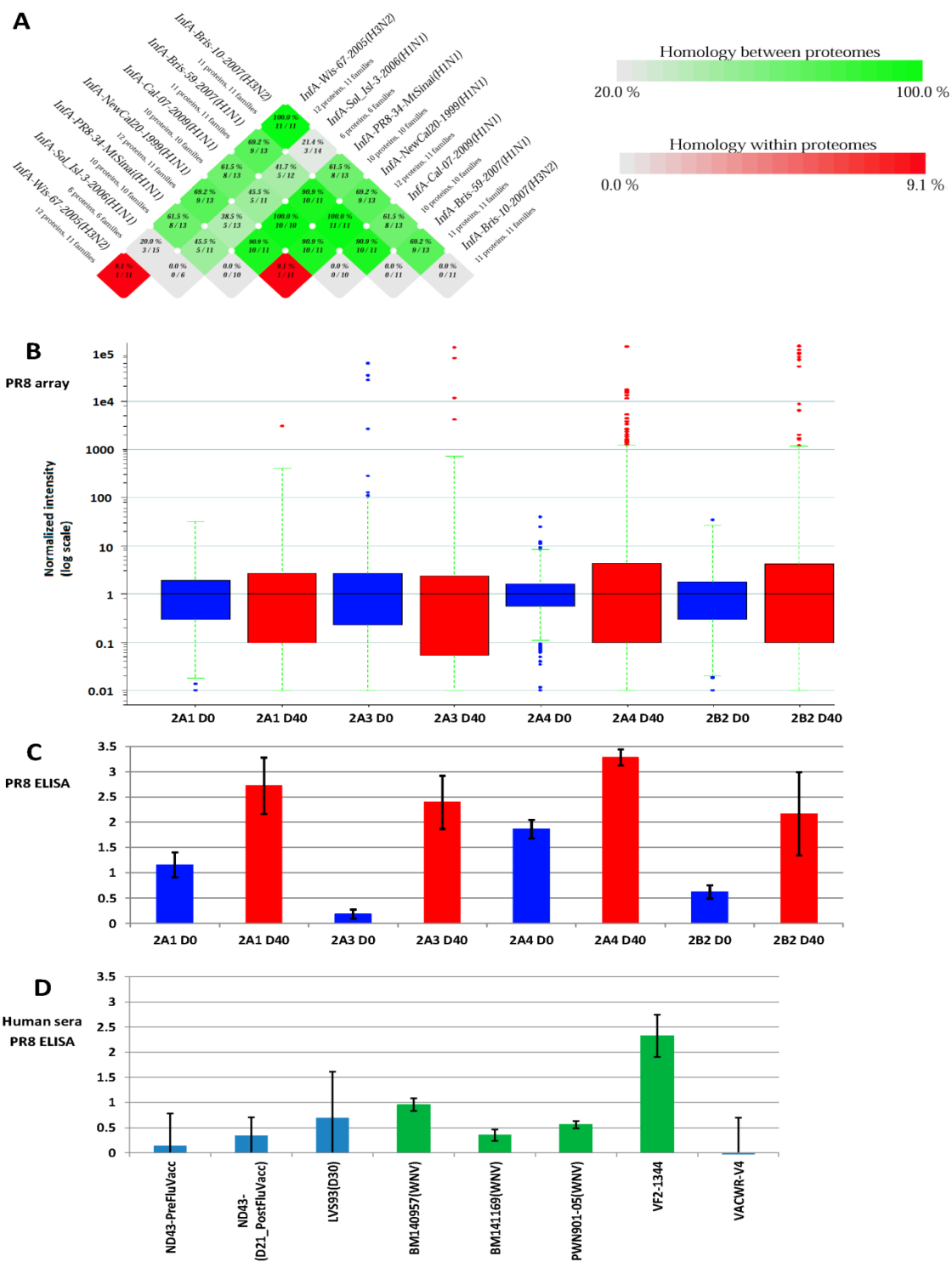


Figure 5-9 Influenza reactivity observed in individuals with non-influenza exposures.

A. Influenza PR8 proteome homology with other human influenza vaccine virus proteomes (60 to 100% homologous) B. Box-Cox plot displaying pre-existing reactivity observed in special pathogen free naïve mice (D0) Influenza Pre (blue) versus 40 days (D40) post infection (red) on 283 influenza PR8 peptides from pathogen proteome peptide array. The line in the center of the box represents the median signal intensity. C. PR8 ELISA (blue bars), a measure of antibody reactivity observed in naïve mice (D0 = Day 0) along with reactivity from same sera on day 40 (red bars). D. Reactivity of serum antibodies in a whole virus (PR8) ELISA for some human donors whose serum antibodies strongly bound PR8 epitope peptides on the pathogen array (green bars). Averaged values from 3 replicates per ELISA measurement are shown and error bars in panels B and D represent standard deviation. The Y axes represent relative fluorescence on array in panel B and absorbance at 405 nm in panels C & D. The data reported in panels C and D is from 1:50 serum dilution for both mouse and human sera.

Figure 5- 9, Panel A is a BLAST matrix obtained through CMG-biotools representing the extent of proteome overlap between Influenza PR8 and human vaccine strains. The matrix represents 49 comparisons (7X7) of pathogen proteomes. Every cell of the BLAST matrix represents BLAST queries with a 50% homology cut-off between a total of 72 proteins summarizing the results of 4,418 BLAST searches. The 2006-2009 human influenza vaccine strains were 60%-100% homologous with PR8. In order to determine if influenza peptides could compete for non-influenza infection specific antibody response, some patient sera with sufficient volumes available were tested for cross-reactivity using a whole PR8 virus ELISA. We hypothesize that the change in

antibody binding observed from non-influenza infections might be due to competition for antibodies between influenza peptides and cognate priority pathogen's peptides. To test this hypothesis without potentially confounding vaccination history from human sera, specific pathogen free (SPF) Naïve mouse sera were collected before and 40 days after PR8 infection and their antibody response was measured on both the PPP-15 microarray (*Figure 5- 9*, Panel B) and PR8 ELISA (*Figure 5- 9*, Panel C). All mice tested including Naïve, showed pre-PR8 exposure antibody cross-reactivity to Influenza PR8 in the ELISA and on the pathogen proteome array. Using Gnotobiotic mice instead of SPF mice might show lesser PR8 reactivity pre-exposure; however, this does not exclude the ability of influenza peptides to non-specifically capture antibody reactivity not related to PR8 exposure.

Figure 5- 9, Panel D shows antibody cross-reactivity as measured by an ELISA from infected human sera (green bars) having non-influenza pathogen exposures. The blue bars represent un-infected pre and post-vaccine sera from one 2006-2007 seasonal influenza vaccinee (ND43) and one *Francisella tularensis* Live vaccine strain (LVS) recipient sera collected in 2009 (LVS93). The probability that LVS93 might have either received or been exposed to the strains in 2006-2007 seasonal Influenza vaccine cannot be excluded. The Influenza vaccine (ND43) pre and post-vaccine serum was included to demonstrate the specificity of the PR8 ELISA. This individual had received the 2006-2007 seasonal influenza vaccine which included another H1N1-like virus A/New Caledonia/20/99 strain, 90.9% homologous to the PR8 strain. ND43's pre and post-vaccine sera did not show significant antibody reactivity on the A/Puerto Rico/8/1934

H1N1 ELISA. This was not an end-point ELISA because it was performed as an alternative measurement of the cross-reactivity observed from non-influenza infection on the PPP array. Average absorbance values were calculated for the most descriptive dilution. The remaining dilutions till 1:800 were processed to observe a linear trend in data so as to verify the observations from 1:50 diluted sera. The sensitivity of a peptide microarray is higher as compared to that of an ELISA [158]. Therefore, the 1:50 dilution was more informative on an ELISA as compared to the 1:500 used for the peptide microarray. Additionally, arrays were processed using 1:50 and 1:100 serum dilution to estimate if concentrating the serum amount would overcome the influenza peptide directed cross-reactivity. The assumption was that increasing the concentration of sera would saturate the influenza peptides sufficiently to reduce competition, thereby, allowing priority pathogen specific antibodies to bind their appropriate target peptides. The two serum concentrations tested, 1:50 and 1:100, however were not sufficient to improve the ability of priority pathogen peptides to capture additional reactivity. *Figure 5- 10* shows two WNV infected individuals sera in panels A and B at the default standard 1:500 serum dilution versus 1:50 and 1:100. The arrays were processed under thermodynamic conditions previously optimized for this platform to reduce cross-reactivity, primary sera incubated for 16 hours at 23°C. At both higher concentrations the average antibody reactivity captured by influenza peptides and several other non-cognate infection pathogen groups is higher than the average antibody reactivity captured by cognate WNV peptides. A similar experiment was repeated using arrays without influenza peptides to observe the antibody reactivity at varying concentrations of serum

dilution. The average signal response from pathogen groups of peptides for three VF infected individuals is depicted in panels A, B, and C of *Figure 5- 11* at the standard 1:500 versus 1:50 and 1:100 serum dilution. As depicted in the figure at 1:500 serum dilution, two out of three individuals' VF reactivity is higher than that of other pathogen groups of peptides. This suggests that the 1:500 serum dilution as previously optimized for this assay is appropriate to allow cognate pathogen antibodies to bind their target pathogen peptides under thermodynamic conditions optimized for this assay.

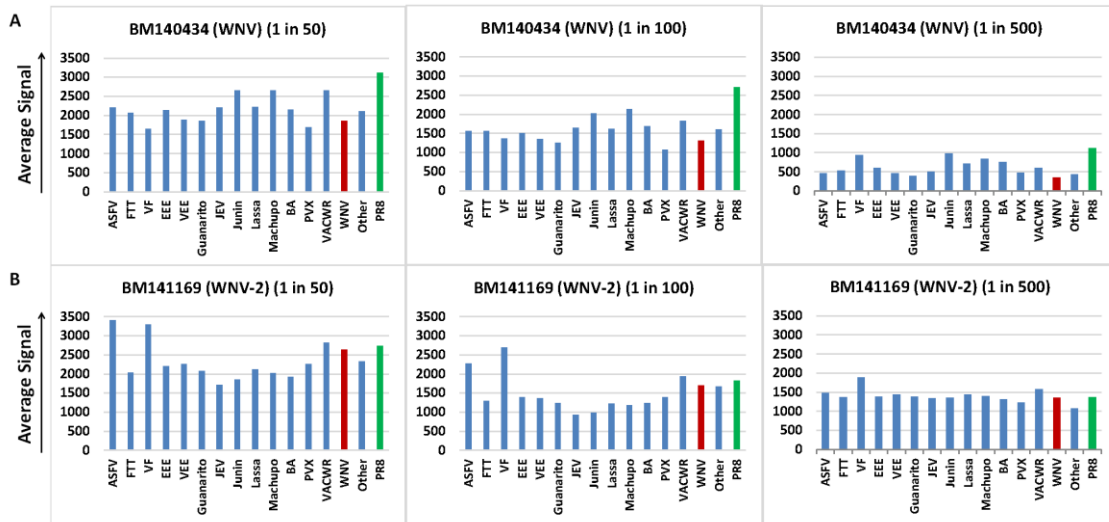


Figure 5- 10 WNV Patients sera processed at three dilutions on PPP-15.

The average signal per pathogen groups of peptides is plotted on the Y-axis. Two WNV infected individuals sera at varying antibody dilutions are presented in panels A and B. The average signal per pathogen groups of peptides is plotted with WNV group antibody signal highlighted in red and Influenza PR8 group antibody signal highlighted in green.

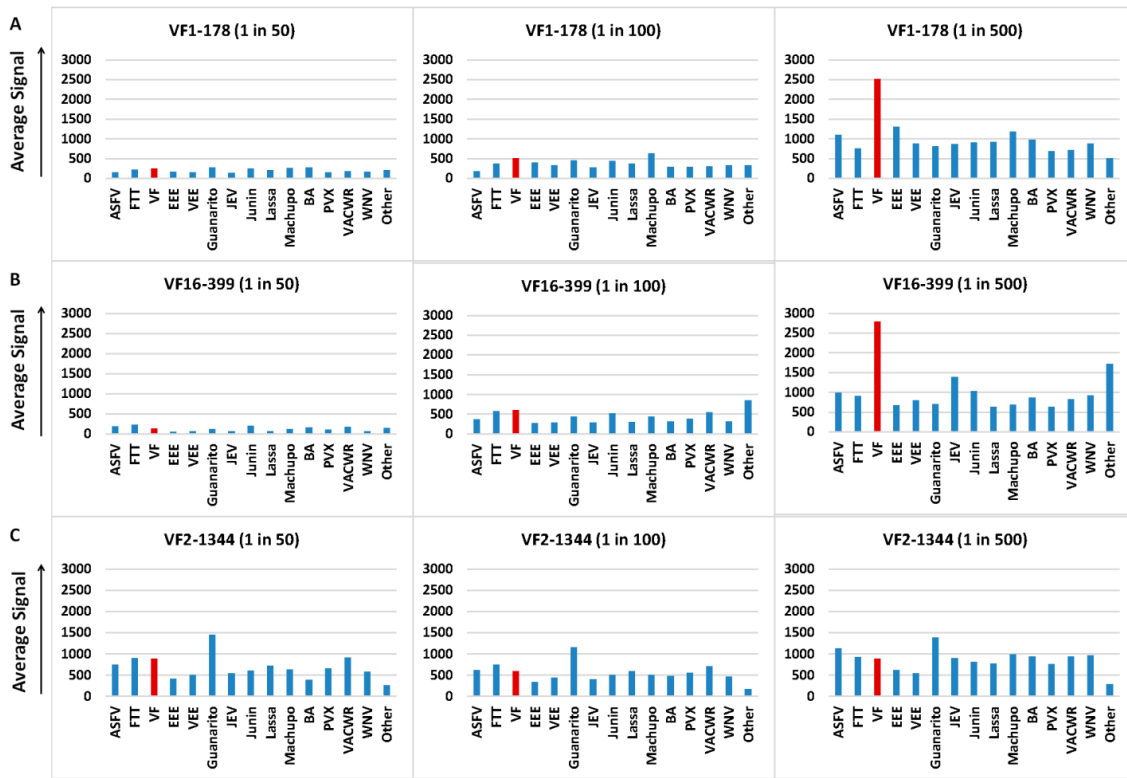


Figure 5- 11 VF Patient sera processed at three dilutions on PPP-14.

Three VF infected individuals at varying antibody dilutions as listed in the figure are plotted in panels A, B and C. The average signal per pathogen group of peptides is plotted on the Y-axis with signal from 83 VF epitope peptides averaged together and highlighted in red.

Taken together these observations indicate that, increasing the concentration of serum on the platform is not sufficient to retrieve cognate infection reactivity from competing influenza peptides. Including influenza peptides might compete for the antibody response captured by priority pathogen peptides on the PPP array. Antibody binding data obtained from arrays containing influenza peptides would be impossible to

re-attribute to the original infection using the eight statistical metrics developed for data analysis likely requiring bioinformatic intervention.

Defining the umbrella of antibody reactivity observed on the pathogen array

Using standard statistical metrics previously designed for this assay, the pathogen peptide ranking system failed to classify priority pathogen infection on an array including influenza peptides. The cross-reactivity observed on this assay might be likely attributable to short, identical amino acid sequences in common between influenza peptides and other priority pathogen peptides. As attempted earlier by Ulrich *et al.* [92], we utilized the pattern of cross-reactivity due to short, identical amino acid sequences in common between unrelated pathogens to re-attribute cross-reactivity observed towards influenza peptides. A regular expression search algorithm developed by Richer *et al.* [153] was used to select the most statistically significant n-mers per individual patient based on averaging signal intensities above background (>500 FIU).

Table 5- 3 displays the results from using the pattern of number of 2-7mer epitopes in common between individual patients classified using SVM with leave one out cross-validation (LOOCV). The classification method is applied to all three versions of the array. Panel C shows the recovery from cross-reactivity and incorrect infection assignment when using SVM to classify samples based on n-mer commonality.

Table 5- 3 SVM (LOOCV) results from PPP-15 using the n-mer analysis for classification

A.) Infections tested on PPP-12	Total samples	No. correctly classified	%Correctly classified
Malaria	3	0	0
ASFV	NA	Not processed, no peptides	NA
WNV	5	4	80
LVS	5	1	20
Vaccinia	NA	Not processed, no peptides	NA
VF	6	6	100

B.) Infections tested on PPP-14	Total samples	No. correctly classified	%Correctly classified
Malaria	2	0	0
ASFV	4	4	100
WNV	6	6	100
LVS	5	1	20
Vaccinia	5	4	80
VF	3	2	67

C.) Infections tested on PPP-15	Total samples tested	No. correctly classified	%Correctly classified
Malaria	3	1	33
ASFV	4	4	100
WNV	6	5	83
LVS	3	1	33
Vaccinia	5	5	100
VF	3	3	100
Influenza	5	5	100

Due to comparing the count of unique 2-mers, 3-mers through 7-mers in common within individual patients, the fundamental assumption of independence among features required for using machine learning algorithms like SVM is not violated. The n-mers in one individual are compared to the n-mers in another completely independent individual. Using n-mer umbrella classification arrays containing influenza virus peptides, PPP-15, showed 100% correct classification for ASFV, Vaccinia, VF and Influenza samples. This method was able to partially recover the accuracy of this assay to detect WNV, 5/6 sera correctly detected 83% correct. The WNV infected patient serum set contained one patient whose sera was part of a longitudinal seroconversion panel from SeraCare (PWN-901) [159]. On day 0 time point of this panel when the patient was still sero-negative on 2 different standard WNV EIA tests (Focus IgG, IgM and PANBIO IgG, IgM) for IgG & IgM and the Taqman RNA was <30 copies/ml, it was accurately detected on the PPP-15 array as having WNV using n-mer umbrella classification. This demonstrates the utility of such an n-mer approach in sensitively classifying disease. LVS and Malaria sera tested however could not be accurately detected (1/3 sera correctly classified).

Discussion

My goal in this study was to increase the accuracy of the multiplexed PPP array and test its limitations. For de-convoluting whether or not the addition of common exposure pathogen peptides on PPP array improves the accuracy of detection of the priority pathogen, three versions of arrays were made with incremental addition of common exposure pathogen peptides. Initially we created a pathogen proteome peptide

array representing 12 priority NIAID categories A, B, C pathogens (PPP-12) and tested sera from 4 exposures (VF, WNV, Malaria and *F. tularensis* LVS) to discern the predictive potential of such a system. VF and WNV out of the four exposures tested could be successfully distinguished using cognate peptides from those pathogens. We added ASFV and Vaccinia peptides to this existing array (PPP-14) and re-tested its accuracy at discerning 6 exposures apart. VF, ASFV, WNV, and Vaccinia could be distinguished with AUC-ROC >90%. There was moderate improvement in the AUC for *F. tularensis* and Malaria exposures as compared to the previous 12 pathogen peptide platform. It was estimated that the addition of Vaccinia and ASFV pathogen peptides represented sufficient double stranded DNA virus related peptides to be able to capture Herpes virus related reactivity. The hypothesis was that the addition of common pathogen peptides might improve the accuracy of distinguishing priority pathogen exposure. This was tested by processing Herpes virus infected patient sera on the array to observe cross-reactivity with ASFV and Vaccinia and several other pathogen peptides on the array despite not directly representing any Herpes virus specific peptides. To test this concept further, PR8 influenza peptides were added to this 14 pathogen array (PPP-15) given that the H1N1 PR8 strain overlaps significantly with other human influenza virus vaccine strains. The addition of influenza peptides significantly reduced the ROC-AUC of detecting priority pathogen specific antibody response on the multiplexed PPP array.

The arrays without influenza peptides showed the best ROC-AUC classification accuracy. The addition of influenza peptides to the array resulted in adversely affecting the detection capability of the platform for exposures such as WNV, Vaccinia, *F.*

tularensis and Malaria. VF, ASFV and Influenza reactivity was not adversely affected by the addition of Influenza peptides. Cross-reactivity to influenza within VF, WNV, LVS exposure patient sera was confirmed on a PR8 ELISA. Several special pathogen free naïve mice also showed PR8 cross-reactive antibodies in an ELISA before being experimentally infected with PR8. Since antibodies cross-reactive to influenza were found to be present in un-related pathogen exposures, it was deemed best to avoid including influenza peptides within a priority pathogen array so as to maintain its ability to discern multiple priority pathogen infections apart. One strategy to improve the assay's detection ability was to remove cross-reacting common pathogen representing peptides. An alternative strategy would be to develop a bioinformatic analysis pipeline that would discern the appropriate cognate infection while circumventing the cross-reactivity observed on the assay.

In order to delineate whether or not changing the peptide diversity on the array lead to significantly different antibody binding, an artificial infection sera, including eight well-characterized monoclonal antibodies, was processed on each array. Change in peptide diversity significantly altered the binding pattern observed on the platform between PPP-12, 14 and 15 as depicted by Figure 5-8 panels A, C and E. Monoclonal antibodies to linear peptide epitopes not directly related to influenza epitopes appeared to bind influenza PR8 peptides. The presence or absence of influenza polyclonal antibody component within the mix of 8 monoclonal antibodies did not have a statistically significant contribution to directing the binding observed on the assay in contrast to the effect observed by adding or removing influenza peptides.

One explanation for the observed change in binding after adding influenza peptides could be that on an amino acid frequency level, influenza, unlike any other pathogen represented on the assay has a greater frequency of the negatively charged, glutamic acid within their proteome. And while this difference in amino acid frequencies might not be significantly high, it appears to be enough to redirect other pathogen antibody reactivity and even unrelated monoclonal antibodies to influenza peptides. The charge on an antigen is known to increase non-specific cross-reactive binding in immunoassays [160]. Herpes viruses, for example, have more Arginine's (positively charged amino acid) in their proteome as compared to any other priority pathogen tested on this array. For the purpose of this study though, it is empirically evident that exclusion of influenza peptides from a multiplexed assay designed to distinguish multiple priority pathogen infections might be an appropriate strategy to accurately detect priority pathogen infection.

A bioinformatic strategy was implemented to trace the original groups of antibodies generating the signature response on the array, thereby de-convoluting the cross-reactivity observed. We ignored existing peptide annotations obtained from amino acid position within pathogen proteomes and instead re-analyzed the datasets based on signal intensities of '*umbrellas of antibody reactivity*'. The ultimate goal was to generate an algorithm capable of bioinformatically discerning the umbrellas of antibody reactivity observed on the assay despite apparent cross-reactivity allowing distinction of the correct infection/antigen (exposure) regardless of changes in the platforms peptide diversity. This strategy aims to delineate the antibody n-mer umbrella of reactivity per infection,

measuring how many n-mers overlap within individual patients and using those set of infection specific umbrella patterns to de-convolute the original infection. This strategy of counting the number of occurrences of a given n-mer or string to create a mathematical signature which could then be used to classify data is typically used in natural language processing for example, when creating e-mail spam-filters [161]. The signature response represents the number of n-mers in common per patient with a given infection versus all other infections. All individuals having a given infection have a specific pattern of overlapping n-mers in common with individuals having other infections and thus based on the extent of overlapping n-mers, get classified into a specific infection group. The antibodies from infected individuals and therefore, high signal intensity peptides they bind on PPP array as well as n-mer umbrellas observed within individuals sera having a given exposure are not always the same for all individuals having that exposure. This individual variation in immune response for one infection could be explained by the observation that immunizing animals experimentally with the same antigen yields antibodies reacting to different epitopes within that antigen per individual animal within the group [162].

Representing the complete proteome of a pathogen ensures accurate detection on the assay. While this trend has been observed for small viruses such as WNV and Influenza on PPP array, it is yet to be tested for larger pathogens in a multiplexed format. The assay has tremendous utility if all known encephalitis viruses are represented on it, as it would reduce the need for central nervous system infection diagnosis requiring invasive procedures such as lumbar puncture. Given the limited diagnostic algorithms

applied to this data, it might be best to avoid inclusion of common pathogens such as influenza alongside priority pathogens. In conclusion, the addition of influenza virus peptides, to the PPP array does not improve its diagnostic ability.

Grant Acknowledgement

This work was supported by the Chemical Biological Technologies Directorate contracts HDTRA-11-1-0010 from the Department of Defense Chemical and Biological Defense program through the Defense Threat Reduction Agency (DTRA) to SAJ.

Acknowledgement

The authors wish to thank Lawrence Livermore National Laboratory for providing infected patient sera for West Nile virus and Malaria infections originally acquired from SeraCare. We thank Dr. Ian Lipkin at Columbia University for contributing Herpes virus infected patient serum samples. We thank Dr. John Galgiani from the Valley Fever Center for Excellence for providing VF infected IDCF characterized longitudinal patient samples. We thank Sara Matsumoto and Daniel Wrapp for helping analyze microarray slide image data and Jameson Berry for processing an ELISA.

Supplementary Information

Supplementary Table 5- 1 Monoclonal and polyclonal antibodies used on PPP array

Antibody Name	Protein Target	Ab Clone	Epitope	Epitope Length (aa)	Source	Cat #	Host Species	Isotype
Monoclonal antibodies to linear epitopes								
FLAG	KAX71_P ANIM Potassium channel toxin alpha-KTx 7.1	F- tag- 01	DYKDDDDK	8	Novus Biolog icals	NB500 -554	Mou se	IgG1
P53Ab 1	P53_HUM AN Cellular tumor antigen p53	pAb2 40	RHSVV	5	Millip ore	CBL40 4	Mou se	IgG1
[Leu5] - Enkeph alin	PDYN_H UMAN Proenkeph alin-B	1193/ 220	YGGFL	5	AbD Serote c	4140- 0159	Mou se	IgG1
P53Ab 8	P53_HUM AN Cellular tumor antigen p53	P53A b8	SDLWKL	6	Therm o	MA1- 19055	Mou se	IgG2 b
DM1 A	TBA1A_H UMAN Tubulin alpha-1A chain	DM1 A	AALEKD	6	Millip ore	05-829	Mou se	IgG1 kapp a
Biotin	BiotinMim ic	-	SGGGPCHPQ FPRCYA	15	Santa Cruz Biotec h	sc- 101339	Mou se	IgG1

cMyc	MYC_HUMAN Myc proto-oncogene protein	9E-10	EQKLISEEDL	10	AbD Serotec	MCA2200G	Mouse	IgG1
V5	V_SV5 Non-structural protein V	SV5-Pk2	GKPIPPLLGLDST	14	AbD Serotec	MCA2892	Mouse	IgG1

Influenza polyclonal antibodies

HA	Influenza A PR8(H1N1) HA	IC5-4F8	native HA	565	BEI Resources	NR4542	Mouse	IgG3.k
NA	Influenza A PR8(H1N1) NA	NA2-1C1	NA-tetramer	454	BEI Resources	NR4540	Mouse	IgG1.k
NP	Influenza A Okada(H2N2) nucleoprotein	C43	nucleoprotein	498	Abcam	ab128193	Mouse	IgG2a

CHAPTER 6

CONCLUSION

Coccidioidomycosis

The first cases of Valley Fever (VF) were observed in agricultural workers from central California in 1890's. In 1892, a physician named Alejandro Posada, diagnosed the cutaneous inflammation in an Argentinian soldier originally misdiagnosed as cancer as instead emanating from an infectious source, *Coccidioides* [163,164]. The infection initiates post exposure of hosts to spores namely, Arthroconidia. The weaponization potential of *Coccidioides* (Lethal Dose LD50, 300 arthroconidia in non-human primates) is greater than that of *Bacillus anthracis* (LD50, 8000 spores in monkeys), which was why it was included in the NIAID Priority pathogen list [165]. Johnson *et al.* [63] estimated that a single arthroconidia was sufficient to cause infection in mice. Between 1 to 10, arthroconidia are sufficient to establish infection in humans [166]. Once infected the arthroconidia convert into spherules with sizes ranging from 3 μm [167-169] to 200 μm [170] with the largest recorded at 262 μm [171]. The size of the spherule depends on the immune status of the host, with observable differences in C57BL/6 VF susceptible mice versus resistant mice to *Coccidioides*, Swiss-Webster [169]. Galgiani *et al.* documented that spherules sizes observed in-vitro (80-100 μm) were smaller than those observed in vivo [172]. The size of B and T cells typically ranges between 7-10 μm in diameter and that of antigen presenting cells such as dendritic cells and macrophages is between 10-22 μm [173] rendering them partially ineffective when responding to larger

spherules. Given that the immune machinery of hosts is severely overwhelmed by this pathogen, early detection of disease is crucial to facilitate appropriate anti-fungal treatment. Newer drugs like Nikkomycin Z have shown promising results in murine models by eradicating infections if given 5 days post-exposure [174] and also in dogs [175].

The recovery rate of this fungus from blood unlike *Mycobacterium tuberculosis* is very low, 0.4% i.e. 20 out of a total of 5,026 samples (6-year retrospective study); making direct pathogen detection based diagnostics less sensitive [65]. To date, depending on the site of primary infection and symptoms manifested due to this disease, the presumptive differential diagnosis can include everything on the spectrum from cancer (fungal granuloma/swollen lymph nodes), arthritis (joint pain), community acquired pneumonias such as tuberculosis (lung nodule/patch, respiratory distress), psychological distress/ depression (meningitis) to chronic fatigue syndrome (chronic muscular pain). Early detection of VF infection would also help obviate unnecessary costs associated with incorrect differential diagnosis.

Development of a microarray diagnostic that exceeds existing diagnostic standards

Developing higher sensitivity assays often comes at the cost of specificity. After selecting random peptide features for the valley fever diagnostic sub-array, we learnt that using as broad a training dataset representing as many confounding conditions during feature selection was crucial to maintaining high assay specificity. The ‘VF-diagnostic’ sub-array (Chapter 2) is a 100% sensitive diagnostic and could be used in combination

with the higher specificity immunodiffusion (IDCF) and enzyme immunoassays (EIA) for differential diagnosis of disease [164]. The comparison of natural epitopes to non-natural mimotopes has been reviewed on multiple occasions both structurally and informatically [31,89,176]. Chapter 3 shows an empirical comparison of life-space epitopes versus non-natural sequence peptides in the context of a diagnostic assay. Life-space VF epitope peptides show higher specificity when distinguishing VF from LVS and normal, but random peptides show higher sensitivity. An interesting aspect of this work was the di-peptide modulation suggested to improve the accuracy of the Smith-Waterman [33] local alignment algorithm in a sequence alignment program, GuiTope [34]. This observation was made when de-convoluting why random VF predictor peptides performed with higher sensitivity than VF epitope peptides. GuiTope found several short sequence motifs in common between random peptides and VF antigens. The frequencies of di-peptides within a given protein, have been used to classify them into functional protein families [85], for designing tumor homing peptides, anti-cancer peptides [177,178] and designing cell penetrating peptides [179]. Rubenstein *et al.* [180] and Sun *et al.* [89] while characterizing epitopes noticed cooperativeness of certain di-peptide pairs as being observed at a higher frequency within epitopes as compared to non-epitope regions on antigens. Inverse-docking also known as ‘target fishing’ has been informatically viable when applied in molecular docking software for searching ‘target-like’ structures [181]. The high binding associated with short sequences having di-peptide inversions in common between life-space VF antigens and VF-predictor random peptides is empirical proof of the viability of the inverse-docking approach.

Bioinformatic analysis of pathogen proteomes toward the development of a multiplexed life-space peptide microarray diagnostic

While creating a multiplexed pathogen proteome peptide array (Chapter 4), our work assessed the various informatics strategies applied for epitope mapping. A T-cell epitope typically ranges in length from 8-12 amino acids [182] and linear B-cell epitopes range from 4-12 amino acids [88]. A conformational B-cell epitope is estimated to contain 3-mer (60%) to 5-mer (85%) linear stretches involved in epitope-paratope binding [99]. While selecting the epitopes to be represented on the multiplexed PPP array, for larger pathogens we represented protein antigens predicted to be surface proteins (ASFV) or empirically documented to be immunodominant (IEDB). For some small viruses such as WNV, we represented the whole viral proteome. Given that the human population has >3000 different MHC alleles [183], it might be prudent to represent every pathogen using their whole proteome to enable accurately capturing individual variance in antibody response to an infection. Whole proteome based protein microarray experiments performed by Felgner *et al.* document that a small portion of the pathogen's proteome is immunoreactive (~26%, Vaccinia) [109]. Due to the fine resolution obtained when using peptide microarrays as compared to using protein microarrays, it is very likely that no *a priori* selection of immunodominant or surface antigens was necessary. This concept however might need additional testing using larger patient serum sets and pathogen peptide groups to specifically compare whole proteomes peptides versus partial proteome peptides ability to capture infection specific immune response in a side by side comparison. In our comparison, the immunodominant antigen

peptides (partial proteome) were sufficient and capable of capturing and distinguishing infection specific response from other pathogen peptides. The multiplexed pathogen proteome array was capable of distinguishing 4 priority pathogen infections (VF, WNV, Vaccinia, and ASFV) apart simultaneously despite moderate cross-reactivity with greater than 90% ROC- AUC accuracy.

Designing a multiplexed pathogen proteome peptide microarray – Future directions

Although there was substantial measurable (and in many cases predictable) cross-reactivity between host antibodies and peptide antigens, there were a number of non-obvious causes for this observation on the PPP array. Given the amount of cross-reactivity observed, the discussion addresses a number of methods, both bioinformatic and biochemical, to ameliorate this seemingly intractable specificity problem. Antigen-antibody interactions observed on a multiplexed PPP array are a function of both the human patient sample being tested as well as the extensive overlap between natural pathogen sequences. The workarounds illustrate some important and quite fundamental aspects of physical characteristics of peptides, their presentation on the assay, and the intricate ways in which antibodies interact with them.

While creating the multiplexed pathogen proteome peptide (PPP) array we printed the 15 pathogen peptides in no specific physical order together in a single array (Chapter 4). Under thermodynamically optimized conditions to reduce cross-reactivity the array functioned with greater than 90% ROC-AUC at distinguishing 4 infections apart (VF, WNV, Vaccinia, and ASFV) simultaneously while it had 14 pathogen peptides. Upon

Using such an analysis, the cross-reactivity observed in Japanese, Dengue virus infected individuals to JEV could be explained [149]. Figure 6- 2 is a blast matrix generated by comparing the proteomes of various Flaviviruses using CMG-biotools [155]. 7 proteomes (7 X 7=49 comparisons, 96 total proteins) are compared through 7,886 BLAST searches using the 50% identity and 50% length match compared fragments homology criteria. Between Japanese encephalitis virus, West Nile virus and Dengue viruses there is a significant proteome level overlap ranging from 12% to 100% and this might explain some of the cross-reactivity observed on immunoassays between these Flaviviruses [148].

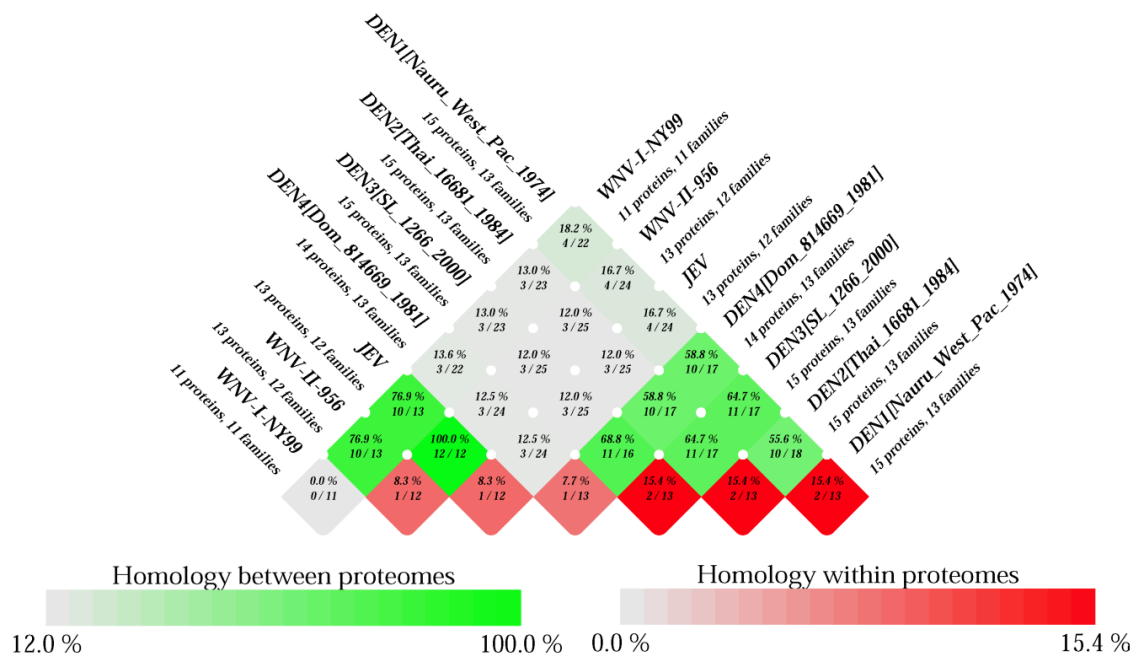


Figure 6- 2 Blast matrix depicting proteome level overlap between the four main races of Dengue virus (reference proteomes) and WNV-I and II and JEV

A BLAST hit within the CMG-biotools program is considered significant (green) if at least 50% of the two protein sequences being compared are aligned and 50% of amino acids within the alignment are identical. The last row at the bottom of this matrix depicts homology within a given pathogen proteome under the strict BLAST search match criteria (grey to red scale).

If significant overlap is observed between pathogen proteomes, those pathogen peptides could either be excluded from being multiplexed together or they could be printed on a physically separate sub-array such as that depicted in the 24-sub array format in *Figure 6- 1*. Additionally, each individual pathogen's peptides could be printed separately within a sub-array on a single glass slide representing up to 24 pathogen proteomes. Alternatively, multiple pathogen peptides could be multiplexed together based on lack of obvious proteome level overlap allowing representation of more than 24 pathogens on a single chip. In summary, when detecting Flaviviruses using pathogen epitope peptides, it might be advisable to print them on separate sub-arrays and process patient sera on them separately.

Another example where a proteome level overlap analysis would be sufficient to explain lower specificity (46 - 97%) observed on an immunoassay is on the ToRCH assay [37].

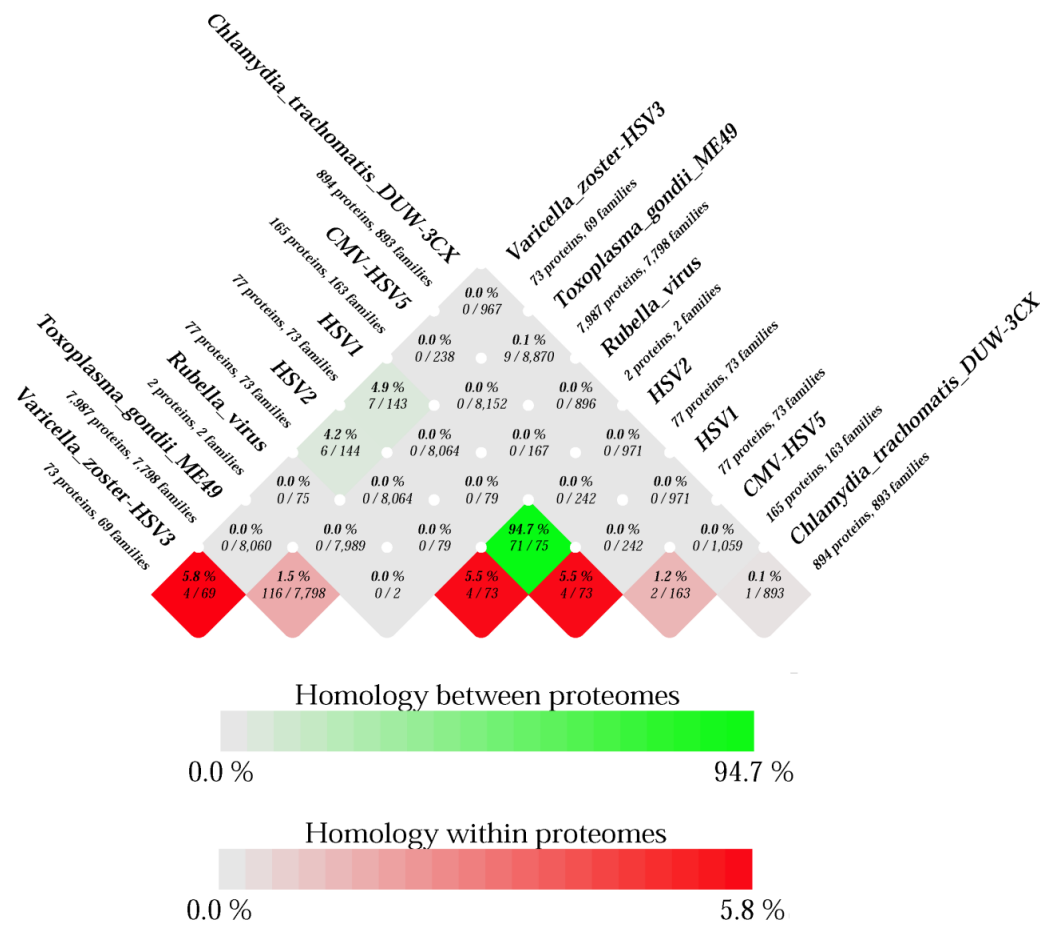


Figure 6-3 Blastmatrix showing ToRCH assay pathogen proteome overlap.

Proteomes included: *Toxoplasma gondii*, *Rubella*, *Chlamydia trachomatis*, *HSV-1*, *HSV-2*, *HSV-3* and *CMV*. A BLAST hit within the CMG-biotools program is considered significant (green) if at least 50% of the two protein sequences being compared are aligned and 50% of amino acids within the alignment are identical. The last row at the bottom of this matrix depicts homology within a given pathogen proteome under the strict BLAST search match criteria (grey to red scale).

Figure 6- 3 summarizes 86 million BLAST searches generated from pathogen proteomes represented on the ToRCH assay using the Blastmatrix program in CMG-biotools [155]. The figure summarizes a BLAST comparison of 9275 total proteins in 7 proteomes (7x7=49 comparisons). From this comparison given that HSV-1 and HSV-2 show greater than 94.7% proteome level overlap (50% identity, 50% length match criteria), it might be prudent to include them on separate sub-arrays to avoid cross-reactivity. Despite printing pathogen proteomes showing a high level of proteome level overlap on separate sub-arrays, it is likely that infected individual's sera might still display cross-reactivity to both sub-arrays. While they may still display cross-reactivity, the peptides of one pathogen will not be able to compete for reactivity from antibodies generated against another pathogen sharing multiple identical short peptides. A new data analysis pipeline would need to be developed from training on well-characterized serum samples to evaluate the extent of expected cross-reactivity. A probabilistic model based on log-odds ratios might need to be developed as has been done for the LLMDA (Lawrence Livermore Microbial detection array) [47,184] to estimate which infection, HSV-1 or HSV-2 or both is more likely based on prior empirical observations from sera for both infections respectively and co-infections processed on such an array.

If there is no obvious overlap observed through a BLAST matrix analysis then an n-mer level analysis of overlap should be conducted on both a peptide level and between peptides and pathogen proteomes if representing partial proteomes. Given that B-cell linear epitopes range from 4-12 amino acids in length and a conformational epitope shows 3-mer to 5-mer contiguous contact points within the antibody paratope as

ascertained in structural studies, it might be appropriate to note the 3-12 mer overlap and exclude pathogens showing significant overlap or print their peptides on a separate sub-array. A peptide to peptide comparison will allow *a priori* estimation of 3-mers to 12-mers in common between genetically unrelated pathogens and expected cross-reactivity attributable to these short motifs.

An example of the benefit of such n-mer short sequence level analysis can be provided using data from Andresen *et al* [36]. They developed a 900 peptide microarray representing peptides from closely related Herpes viruses (HSV-1, HSV-2, CMV, EBV) and Hepatitis C virus. They observed specific reactivity to CMV and EBV peptides from infected sera tested for those infections. However they were unsuccessful at distinguishing these Herpes viruses apart from Hepatitis C infected sera due to broad cross-reactivity observed from HCV infected sera towards Herpes virus peptides. Figure 6- 4 summarizes 173K BLAST searches generated using CMG-biotools representing pathogen proteomes from the Andresen *et al.* study. It represents a comparison of 416 total proteins in 5 proteomes ($5 \times 5 = 25$ comparisons). On a proteome level, there is no obvious overlap under stringent BLAST search criteria between HCV and the herpes viruses. However, on a 5-amino acid short sequence (n-mer) level, the extent of overlap between these proteomes is obvious as summarized in Table 6- 1, Panel A. As expected this 5-mer overlap diminishes when searching for identical 9-mers between these proteomes (*Table 6- 1*, Panel B).

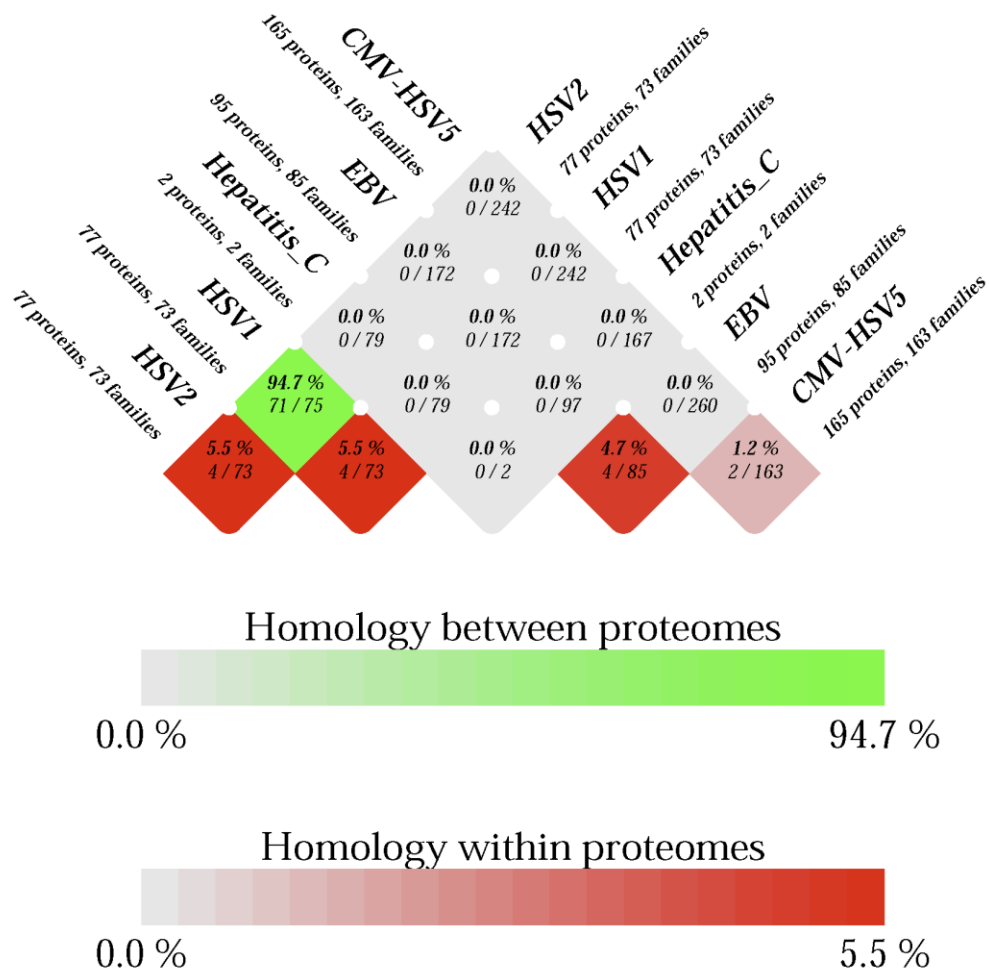


Figure 6- 4 Pathogen proteome level overlap for pathogens represented in a multiplexed 900 peptide microarray showing cross-reactivity in *Andresen et al (2009)*.

The pathogen proteomes included in this comparison are HSV-1, HSV-2, CMV, EBV and Hepatitis C. A BLAST hit within the CMG-biotools program is considered significant (green) if at least 50% of the two protein sequences being compared are aligned and 50% of amino acids within the alignment are identical. The last row at the bottom of this matrix depicts homology within a given pathogen proteome under the strict BLAST search match criteria (grey to red scale).

Table 6- 1 Unique 5-mers and 9-mers in-common between pathogens tested on the Andresen assay

A.) Unique 5-mers in common	HSV2	EBV	CMV- HSV5	Hepatitis C	HSV1
HSV2	36488	2212	2795	173	18833
EBV	2212	38977	2556	144	2116
CMV-HSV5	2795	2556	58960	169	2703
Hepatitis C	173	144	169	3151	167
HSV1	18833	2116	2703	167	36444

B.) Unique 9-mers in common	HSV2	EBV	CMV- HSV5	Hepatitis C	HSV1
HSV2	38159	26	15	0	12186
EBV	26	39939	11	0	24
CMV-HSV5	15	11	60809	0	15
Hepatitis C	0	0	0	3154	0
HSV1	12186	24	15	0	37715

From our own pathogen proteome peptide (PPP) array data, we observed cross-reactivity to ASFV and Vaccinia peptides from Herpes virus infected individuals (Chapter 5). We also noted ASFV peptide cross-reactivity from Vaccinia vaccine recipient sera. This cross-reactivity to ASFV and Vaccinia peptides from herpes virus infections could not be explained on a proteome level overlap as depicted in Figure 6- 5. The Blastmatrix generated using CMG-biotools [155] compares proteomes of the 8 known variants of herpes simplex virus with Vaccinia and ASFV representing 1294 total proteins comparisons (11X11) summarizing 1.49 million BLAST searches. The stringent

homology cut-off of 50% identity and 50% length match between query sequences was applied. HSV-1 and 2 showed 94.7% identity, HSV-3 showed 4.9% and 4.2% identity with HSV-1 and 2 respectively. The two HSV-6 strains showed 65.4% identity among themselves and HSV-6 and HSV-7 showed 28.3% (HSV-6 strain: U1102) and 32.6% (HSV-6 strain: Z29) identity. On a pathogen proteome protein level there is no overlap between ASFV and Vaccinia proteomes with Herpes virus proteomes.

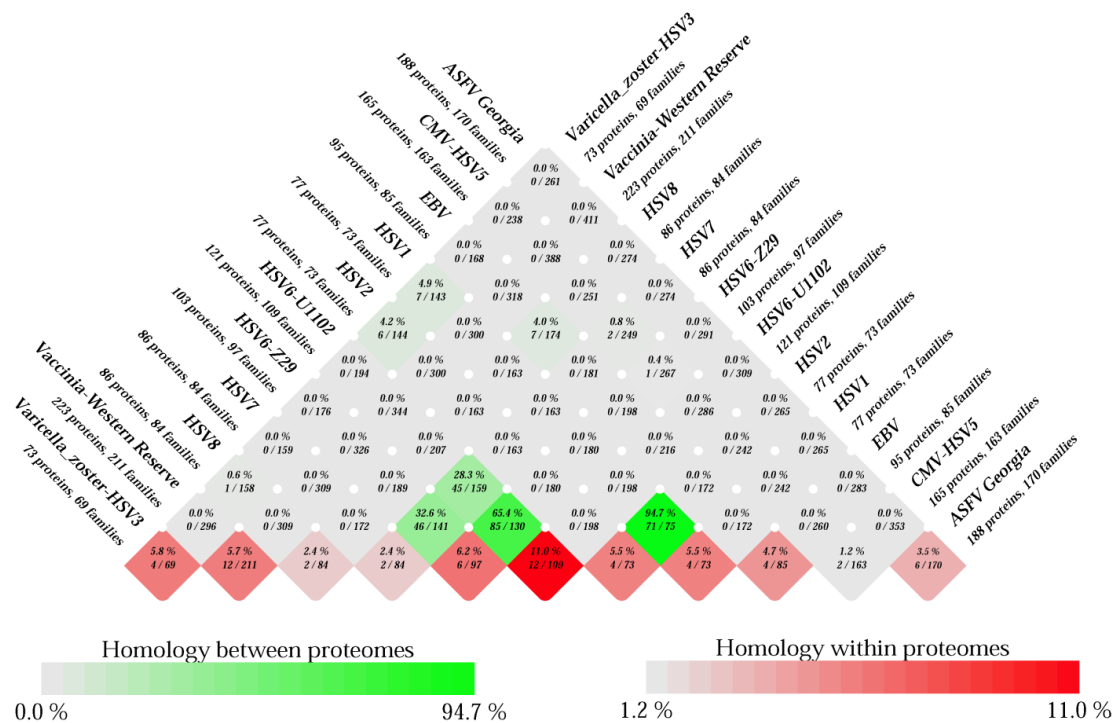


Figure 6- 5 Blast matrix depicting proteome level overlap between Herpes viruses (*Herpesviridae*) and other pox-viruses ASFV (*Asfarviridae*) and Vaccinia (*Orthopoxviridae*)

A BLAST hit within the CMG-biotools program is considered significant (green) if at least 50% of the two protein sequences being compared are aligned and 50% of amino

acids within the alignment are identical. The last row at the bottom of this matrix depicts homology within a given pathogen proteome under the strict BLAST search match criteria (grey to red scale).

This cross-reactivity could however be explained by annotating the high number of 5-mers in common between these double stranded DNA viruses belonging to distinct viral families. Table 6- 2 summarizes the number of 5-mer identical epitopes in common between ASFV, Vaccinia and all eight Herpes virus strains. Cells in the table are colored with red if the value is greater than 1000 identical 5-mers in common. On a 5 amino acid peptide motif level the number of identical unique 5-mers in common between all herpes viruses and ASFV ranged from 1,043 to 1,716. There are 1,140 to 1,846 identical 5-mers in common between Vaccinia and herpes viruses. Between ASFV and Vaccinia there are 2,161 identical 5-mers in common. This implies that the probability of humoral antibodies generated against one herpes virus infection showing cross-reactivity with an identical 5-mer epitope within an ASFV or Vaccinia peptides is plausible.

Table 6- 2 Five mers in common between ASFV and Vaccinia proteomes (orange) and several Herpes viruses (yellow).

5-mers in Common between Pathogen proteomes	ASFV-Georgia	Epstein Barr virus	CMV-HSV5	HSV1	HSV6-U1102	HSV6-strain Z29	HSV7	HSV8	HumanH SV2	Varicella zoster-HSV3	Vaccinia-Western Reserve
ASFV-Georgia	52206	1253	1716	1036	1482	1527	1661	1170	1043	1061	2161
Epstein Barr virus	1253	38977	2556	2116	1306	1294	1072	2291	2212	1274	1153
CMV-HSV5	1716	2556	58960	2703	2224	2266	1810	2109	2795	1772	1846
HSV1	1036	2116	2703	36444	1030	1053	826	1589	18833	2462	990
HSV6-U1102	1482	1306	2224	1030	41794	28828	4336	1125	1053	1076	1651
HSV6-strain Z29	1527	1294	2266	1053	28828	42332	4494	1193	1071	1108	1695
HSV7	1661	1072	1810	826	4336	4494	38805	1040	781	972	1730
HSV8	1170	2291	2109	1589	1125	1193	1040	36941	1650	1207	1185
HumanHSV2	1043	2212	2795	18833	1053	1071	781	1650	36488	2409	965
Varicella zoster-HSV3	1061	1274	1772	2462	1076	1108	972	1207	2409	34622	1140
Vaccinia-Western Reserve	2161	1153	1846	990	1651	1695	1730	1185	965	1140	53911

Noting the peptide to pathogen proteome commonality is recommended because pathogen proteome space is extremely conserved resulting in overlaps within distinct pathogens. To assess if the extent of overlap between life-space pathogens versus those randomly generated, is greater than that possible by chance, pathogen proteomes matching the original size of the priority pathogens represented on the PPP array were generated in-silico using a custom script written in R. The amino acid frequency of priority and common pathogen proteomes was calculated using MEGA5 [185]. This amino acid frequency observed in life space pathogen proteomes, depicted in Table 6- 3 was intentionally ignored while generating the random proteomes. The Blast matrix program within the CMG-biotools environment was used as before to assess the extent of overlap between pathogens due to random chance. There was no overlap observed within any of the randomly generated proteomes indicating that amino acid bias is essential for inter-pathogen overlap.

Table 6- 3 Amino acid frequencies in proteomes of priority pathogens and common pathogens

All frequencies are given in percent, average values reported																						
Pathogen	Ala	Cys	Neg Asp	Neg Glu	Phe	Gly	Pos His	Pos Ile	Pos Lys	Leu	Met	Asn	Pro	Gln	Pos Arg	Ser	Thr	Val	Trp	Tyr	Protein(aa)	
Influenza viruses																						
Influenza PR8-H1N1	5.78	1.75	4.43	7.42	3.84	6.77	1.66	6.54	5.93	8.14	3.96	5.53	3.93	3.82	6.63	7.69	6.20	5.51	1.62	2.83	4449	
Influenza-A-Brisbane-10-2007																						
H3N2	5.51	1.87	4.63	7.16	3.89	6.54	1.76	6.81	6.08	7.93	3.78	5.58	3.82	4.19	6.66	7.55	6.48	5.58	1.60	2.61	4555	
Influenza-A-Brisbane-59-2007(H1N1)-NS2 not found	5.77	1.75	4.49	7.30	3.91	6.74	1.72	6.43	5.95	7.92	3.76	5.68	3.87	3.94	6.37	7.63	6.41	5.93	1.61	2.83	4523	
Influenza-A-California-07-2009	5.73	1.80	4.58	7.30	3.91	6.71	1.66	6.67	5.93	7.90	3.75	5.64	3.89	3.80	6.49	7.75	6.24	5.79	1.64	2.83	4453	
Influenza-A-NewCaledonia20-1999(H1N1)	5.62	1.70	4.48	7.28	3.98	6.78	1.79	6.48	5.92	8.06	3.81	5.51	3.77	4.07	6.42	7.69	6.42	5.77	1.64	2.80	4643	
Influenza-A-Solomon_Islands-3-2006(H1N1)[incomplete proteome]	6.28	2.36	4.12	6.83	3.42	7.99	1.81	6.63	5.23	7.69	2.76	6.43	3.67	3.52	5.63	8.79	5.98	5.78	1.86	3.22	1990	
Influenza-A-Wisconsin-67-2005(H3N2)	5.43	1.82	4.59	7.21	3.90	6.52	1.72	6.71	6.00	8.13	3.86	5.62	3.69	4.29	6.73	7.57	6.41	5.58	1.61	2.62	4663	
Herpes viruses																						
HSV-1	12.95	1.78	5.38	4.81	3.31	8.05	2.47	2.75	1.70	9.56	1.67	2.23	9.13	3.01	8.52	6.24	5.85	6.94	1.15	2.48	41030	
HSV-2	14.03	1.75	5.33	4.84	3.26	7.95	2.53	2.63	1.87	9.45	1.80	2.01	9.23	2.80	8.86	6.21	5.48	6.86	1.17	2.42	41552	
HRV-3	7.57	2.14	5.35	5.16	4.05	6.18	2.61	5.55	3.48	9.60	2.08	4.08	6.09	3.52	6.56	7.41	7.29	6.82	1.07	3.37	37717	
EBV-HHV4	9.38	1.96	4.32	5.16	3.37	7.92	2.64	3.31	2.90	10.09	1.80	2.70	9.65	4.11	7.22	7.68	5.88	6.30	1.19	2.54	46450	
CMV-HHV5 [strain:Merlin]	7.89	2.52	4.99	5.37	3.80	6.05	3.15	3.51	2.91	10.48	2.07	3.27	5.92	3.63	7.69	7.59	6.84	7.56	1.43	3.31	63120	
HHV6 [strain:Z9]	5.27	2.53	4.95	5.79	5.22	4.42	2.57	6.42	6.12	10.10	2.42	5.29	4.52	3.54	5.42	8.42	6.37	6.20	0.96	3.48	45341	
HHV6 [strain:U102]	5.26	2.90	4.93	5.50	5.26	4.47	2.51	6.37	5.99	9.91	2.50	5.30	4.56	3.45	5.63	8.15	6.26	6.60	0.95	3.46	46409	
HHV-7	4.30	2.46	4.85	5.92	6.09	3.46	2.49	7.68	7.21	10.78	2.20	6.48	3.74	3.89	4.07	7.95	6.33	5.38	0.84	3.88	41001	
HHV-8	7.59	2.55	4.68	5.57	4.16	6.16	2.75	4.54	3.76	10.38	2.05	3.22	6.96	4.45	5.85	7.59	6.58	6.98	1.22	2.97	38731	
Other dsDNA viruses																						
ASFV	5.09	2.11	4.58	6.25	4.82	4.28	2.94	8.41	7.40	10.39	2.68	6.07	4.15	4.21	4.06	6.04	5.92	5.10	1.13	4.77	55884	
ASFV Proteins represented on the array	5.15	1.82	4.85	6.36	4.57	4.44	2.65	8.33	6.78	9.97	2.47	6.39	4.38	4.51	4.31	6.53	5.94	5.05	0.96	4.55	18114	
Vaccinia-WR	3.84	2.08	6.74	5.45	4.64	4.03	2.08	9.50	7.40	8.73	2.83	6.86	3.38	2.23	4.33	7.70	6.11	6.16	0.73	5.18	57833	
Encephalitis viruses																						
WNV-LNY99	7.98	1.81	4.52	6.18	3.03	8.51	1.86	5.10	5.48	9.09	3.35	3.67	4.11	2.65	6.23	5.77	7.28	8.13	2.71	2.56	3433	
WNV-H1996	8.34	1.72	4.32	6.04	3.10	8.59	1.91	5.12	5.90	9.14	3.41	3.77	4.10	2.44	6.04	5.79	7.23	7.87	2.71	2.47	3610	
JEV	8.44	1.52	4.54	5.87	3.24	8.75	2.02	4.82	6.79	9.03	3.27	3.65	4.15	2.57	6.20	5.99	7.14	8.19	2.69	2.52	3672	
VEE	8.46	2.77	4.75	6.22	3.26	5.74	2.91	4.96	6.56	7.82	2.05	3.79	6.32	3.20	5.39	6.70	6.94	7.58	0.96	3.63	3748	
EEE	8.14	2.92	5.12	5.12	3.40	5.63	2.97	5.49	6.11	7.34	2.04	4.05	6.56	3.27	5.46	6.43	7.18	8.04	1.02	3.72	3733	
Arenaviruses																						
Junin	4.15	2.65	5.99	6.11	5.01	5.16	2.15	5.55	6.89	12.14	2.56	4.92	3.64	3.88	5.25	8.53	4.80	6.59	1.16	2.86	3353	
Machupo	3.95	2.62	5.71	6.16	4.88	5.62	2.23	5.38	7.34	12.19	2.68	5.41	3.54	3.68	4.52	8.98	4.76	6.68	1.13	2.71	3363	
Lassa	4.83	2.55	5.77	6.01	4.18	5.54	2.28	5.77	6.66	11.79	2.87	5.00	3.52	3.91	4.80	8.50	5.30	6.01	1.13	3.58	3337	
Guariato	3.78	2.82	5.40	7.08	4.86	5.31	2.22	5.25	7.08	12.67	2.37	4.92	3.78	3.18	4.80	8.70	4.92	6.90	1.14	2.79	3352	
Bacteria																						
FTT-SchuS4	6.92	1.11	5.60	5.59	4.93	5.71	1.77	9.31	7.99	9.66	2.30	5.83	3.08	3.75	3.33	6.74	5.09	6.23	0.88	4.17	497851	
FTT-LVS	7.01	1.12	5.55	5.48	4.96	5.79	1.79	9.32	7.89	9.66	2.32	5.80	3.06	3.74	3.34	6.71	5.14	6.31	0.89	4.13	498451	
Bacillus anthracis-Ames	6.67	0.84	4.65	7.56	4.70	6.64	2.12	8.08	7.47	9.49	2.86	4.64	3.39	3.70	3.76	5.80	5.59	7.25	1.03	3.76	1496823	
Bacillus anthracis-Sterne	6.72	0.84	4.64	7.52	4.69	6.70	2.12	8.09	7.40	9.51	2.88	4.62	3.41	3.69	3.72	5.80	5.63	7.27	1.03	3.72	1460522	
Ba-Protective Ag on array from Sterne	5.30	0.00	6.39	6.66	3.26	4.76	1.36	7.34	7.74	7.74	1.22	9.24	3.80	4.21	3.80	9.38	7.61	5.43	0.95	3.80	796	
Plasmodium vivax [strain:Sal I]																						
Plasmodium vivax [strain:Sal I]	5.29	1.83	5.46	7.72	4.27	6.63	2.73	5.58	9.00	8.23	2.02	7.24	3.59	3.28	4.93	8.07	4.27	5.26	0.61	3.97	3635402	
Fungus																						
Coccidioides immitis [strain:RS]	7.95	1.32	5.51	6.36	3.69	6.48	2.46	5.16	5.32	8.98	2.16	3.85	6.13	4.10	6.42	8.55	5.66	5.83	1.35	2.71	4445892	
Coccidioides immitis[RS] proteins represented on the array	8.77	1.85	5.56	4.97	3.80	9.65	1.66	3.90	5.07	8.28	2.34	5.28	6.73	2.44	3.02	7.99	7.60	6.34	1.46	3.31	1026	

When representing partial proteomes for larger pathogens, while certain peptide sequences may be excluded from the array they might be represented through another unrelated pathogen's peptides. If an infected individual's sera shows antibody reactivity against these excluded motifs due to them being presented by the pathogen to their immune system, that might result in cross-reactivity. For antibody association on peptide microarrays short sequence identities are sufficient, but so is the context of presentation (surrounding sequence). The surrounding context within a peptide might be inhibitory to antibody association. If the context is not inhibitory, then from our experience with monoclonal antibody binding (e.g. p53Ab1) we have observed non-cognate reactivity. An analysis to estimate commonality between the peptides chosen to be represented on the assay and all pathogen proteomes of interest for the assay can help decide whether that pathogen's peptides might need to be presented in a separate sub-array to avoid competition between peptides for antibodies.

Cross-reactivity attributable to common exposures and vaccinations:

Certain pathogen proteomes might have to be excluded when multiplexing priority pathogens on an epitope peptide microarray format to avoid observing residual memory antibodies from vaccinations or common infections. Miller *et al.* [54] have demonstrated through their longitudinal study characterizing Influenza A and Cytomegalovirus (CMV) serum antibody in 40 individuals for 20 years that influenza antibodies capable of neutralizing the virus increase during the lifetime of an individual. CMV antibody titers on the other hand remained stable in the 15 out of 40 individuals

that tested positive for CMV in the first assessment. The duration of circulating antibodies to common exposure pathogens such as Varicella and Epstein Barr virus (EBV) or common vaccinations such as Measles, Mumps, Rubella (MMR vaccine), Vaccinia (small-pox vaccine), *Clostridium tetani* (Tetanus) and *Corynebacterium diphtheriae* (Diphtheria) measured by Slifka and colleagues [53] ranged with half-lives from 50 to 200 years and were short-lived for Tetanus (11 years) and Diphtheria (19 years). Herpes simplex viruses are ubiquitous human pathogens that have a worldwide sero-prevalence in the population of up to 90% [186-188].

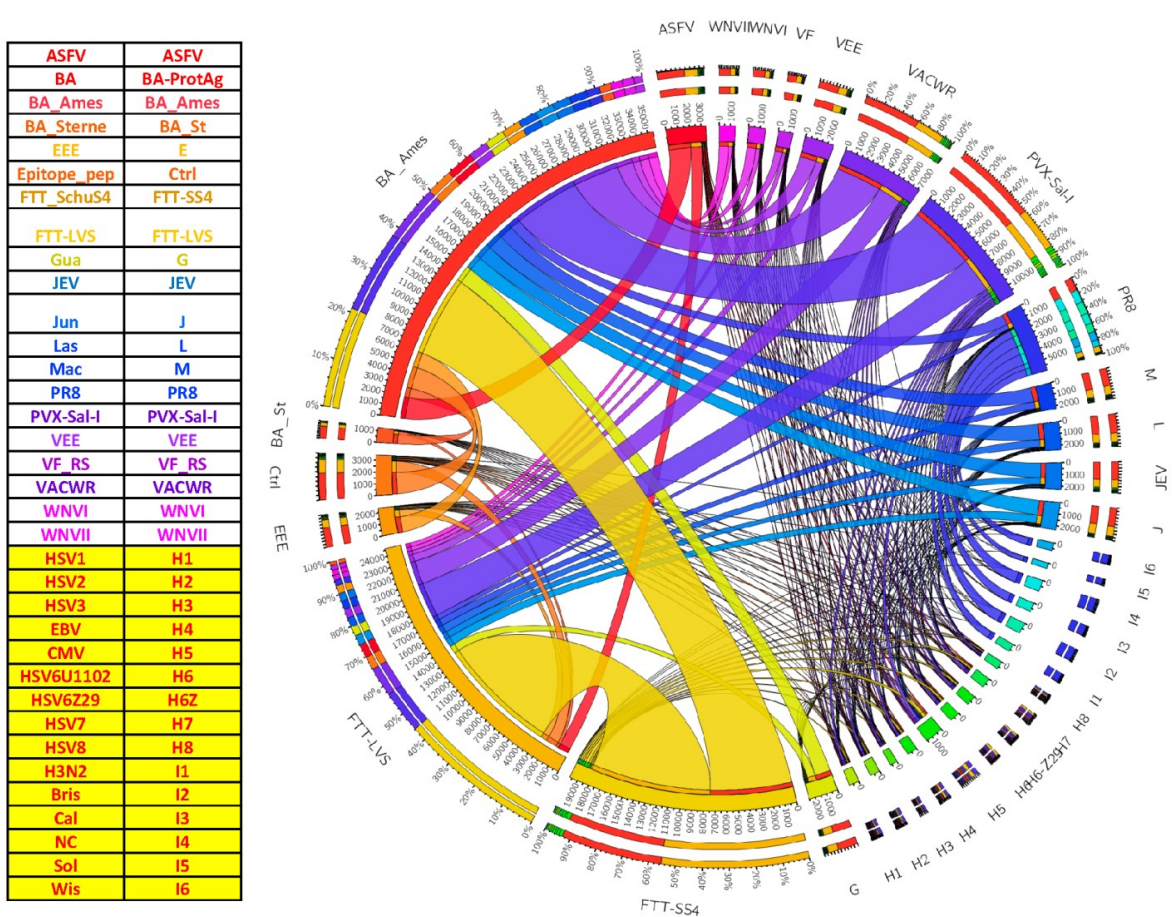


Figure 6- 6 Commonality on a 5-mer sequence level between priority pathogen proteomes and common pathogen proteomes such as Herpes viruses and influenza vaccine proteomes (highlighted in the legend in yellow).

In context to the priority pathogens represented on the PPP array, Figure 6- 6 represents the number of unique 5-mer sequences in common between the priority pathogen peptides and common pathogens. The common pathogen proteomes included for this analysis were eight herpes viruses and influenza vaccine strains (2006-2009) not intentionally represented on the array. The connectogram was generated using an online

tool, Circos [154]. The size of the ribbon represents the number of 5-mer sequences in common between peptides represented on the array and pathogen proteomes of priority and common pathogens. While the extent of overlap between common pathogens apparent on a 5-mer level is less in comparison to that observed between some unrelated priority pathogens it might be sufficient to drive competition on the assay.

Thus, when developing extremely sensitive multiplexed pathogen specific assays the contribution and presence of these circulating antibodies to persistent common pathogens; common vaccinations and homologous pathogens cannot be neglected. To summarize this with respect to a multiplexed peptide microarray platform, the antibody response observed post exposure to a new priority pathogen could potentially have 3 primary components. An adaptive immune response specific to the priority pathogen, a component representing specific reactivity to epitopes not represented on the array and a component representing non-specific, residual reactivity from prior exposure to a homologous or unrelated pathogen either part of a vaccination or persistent chronic infection.

REFERENCES

1. Stafford P (2007) Biochips as Pathways to Drug Discovery. In: Carmen A, Hardiman G, editors. Drug Discovery Series. pp. 281-320.
2. Stafford P, Halperin R, Legutki JB, Magee DM, Galgiani J, et al. (2012) Physical Characterization of the "Immunosignaturing Effect". *Molecular & Cellular Proteomics* 11.
3. Gaseitsiwe S, Valentini D, Mahdavi S, Magalhaes I, Hoft DF, et al. (2008) Pattern Recognition in Pulmonary Tuberculosis Defined by High Content Peptide Microarray Chip Analysis Representing 61 Proteins from *M. tuberculosis*. *Plos One* 3.
4. Nahtman T, Jernberg A, Mahdavi S, Zerweck J, Schutkowski M, et al. (2007) Validation of peptide epitope microarray experiments and extraction of quality data. *Journal of Immunological Methods* 328: 1-13.
5. List C, Qi WH, Maag E, Gottstein B, Muller N, et al. (2010) Serodiagnosis of *Echinococcus* spp. Infection: Explorative Selection of Diagnostic Antigens by Peptide Microarray. *Plos Neglected Tropical Diseases* 4.
6. Chow SCS, Ho CYS, Tam TTY, Wu C, Cheung T, et al. (2006) Specific epitopes of the structural and hypothetical proteins elicit variable humoral responses in SARS patients. *Journal of Clinical Pathology* 59: 468-476.
7. Guo JP, Petric M, Campbell W, McGeer PL (2004) SARS corona virus peptides recognized by antibodies in the sera of convalescent cases. *Virology* 324: 251-256.
8. Andresen H, Zarse K, Grotzinger C, Hollidt JM, Ehrentreich-Forster E, et al. (2006) Development of peptide microarrays for epitope mapping of antibodies against the human TSH receptor. *Journal of Immunological Methods* 315: 11-18.
9. Johnston SA, Stafford P (2010) Compound arrays for sample profiling. In: office UPaT, editor. USA: The Arizona Board of Regents, A body corporate of the state of Arizona for and on behalf of Arizona State University [US/US]; 699 S. Mill Avenue The Brickyard, Suite 601 Room 691 AA Tempe, Arizona 85281 (US) (For All Designated States Except US).

10. Sykes KF, Legutki JB, Stafford P (2013) Immunosignaturing: a critical review. *Trends in Biotechnology* 31: 45-51.
11. Legutki JB, Magee DM, Stafford P, Johnston SA (2010) A general method for characterization of humoral immunity induced by a vaccine or infection. *Vaccine* 28.
12. Restrepo L, Stafford P, Magee DM, Johnston SA (2011) Application of Immunosignatures to the Assessment of Alzheimer's Disease. *Annals of Neurology* 70: 286-295.
13. Kukreja M, Johnston S, Stafford P (2012) Immunosignaturing microarrays distinguish antibody profiles of related pancreatic diseases. *Journal of Proteomics and Bioinformatics* S6:001.
14. Vigil A, Chen C, Jain A, Nakajima-Sasaki R, Jasinskas A, et al. (2011) Profiling the Humoral Immune Response of Acute and Chronic Q Fever by Protein Microarray. *Molecular & Cellular Proteomics* 10.
15. Rup L (2012) The Human Microbiome Project. *Indian Journal of Microbiology* 52: 315-315.
16. Mariat D, Firmesse O, Levenez F, Guimaraes VD, Sokol H, et al. (2009) The Firmicutes/Bacteroidetes ratio of the human microbiota changes with age. *Bmc Microbiology* 9.
17. Golby S, Hackett M, Boursier L, Dunn-Walters D, Thiagamoorthy S, et al. (2002) B cell development and proliferation of mature B cells in human fetal intestine. *Journal of Leukocyte Biology* 72: 279-284.
18. Wesemann DR, Portuguese AJ, Meyers RM, Gallagher MP, Cluff-Jones K, et al. (2013) Microbial colonization influences early B-lineage development in the gut lamina propria. advance online publication.
19. Galgiani JN, Ampel NM, Blair JE, Catanzaro A, Johnson RH, et al. (2005) Coccidioidomycosis. *Clinical infectious diseases* 41: 1217.

20. Arizona Department of Health Services-Valley Fever Annual Report 2007.
21. Adams DA, Gallagher KM, Jajosky RA, Kriseman J, Sharp P, et al. (2013) Summary of Notifiable Diseases – United States, 2011.
22. Panackal AA, Hajjeh RA, Cetron MS, Warnock DW (2002) Fungal infections among returning travelers. *Clinical Infectious Diseases* 35: 1088-1095.
23. CDC Coccidioidomycosis webpage.
24. US Census Bureau.
25. Parish JM, Blair JE (2008) Coccidioidomycosis. *Mayo Clinic proceedings* 83: 343.
26. DiCaudo DJ (2006) Coccidioidomycosis: A review and update. *Journal of the American Academy of Dermatology* 55: 929.
27. Cox RA, Magee DM (1998) Protective immunity in coccidioidomycosis. *Research in Immunology* 149: 417-428.
28. Cordeiro RD, Brilhante RSN, Rocha MFG, Moura FEA, de Camargo ZP, et al. (2007) Rapid diagnosis of coccidioidomycosis by nested PCR assay of sputum. *Clinical Microbiology and Infection* 13: 449-451.
29. Duarte-Escalante E, Frías-De-León MG, Zúñiga G, Martínez-Herrera E, Acosta-Altamirano G, et al. (2014) Molecular markers in the epidemiology and diagnosis of coccidioidomycosis. *31: 49-53.*
30. Munson E, Endes T, Vaughan K, Block T, Hryciuk JE (2009) Two cases of recovery of dimorphic pathogenic fungi via conventional BacT/ALERT microbial detection system media. *Mycopathologia* 167: 191.
31. De Lucrezia D, Slanzi D, Poli I, Polticelli F, Minervini G (2012) Do Natural Proteins Differ from Random Sequences Polypeptides? Natural vs. Random Proteins Classification Using an Evolutionary Neural Network. *Plos One* 7.

32. Minervini G, Evangelista G, Villanova L, Slanzi D, De Lucrezia D, et al. (2009) Massive non-natural proteins structure prediction using grid technologies. *Bmc Bioinformatics* 10.
33. Smith TF, Waterman MS (1981) Identification of common molecular subsequences. *Journal of Molecular Biology* 147: 195-197.
34. Halperin RF, Stafford P, Emery JS, Navalkar KA, Johnston SA (2012) GuiTope: an application for mapping random-sequence peptides to protein sequences. *Bmc Bioinformatics* 13.
35. Miller JJ, Valdes R (1992) Methods for calculating cross-reactivity in Immunoassays. *Journal of Clinical Immunoassay* 15: 97-107.
36. Andresen H, Grotzinger C (2009) Deciphering the Antibodyome - Peptide Arrays for Serum Antibody Biomarker Diagnostics. *Current Proteomics* 6: 1-12.
37. Ardizzoni A, Capuccini B, Baschieri MC, Orsi CF, Rumpianesi F, et al. (2009) A protein microarray immunoassay for the serological evaluation of the antibody response in vertically transmitted infections. *European Journal of Clinical Microbiology & Infectious Diseases* 28: 1067-1075.
38. Diseases NIOAaI (2013) NIAID Category A, B, and C Priority Pathogens.
39. Registry NSA HHS and USDA Select Agents and Toxins List.
40. Loh J, Zhao GY, Presti RM, Holtz LR, Finkbeiner SR, et al. (2009) Detection of Novel Sequences Related to African Swine Fever Virus in Human Serum and Sewage. *Journal of Virology* 83: 13019-13025.
41. Basile AJ, Horiuchi K, Panella AJ, Laven J, Kosoy O, et al. (2013) Multiplex Microsphere Immunoassays for the Detection of IgM and IgG to Arboviral Diseases. *Plos One* 8.

42. Ngo Y, Advani R, Valentini D, Gaseitsiwe S, Mahdavifar S, et al. (2009) Identification and testing of control peptides for antigen microarrays. *Journal of Immunological Methods* 343: 68-78.
43. Panse S, Dong L, Burian A, Carus R, Schutkowski M, et al. (2004) Profiling of generic anti-phosphopeptide antibodies and kinases with peptide microarrays using radioactive and fluorescence-based assays. *Molecular Diversity* 8: 291-299.
44. Choi J-j, Kim C, Park H (2009) Peptide Nucleic Acid-Based Array for Detecting and Genotyping Human Papillomaviruses. *Journal of Clinical Microbiology* 47: 1785-1790.
45. Luminex C xMAP® Technology Technical Note: Overcoming the Cost and Performance Limitations of ELISA with xMAP® Technology. The Thomas Joos laboratory at Natural and Medical Sciences Institute (NMI) at the University of Tuebingen.
46. Rider TH, Petrovick MS, Nargi FE, Harper JD, Schwoebel ED, et al. (2003) A B cell-based sensor for rapid identification of pathogens. *Science* 301: 213-215.
47. Erlandsson L, Rosenstjerne MW, McLoughlin K, Jaing C, Fomsgaard A (2011) The Microbial Detection Array Combined with Random Phi29-Amplification Used as a Diagnostic Tool for Virus Detection in Clinical Samples. *Plos One* 6.
48. Gardner SN, Jaing CJ, McLoughlin KS, Slezak TR (2010) A microbial detection array (MDA) for viral and bacterial detection. *Bmc Genomics* 11.
49. Simoes EAF, Patel C, Sung W-K, Lee CWH, Loh KH, et al. (2013) Pathogen Chip for Respiratory Tract Infections. *Journal of Clinical Microbiology* 51: 945-953.
50. Quan P-L, Palacios G, Jabado OJ, Conlan S, Hirschberg DL, et al. (2007) Detection of respiratory viruses and subtype identification of influenza A viruses by GreeneChipResp oligonucleotide microarray. *Journal of Clinical Microbiology* 45: 2359-2364.
51. Miller S, Chen E, Naccache S, Pinsky BA, Chiu C (2010) Virochip Analysis Utility of a Pan Viral Microarray for Identification of Viral Causes of Acute Clinical Illness and Outbreak Investigations. *Journal of Molecular Diagnostics* 12: 883-883.

52. Glanville J, Zhai W, Berka J, Telman D, Huerta G, et al. (2009) Precise determination of the diversity of a combinatorial antibody library gives insight into the human immunoglobulin repertoire. *Proceedings of the National Academy of Sciences of the United States of America* 106: 20216-20221.
53. Amanna IJ, Carlson NE, Slifka MK (2007) Duration of humoral immunity to common viral and vaccine antigens. *New England Journal of Medicine* 357: 1903-1915.
54. Miller MS, Gardner TJ, Krammer F, Aguado LC, Tortorella D, et al. (2013) Neutralizing Antibodies Against Previously Encountered Influenza Virus Strains Increase over Time: A Longitudinal Analysis. *Science Translational Medicine* 5.
55. Kruszon-Moran Deanna, Porter Kathryn S, McQuillan Geraldine, Goud Billioux Veena, Kim-Farley Robert, et al. (2012) Infectious disease prevalence in Los Angeles County- A comparison to national estimates, 1999-2004. Hyattsville, MD: NCHS data brief, no 90. National Center for Health Statistics.
56. Kaitlin B, Tsang C, Tabnak F, Chiller T (March 29, 2013) Increase in Reported Coccidioidomycosis-United States, 1998-2011.: *Morbidity and Mortality Weekly Report (MMWR)*, Centers for Disease Control and Prevention. pp. 217-221.
57. (February 13, 2009 / 58(05);105-109) Increase in Coccidioidomycosis-California, 2000-2007.: *Morbidity and Mortality Weekly Report (MMWR)*-Weekly.
58. Tamerius JD, Comrie AC (2011) Coccidioidomycosis Incidence in Arizona Predicted by Seasonal Precipitation. *Plos One* 6.
59. Galgiani JN (1999) Coccidioidomycosis: A Regional Disease of National Importance: Rethinking Approaches for Control. *Annals of Internal Medicine* 130: 293.
60. Becker-Merok A, Nikolaisen C, Nossent HC (2006) B-lymphocyte activating factor in systemic lupus erythematosus and rheumatoid arthritis in relation to autoantibody levels, disease measures and time. *Lupus* 15: 570 - 576.
61. Mark D. Lindsley DWW, Christine J. Morrison (2006) Serological and Molecular Diagnosis of Fungal Infections. In: Detrick BH, Robert G. Folds, James D., editor.

Manual of Molecular and Clinical Laboratory Immunology. 7th ed. Washington, DC, USA: ASM Press. pp. 569-605.

62. Pappagianis D (2001) Serologic studies in Coccidioidomycosis. *Seminars in Respiratory Infections* 16: 242-250.

63. Stevens DA, Clemons KV, Levine HB, Pappagianis D, Baron EJ, et al. (2009) Expert Opinion: What To Do When There Is Coccidioides Exposure in a Laboratory. *Clinical Infectious Diseases* 49: 919-923.

64. Ditomasso JP, Ampel NM, Sobonya RE, Bloom JW (1994) Bronchoscopic diagnosis of pulmonary Coccidioidomycosis - Comparison of cytology, culture and transbronchial biopsy. *Diagnostic Microbiology and Infectious Disease* 18: 83-87.

65. Saubolle MA (2007) Laboratory aspects in the diagnosis of coccidioidomycosis. *Coccidioidomycosis: Sixth International Symposium* 1111: 301-314.

66. Chase BA, Johnston SA, Legutki JB (2012) Evaluation of Biological Sample Preparation for Immunosignature-Based Diagnostics. *Clinical and Vaccine Immunology* 19.

67. Mathisen G, Shelub A, Truong J, Wigen C (2010) Coccidioidal Meningitis Clinical Presentation and Management in the Fluconazole Era. *Medicine* 89: 251-284.

68. Drake KW, Adam RD (2009) Coccidioidal meningitis and brain abscesses Analysis of 71 cases at a referral center. *Neurology* 73: 1780-1786.

69. E B, JS D, WL H, RD M (1981) Coccidioidal Meningitis. An analysis of thirty one cases and review of the literature. *Medicine* 60: 139-172.

70. Ihaka R, Gentleman R (1996) R: A Language for Data Analysis and Graphics. 5: 299-314.

71. Weihs C, Ligges U, Luebke K, Raabe N (2005) *klaR Analyzing German Business Cycles*. Berlin: Springer-Verlag.

72. Torgo L (2010) *Data Mining with R: Learning with Case Studies*: Chapman and Hall/CRC.
73. Johnson WE, Li C, Rabinovic A (2007) Adjusting batch effects in microarray expression data using empirical Bayes methods. *Biostatistics* 8: 118-127.
74. Chen C, Grennan K, Badner J, Zhang D, Gershon E, et al. (2011) Removing Batch Effects in Analysis of Expression Microarray Data: An Evaluation of Six Batch Adjustment Methods. *Plos One* 6.
75. Legutki JB, Johnston SA (2013) Immunosignatures can predict vaccine efficacy. *Proceedings of the National Academy of Sciences of the United States of America* 110: 18614-18619.
76. Brown GD, Denning DW, Gow NAR, Levitz SM, Netea MG, et al. (2012) Hidden Killers: Human Fungal Infections. *Science Translational Medicine* 4.
77. Saubolle MA, McKellar PP, Sussland D (2007) Epidemiologic, clinical, and diagnostic aspects of coccidioidomycosis. *Journal of Clinical Microbiology* 45: 26-30.
78. Polage CR, Billetdeaux E, Litwin CM, Petti CA (2006) Revisiting the sensitivity of serologic testing in culture positive coccidioidomycosis. *Abstracts of the General Meeting of the American Society for Microbiology* 106: 244-245.
79. Blair JE, Coakley B, Santelli AC, Hentz JG, Wengenack NL (2006) Serologic testing for symptomatic coccidioidomycosis in immunocompetent and immunosuppressed hosts. *Mycopathologia* 162: 317-324.
80. Navalkar KA, Johnston SA, Stafford P, Galgiani J, Magee DM (2014) Application of Immunosignaturing to diagnosis of Valley Fever. In: Center for Innovations in Medicine TBI, Arizona State University, Tempe, AZ, Center for Personalized Diagnostics TBI, Arizona State University, Tempe, AZ, Valley Fever Center for Excellence UoA, Tucson, AZ, editors. [manuscript in submission] ed.
81. Yang MC, Magee DM, Cox RA (1997) Mapping of a *Coccidioides immitis*-specific epitope that reacts with complement-fixing antibody. *Infection and Immunity* 65: 4068-4074.

82. Zhu YF, Tryon V, Magee DM, Cox RA (1997) Identification of a *Coccidioides immitis* antigen 2 domain that expresses B-cell-reactive epitopes. *Infection and Immunity* 65: 3376-3380.
83. Ivey FD, Magee DM, Woitaske MD, Johnston SA, Cox RA (2003) Identification of a protective antigen of *Coccidioides immitis* by expression library immunization. *Vaccine* 21: 4359-4367.
84. Pan SC, Cole GT (1995) Molecular and Biochemical-characterization of a *Coccidioides immitis*-specific antigen. *Infection and Immunity* 63: 3994-4002.
85. Petrilli P (1993) Classification of protein sequences by their dipeptide composition. *Computer Applications in the Biosciences* 9: 205-209.
86. Huang J, Ru B, Zhu P, Nie F, Yang J, et al. (2012) MimoDB 2.0: a mimotope database and beyond. *Nucleic Acids Research* 40: D271-D277.
87. Grantham R (1974) AMINO-ACID DIFFERENCE FORMULA TO HELP EXPLAIN PROTEIN EVOLUTION. *Science* 185: 862-864.
88. Buus S, Rockberg J, Forsstrom B, Nilsson P, Uhlen M, et al. (2012) High-resolution Mapping of Linear Antibody Epitopes Using Ultrahigh-density Peptide Microarrays. *Molecular & Cellular Proteomics* 11: 1790-1800.
89. Sun J, Xu T, Wang S, Li G, Wu D, et al. (2011) Does difference exist between epitope and non-epitope residues? Analysis of the physicochemical and structural properties on conformational epitopes from B-cell protein antigens. *Immunome Research* 7.
90. Centers for Disease Control and Prevention: Tularemia webpage.
91. Altschul SF, Wootton JC, Gertz EM, Agarwala R, Morgulis A, et al. (2005) Protein database searches using compositionally adjusted substitution matrices. *Febs Journal* 272: 5101-5109.

92. Keasey SL, Schmid KE, Lee MS, Meegan J, Tomas P, et al. (2009) Extensive Antibody Cross-reactivity among Infectious Gram-negative Bacteria Revealed by Proteome Microarray Analysis. *Molecular & Cellular Proteomics* 8: 924-935.
93. Kuberski T, Myers R, Wheat LJ, Durkin M, Connolly P, et al. (2007) Diagnosis of coccidioidomycosis by antigen detection using cross-reaction with a histoplasma antigen. *Clinical Infectious Diseases* 44: 50-54.
94. RH J, S B (2008) *Coccidioidomycosis Infectious Disease*. In: Hospenthal D, Rinaldi M, editors. *Diagnosis and Treatment of Human Mycoses*. Totowa, NJ.: Humana Press Inc. pp. 295-315.
95. Blair JE (2009) Coccidioidal meningitis: Update on epidemiology, clinical features, diagnosis, and management. *Current Infectious Disease Reports* 11: 289-295.
96. Smith CE, Saito MT, Simons SA (1956) Pattern of 39,500 serologic tests in Coccidioidomycosis. *Jama-Journal of the American Medical Association* 160: 546-552.
97. Thompson GR, Lunetta JM, Johnson SM, Taylor S, Bays D, et al. (2011) Early Treatment With Fluconazole May Abrogate the Development of IgG Antibodies in Coccidioidomycosis. *Clinical infectious diseases* 53: e20-e24.
98. Marr KA, Balajee SA, McLaughlin L, Tabouret M, Bentsen C, et al. (2004) Detection of galactomannan antigenemia by enzyme immunoassay for the diagnosis of invasive aspergillosis: Variables that affect performance. *Journal of Infectious Diseases* 190: 641-649.
99. Kringelum JV, Nielsen M, Padkjaer SB, Lund O (2013) Structural analysis of B-cell epitopes in antibody:protein complexes. *Molecular Immunology* 53: 24-34.
100. Graybill JR, Stevens DA, Galgiani JN, Dismukes WE, Cloud GA (1990) Itraconazole treatment of Coccidioidomycosis. *American Journal of Medicine* 89: 282-290.
101. Notkins AL (2004) Polyreactivity of antibody molecules. *Trends in Immunology* 25: 174-179.

102. Halperin RF, Stafford P, Johnston SA (2011) Exploring Antibody Recognition of Sequence Space through Random-Sequence Peptide Microarrays. *Molecular & Cellular Proteomics* 10.
103. Mouquet H, Nussenzweig MC (2012) Polyreactive antibodies in adaptive immune responses to viruses. *Cellular and Molecular Life Sciences* 69: 1435-1445.
104. Mezzasoma L, Bacarese-Hamilton T, Di Cristina M, Rossi R, Bistoni F, et al. (2002) Antigen microarrays for serodiagnosis of infectious diseases. *Clinical Chemistry* 48: 121-130.
105. Reverberi R, Reverberi L (2007) Factors affecting the antigen-antibody reaction. *Blood Transfusion* 5: 227-240.
106. Barderas MG, Rodriguez F, Gomez-Puertas P, Aviles M, Beitia F, et al. (2001) Antigenic and immunogenic properties of a chimera of two immunodominant African swine fever virus proteins. *Archives of Virology* 146: 1681-1691.
107. GomezPuertas P, Rodriguez F, Oviedo JM, RamiroIbanez F, RuizGonzalvo F, et al. (1996) Neutralizing antibodies to different proteins of African swine fever virus inhibit both virus attachment and internalization. *Journal of Virology* 70: 5689-5694.
108. Neilan JG, Zsak L, Lu Z, Burrage TG, Kutish GF, et al. (2004) Neutralizing antibodies to African swine fever virus proteins p30, p54, and p72 are not sufficient for antibody-mediated protection. *Virology* 319: 337-342.
109. Davies DH, Molina DM, Wrammert J, Miller J, Hirst S, et al. (2007) Proteome-wide analysis of the serological response to vaccinia and smallpox. *Proteomics* 7: 1678-1686.
110. Benhnia MR-E-I, McCausland MM, Su H-P, Singh K, Hoffmann J, et al. (2008) Redundancy and Plasticity of Neutralizing Antibody Responses Are Cornerstone Attributes of the Human Immune Response to the Smallpox Vaccine. *Journal of Virology* 82: 3751-3768.
111. Davies DH, Wyatt LS, Newman FK, Earl PL, Chun S, et al. (2008) Antibody profiling by proteome microarray reveals the immunogenicity of the attenuated smallpox

vaccine modified vaccinia virus Ankara is comparable to that of Dryvax. *Journal of Virology* 82: 652-663.

112. Sundaresh S, Randall A, Unal B, Petersen JM, Belisle JT, et al. (2007) From protein microarrays to diagnostic antigen discovery: a study of the pathogen *Francisella tularensis*. *Bioinformatics* 23: I508-I518.

113. Eyles JE, Unal B, Hartley MG, Newstead SL, Flick-Smith H, et al. (2007) Immunodominant *Francisella tularensis* antigens identified using proteome microarray. ©Crown Copyright 2007 Dstl. 7: 2172-2183.

114. Baillie L, Townend T, Walker N, Eriksson U, Williamson D (2004) Characterization of the human immune response to the UK anthrax vaccine. *Fems Immunology and Medical Microbiology* 42: 267-270.

115. Crowe SR, Ash LL, Engler RJM, Ballard JD, Harley JB, et al. (2010) Select Human Anthrax Protective Antigen Epitope-Specific Antibodies Provide Protection from Lethal Toxin Challenge. *Journal of Infectious Diseases* 202: 251-260.

116. Gubbins MJ, Schmidt L, Tsang RS, Berry JD, Kabani A, et al. (2007) Development of a Competitive Enzyme Linked Immunosorbent Assay to Identify Epitope Specific Antibodies in Recipients of the U.S. Licensed Anthrax Vaccine. *Journal of Immunoassay and Immunochemistry* 28: 213-225.

117. Chen JH, Jung JW, Wang Y, Ha KS, Lu F, et al. (2010) Immunoproteomics Profiling of Blood Stage *Plasmodium vivax* Infection by High-Throughput Screening Assays. *Journal of Proteome Research* 9: 6479-6489.

118. Cole GT, Kruse D, Seshan KR (1991) Antigen complex of *Coccidioides immitis* which elicits a precipitin antibody-response in patients. *Infection and Immunity* 59: 2434-2446.

119. Cox RA, Magee DM (2004) *Coccidioidomycosis*: Host response and vaccine development. *Clinical Microbiology Reviews* 17: 804-+.

120. Emini EA, Hughes JV, Perlow DS, Boger J (1985) Induction of Hepatitis-A virus-neutralizing antibody by a virus-specific synthetic peptide. *Journal of Virology* 55: 836-839.
121. Parker JMR, Guo D, Hodges RS (1986) New Hydrophilicity scale derived from High-performance liquid-chromatography peptide retention data - Correlation of predicted surface residues with antigenicity and X-ray-derived accessible sites. *Biochemistry* 25: 5425-5432.
122. Kolaskar AS, Tongaonkar PC (1990) A Semiempirical method for prediction of antigenic determinants of protein antigens. *Febs Letters* 276: 172-174.
123. Karplus PA, Schulz GE (1985) Prediction of chain flexibility in proteins - A tool for the selection of peptide antigens. *Naturwissenschaften* 72: 212-213.
124. Zweig MH, Campbell G (1993) RECEIVER-OPERATING CHARACTERISTIC (ROC) PLOTS - A FUNDAMENTAL EVALUATION TOOL IN CLINICAL MEDICINE. *Clinical Chemistry* 39: 561-577.
125. Oh SJ, Ju JM, Kim BC, Ko E, Hong BJ, et al. (2005) DNA microarrays on a dendron-modified surface improve significantly the detection of single nucleotide variations in the p53 gene. *Nucleic Acids Research* 33.
126. Halperin R (2011) Characterization and Analysis of a Novel Platform for Profiling the Antibody Response In: University AS, editor. Tempe, AZ.
127. Sagawa T, Oda M, Ishimura M, Furukawa K, Azuma T (2003) Thermodynamic and kinetic aspects of antibody evolution during the immune response to hapten. *Molecular Immunology* 39: 801-808.
128. Kusnezow W, Syagailo YV, Rueffer S, Baudenstiel N, Gauer C, et al. (2006) Optimal design of microarray immunoassays to compensate for kinetic limitations - Theory and experiment. *Molecular & Cellular Proteomics* 5: 1681-1696.
129. Warter L, Appanna R, Fink K (2012) Human poly- and cross-reactive anti-viral antibodies and their impact on protection and pathology. *Immunologic Research* 53: 148-161.

130. Waag DM, McKee KT, Sandstrom G, Pratt LLK, Bolt CR, et al. (1995) Cell-mediated and Humoral immune-responses after vaccination of human volunteers with the Live Vaccine Strain of *Francisella tularensis*. *Clinical and Diagnostic Laboratory Immunology* 2: 143-148.

131. Saeed M, Roeffen W, Alexander N, Drakeley CJ, Targett GAT, et al. (2008) Plasmodium falciparum Antigens on the Surface of the Gametocyte-Infected Erythrocyte. *Plos One* 3.

132. Yoshinoya S, Cox RA, Pope RM (1980) Circulating immune-complexes in Coccidioidomycosis - Detection and Characterization. *Journal of Clinical Investigation* 66: 655-663.

133. Sigounas G, Kolaitis N, Monelltorrens E, Notkins AL (1994) Polyreactive IgM antibodies in the circulation are masked by Antigen-binding. *Journal of Clinical Immunology* 14: 375-381.

134. Chumpitazi B, Lepers JP, Rason M, Meunier A, Boudin C, et al. (1993) Circulating stable antigens at higher levels down-regulate antibody-responses to *Plasmodium falciparum*. *Parasitology Research* 79: 163-167.

135. de Dominguez N, Rodriguez-Acosta A (2000) A 33-35 kDa circulating antigen from Plasmodium falciparum. *Folia Parasitol (Praha)* 47: 267-272.

136. Durkin M, Estok L, Hospenthal D, Crum-Cianflone N, Swartzentruber S, et al. (2009) Detection of Coccidioides Antigenemia following Dissociation of Immune Complexes. *Clinical and Vaccine Immunology* 16: 1453-1456.

137. Mathers C, Fat DM, Boerma JT, World Health O (2008) The global burden of disease : 2004 update. Geneva, Switzerland: World Health Organization.

138. Khetsuriani N, Quiroz ES, Holman RC, Anderson LJ (2003) Viral meningitis-associated hospitalizations in the United States, 1988-1999. *Neuroepidemiology* 22: 345-352.

139. Chow FC, Marra CM, Cho TA (2011) Cerebrovascular disease in central nervous system infections. *Semin Neurol* 31: 286-306.

140. Kusalik A, Trost B, Bickis M, Fasano C, Capone G, et al. (2009) Codon number shapes peptide redundancy in the universal proteome composition. *Peptides* 30: 1940-1944.
141. Navalkar KA, Johnston SA, Stafford P, Halperin R (2014) Multi-pathogen peptide based serological diagnostic. In: Center for Innovations in Medicine TBI, Arizona State University, editor. [manuscript in preparation] ed. Tempe, Arizona.
142. Balakrishnan T, Bela-Ong DB, Toh YX, Flamand M, Devi S, et al. (2011) Dengue Virus Activates Polyreactive, Natural IgG B Cells after Primary and Secondary Infection. *Plos One* 6.
143. Greenbaum JA, Kotturi MF, Kim Y, Oseroff C, Vaughan K, et al. (2009) Pre-existing immunity against swine-origin H1N1 influenza viruses in the general human population. *Proceedings of the National Academy of Sciences of the United States of America* 106: 20365-20370.
144. Konishi E (2009) Status of natural infection with Japanese encephalitis virus in Japan: Prevalence of antibodies to the nonstructural 1 protein among humans and horses. *Vaccine* 27: 7129-7130.
145. Fange Y, Banner D, Kelvin AA, Huang SSH, Paige CJ, et al. (2012) Seasonal H1N1 Influenza Virus Infection Induces Cross-Protective Pandemic H1N1 Virus Immunity through a CD8-Independent, B Cell-Dependent Mechanism. *Journal of Virology* 86: 2229-2238.
146. Throsby M, van den Brink E, Jongeneelen M, Poon LLM, Alard P, et al. (2008) Heterosubtypic Neutralizing Monoclonal Antibodies Cross-Protective against H5N1 and H1N1 Recovered from Human IgM(+) Memory B Cells. *Plos One* 3.
147. Whittle JRR, Zhang RJ, Khurana S, King LR, Manischewitz J, et al. (2011) Broadly neutralizing human antibody that recognizes the receptor-binding pocket of influenza virus hemagglutinin. *Proceedings of the National Academy of Sciences of the United States of America* 108: 14216-14221.
148. Vaughan K, Greenbaum J, Blythe M, Peters B, Sette A (2010) Meta-analysis of All Immune Epitope Data in the Flavivirus Genus: Inventory of Current Immune Epitope

Data Status in the Context of Virus Immunity and Immunopathology. *Viral Immunology* 23: 259-284.

149. Yamada KI, Takasaki T, Nawa M, Yabe S, Kurane I (2003) Antibody responses determined for Japanese dengue fever patients by neutralization and hemagglutination inhibition assays demonstrate cross-reactivity between dengue and Japanese encephalitis viruses. *Clinical and Diagnostic Laboratory Immunology* 10: 725-728.

150. Kanduc D, Stufano A, Lucchese G, Kusalik A (2008) Massive peptide sharing between viral and human proteomes. *Peptides* 29: 1755-1766.

151. Patel A, Dong JC, Trost B, Richardson JS, Tohme S, et al. (2012) Pentamers Not Found in the Universal Proteome Can Enhance Antigen Specific Immune Responses and Adjuvant Vaccines. *PLoS ONE* 7: e43802.

152. FluView: 2012-2013 Influenza Season Surveillance Summary (CDC) Centers for disease control and prevention.

153. Richer J, Stafford P, Johnston SA (2014) Epitope identification from fixed-complexity random-sequence peptide microarrays. In: Center for Innovations in Medicine TBI, Arizona State University., editor. [Manuscript in preparation] ed. Tempe, Arizona.

154. Krzywinski M, Schein J, Birol I, Connors J, Gascoyne R, et al. (2009) Circos: An information aesthetic for comparative genomics. *Genome Research* 19: 1639-1645.

155. Vesth T, Lagesen K, Acar Ö, Ussery D (2013) CMG-Biotools, a Free Workbench for Basic Comparative Microbial Genomics. *PLoS ONE* 8: e60120.

156. Mina MJ, Klugman KP, McCullers JA (2013) Live Attenuated Influenza Vaccine, But Not Pneumococcal Conjugate Vaccine, Protects Against Increased Density and Duration of Pneumococcal Carriage After Influenza Infection in Pneumococcal Colonized Mice. *Journal of Infectious Diseases* 208: 1281-1285.

157. Roy S, Patil D, Dahake R, Mukherjee S, Athlekar SV, et al. (2012) Prevalence of influenza virus among the paediatric population in Mumbai during 2007-2009. *Indian Journal of Medical Microbiology* 30: 155-158.

158. Prim D, Rebeaud F, Cosandey V, Marti R, Passeraub P, et al. (2013) ADIBO-Based "Click" Chemistry for Diagnostic Peptide Micro-Array Fabrication: Physicochemical and Assay Characteristics. *Molecules* 18: 9833-9849.

159. West Nile virus seroconversion panel No. PWN901. Fisher Scientific. SeraCare Life Sciences Inc.

160. Chamczuk AJ, Ursell M, O'Connor P, Jackowski G, Moscarello MA (2002) A rapid ELISA-based serum assay for myelin basic protein in multiple sclerosis. *Journal of Immunological Methods* 262: 21-27.

161. Narayanan S, Jurafsky D (1998) Bayesian models of human sentence processing. In: Gernsbacher MA, Derry SJE, editors. *Proceedings of 20th Annual Conference of the Cognitive Science Society*. University of Wisconsin-Madison: Lawrence Erlbaum Associates. pp. 752-757.

162. Hjelm B, Forsström B, Löfblom J, Rockberg J, Uhlén M (2012) Parallel Immunizations of Rabbits Using the Same Antigen Yield Antibodies with Similar, but Not Identical, Epitopes. *PLoS ONE* 7: e45817.

163. Hirschmann JV (2007) The early history of coccidioidomycosis: 1892-1945. *Clinical Infectious Diseases* 44: 1202-1207.

164. Lalkhen AG, McCluskey A (2008) Clinical tests: sensitivity and specificity. *Continuing Education in Anaesthesia, Critical Care & Pain* 8: 221-223.

165. Casadevall A, Pirofski L-A (2006) The weapon potential of human pathogenic fungi. *Medical Mycology* 44: 689-696.

166. Clemons KV, Capilla J, Stevens DA (2007) Experimental animal models of coccidioidomycosis. *Coccidioidomycosis: Sixth International Symposium* 1111: 208-224.

167. Tager M, Liebow AA (1942) Intranasal and intraperitoneal infection of the mouse with *Coccidioides immitis*. *Yale Jour Biol and Med* 15: 41-60.

168. Tarbet JE, Wright ET, Newcomer VD (1952) Experimental Coccidioidal Granuloma-Developmental stages of Sporangia in mice. *American Journal of Pathology* 28: 901-917.
169. Shubitz LF, Dial SM, Perrill R, Casement R, Galgiani JN (2008) Vaccine-Induced Cellular Immune Responses Differ from Innate Responses in Susceptible and Resistant Strains of Mice Infected with *Coccidioides posadasii*. *Infection and Immunity* 76: 5553-5564.
170. Taxy JB, Kodros S (2005) Musculoskeletal coccidioidomycosis - Unusual sites of disease in a nonendemic area. *American Journal of Clinical Pathology* 124: 693-696.
171. Schenken JR, Palik EE (1942) Coccidioidomycosis in states other than California, with report of a case in Louisiana. *Archives of Pathology* 34: 484-494.
172. Dionne SO, Podany AB, Ruiz YW, Ampel NM, Galgiani JN, et al. (2006) Spherules derived from *Coccidioides posadasii* promote human dendritic cell maturation and activation. *Infection and Immunity* 74: 2415-2422.
173. Smith DM, Simon JK, Baker JR, Jr. (2013) Applications of nanotechnology for immunology. *Nature Reviews Immunology* 13: 592-605.
174. Shubitz LF, Trinh HT, Perrill RH, Thompson CM, Hanan NJ, et al. (2014) Modeling Nikkomycin Z Dosing and Pharmacology in Murine Pulmonary Coccidioidomycosis Preparatory to Human Phase II Trials. *Journal of Infectious Diseases*.
175. Shubitz LF, Roy ME, Nix DE, Galgiani JN (2013) Efficacy of Nikkomycin Z for respiratory coccidioidomycosis in naturally infected dogs. *Medical Mycology* 51: 747-754.
176. Munteanu CR, Gonzalez-Diaz H, Borges F, de Magalhaes AL (2008) Natural/random protein classification models based on star network topological indices. *Journal of Theoretical Biology* 254: 775-783.
177. Sharma A, Kapoor P, Gautam A, Chaudhary K, Kumar R, et al. (2013) Computational approach for designing tumor homing peptides. *Scientific Reports* 3.

178. Tyagi A, Kapoor P, Kumar R, Chaudhary K, Gautam A, et al. (2013) In Silico Models for Designing and Discovering Novel Anticancer Peptides. *Scientific Reports* 3.
179. Gautam A, Chaudhary K, Kumar R, Sharma A, Kapoor P, et al. (2013) In silico approaches for designing highly effective cell penetrating peptides. *Journal of Translational Medicine* 11.
180. Rubinstein ND, Mayrose I, Halperin D, Yekutieli D, Gershoni JM, et al. (2008) Computational characterization of B-cell epitopes. *Molecular Immunology* 45: 3477-3489.
181. Yuriev E, Ramsland PA (2013) Latest developments in molecular docking: 2010-2011 in review. *Journal of Molecular Recognition* 26: 215-239.
182. Binkowski TA, Marino SR, Joachimiak A (2012) Predicting HLA Class I Non-Permissive Amino Acid Residues Substitutions. *Plos One* 7.
183. Flower DR (2013) Designing immunogenic peptides. *Nature Chemical Biology* 9: 748-752.
184. Jaing C, Gardner S, McLoughlin K, Thissen JB, Slezak T (2011) Detection of Adventitious Viruses from Biologicals Using a Broad-Spectrum Microbial Detection Array. *PDA Journal of Pharmaceutical Science and Technology* 65: 668-674.
185. Tamura K, Peterson D, Peterson N, Stecher G, Nei M, et al. (2011) MEGA5: Molecular Evolutionary Genetics Analysis Using Maximum Likelihood, Evolutionary Distance, and Maximum Parsimony Methods. *Molecular Biology and Evolution* 28: 2731-2739.
186. Bradley H, Markowitz LE, Gibson T, McQuillan GM (2013) Seroprevalence of Herpes Simplex Virus Types 1 and 2—United States, 1999-2010. *Journal of Infectious Diseases*.
187. Chayavichitsilp P, Buckwalter JV, Krakowski AC, Friedlander SF (2009) Herpes Simplex. *Pediatrics in Review* 30: 119-130.

188. Smith JS, Robinson NJ (2002) Age-Specific Prevalence of Infection with Herpes Simplex Virus Types 2 and 1: A Global Review. *Journal of Infectious Diseases* 186: S3-S28.
189. Weiner MH (1983) Antigenemia detected in Human Coccidioidomycosis. *Journal of Clinical Microbiology* 18: 136-142.
190. Galgiani JN, Grace GM, Lundergan LL (1991) New serologic tests for early detection of Coccidioidomycosis. *Journal of Infectious Diseases* 163: 671-674.
191. Johnson SM, Simmons KA, Pappagianis D (2004) Amplification of coccidioidal DNA in clinical specimens by PCR. *Journal of Clinical Microbiology* 42: 1982-1985.
192. Ascioğlu S, Rex JH, de Pauw B, Bennett JE, Bille J, et al. (2002) Defining opportunistic invasive fungal infections in immunocompromised patients with cancer and hematopoietic stem cell transplants: An international consensus. *Clinical Infectious Diseases* 34: 7-14.
193. Telenti A, Roberts GD (1989) Fungal Blood Cultures. *European Journal of Clinical Microbiology & Infectious Diseases* 8: 825-831.
194. Rempe S, Sachdev MS, Bhakta R, Pineda-Roman M, Vaz A, et al. (2007) *Coccidioides immitis* fungemia: Clinical features and survival in 33 adult patients. *Heart & Lung* 36: 64-71.
195. Keckich DW, Blair JE, Vikram HR (2010) *Coccidioides* Fungemia in Six Patients, with a Review of the Literature. *Mycopathologia* 170: 107-115.
196. Idriss MH, Khalil A, Elston D (2013) The diagnostic value of fungal fluorescence in onychomycosis. *Journal of Cutaneous Pathology* 40: 385-390.
197. Plewig G, Marples RR (1970) Regional Differences of Cell sizes in Human Stratum Corneum Part I. *Journal of Investigative Dermatology* 54: 13-&.
198. Fetsch PA, Abati A (2001) Immunocytochemistry in effusion cytology - A contemporary review. *Cancer Cytopathology* 93: 293-308.

199. Pass HI, Stevens EJ, Oie H, Tsokos MG, Abati AD, et al. (1995) Characteristics of nine newly-derived mesothelioma cell lines. *Annals of Thoracic Surgery* 59: 835-844.
200. Kaplan W (1967) Application of the fluorescent antibody technique to the diagnosis and study of coccidioidomycosis. *Proceedings of the Second Symposium on Coccidioidomycosis*, 8-10 December, 1965, Phoenix, Ariz: 227-231.
201. Graham AR (1983) Fungal Autofluorescence with Ultraviolet illumination. *American Journal of Clinical Pathology* 79: 231-234.
202. Elston DM (2001) Fluorescence of fungi in superficial and deep fungal infections. *BMC Microbiology* 1: 1-4.
203. Rao S, Rajkumar A, Ehtesham M, Prathiba D (2008) Autofluorescence: A screening test for mycotic infection in tissues. *Indian Journal of Pathology and Microbiology* 51: 215-217.
204. Jiang CY, Magee DM, Ivey FD, Cox RA (2002) Role of signal sequence in vaccine-induced protection against experimental coccidioidomycosis. *Infection and Immunity* 70: 3539-3545.
205. Cenci S, Sitia R (2007) Managing and exploiting stress in the antibody factory. *Febs Letters* 581: 3652-3657.
206. Chen Y, Cai J, Xu Q, Chen ZW (2004) Atomic force bio-analytics of polymerization and aggregation of phycoerythrin-conjugated immunoglobulin G molecules. *Molecular Immunology* 41: 1247-1252.
207. Henry N, Parce JW, McConnell HM (1978) Visualization of specific antibody and C1q binding to hapten-sensitized lipid vesicles. *Proceedings of the National Academy of Sciences of the United States of America* 75: 3933-3937.
208. Chan KH, To KKW, Hung IFN, Zhang AJX, Chan JFW, et al. (2011) Differences in Antibody Responses of Individuals with Natural Infection and Those Vaccinated against Pandemic H1N1 2009 Influenza. *Clinical and Vaccine Immunology* 18: 867-873.

209. Cretich M, Damin F, Longhi R, Gotti C, Galati C, et al. (2010) Peptide Microarrays on Coated Silicon Slides for Highly Sensitive Antibody Detection. *Small Molecule Microarrays: Methods and Protocols* 669: 147-160.

210. Whitlock GC, Robida MD, Judy BM, Qazi O, Brown KA, et al. (2011) Protective antigens against glanders identified by expression library immunization. *Frontiers in Microbiology* 2.

211. Borca MV, Irusta P, Carrillo C, Afonso CL, Burrage T, et al. (1994) African swine fever virus structural protein p72 contains a conformational neutralizing epitope. *Virology* 201: 413-418.

212. Pedelacq JD, Cabantous S, Tran T, Terwilliger TC, Waldo GS (2006) Engineering and characterization of a superfolder green fluorescent protein. *Nature Biotechnology* 24: 79-88.

213. Sykes KF, Johnston SA (1999) Linear expression elements: a rapid, in vivo, method to screen for gene functions. *Nature Biotechnology* 17: 355-359.

214. Montor WR, Huang J, Hu YH, Hainsworth E, Lynch S, et al. (2009) Genome-Wide Study of *Pseudomonas aeruginosa* Outer Membrane Protein Immunogenicity Using Self-Assembling Protein Microarrays. *Infection and Immunity* 77: 4877-4886.

APPENDIX I

COCCIDIOIDES SPHERULES IN SERA

INTERFERENCE IN MICROARRAYS – SUPPLEMENTAL FIGURES AND TABLES

FOR CHAPTER 2

The recovery of culturable *Coccidioides* spherules from blood is 0.4% (n=5,026; 0.4% = 20 samples) as per a retrospective study from processing 55,788 samples in a diagnostic lab in Phoenix (endemic for *Coccidioides*) [77]. The highest recovery rate of this pathogen through culturing techniques is directly from the primary site of infection, i.e. respiratory tract specimens is 8.3% (n=10,372; 8.3% = 861 samples). Coccidioidal antigenemia to galactomannan [136] or coccidioides specific antigens [189,190] has been detected in patient sera through ELISA's for antigens and DNA using PCR [191]. Fungemia [192] is a common feature of several fungal infections, but only observed in the disseminated form of Coccidioidomycosis [193]. The prognosis of these patients is poor with mortality rates up to 73% [194] Till date, 113 cases showing fungemia have been reported in literature as reviewed by Blair *et al.* in 2010 [195]. The detection of fungemia in Coccidioidomycosis is impeded due to physician's not ordering the fungal blood culture assay or the assay not being performed in clinical laboratories with modifications providing higher recovery rates from blood [193]. One such modification is the lysis centrifugation system whereby, whole blood is lysed and centrifuged so that the microorganisms are released from polymorphonuclear leukocytes and the sediment is cultured on appropriate fungal culture media [193].

The spherules of *Coccidioides* range in size from 3 μm to the largest recorded in literature from a patient, 262 μm [171]. The following observation is the first report on Coccidioidal spherules-like objects observed in Valley Fever (VF) infected patient sera and the probable interference they might impose on antibody detecting peptide microarrays. Coccidioidal antigenemia in sera is reported to interfere with antigen

detection based assays yielding lower true positives. For example, in the MiraVista Diagnostic Coccidioidal anti-galactomannan antibodies were used to detect antigenemia in EDTA and heat treated sera (73.1% positive) versus untreated sera (28.6% true positives detected). In context to the peptide microarray, if Coccidioidal spherules capture VF infected individuals antibody, a protocol change allowing dissociation of circulating antigen-antibody complexes without degrading antibodies from VF infected sera might enhance detection of antibodies on our assay.

I noted the presence of brightly fluorescent spherule-like globular objects when processing patient sera from VF infected individuals (Figure A1- 1, Figure A1- 2). A summary of these incidental observations is presented in Table A1- 1. The diameter of these N=15 spherule-like globules observed from 12 patient sera falls within the range observed in clinical samples with the exception of the larger spherules (290 to 486 μ m). The size of these objects made it unlikely that they were T or B cells (7-10 μ m), Dendritic cells or Macrophages (10-22 μ m) Neutrophils (8-15 μ m) and Eosinophils (10-12 μ m) [173] or auto-fluorescent human skin cells [196] from the stratum-corneum (34-44 μ m) [197]. The spherule-like objects likely showed high fluorescence in both red (IgM-Median fluorescence intensity units (FIU) range: 6,237.5 to 50,358) and green channels (IgG-Median FIU range: 1,040 to 11,711). These images were obtained during routine scanning of 1:500 diluted patient sera which was incubated on the VF diagnostic peptide sub-array and detected using anti-human secondary antibodies. Such globular objects were not observed on slides when processing any other infected sera (West Nile Virus (WNV) infected human sera, *F.tularensis* Live Vaccine Strain (LVS) vaccinated

human sera, Normal human sera, African Swine Fever Virus (ASFV) infected swine sera, Influenza PR8 strain infected mouse sera, Vaccinia-Western Reserve strain vaccinated human sera) under similar microarray processing conditions.

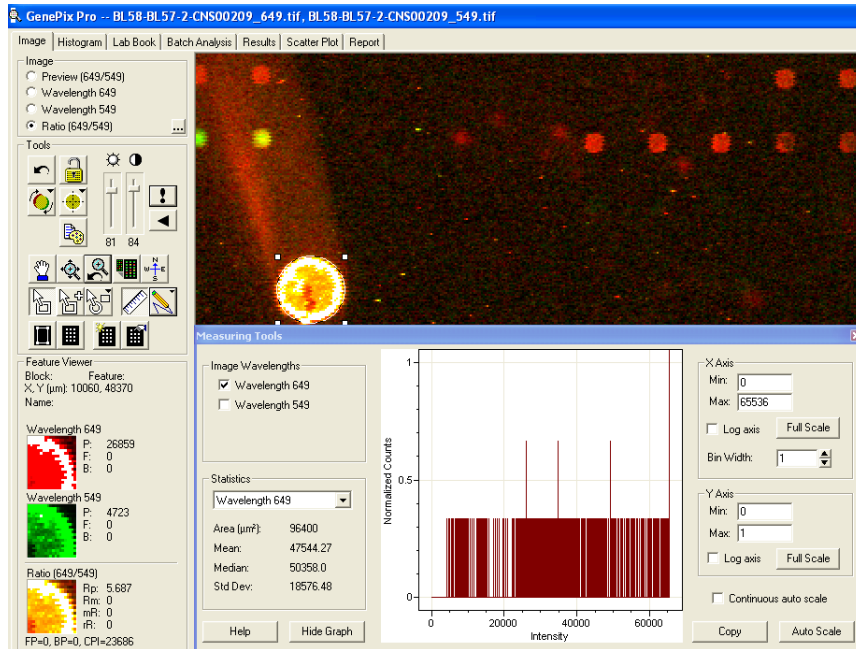


Figure A1- 1 A screenshot of a spherule-like object (Slide No. CNS00209) as captured using GenePix Pro on the VF diagnostic sub-array (slide surface: Aminosilane).

The distribution of signal in fluorescence intensity (FIU) within the encircled area selected is depicted at a wavelength of 649 nm.

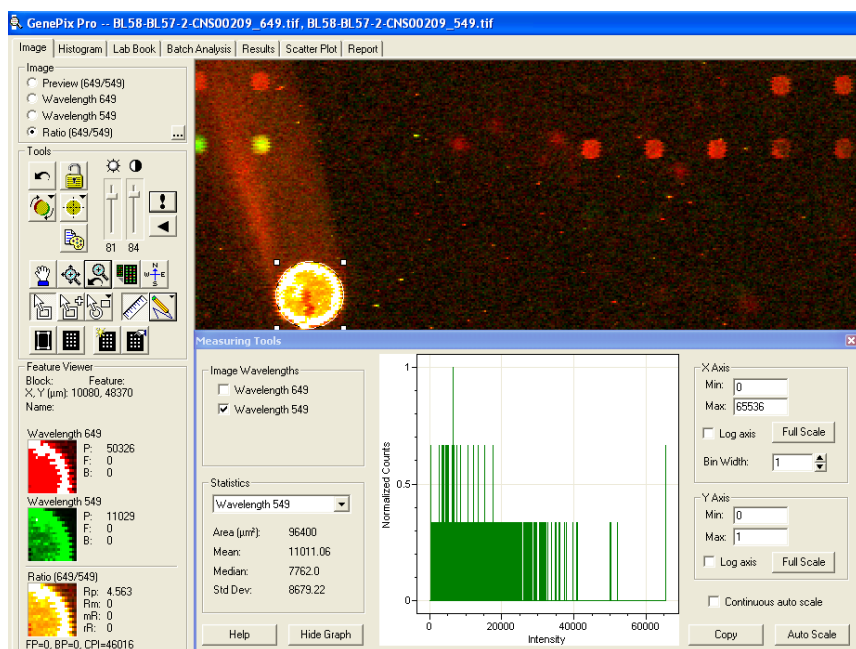
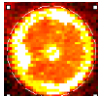
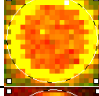
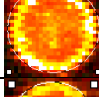
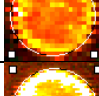
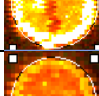
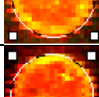
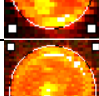
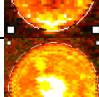
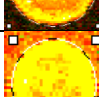
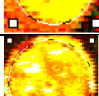



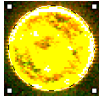
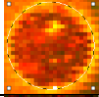

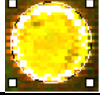
Figure A1- 2 A screenshot of a spherule-like object (Slide No. CNS00209) as captured within GenePix on the VF diagnostic sub-array (slide surface: Aminosilane)

The distribution of signal in fluorescence intensity units (FIU) within the encircled area selected is depicted at a wavelength of 549 nm.

Table A1- 1 Summary of Spherules-like objects observed in VF infected individuals sera when incubated on aminosilane surface VF diagnostic sub-arrays.

Signals depicted in Fluorescence intensity units (FIU).

No.	Patient No.	Slide Number	Area-GenePix estimate(μm^2)	GenePix estimated Diameter (μm)	Mean Signal FIU (649nm)	Mean Signal FIU (549nm)	Spherule-like objects
1	BL55 (0-407)	CNS0 0206	78400	316	39527	3184	
2	32-555	CNS0 0146	21800	167	13817	3016	
3	BL58 (1-412)	CNS0 0208	44000	237	31604	3842	
4	BL58 (1-412)	CNS0 0208	21800	167	21461	3034	
5	BL57 (0-412)	CNS0 0209	96400	350	47544	11011	
6	BL58 (1-412)	CNS0 0209	29200	193	26146	2568	
7	BL61 (0-413)	CNS0 0210	29200	193	22687	2814	
8	BL62 (0-413)	CNS0 0213	73600	306	25863	3040	
9	BL68 (0-472)	CNS0 0216	166100	460	25608	2690	
10	32-1280	CNS0 0149	53600	261	16971	2935	
11	BL49 (0-391)	CNS0 0201	151700	440	34247	6707	

12	BL49 (0-391)	CNS0 0201	185600	486	24104	11521	
13	2-7	CNS0 0123	35200	212	11996	1602	
14	64-607	CNS0 0152	66400	291	25537	3474	
15	BL52 (0-401)	CNS0 0205	38500	221	32862	13208	

Several aspects of processing peptide microarrays are identical to pre-processing conditions applied in Immunohistochemistry (IHC). For example, the peptide microarray slide surface used in this analysis was Aminosilane activated with SMCC (primary amines present on surface at a density of one free primary amine group ~ per 1nm). In IHC cytospin protocols, cells are fixed on silanated glass slides [198]. The patient sera in this assay was diluted 1:500 in the standard microarray incubation buffer and incubated on the array at 37°C for 1 hour using the Tecan Pro automated hybridization station. In IHC a short fixing protocol involves fixing the cellular material on plain glass slides for 30 minutes to 1 hour at room temperature [198,199] or on a 37°C slide warmer. Fluorescent dye labeled anti-pathogen antibodies have been used for direct detection and differentiation of *Coccidioides* from other fungal pathogens in microscopy and IHC techniques [200]. The direct detection technique involves fixing the pathogen on a glass slide and detecting the pathogen with fluorescent dye labeled anti-pathogen serum. The indirect detection technique involves fixing the pathogen on a glass slide, incubating patient serum on it and detecting the pathogen bound patient serum using an anti-host fluorescently labeled antibody. The peptide microarray slides were scanned on a Perkin

Elmer ProScan Array HT microarray scanner (Melville, NY) in two channels, 633 nm (Red wavelength) and 543 nm (Green wavelength) at 10µm resolution. This scanner scans slides from the top, slide-facing surface. The secondary anti-host (human) IgM and IgG antibodies are conjugated to fluorescent dyes, Dylight 649 and Dylight 549 respectively. The microarray images included in this Appendix are from the PerkinElmer scanner, but were also scanned using the Agilent 'C' scanner (Santa Clara, CA). The Agilent microarray scanner scans the back of the slide with excitation at 633 nm (Red) and 532 nm (Green) with 10µm resolution.

Hypothesis

In the red and green wavelength, we might be detecting fluorescence from the secondary anti-human IgM (5µ) and anti-human IgG (Fcγ) antibody detecting the Fc portion of pre-bound IgM and IgG antibodies from the patient's serum, on the spherule-like object. The fluorescence intensity estimated by GenePix in both red and green wavelengths is much higher than background fluorescence observed from these slides.

This hypothesis could be tested by either culturing the pathogen from patient sera listed in Table A1- 1 or checking for fungal auto-fluorescence using UV illumination in fluorescence microscopy (serum sediment). Fungi including *Coccidioides* spherules are known to auto-fluoresce upon UV illumination in the green wavelength [201,202]. This fungal auto-fluorescence has been used for diagnosis with a sensitivity of 97.8% and specificity of 100% (n=64) to distinguish *Aspergillus*, *Candida* and *Zygomycetes* cases in Hematoxylin and Eosin stained tissue sections from several tissue sites by Rao *et al*

[203]. A more sensitive confirmation could be made utilizing PCR to confirm the presence of DNA from *Coccidioides* in centrifuged patient serum sediment [191] Given the paucity of accurate VF diagnostics and variability of symptoms, any approach enabling direct detection of VF is useful and is therefore documented in this report.

Bibliography

1. Saubolle MA, McKellar PP, Sussland D. 2007. Epidemiologic, clinical, and diagnostic aspects of coccidioidomycosis. *Journal of Clinical Microbiology* 45:26-30.
2. Durkin M, Estok L, Hospenhal D, Crum-Cianflone N, Swartzentruber S, Hackett E, Wheat LJ. 2009. Detection of *Coccidioides* Antigenemia following Dissociation of Immune Complexes. *Clinical and Vaccine Immunology* 16:1453-1456.
3. Weiner MH. 1983. Antigenemia detected in Human Coccidioidomycosis. *Journal of Clinical Microbiology* 18:136-142.
4. Galgiani JN, Grace GM, Lundergan LL. 1991. New serologic tests for early detection of Coccidioidomycosis. *Journal of Infectious Diseases* 163:671-674.
5. Johnson SM, Simmons KA, Pappagianis D. 2004. Amplification of coccidioidal DNA in clinical specimens by PCR. *Journal of Clinical Microbiology* 42:1982-1985.
6. Ascoglu S, Rex JH, de Pauw B, Bennett JE, Bille J, Crokaert F, Denning DW, Donnelly JP, Edwards JE, Erjavec Z, Fiere D, Lortholary O, Maertens J, Meis JF, Patterson TF, Ritter J, Selleslag D, Shah PM, Stevens DA, Walsh TJ, Invasive Fungal Infections C. 2002. Defining opportunistic invasive fungal infections in immunocompromised patients with cancer and hematopoietic stem cell transplants: An international consensus. *Clinical Infectious Diseases* 34:7-14.
7. Telenti A, Roberts GD. 1989. Fungal Blood Cultures. *European Journal of Clinical Microbiology & Infectious Diseases* 8:825-831.
8. Rempe S, Sachdev MS, Bhakta R, Pineda-Roman M, Vaz A, Carlson RW. 2007. *Coccidioides immitis* fungemia: Clinical features and survival in 33 adult patients. *Heart & Lung* 36:64-71.

9. Keckich DW, Blair JE, Vikram HR. 2010. *Coccidioides* Fungemia in Six Patients, with a Review of the Literature. *Mycopathologia* 170:107-115.
10. Schenken JR, Palik EE. 1942. Coccidioidomycosis in states other than California, with report of a case in Louisiana. *Archives of Pathology* 34:484-494.
11. Smith DM, Simon JK, Baker JR, Jr. 2013. Applications of nanotechnology for immunology. *Nature Reviews Immunology* 13:592-605.
12. Idriss MH, Khalil A, Elston D. 2013. The diagnostic value of fungal fluorescence in onychomycosis. *Journal of Cutaneous Pathology* 40:385-390.
13. Plewig G, Marples RR. 1970. Regional Differences of Cell sizes in Human Stratum Corneum Part I. *Journal of Investigative Dermatology* 54:13-&.
14. Fetsch PA, Abati A. 2001. Immunocytochemistry in effusion cytology - A contemporary review. *Cancer Cytopathology* 93:293-308.
15. Pass HI, Stevens EJ, Oie H, Tsokos MG, Abati AD, Fetsch PA, Mew DJY, Pogrebniak HW, Matthews WJ. 1995. Characteristics of nine newly-derived mesothelioma cell lines. *Annals of Thoracic Surgery* 59:835-844.
16. Kaplan W. 1967. Application of the fluorescent antibody technique to the diagnosis and study of coccidioidomycosis. *Proceedings of the Second Symposium on Coccidioidomycosis, 8-10 December, 1965, Phoenix, Ariz.:*227-231.
17. Graham AR. 1983. Fungal Autofluorescence with Ultraviolet illumination. *American Journal of Clinical Pathology* 79:231-234.
18. Elston DM. 2001. Fluorescence of fungi in superficial and deep fungal infections. *BMC Microbiology* 1:1-4.
19. Rao S, Rajkumar A, Ehtesham M, Prathiba D. 2008. Autofluorescence: A screening test for mycotic infection in tissues. *Indian Journal of Pathology and Microbiology* 51:215-217.

APPENDIX II
SUPPLEMENTAL DATA FOR CHAPTER 3 – VALLEY FEVER EPITOPE
PEPTIDES

The raw IgG and IgM antibody reactivities in FIU (Y-axis) captured by 83 life space epitope peptides representing 4 Valley Fever (VF) immuno-dominant antigens is plotted per peptide (X-axis) in these graphs. The 4 antigens were chitinase F (CF) [81], Expression Library Immunization Eli-Ag1 [83], Antigen 2 [82] and *Coccidioides* specific antigen (CSA) [84]. These data show the trend (bright red line) in humoral immune responses at various stages of Valley Fever infection from CF-Titer=0 (primary) to CF-titer=256 (dissemination). The advantage of using peptide microarrays is their ability to separate each component of the humoral immune response to an infection/exposure. This high resolution is advantageous while evaluating whether or not certain VF proteins offer protection and could potentially be used as vaccine candidates against VF. For example, the signal sequence of Ag2 (amino acids 1-18) is known to be protective in BALBc (VF susceptible) mice upon immunization and challenge [204]. In our data as well, some VF patients display a high IgG antibody response to Ag2 peptides at the same amino acid positions (1-17, 13-29 and 25-41) in primary infection (CF-titer = 1, *Figure A2-3*).

At all CF-titers (0, 1, 2, 4, 8, 16, 32, 64, 128, 256) the IgM graphs show higher binding than IgG data at multiple epitope sites displaying the breadth of IgM response. The IgM response might also be broad because IgM is a much larger molecule (36nm x 4nm- planar disk) [205] as compared to IgG (20-40nm) [206,207] and is reactive to many VF epitope peptides in this solid phase assay (antigen peptide attached to solid slide surface). From our own experimental data however, we know that the specificity when using IgM data is lower than that obtained using IgG data for distinguishing VF versus normal (Table 3-2, Panel A) or VF versus non-VF (normal and LVS, Table 3-2, Panel B).

Thus it would be unlikely that IgM array data alone might be sufficient for diagnosis.

This concept would need to be tested on a larger peptide microarray (>96 peptides).

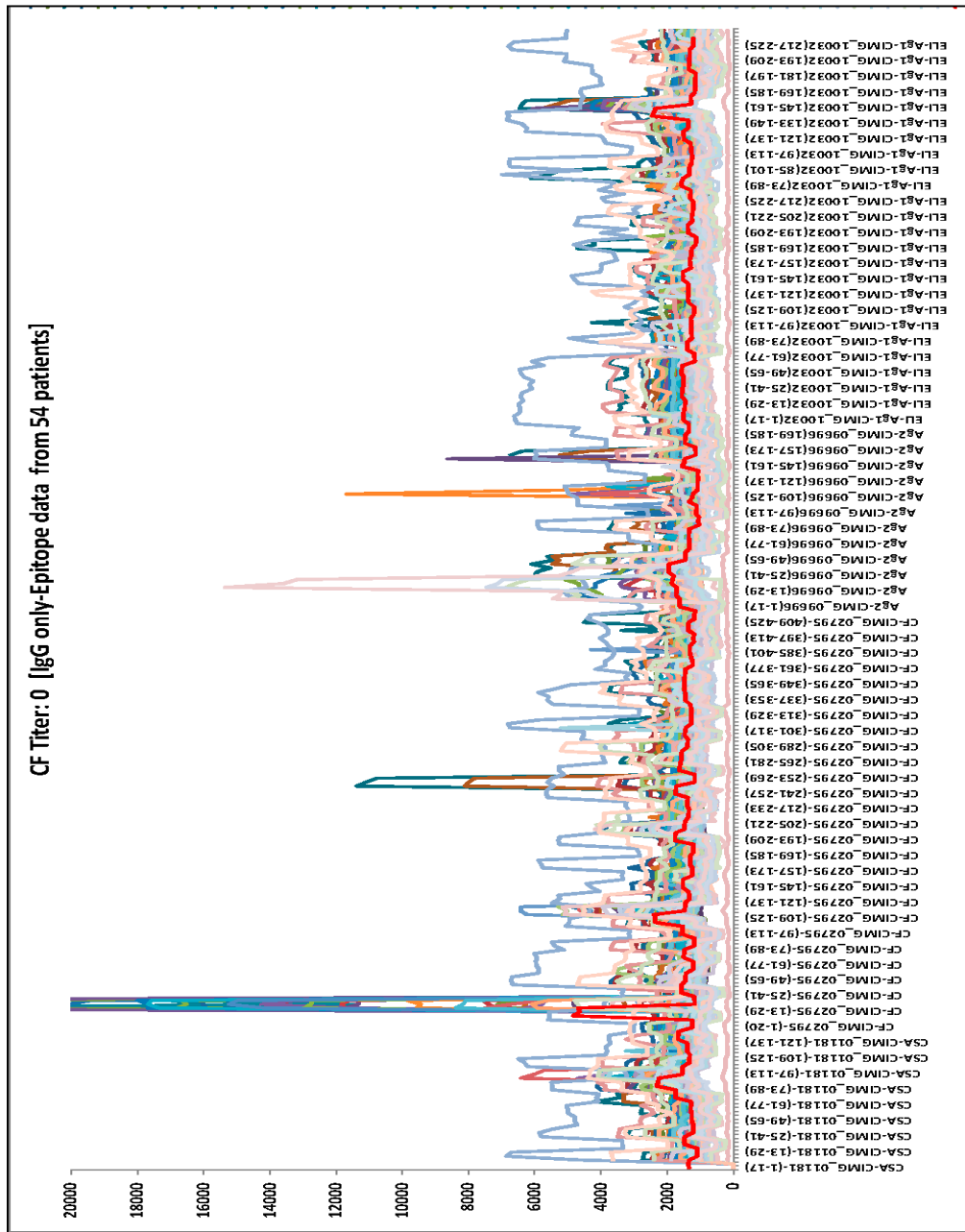


Figure A2-1 IgG antibody reactivity captured on VF epitope peptides (83) from false-negative CF-titer=0 patients sera (N=54). Each line on the graph represents antibody response from one VF sample.

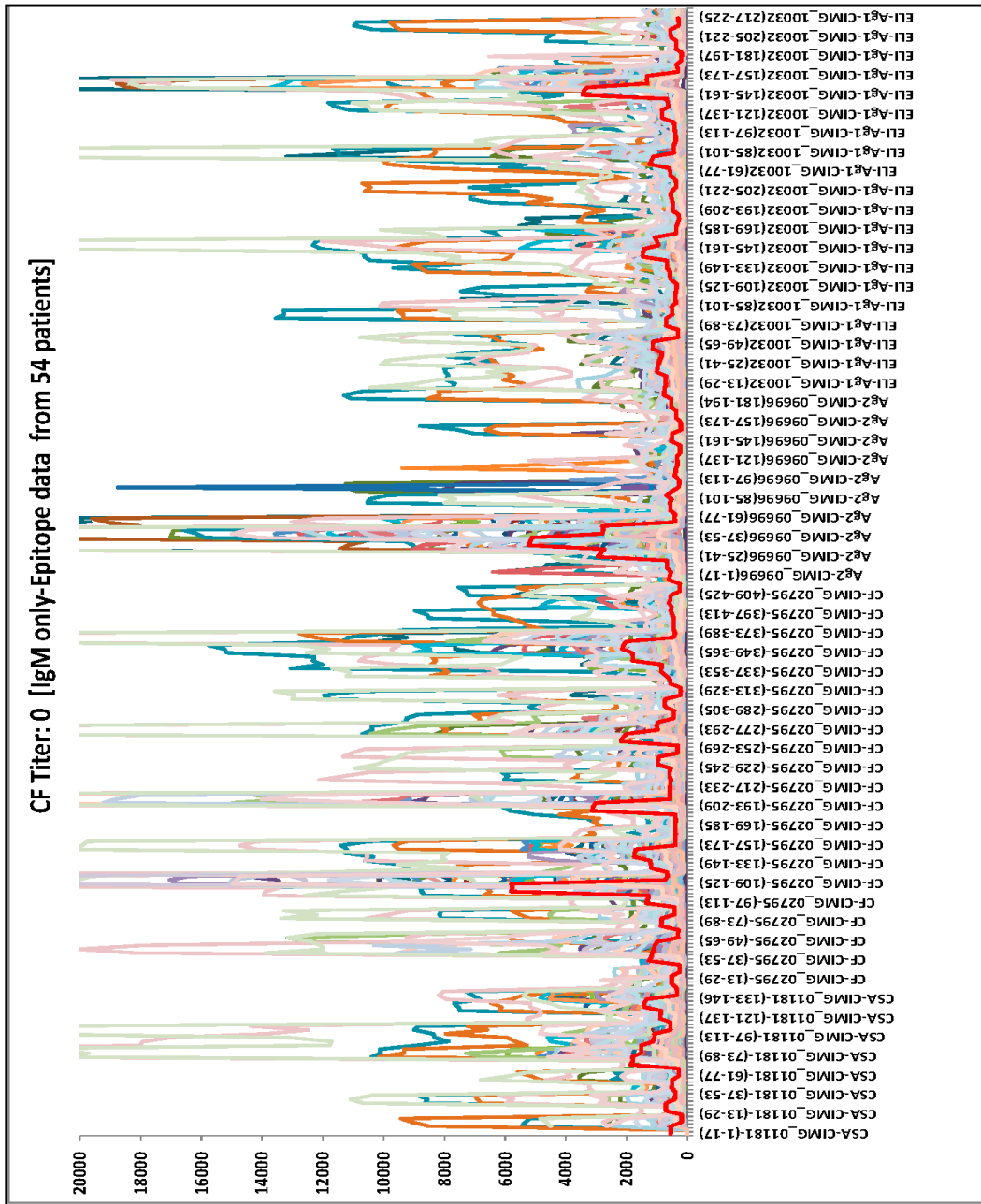


Figure A2-2 IgM antibody reactivity captured on VF epitope peptides (83) from false-negative CF-titer=0 patients sera (N=54) Each line on the graph represents antibody response from one VF sample.

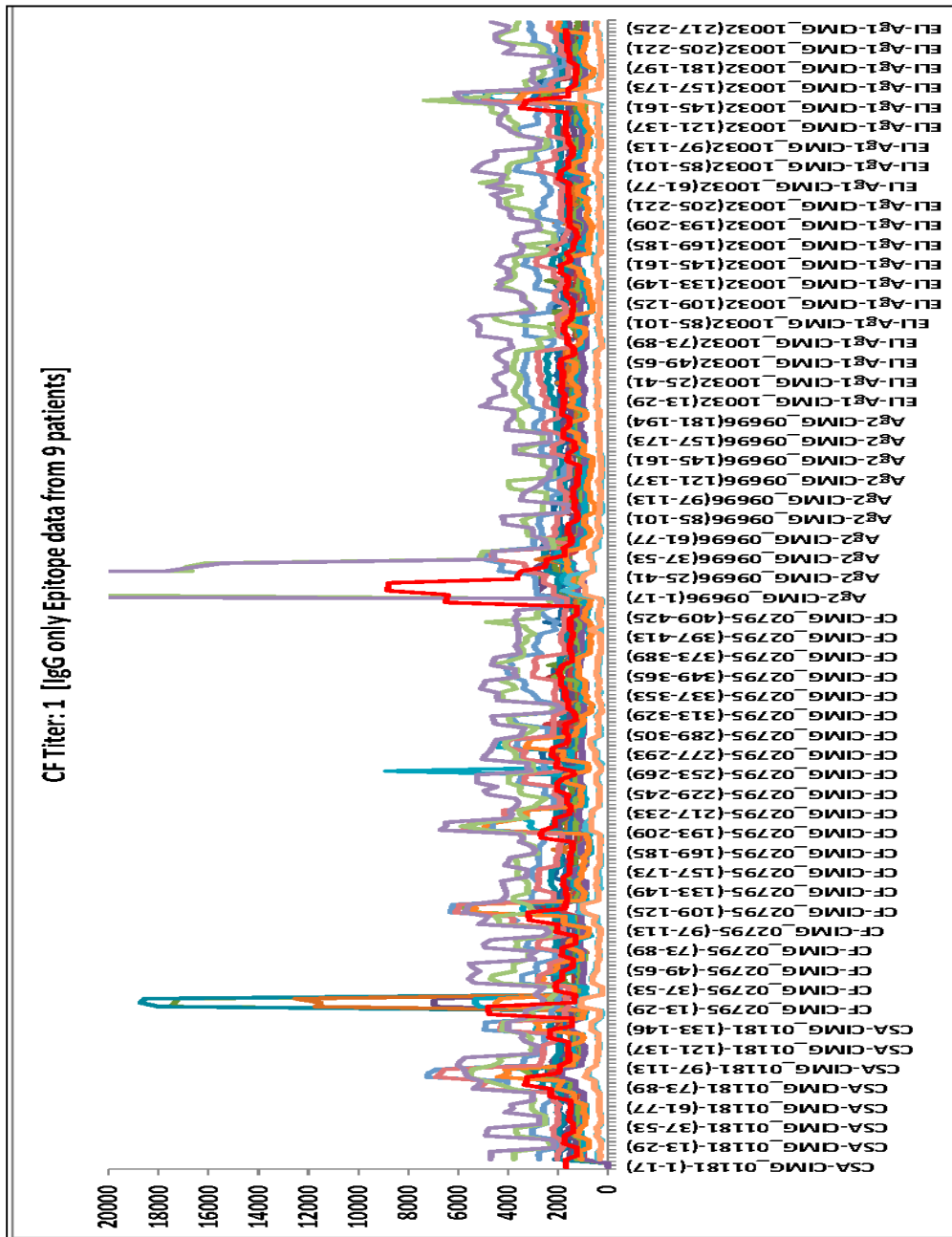


Figure A2-3 IgG antibody reactivity captured on VF epitope peptides (83) from CF-titer=1 patients sera (N=9). Each line on the graph represents antibody response from one VF sample.

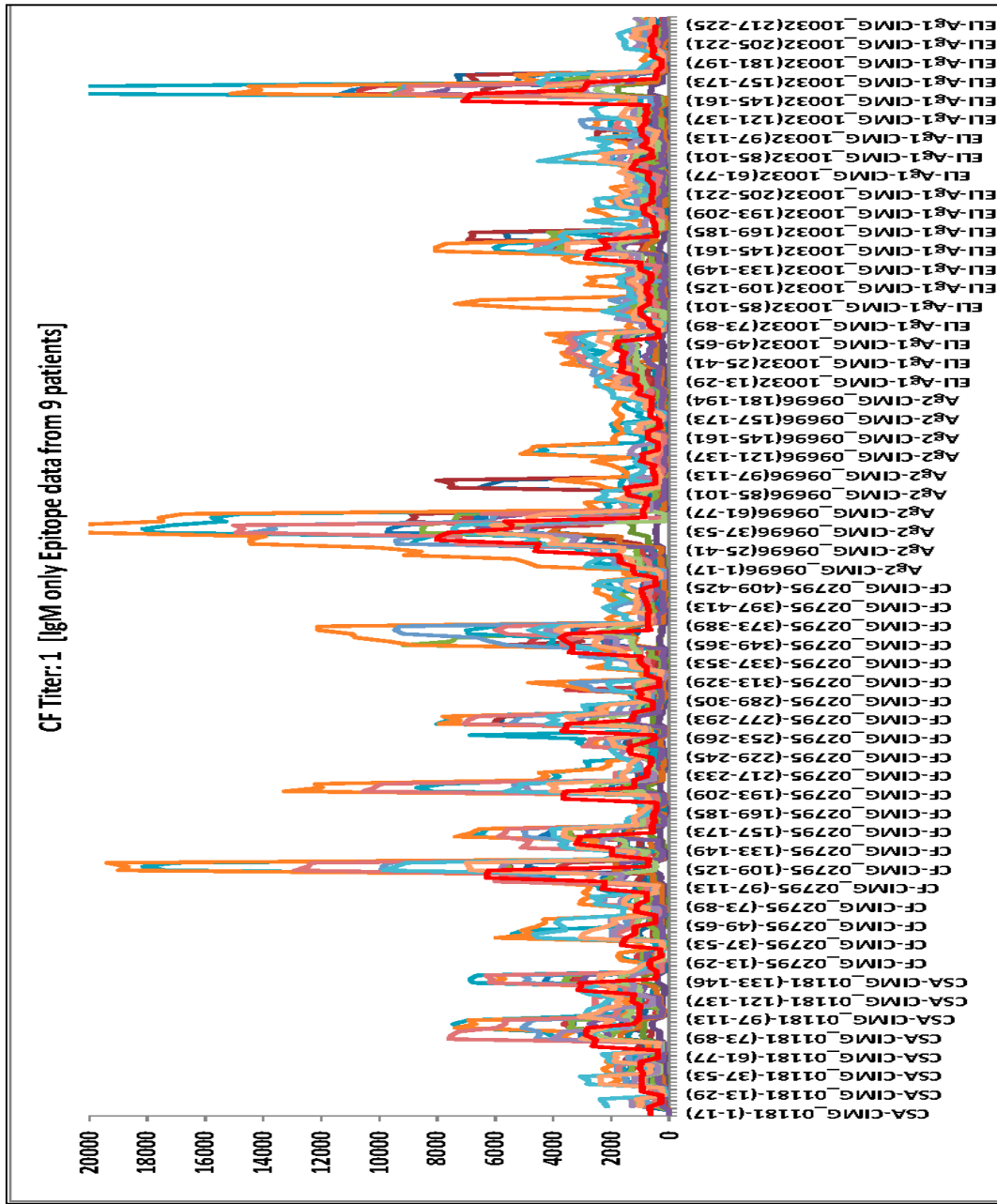


Figure A2-4 IgM antibody reactivity captured on VF epitope peptides (83) from CF-titer=1 patients sera (N=9). Each line on the graph represents antibody response from one VF sample.

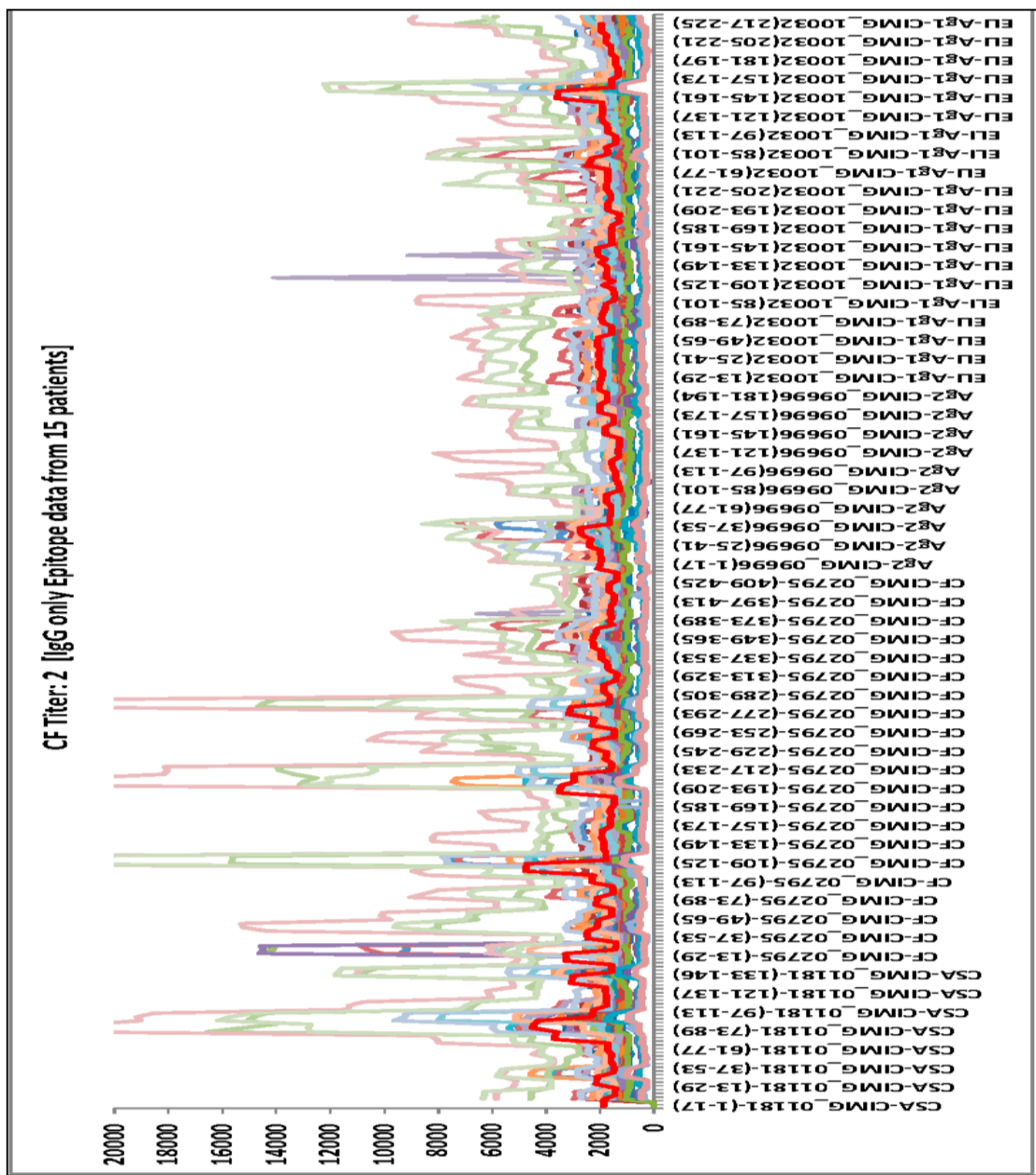


Figure A2-5 IgG antibody reactivity captured on VF epitope peptides (83) from CF-titer=2 patients sera (N=15). Each line on the graph represents antibody response from one VF sample.

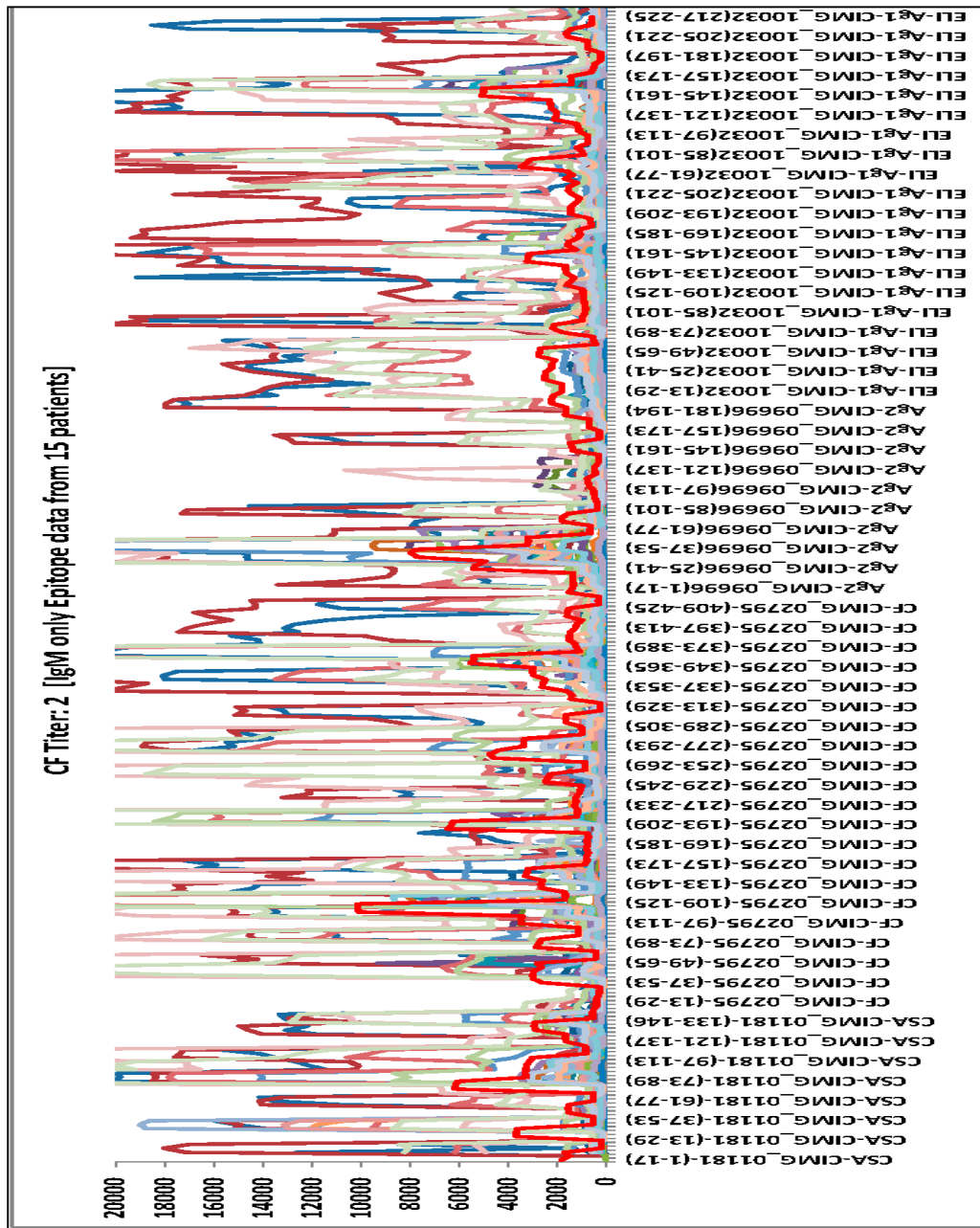


Figure A2-6 IgM antibody reactivity captured on VF epitope peptides (83) from CF-titer=2 patients sera (N=15). Each line on the graph represents antibody response from one VF sample.

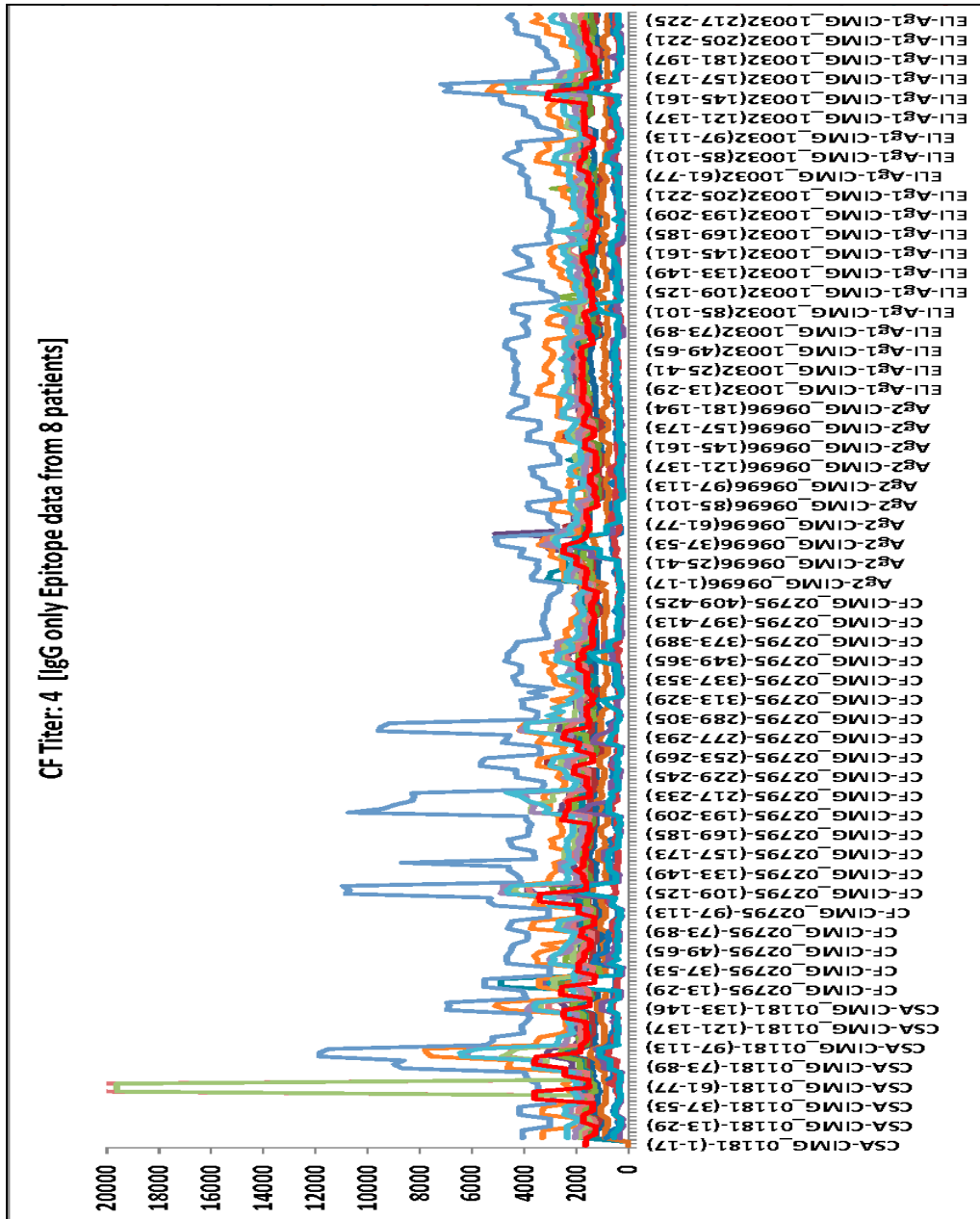


Figure A2-7 IgG antibody reactivity captured on VF epitope peptides (83) from CF-titer=4 patients sera (N=8). Each line on the graph represents antibody response from one VF sample.

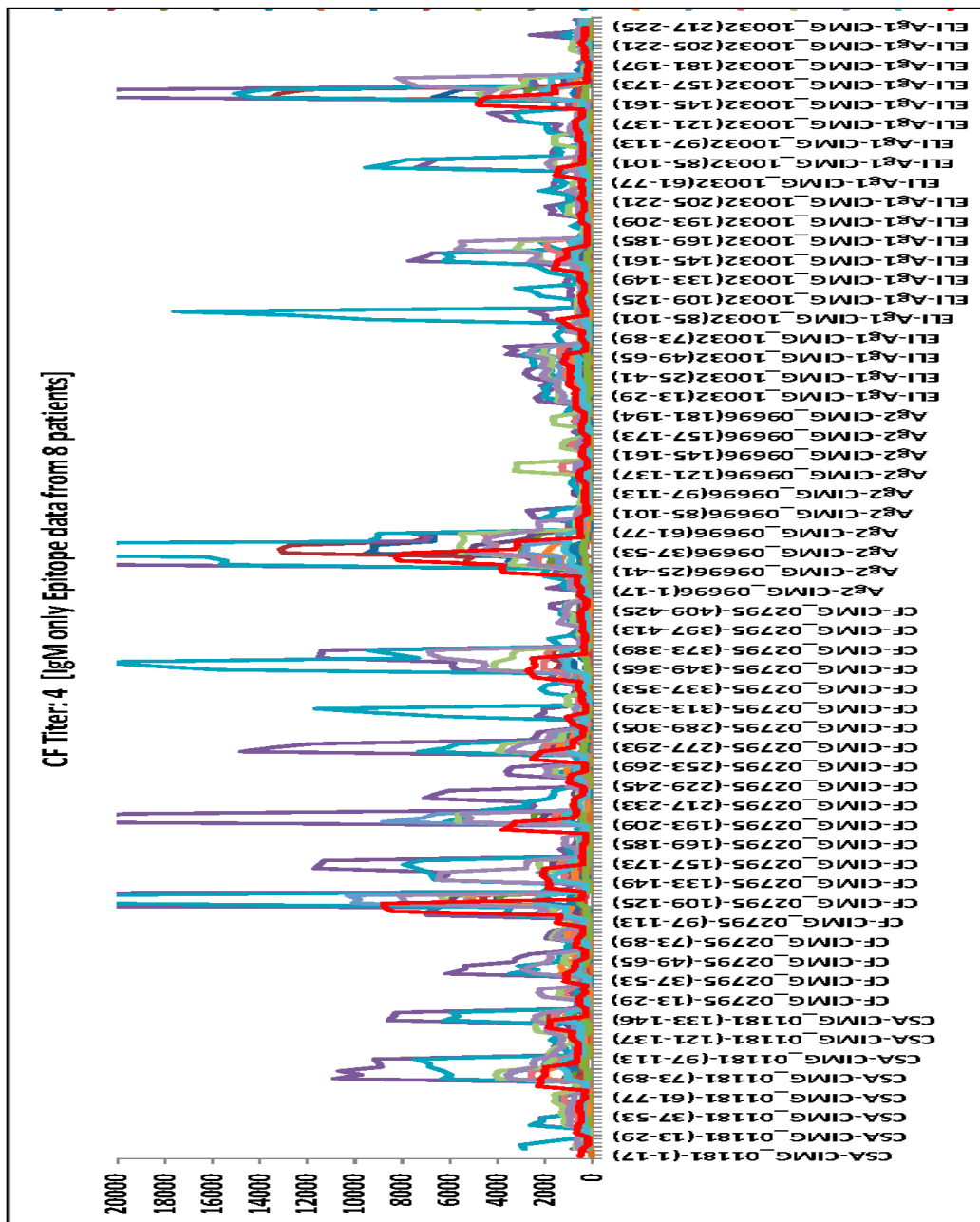


Figure A2-8 IgM antibody reactivity captured on VF epitope peptides (83) from CF-titer=4 patients sera (N=8). Each line on the graph represents antibody response from one VF sample.

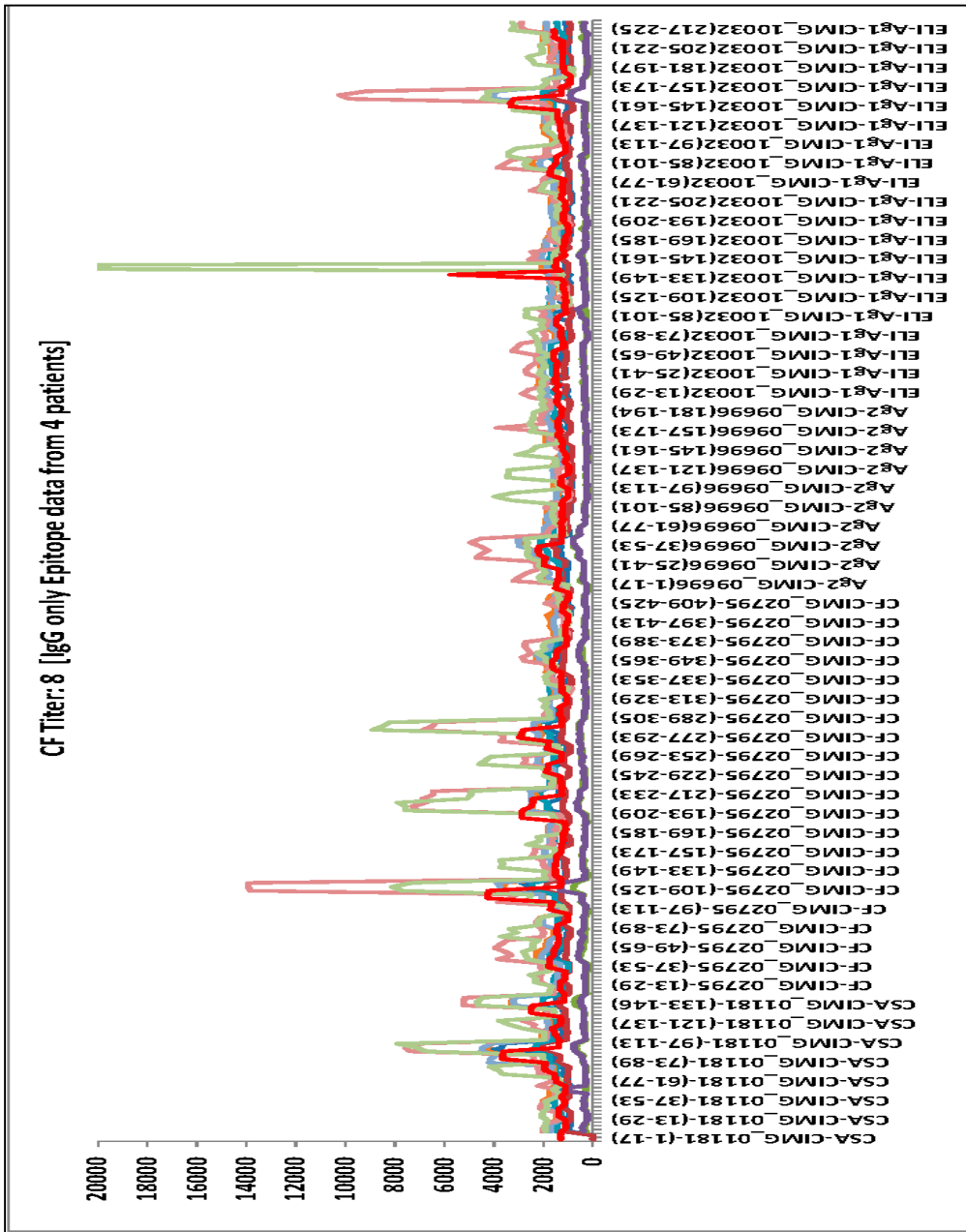


Figure A2-9 IgG antibody reactivity captured on VF epitope peptides (83) from CF-titer=8 patients sera (N=4). Each line on the graph represents antibody response from one VF sample.

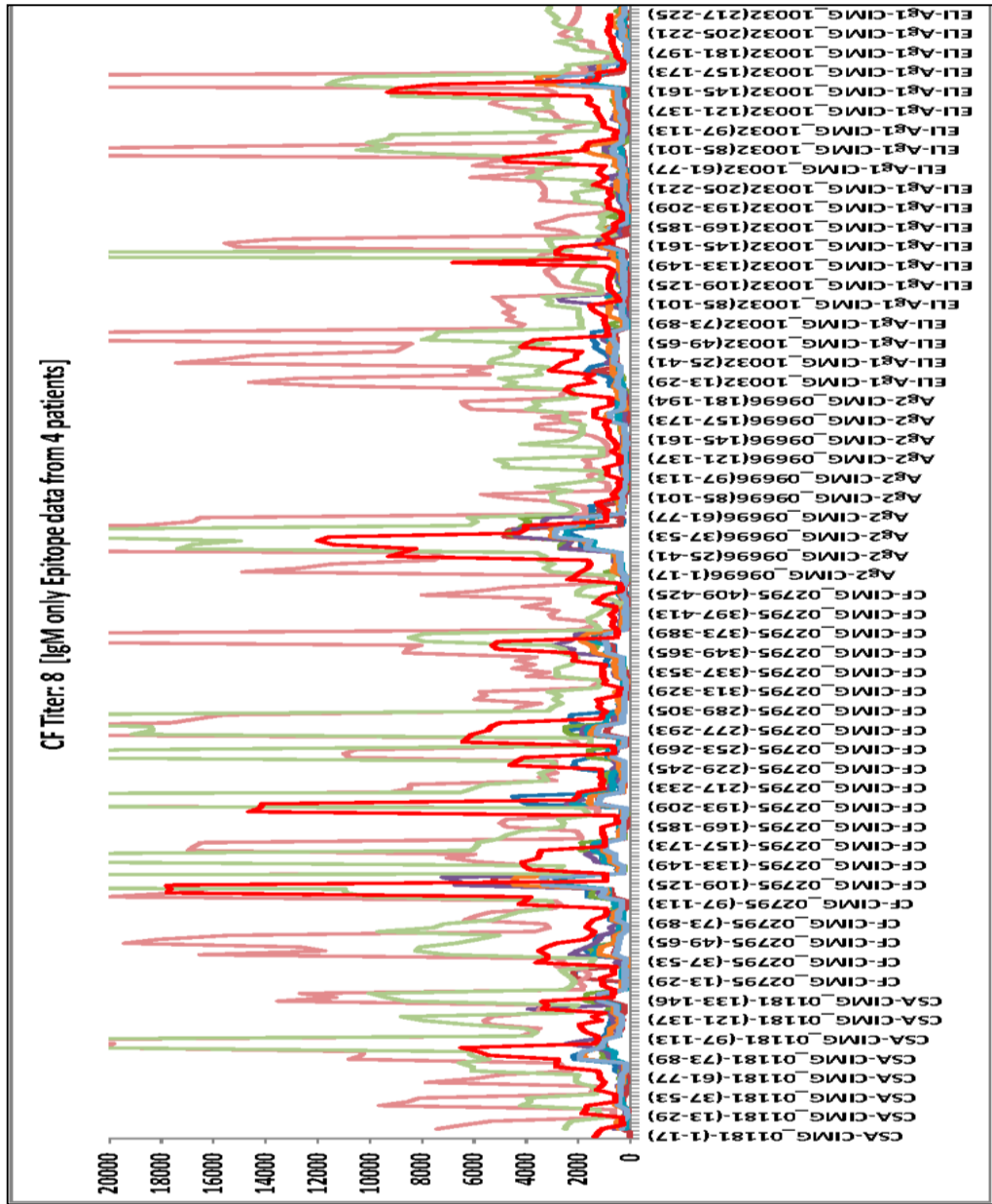


Figure A2-10 IgM antibody reactivity captured on VF epitope peptides (83) from CF-titer=8 patients sera (N=4). Each line on the graph represents antibody response from one VF sample.

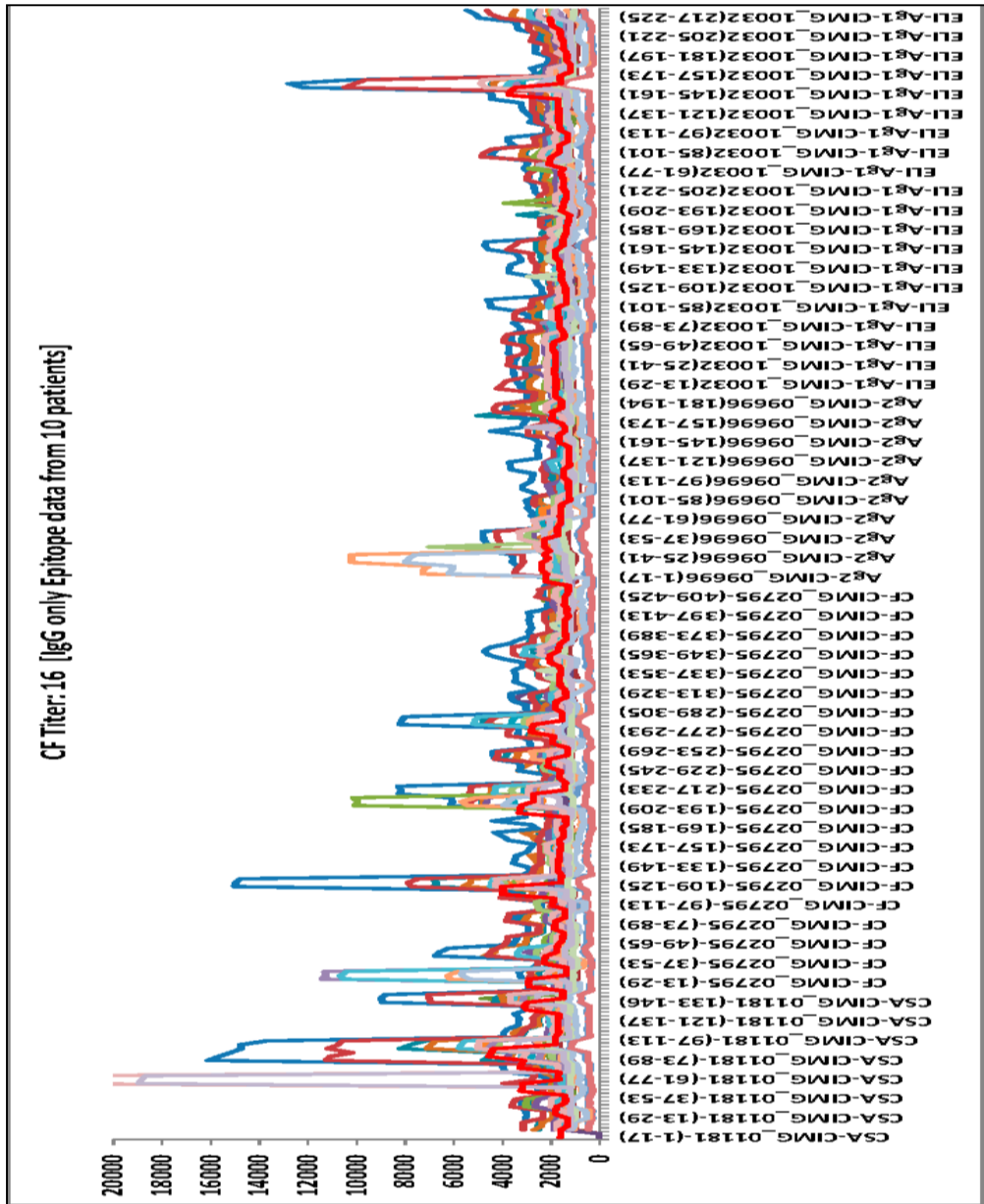


Figure A2-11 IgG antibody reactivity captured on VF epitope peptides (83) from CF-titer=16 patients sera (N=10). Each line on the graph represents antibody response from one VF sample.

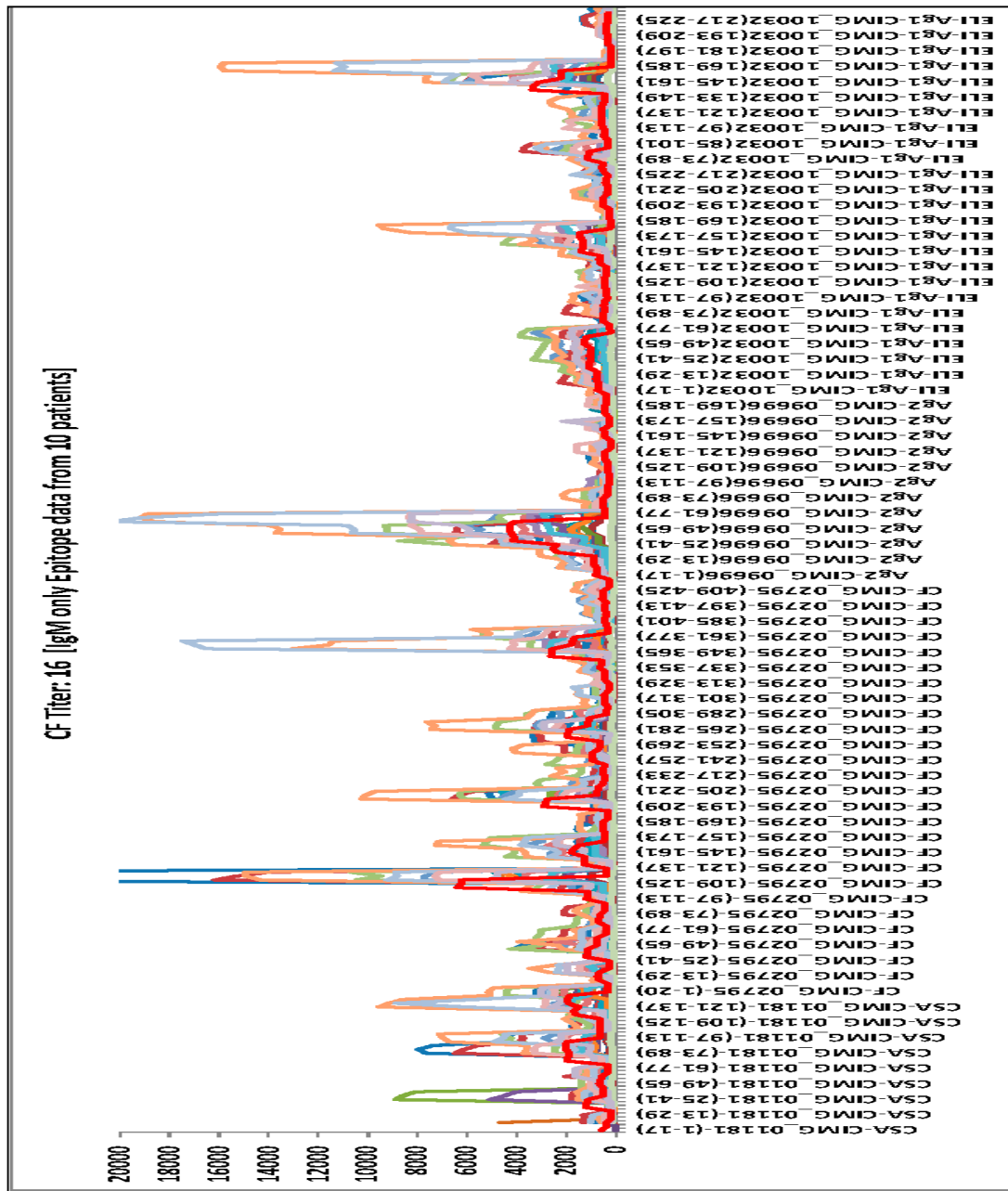


Figure A2-12 IgM antibody reactivity captured on VF epitope peptides (83) from CF-titer=16 patients sera (N=10). Each line on the graph represents antibody response from one VF sample.

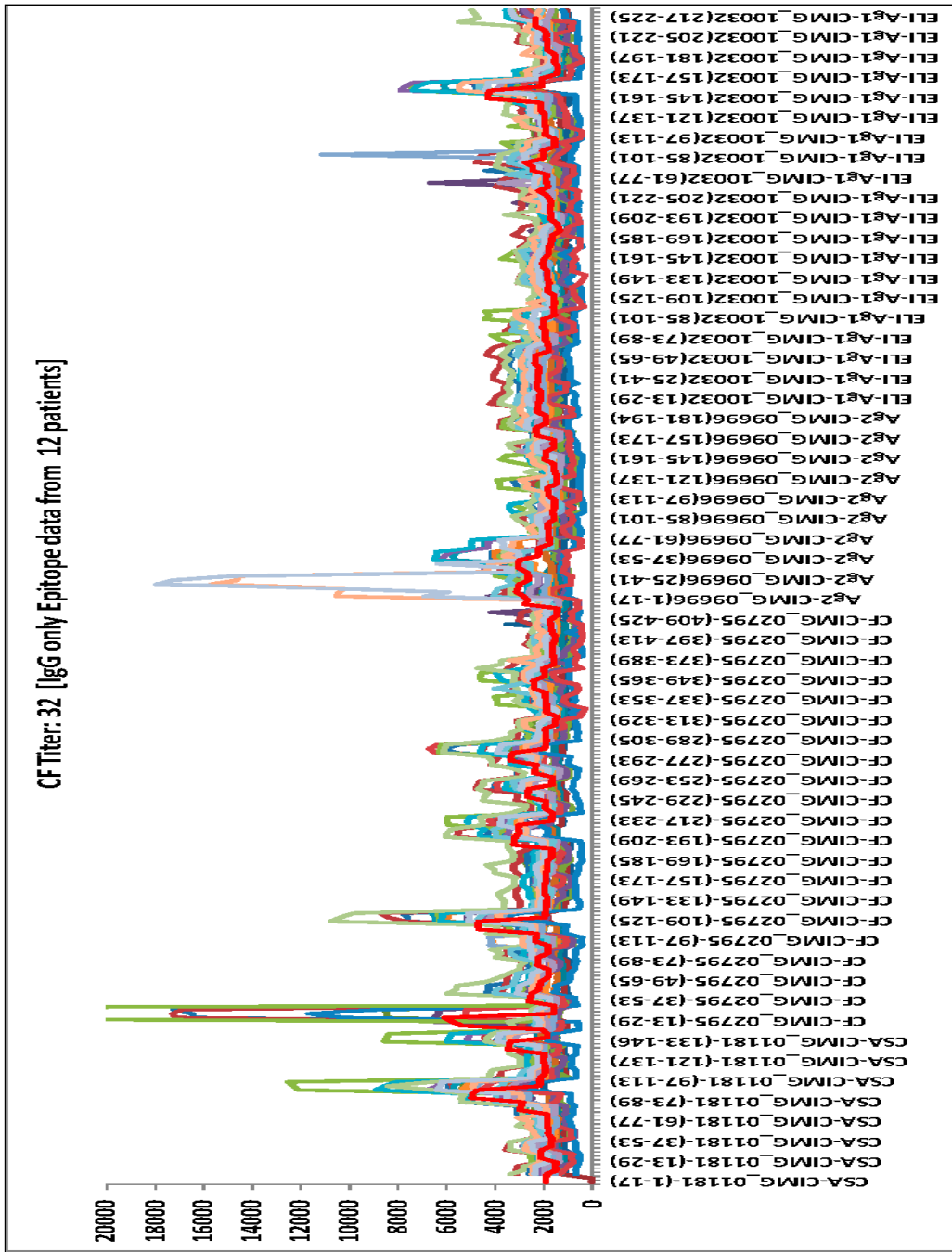


Figure A2-13 IgG antibody reactivity captured on VF epitope peptides (83) from CF-titer=32 patients sera (N=12). Each line on the graph represents antibody response from one VF sample.

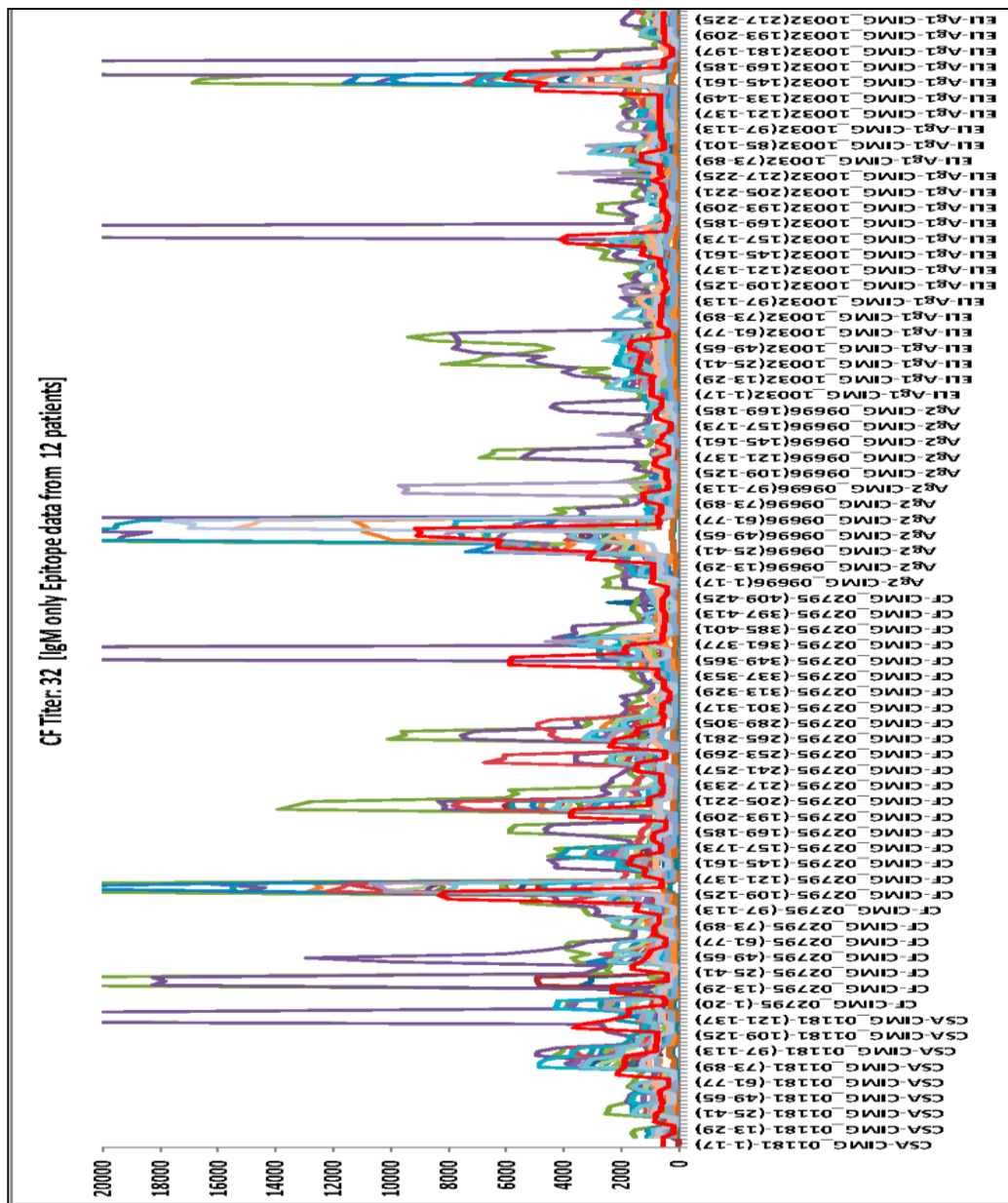


Figure A2-14 IgM antibody reactivity captured on VF epitope peptides (83) from CF-titer=32 patients sera (N=12). Each line on the graph represents antibody response from one VF sample.

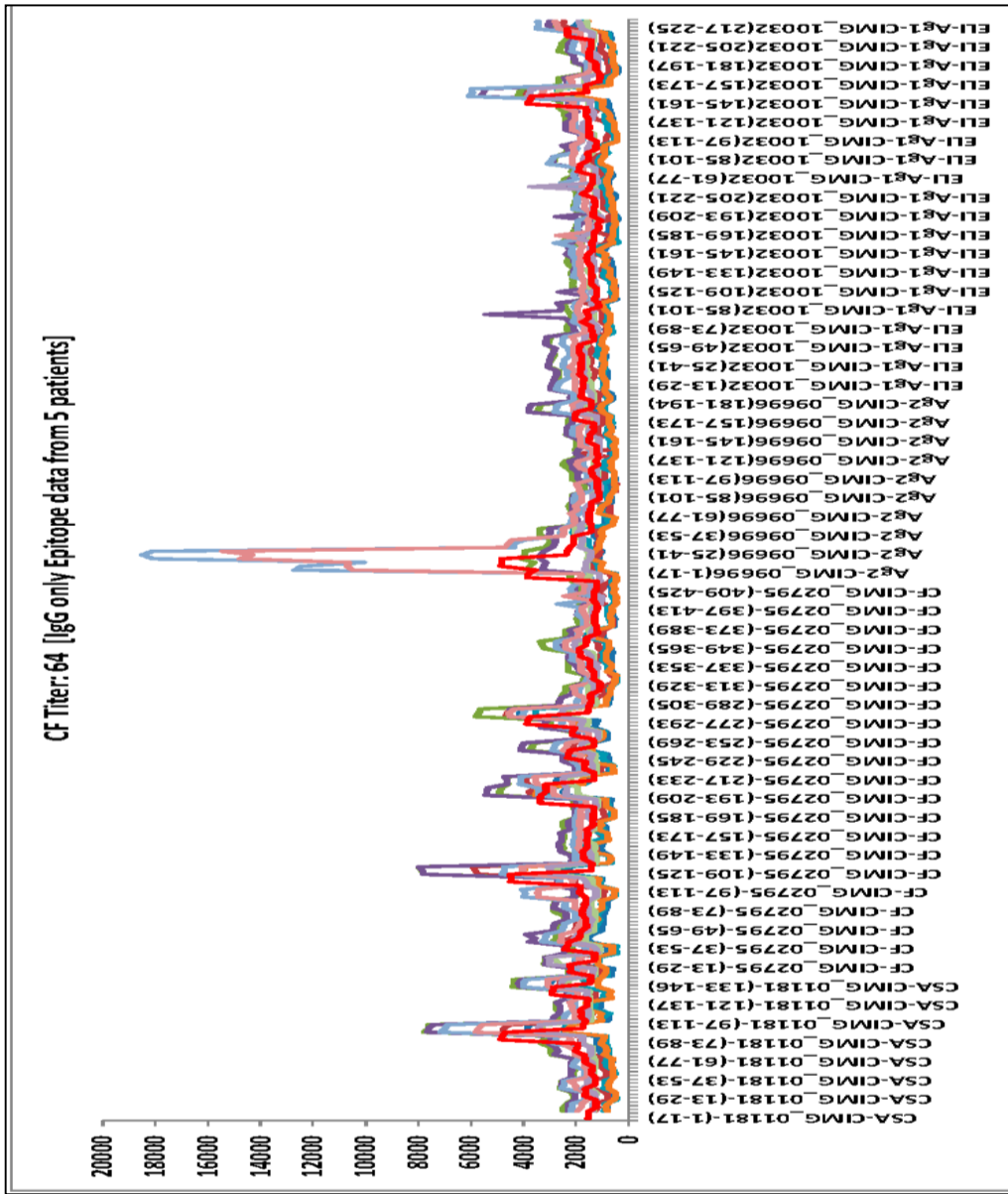


Figure A2-15 IgG antibody reactivity captured on VF epitope peptides (83) from CF-titer=64 patients sera (N=5). Each line on the graph represents antibody response from one VF sample.

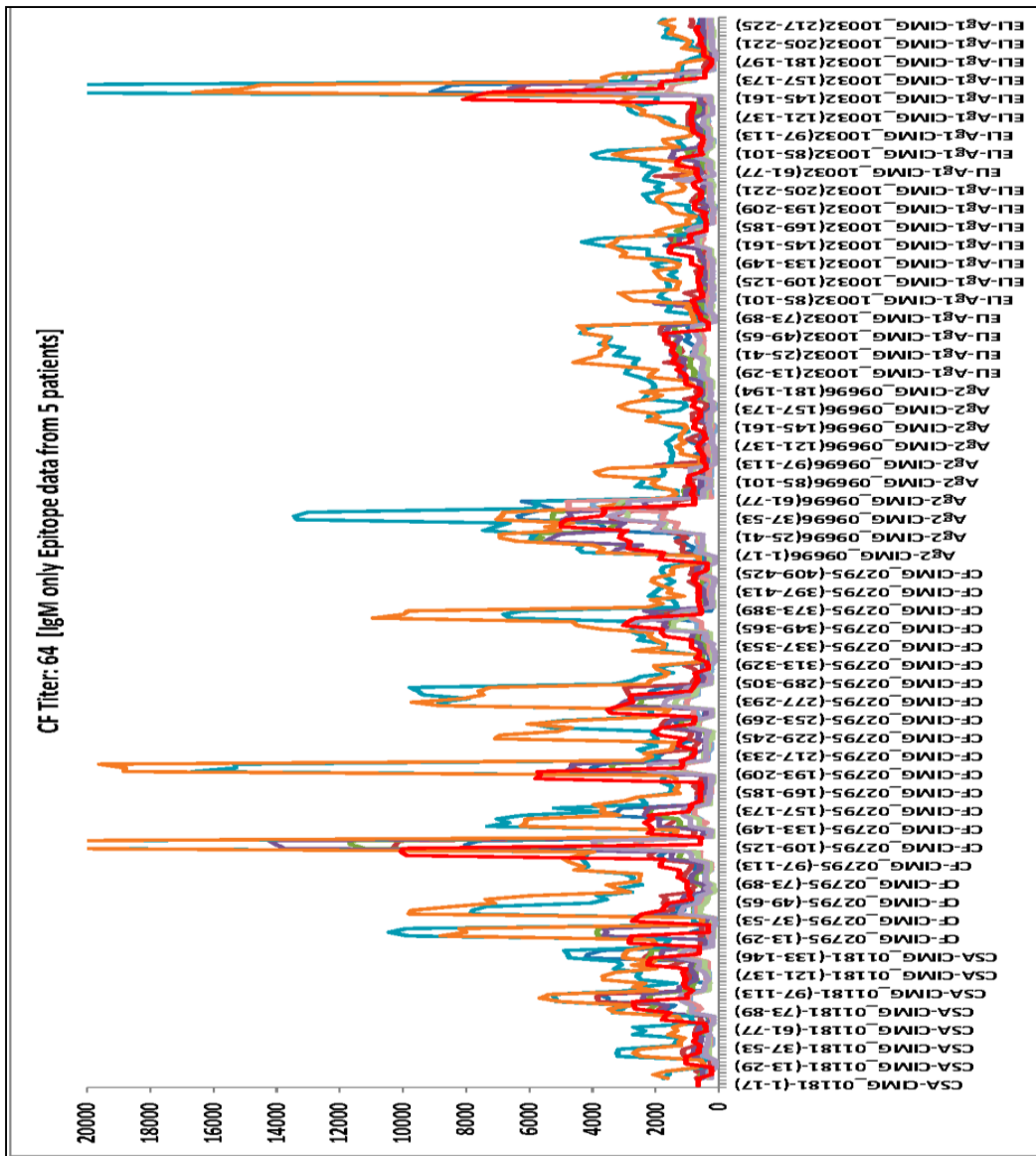


Figure A2-16 IgM antibody reactivity captured on VF epitope peptides (83) from CF-titer=64 patients sera (N=5). Each line on the graph represents antibody response from one VF sample.

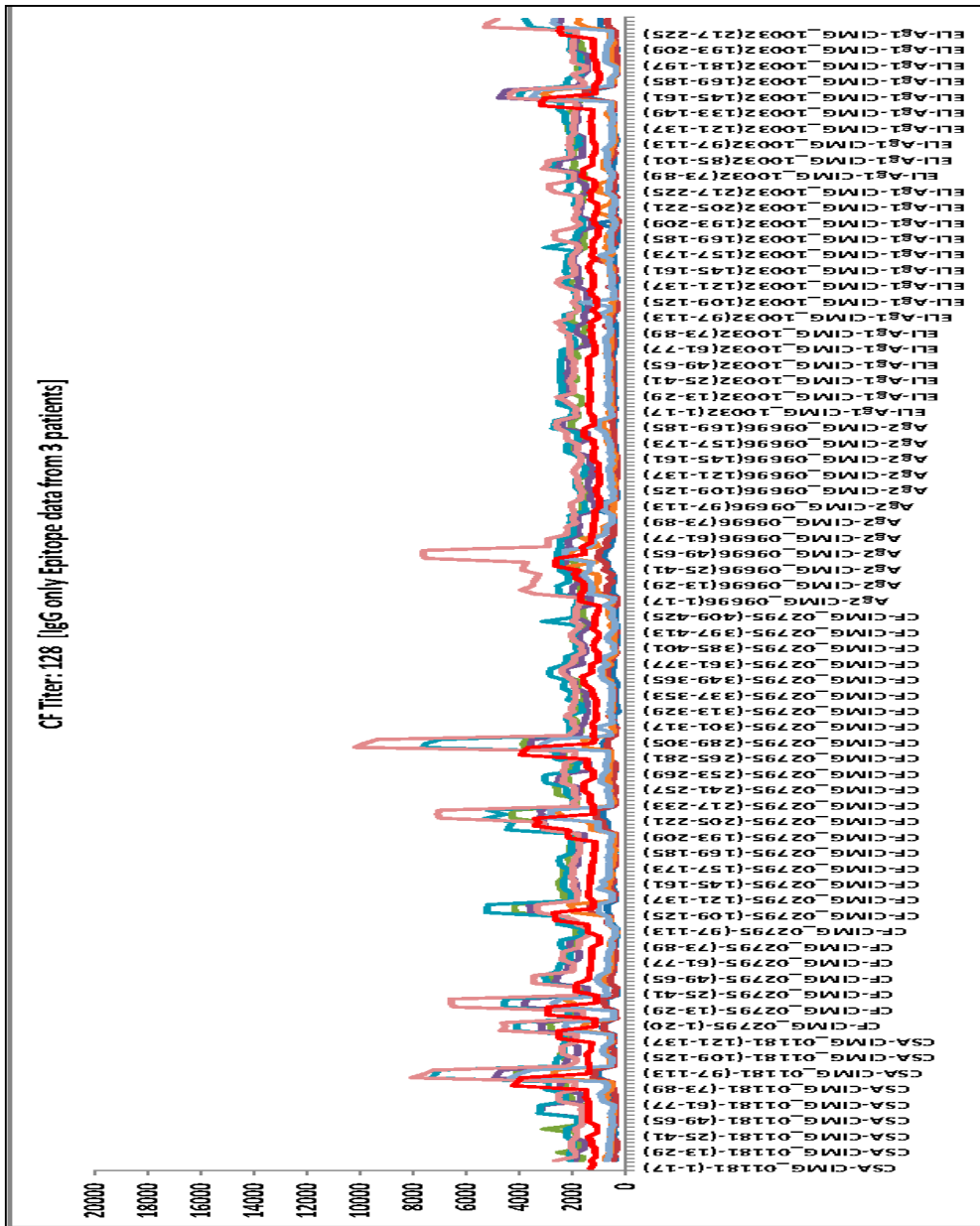


Figure A2-17 IgG antibody reactivity captured on VF epitope peptides (83) from CF-titer=128 patients sera (N=3). Each line on the graph represents antibody response from one VF sample.

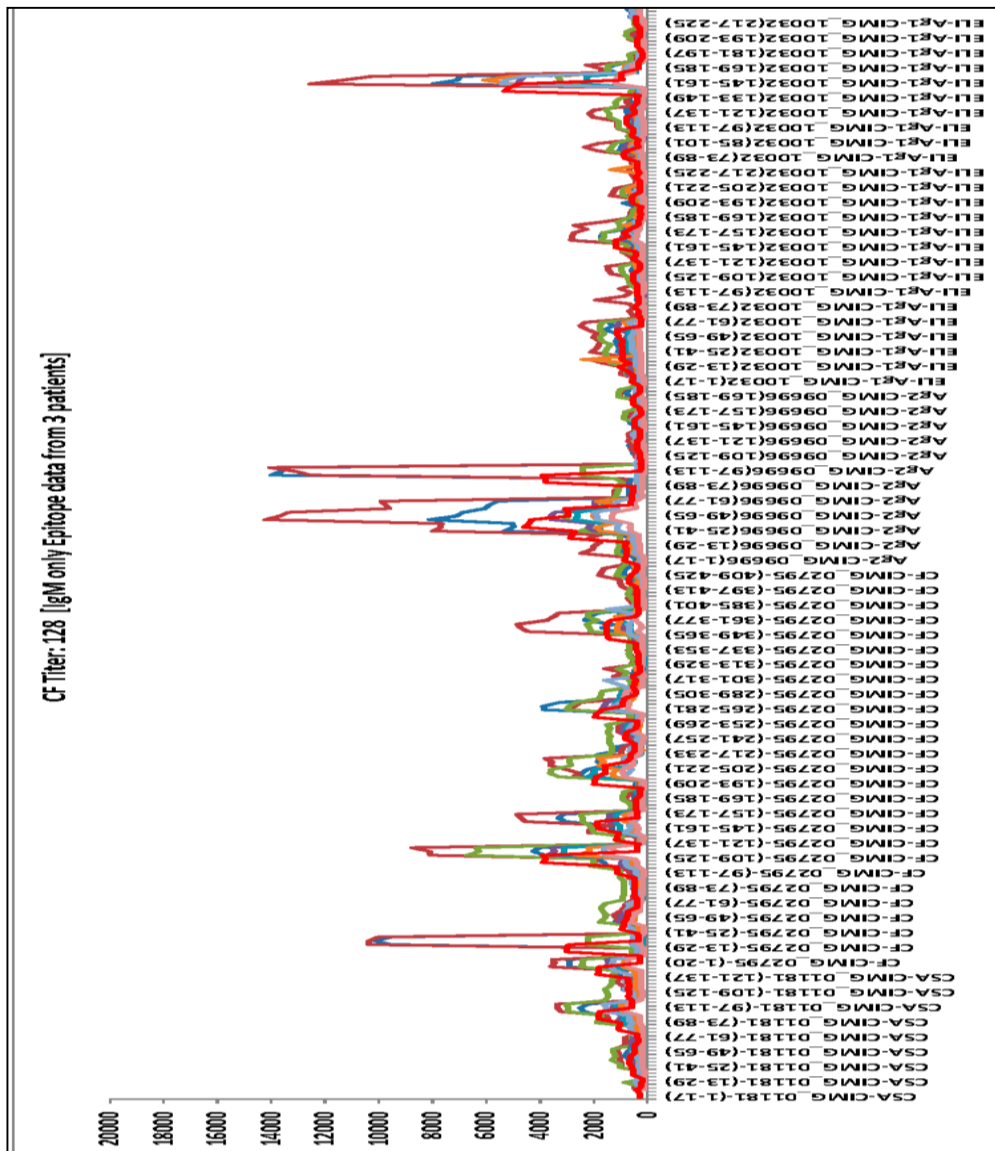


Figure A2-18 IgM antibody reactivity captured on VF epitope peptides (83) from CF-titer=128 patients sera (N=3). Each line on the graph represents antibody response from one VF sample.

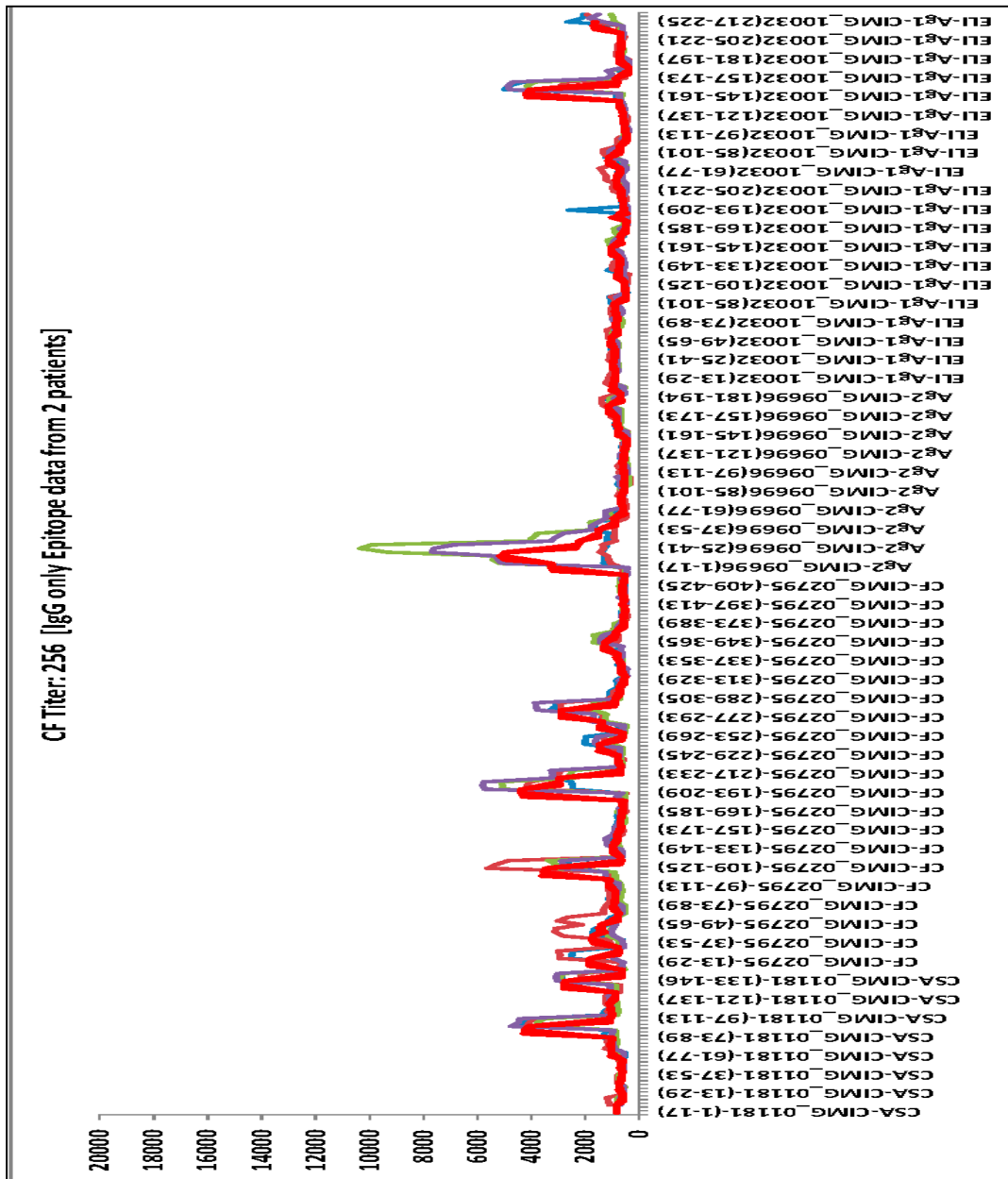


Figure A2-19 IgG antibody reactivity captured on VF epitope peptides (83) from CF-titer=256 patients sera (N=2). Each line on the graph represents antibody response from one VF sample.

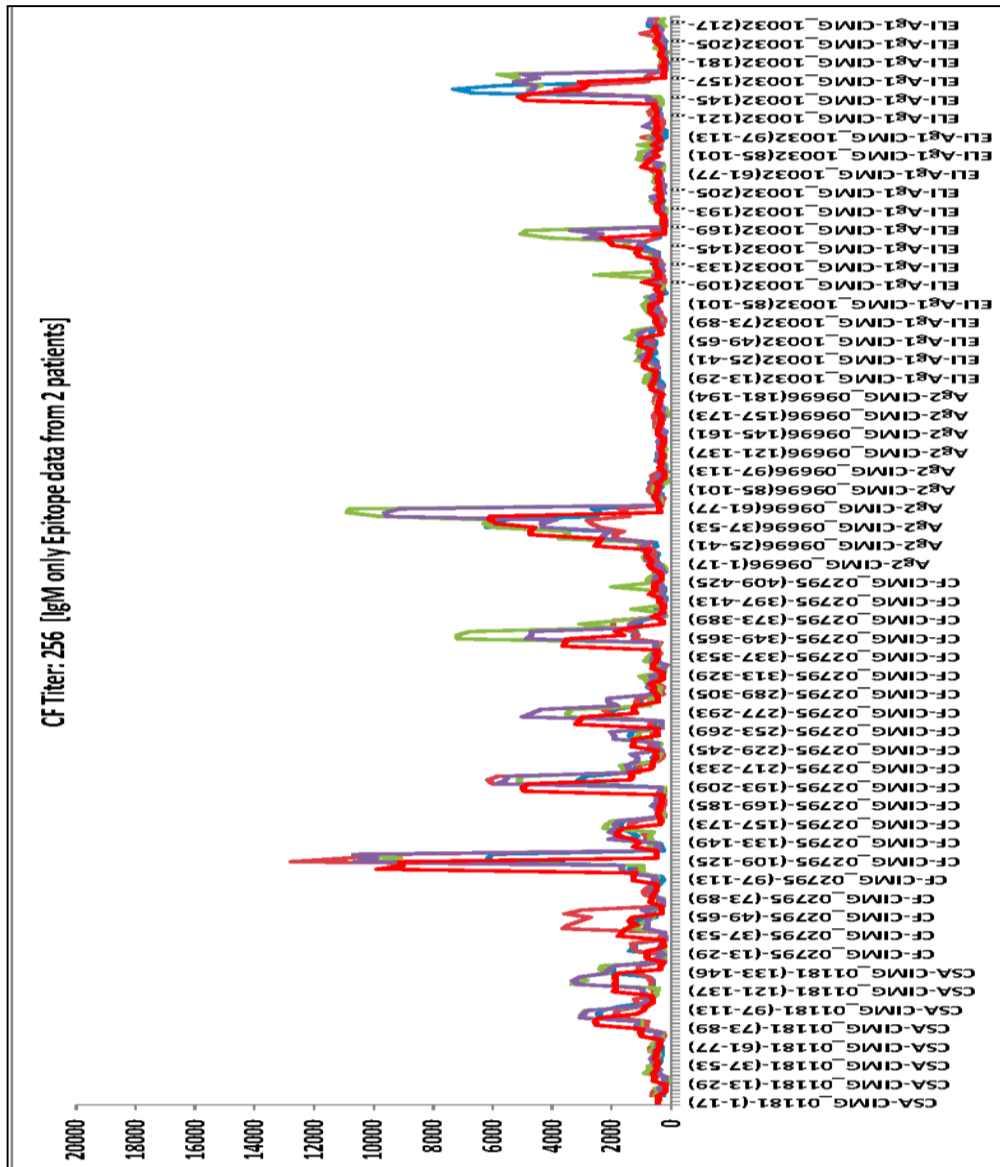


Figure A2-20 IgM antibody reactivity captured on VF epitope peptides (83) from CF-titer=256 patients sera (N=2). Each line on the graph represents antibody response from one VF sample.

Bibliography

1. Yang MC, Magee DM, Cox RA. 1997. Mapping of a *Coccidioides immitis*-specific epitope that reacts with complement-fixing antibody. *Infection and Immunity* 65:4068-4074.
2. Ivey FD, Magee DM, Woitaske MD, Johnston SA, Cox RA. 2003. Identification of a protective antigen of *Coccidioides immitis* by expression library immunization. *Vaccine* 21:4359-4367.
3. Zhu YF, Tryon V, Magee DM, Cox RA. 1997. Identification of a *Coccidioides immitis* antigen 2 domain that expresses B-cell-reactive epitopes. *Infection and Immunity* 65:3376-3380.
4. Pan SC, Cole GT. 1995. Molecular and Biochemical-characterization of a *Coccidioides immitis*-specific antigen. *Infection and Immunity* 63:3994-4002.
5. Jiang CY, Magee DM, Ivey FD, Cox RA. 2002. Role of signal sequence in vaccine-induced protection against experimental coccidioidomycosis. *Infection and Immunity* 70:3539-3545.
6. Cenci S, Sitia R. 2007. Managing and exploiting stress in the antibody factory. *Febs Letters* 581:3652-3657.
7. Chen Y, Cai J, Xu Q, Chen ZW. 2004. Atomic force bio-analytics of polymerization and aggregation of phycoerythrin-conjugated immunoglobulin G molecules. *Molecular Immunology* 41:1247-1252.
8. Henry N, Parce JW, McConnell HM. 1978. Visualization of specific antibody and C1q binding to hapten-sensitized lipid vesicles. *Proceedings of the National Academy of Sciences of the United States of America* 75:3933-3937.

APPENDIX III
SUPPLEMENTAL DATA FOR CHAPTER 4

1.) *F. tularensis* Vaccine Project: Overcoming ELISA limitations using the pathogen proteome peptide (PPP) array

The pathogen proteome peptide (PPP) array was used to discern the antibody response generated from *Francisella tularensis* vaccinated rat sera. The study involved serum samples from the following 4 groups of immunized rats provided by our collaborators at the University of New Mexico as part of their Tularemia vaccine development consortium (TVDC) project:

- Group 1 – Naïve rats
- Group 2 – *Francisella tularensis* Live Vaccine Strain (LVS) vaccinated
- Group 3 – O-Antigen mutant *Francisella tularensis* SchuS4 strain vaccinated
- Group 4 – Immunized with 23 SchuS4 Proteins [Only 1 protein out of these 23 was represented on the PPP array, in the form of 30 non-contiguous peptides. The PPP array carried 862 *Francisella tularensis* SchuS4 peptides in total].

We anticipated significant differences in the antibody responses among these 4 groups based on observations through similar studies [208]. However, this serum set did not show statistically significant difference between Naïve (Group1) versus Vaccinated (Groups 2, 3, 4) when tested by ELISA. The limit of detection (LOD) of antibodies on peptide microarrays is between 0.5 to 2ng/ml, many-fold lower than an ELISA's LOD, 7ng/ml [158,209]. Therefore, I attempted to use a more sensitive technology to be able to measure subtle differences in immune responses between these 4 different groups. I hypothesized that pathogen specific peptides fixed in a microarray format, such as the PPP array, would enable smaller differences in the immune response to be detected. As a proof of concept, Figure A3- 1 shows the antibody response

generated by individual rats within the 4 groups as captured using 862 *F. tularensis* (SchuS4) peptides on the PPP array.

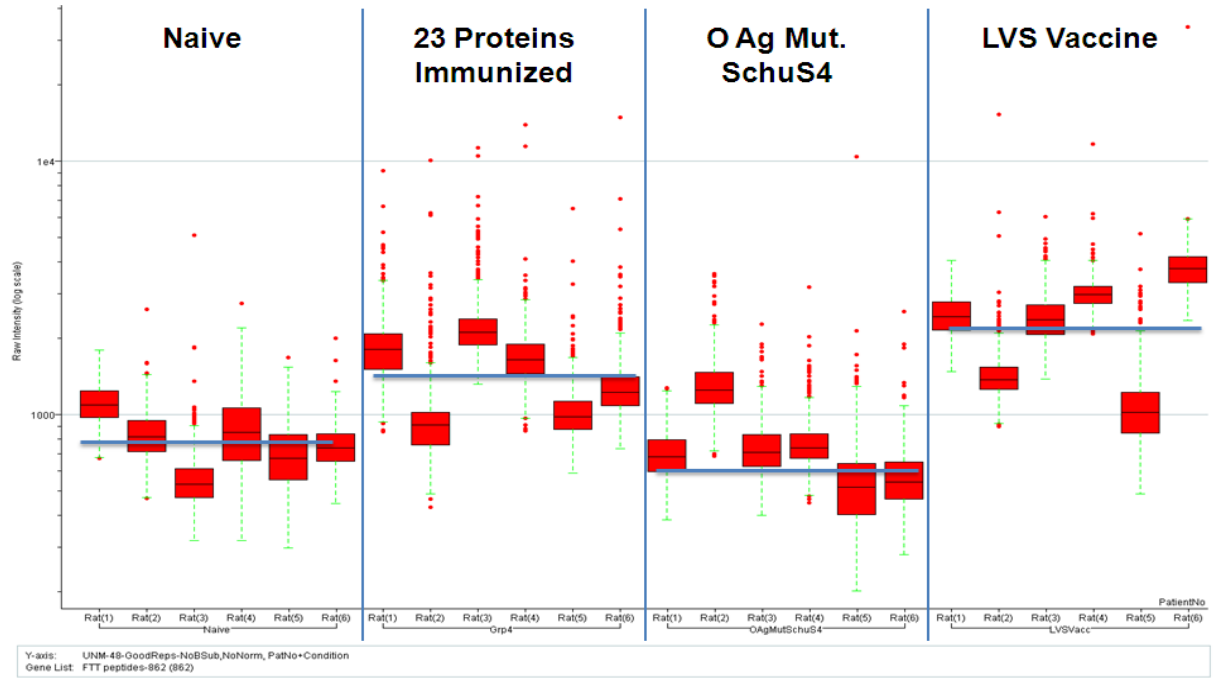


Figure A3- 1 Box plots of immune response from individual rats per group (X-axis) as captured on 862 *F. tularensis* (SchuS4) peptides printed on an array. The raw (un-normalized) fluorescence intensity units (FIU) are plotted on the Y-axis on a log scale. The line at the center of every box represents the median signal intensity for that individual rat.

When these antibodies were measured by ELISA, all animal sera in each group were pooled. However, here on the PPP array, Rat 1 in the Naïve set shows a higher antibody response as compared to other rats within the Naïve group. This disparity in immune response within animals belonging to the same group has been observed in other studies [162]. It is thus obvious through the use of a more sensitive technology such as the pathogen proteome peptide microarray that Rat 1 from the Naïve set might bias the observation in a pooled ELISA leading

to non-observable differences between the 4 groups. This assay could thus be used to trace underlying reasons for lower statistical differences between groups when pooling sera due to single outliers such as Naïve Rat 1 from Group 1. An appropriate analysis to estimate whether or not the response from the treated group is indeed statistically significantly different due to the treatment (vaccination or genetic immunization) as compared to Naïve would be to calculate the statistical differences between the mean responses of Naïve versus treated both with and without the outlier. Table A3- 1 summarizes the statistical differences between Naïve versus the 3 immunization groups using data from PPP array FTT peptides. As expected, the whole pathogen vaccine LVS shows the most significant difference when compared to Naïve. However the average antibody response observed on vaccinating with the O antigen mutant SchuS4 strain (group 3) was lower than that of Naïve rats. In comparison the 23 protein immunization also shows a significant p-value over Naïve above cut-off 0.001. Protection data post-challenge might be more indicative of the impact of these three vaccination strategies on these groups of animals.

Table A3- 1 Difference between immunization groups and Naïve sera using PPP array data

Groups	Mean Signal (FIU)	Standard Deviation	Variance	p-value (single tailed, two-sample unequal variance)
Group 1 - Naïve	300	227	51565	
Group 2 - LVS Vaccine	701	694	481871	6.61E-305
Group 3 - O Ag Mutant SchuS4	207	245	60038	7.08E-89
Group 4 - 23 protein immunization	419	596	355696	8.57E-41

p-value cut off = 1/n = 1/862 FTT peptides = 0.00116

A more informative set of peptides for completing this comparison should be ones representing the whole proteome of *F. tularensis* (SchuS4 and LVS). This would allow a comparison of antibody responses from individual animals vaccinated with the complete pathogens (LVS-Group2 or SchuS4-Group3) versus those that were immunized using 23 proteins from *F. tularensis* (SchuS4)-Group4. These peptides should be printed on an array by themselves instead of within the context of other pathogen peptides. This would reduce competition on the array from other unrelated pathogen peptides for capturing *Francisella* specific antibodies as observed from the addition of influenza peptides to the PPP array in Chapter 5.

Conclusion: The pathogen proteome peptide microarray can be used to segregate minor differences in the immune response generated from individuals within the same group. Additionally it also allows for more sensitive differences in antibody response between immunization groups beyond those observable through an ELISA.

2.) ASFV Vaccine project: Mapping humoral response from genetic immunization using the PPP array

The African Swine fever virus (ASFV) is a double stranded DNA virus from the family Asfarviridae. The disease infects wart-hogs, bush-pigs, domesticated pigs and ticks. Phylogenetically it is very closely related to the human infection causing viruses from Herpesviridae and Poxviridae (Variola-smallpox) families [40]. The swine sera were obtained from Dr. Linda Dixon at the Institute of Animal Health (IAH), Pirbright, UK and the primary goal of that project was to create a vaccine protective in domestic pigs against ASFV. It is a

priority pathogen of interest on the U.S Department of Agriculture (USDA) list [39] due to its ability to potentially infect humans [40].

The following double vaccinia boosted, sera from 4 groups of six inbred pigs/group was obtained from IAH, Pirbright as follows:

Group 1: Randomly selected antigens 1-20 + Vp30, Vp72

Group 2: Randomly selected antigens 21-40 + Vp30, Vp72

Group 3: 12 known surface antigens (including Vp30, Vp72)

Group 4: Vp30, Vp72

The above sera are part of a Genetic Immunization Screen (#2) to optimize the expression library immunization (ELI) [210] protocol for pigs. These animals were not challenged with the virulent strain of ASFV post-genetic immunization. Vp30 and Vp72 proteins in group 4 are immunodominant antigens of ASFV, as established by conventional ELISA and Western blot assays [107,211]. Immunization with these antigens produces neutralizing antibodies against the virus [108]. These proteins were included in every group as a genetic immunization control and their reactivity was measured in all sera by ELISA.

We selected 299 peptides to print on the PPP array that represent antigens from group 3 and group 4. Peptides representing all proteins in group 1 and group 2 would comprise 1000 additional peptides required to complete this analysis. As an initial proof of concept that the peptide microarray is capable of accurately capturing ASFV specific antibody responses post-genetic immunization, Figure A3- 2 displays the range of immune responses per individual animal using Box-Cox plots. Data for groups 1 through 4 immunized animals in comparison to one Day 0 sera from group 1 and the special pathogen free (SPF) out-bred ASFV infected and

uninfected pigs within the French cohort is plotted. The immune response mounted in all 4 groups of genetically immunized animals as captured by 299 peptides is equivalent to that mounted in a real infection (French cohort) and captured by the antigens in group 3. All 4 groups were immunized using Vp30 and Vp72 which were included as peptides on the array, in addition to 20 other antigens in groups 1 and 2 and 12 additional antigens in group 3.

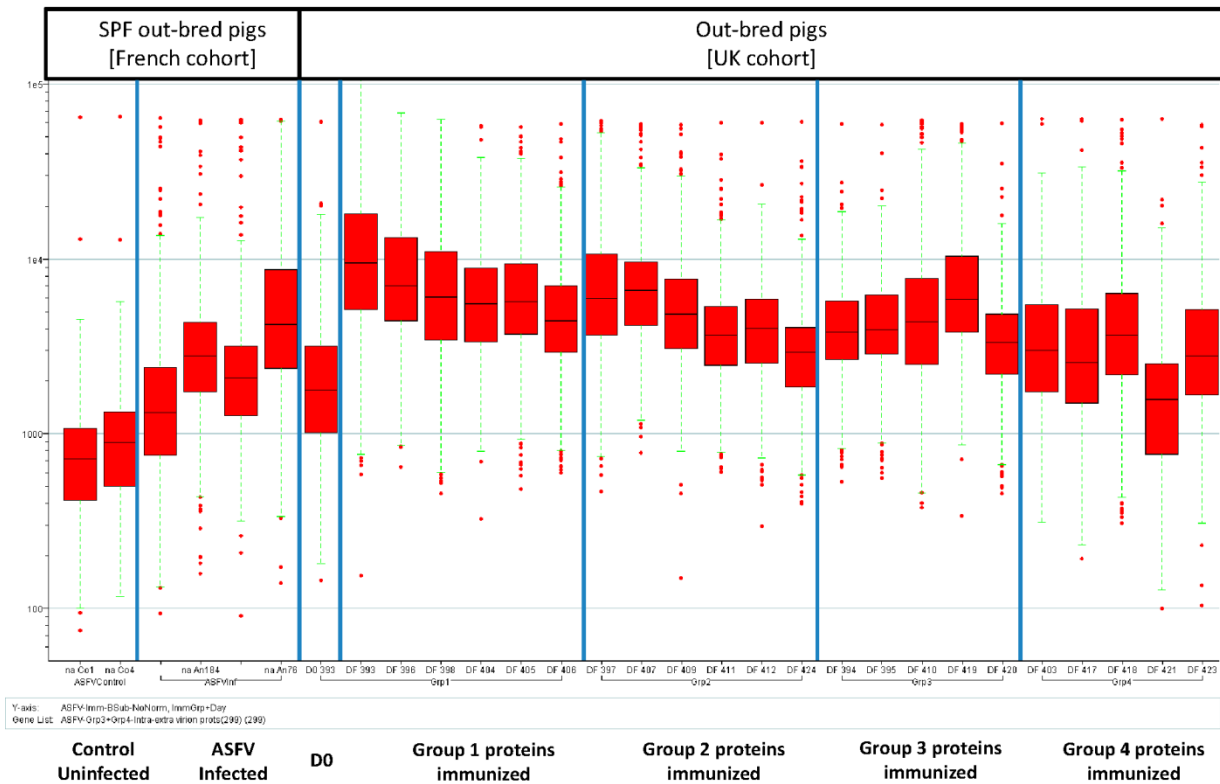


Figure A3- 2 A simultaneous comparison of infectious (French cohort) versus genetic-immunization (UK cohort) antibody responses as captured by 299 ASFV peptides on PPP array.

The box-plot depicts raw (un-normalized) fluorescence intensity units (FIU) plotted per individual animal on the Y-axis using a log scale. The French cohort represents a separate experiment involving ASFV infected and uninfected out-bred pigs. One day zero (D0), pre-

immunization sample and all day final – post-immunization (DF) samples from the UK cohort are presented on the X-axis.

The Day 0 sample from swine no. 393 of group 1 had a higher antibody response even pre-immunization as expected than that of the 2 uninfected negative control SPF pigs in the French cohort. It was processed on the array to test whether it would be worthwhile to subtract the pre-immunization response of individual out-bred pigs (UK cohort) from their post-immunized samples. The medians of antibody responses captured by the 299 ASFV peptides from group 3 and 4 protein immunized animals were comparably higher (except Day Final-DF pig 421 from group 4) than the immune response observed from an infection (French cohort).

Apart from Vp30 and Vp72, none of the 20 distinct antigens of group 1 or 2 were represented on the PPP array. As mentioned in Chapter 4, Supplementary Figure 4-3, the overall reactivity captured on PPP arrays from ASFV sera despite dilution (1:500) was much higher than that observed from any of the human exposures tested (VF, WNV, LVS, Vaccinia). Figure A3- 3 shows a similar trend when using genetically immunized sera from groups 1 through 4. The average signal obtained per individual swine sera in all 4 groups on the PPP array seems roughly proportional to the number of antigens they were exposed to per genetic immunization group (22 constructs each in groups 1 & 2, 14 constructs in group 3 and 2 in group 4). The extent of cross-reactivity observed from this assay to non-ASFV peptides was high due to the total antibody response captured despite processing these arrays under optimized thermodynamic conditions to reduce cross-reactivity (incubating sera for 16 hours at 23°C).

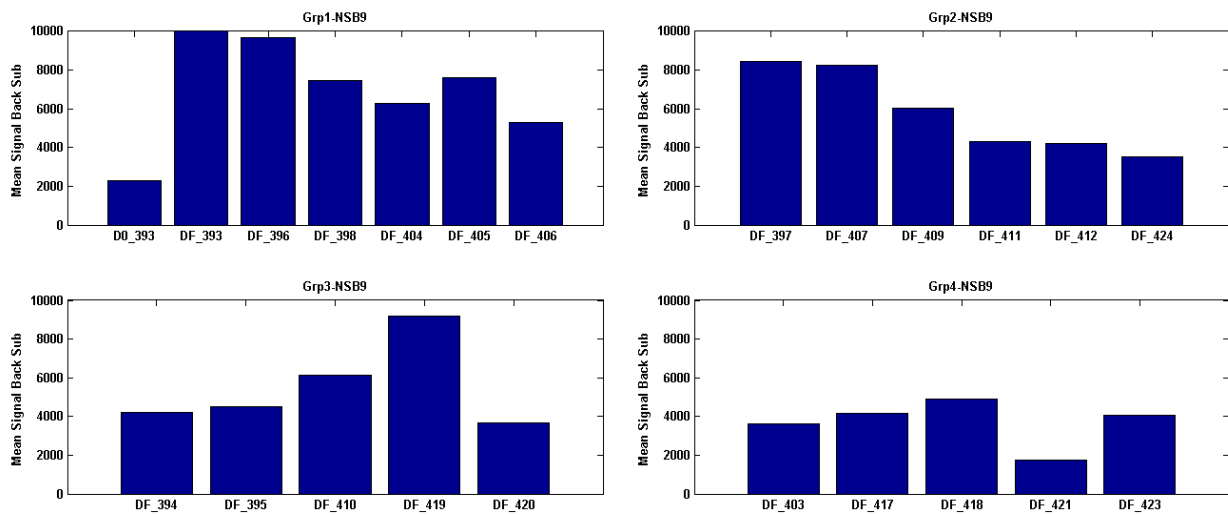


Figure A3- 3 Average signal captured by PPP array for 4 groups of ASFV genetic immunization are depicted with every animal's antibody response represented per bar on the X-axis.

The background subtracted average raw (un-normalized) signal intensity data is plotted on the Y-axis. One Day 0 – pre-immunization (D0_393) and all Day Final – post-genetic immunization (DF) pig sera are depicted in these bar graphs.

Once conditions for the genetic immunization of pigs were established through this experiment, and it was confirmed that the immunization led to both T-cell (Pirbright) and B-cell responses (ELISAs, PPP array-CIM), they were applied to the next two immunization regimes. Both immunization protocols contained a boosting step using recombinant Vaccinia viruses (rVV), each expressing an ASFV gene. A group of such recombinant Vaccinia viruses were then combined into a single inoculum and delivered to the animals 2 and 3 weeks post the gene gun immunization. Each recombinant Vaccinia virus containing one ASFV antigen was present at 10^9 pfu/dose. Each pig received 2×10^9 pfu/100 μ L dose of rVV. A summary of the steps involved in these genetic immunization regimes are as follows:

1. Day 0 & 2/3: Double prime + CPG adjuvant (left & right ear-5 gene gun shots)
2. 2 Weeks later: DNA Boost + CPG adjuvant (left & right ear-5 gene gun shots)
3. 3 Weeks later: 1st recombinant vaccinia boost (intra-dermal)
4. 2 Weeks later: 2nd recombinant vaccinia boost (intra-dermal)

Immunization Protocol # AR000158:

Although Vp30 and Vp72 are immunodominant antigens for ASFV, there are confounding reports on whether or not groups of neutralizing antibodies generated against these antigens are sufficient to protect against challenge with a virulent ASFV strain. Barderas *et al.* have shown that immunization of pigs with a chimeric protein combining Vp30 and Vp54 proteins was sufficient to protect them against a virulent ASFV isolate E75 challenge [106]. Neilan *et al.* immunized pigs with baculovirus expressed ASFV-pr4 isolate Vp30, Vp72, Vp54 and Vp22 antigens and found that they did not survive post-challenge with the pr4 strain [108]. An experiment was conducted to isolate the effect of adding Vp30 along with the bin of antigens in all Groups. The rationale for this experiment was to test if Vp30 alone or in combination with Vp72 was responsible for the non-protective immune response as observed by Neilan *et al.* [108]

Group A: all antigens from previous Groups 1, 2 and 3 [= 37 antigens including Vp30] (6 pigs)

Group B: all antigens except Vp30 (6 pigs)

Group C: no ASFV antigens, irrelevant antigens for challenge control-HA, AAT, gp160 (3 pigs)

Post vaccination, pigs were intramuscularly challenged with 10^4 (50% hemadsorbing doses) HAD50/ml ASFV strain Georgia 2007/1 (Genotype-II). None of these animals survived the challenge and had to be humanely euthanized on day 6 and 7 post-challenge. Collaborators

from IAH sent information on viral load estimated via PCR from blood and tissues (spleen, tonsil, mesenteric & gastro-hepatic lymph nodes) on the third day post-challenge. They also sent other clinical parameters such as weight gain in kg, temperature per individual and clinical scores based on the severity of disease symptoms manifested. Group A pigs showed moderately higher viraemia in blood on day 3 as compared to pigs from group B. Group C pigs showed higher viraemia as expected in comparison to groups A and B. All individual pigs in group A, showed higher weight loss as compared to weight gain observed in 4 out of 6 pigs in group B and 4 out 6 group C pigs. Normal body temperature in pigs is 38-39°C, and temperature of febrile pigs in the immunized groups A and B raised to greater than 40.5 two days post-challenge where as that of group C pigs became febrile three days post-challenge (except pig C5, febrile on day 2). A clear bifurcation in the distribution of viraemia in blood was observed between individual animals in all three groups. The sera for two pigs showing higher viraemia and two showing lower viraemia in blood per group were processed on the PPP array and data presented in Figure A3- 4.

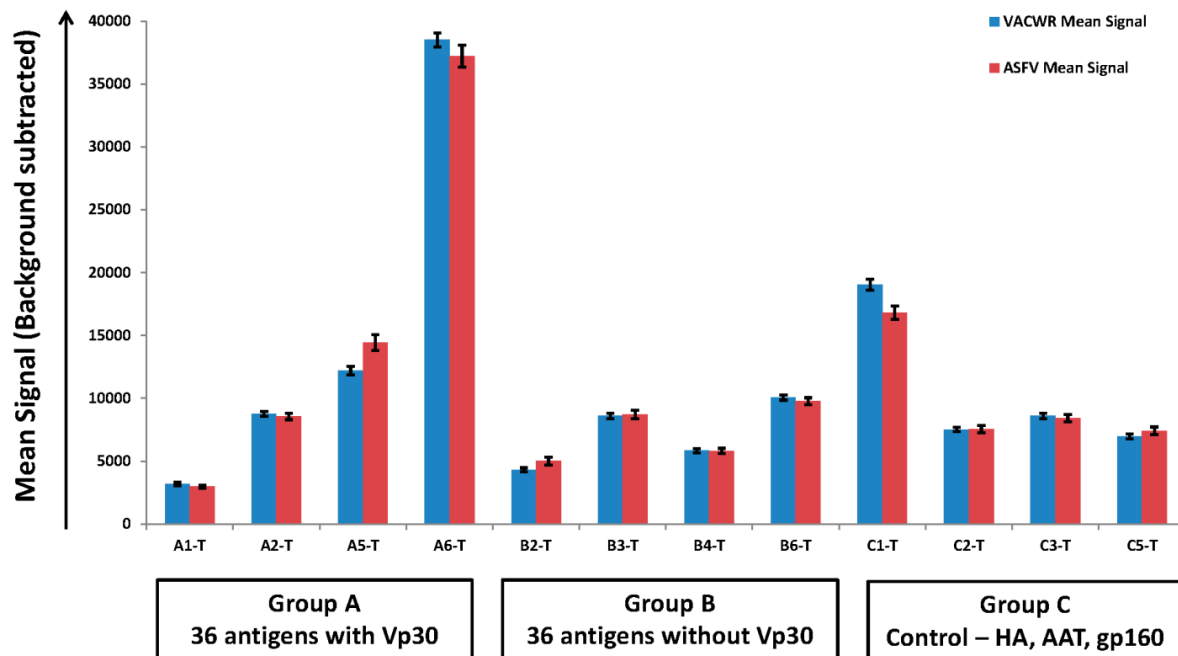


Figure A3- 4 Humoral immune response as measured on PPP array from Group A, B, C pigs sera post-challenge with ASFV

Average signal intensities in FIU (Y-axis) from animals in groups A, B and C (X-axis) as measured using ASFV (red bars) and Vaccinia (blue bars) peptides on the pathogen proteome peptide (PPP) microarray. The error bars represent standard error.

Figure A3- 4 represents the average signal intensities from ASFV as well as Vaccinia (rVV boost) peptides as measured from capturing antibodies from individual pig sera. Pigs A5 and A6 had lower viraemia as compared to pigs A1 and A2 and this seems to correlate with observing a marginally higher relative antibody response in pig A5 and a significantly higher response in pig A6 as compared to A1 and A2. Pigs B4 and B6 had lower viremia as compared to pigs B2 and B3 but the antibody response captured on the PPP array does not reflect a clear correlation between viraemia and antibody response.

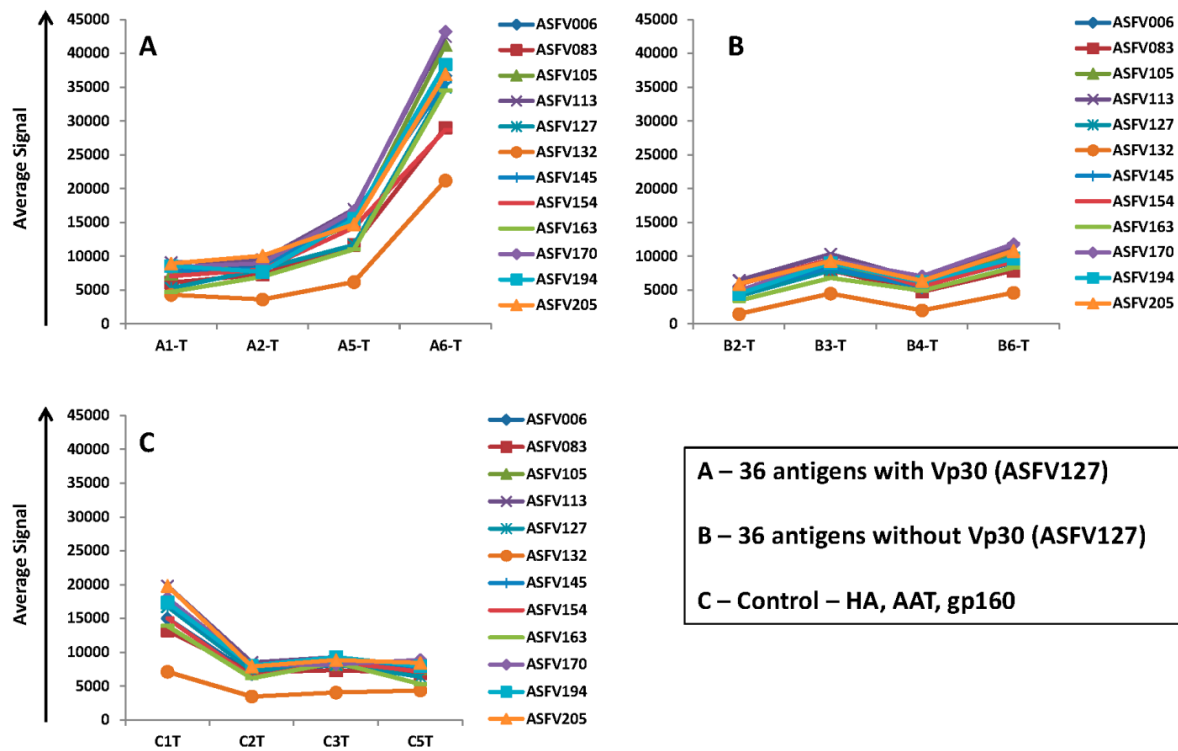


Figure A3- 5 Signal intensities from ASFV peptides averaged per ASFV protein as measured on the PPP array from group A, B and C samples post-ASFV challenge.

Figure A3- 5 represents the signal averaged for peptides per ASFV protein from individual animals in groups A, B and C. The control group C animals were not genetically immunized with ASFV antigens and still mounted a strong antibody response to challenge infection especially pig C1. Additional comparisons might be necessary to establish whether the PPP array platform can be used to correlate protection post-challenge.

The Immunosignature non-natural sequence peptide microarray has been used to distinguish the outcome from different vaccine regimens [75]. The pathogen proteome peptide microarray could be potentially used for similar studies. Figure A3- 6 displays an individual pigs’ antibody response as captured by the PPP array from group A before immunization, after

immunization and post-challenge. Panel B displays an individual pig's antibody response from a separate experiment, before and after immunization with an attenuated ASFV vaccine strain and post-challenge with ASFV Georgia/2007 strain. In both cases the antibody immune response to the challenge was lower as compared to that observed post-immunization. In Panel B, the recombinant vaccinia vector containing ASFV antigens was not used for boosting the immune response from the immunization and yet the peptide microarray captures cross-reactivity to Vaccinia peptides. Ideally, for mapping the protective response post-immunization and challenge the peptides for the complete ASFV viral proteome should be printed on a separate microarray by themselves and not within the context of other pathogen peptides as done here on the PPP array.

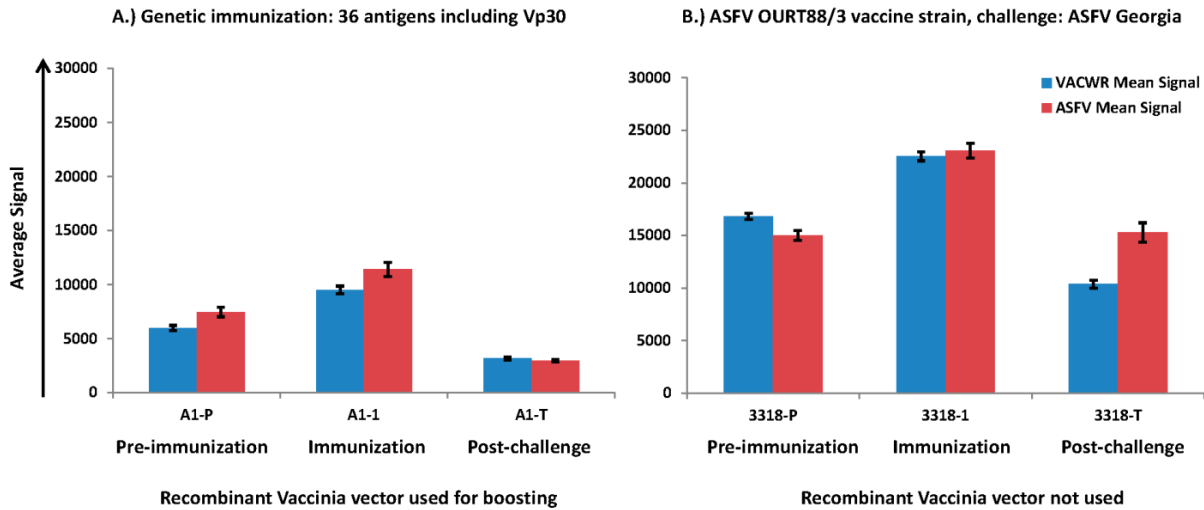


Figure A3- 6 Average signal intensities in FIU (Y-axis) from various stages (X-axis) in two separate immunization and challenge regimes.

Panel A displays the antibody response as captured by PPP array peptides representing ASFV (red bars) and Vaccinia (blue bars) peptides and Panel B displays the antibody response from

another pig immunized with the ASFV OURT88/3, attenuated vaccine strain. Both pigs were challenged with ASFV Georgia/2007 virulent strain. The error bars represent standard error.

Despite the observable cross-reactivity when printing multiple pathogen peptides on a single assay, an advantage of using the PPP microarray is its ability to resolve linear antibody epitope within immunodominant antigens despite significant competition from several other unrelated pathogen peptides. Figure A3- 7 displays the significant epitopes within the hierarchical clustering map of Vp30. Figure A3- 8 displays Vp72 with a high resolution mapping of exactly which linear peptide segments the individual pigs were responding to post-challenge.

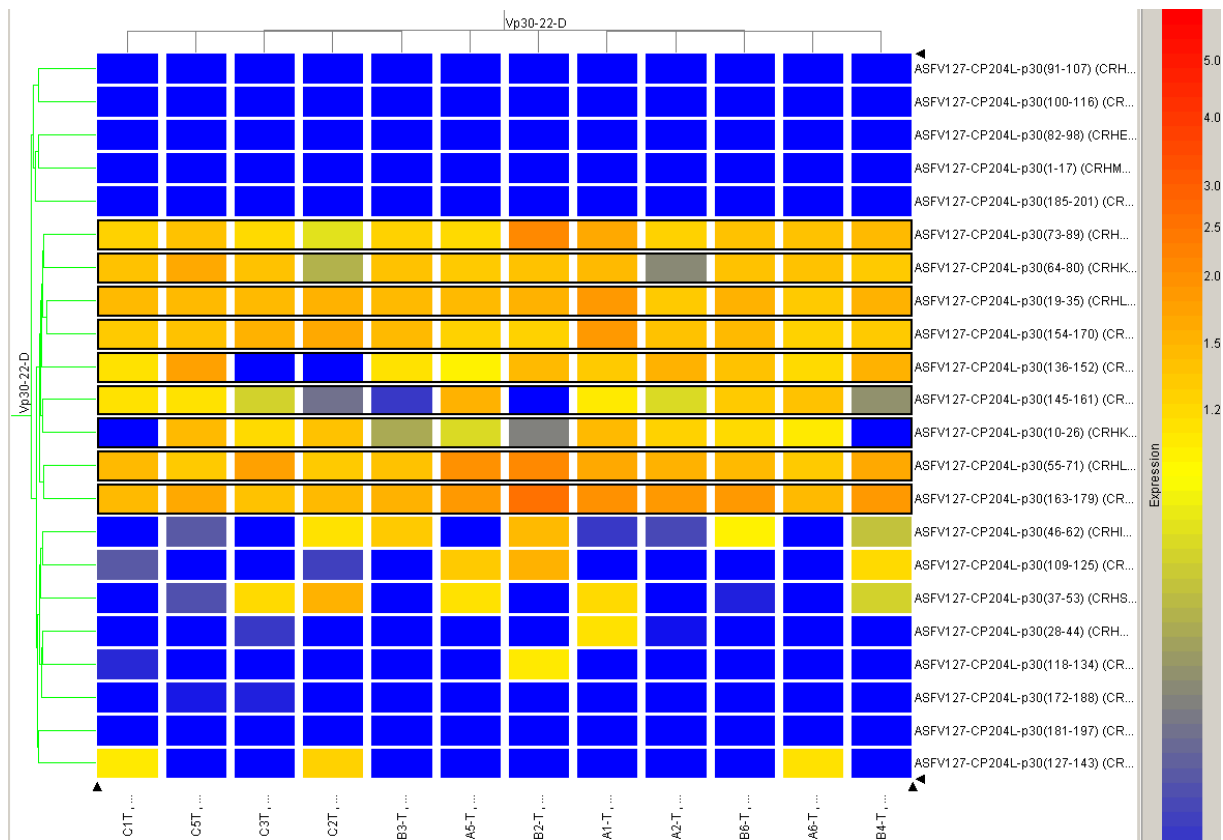


Figure A3- 7 Peptides tiling Vp30 (ASFV127) an immunodominant antigen of ASFV displaying individual (X-axis) responses from sera on PPP array.

Every column represents one individual pig and every row represents one peptide within the ASFV127 protein. The coloring within this heatmap is based on median normalized signal intensities obtained from the microarray. Blue squares represent no antibody binding whereas yellow to orange represent moderate-high binding of antibody to those peptides on a relative scale as colored in GeneSpring GX 7.3.1 (legend on right).

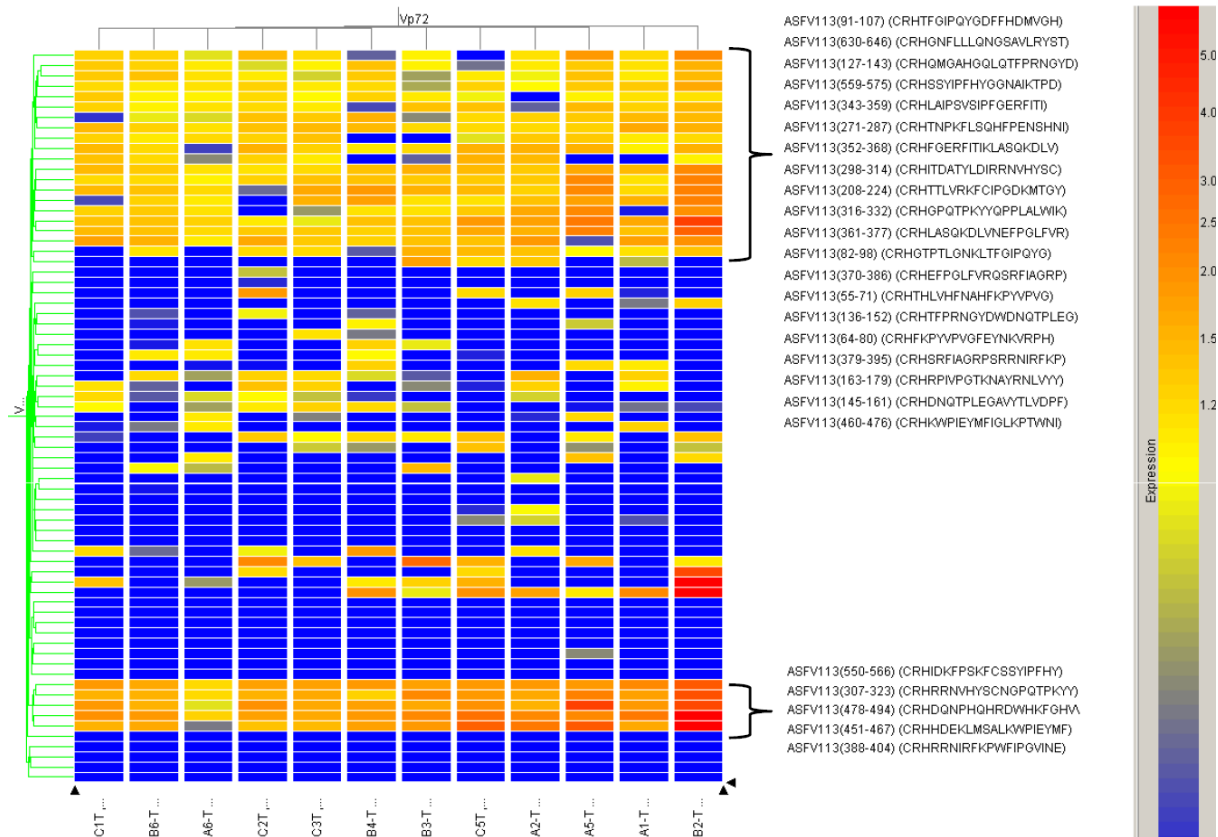


Figure A3- 8 Peptides tiling Vp72 (ASFV113) an immunodominant antigen of ASFV, displaying individual (X-axis) responses from sera on PPP array.

Every column represents one individual pig and every row represents one peptide within the ASFV113 protein. The coloring within this heatmap is based on median normalized signal

intensities obtained from the microarray. Blue squares represent no antibody binding whereas yellow to red represent high binding of antibody to those peptides on a relative scale as colored in GeneSpring GX 7.3.1 (legend on right).

Table A3- 2 summarizes the T-test p-value results reflecting statistical significance of groups A and B over control non-ASFV genetic immunization (group C) sera. The p-value was calculated using antibody signal intensities captured using ASFV and Vaccinia peptides on the PPP array between groups A and B versus group C. Both groups A and B are statistically significantly different as compared to the control group (p-value cut-off = 0.001155). The mean antibody response post-challenge in group B is statistically significantly lower as compared to the control group C. The addition of Vp30 in group A resulted in statistically significantly higher mean antibody response as compared to animals in group C post-challenge.

Table A3- 2 Summary of statistical differences between groups A, B and control group C post-ASFV challenge.

Groups	Mean	Standard Deviation	Variance	p-value (single tailed, paired)
A	15718	16037	257172615	5.00099E-63
B	7254	5173	26764966	1.0717E-106
C	10370	7875	62020663	

p-value cut off = 1/no. of ASFV + Vaccinia peptides = 1/866 = 0.001155

The protective ability of Vp30 however could not be assessed using this immunization regime as all pig's perished post-challenge. It was estimated that the immune system of pigs in group's A and B was likely overwhelmed due to the amount of DNA injected from 37 and 36 ASFV genes respectively. An alternate protocol was therefore attempted with a balanced and reduced DNA load in immunization protocol # AR000302.

Immunization Protocol # AR000302:

Group A: 21 antigens (contains Vp30)

Group B: 16 antigens approximately equivalent in DNA size to 21 antigens in group A. This was done so as to roughly normalize for the amount of genetic material used for immunization between Groups 1 and 2.

Group C: no ASFV antigens, irrelevant antigens for genetic-immunization control-HA, AAT, gp160.

None of the pigs survived post-challenge. Our collaborators from IAH sent us in-vitro T-cell response to virus as measured by an IFN- γ ELISpot assay pre-challenge and post-immunization and boost from Day 70. Pigs from group A (A3, A4 and A5) showed a higher T-cell response as compared to those from groups B and C. This observation correlates with our antibody measurement using PPP array as summarized in Table A3- 3. Group A had a significantly higher mean antibody response as compared to the immunization control group C. The antibody response as measured in group B was not significant at the p-value cut-off of 0.001.

Table A3- 3 T-test p-value from samples on Day 70 post-immunization and boost, pre-challenge as captured using ASFV and Vaccinia peptides on PPP array

Groups	Mean	Standard Deviation	Variance	p-value (single tailed, two-sample, unequal variance)
A	22723	13140	172649302	1.74057E-42
B	18316	11988	143704928	0.017567
C	17575	15348	235549616	

p-value cut-off: $1/n = 1/866 = 0.001155$

Figure A3- 9 summarizes the results from measuring the antibody response on the PPP array. Day 70 is after the second live vaccinia-ASFV construct boost and one day before challenge. Day 76/77 is a time point post-challenge before these animals were humanely euthanized. The immediately observable trend from this data is that of lower signals on Day 76/77 and this might be because these samples were severely hemolyzed and coagulated, making them unusable for this comparison.

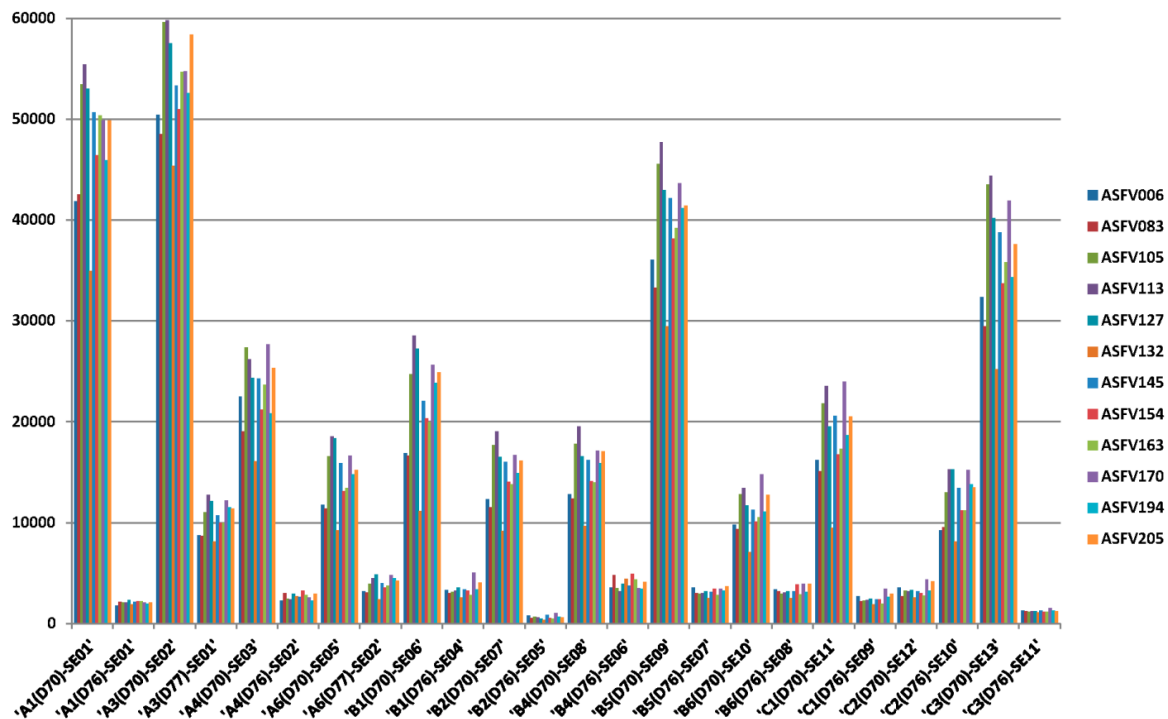


Figure A3- 9 Signal intensities averaged per ASFV protein ($N=12$) tested in the form of peptides on the PPP microarray.

Day 70 (post-immunization and one day pre-ASFV challenge) and Day 76 (post-ASFV challenge) sera per pig are depicted on the X-axis. The Y-axis displays the average raw (non-normalized) signal intensities from background subtracted microarray data in FIU.

In summary, the antibody response obtained from group A, pigs A1 and A3 were higher post-immunization and boost as compared to that obtained from group B pigs, not immunized with Vp30, except pig B5, and group C control pigs (except pig C3). Given that neither of these animals survived post-challenge, the protective effect of including Vp30 could not be isolated.

Conclusion: The PPP microarray can be used to distinguish the immune response generated during various modulations of an immunization regime using genetic-immunization. Additional

sera need to be processed to compare if quantifiable differences in the immune response due to vaccination using an attenuated virus versus genetic-immunization could be accurately distinguished using the PPP array.

3.) IVTT bead protein array–Rapid screening of immunogenic/immunodominant proteins

The IVTT bead protein array is part of the MPID (Membrane proteins in Infectious diseases) grant. Performing in-vitro translation of proteins in the presence of uncoupled (without protein anti-tag antibody) tosyl-activated magnetic beads, results in binding of the membrane proteins to the beads. This is an irreversible hydrophobic interaction which allows the membrane protein to stabilize on the tosyl-activated bead surface. The beads containing proteins are printed onto aminosilane glass surface using sonication printing technology developed by Matt Greving. All proteins printed on the slide have the folding reporter green fluorescent protein (frGFP) construct integrated within their expression cassette. The frGFP construct was included to allow a quick quality control over the spotting and appropriate folding and presentation of these proteins by measuring the fluorescence from frGFP [excitation 490nm, emission 510nm [212]] under the blue wavelength (488 nm) on the Perkin Elmer ProScan Array HT microarray scanner (Melville, NY).

Sonication printing protocols

Three different print protocols were used for printing in the first print run so as to be able to optimize for the best printing conditions going forward. The array was initially printed with 13 reagents, some proteins being captured on Dynabeads MyOne-1 μm diameter bead versus some on M280-2.8 μm beads from Life Technologies (Grand Island, NY) as listed:

- 1.) frGFP LEE (Linear Expression Element) [213] #1 - MyOne

- 2.) frGFP LEE#2 - MyOne
- 3.) ASFV113-F1 - MyOne
- 4.) ASFV113-F2 - MyOne
- 5.) FTT0583-frGFP - MyOne
- 6.) FTT1258-frGFP - MyOne
- 7.) GFP-HA in pET 32 - MyOne
- 8.) Mock IVT (no template) – Negative control
- 9.) My one beads – clean (no protein bound) – Negative control
- 10.) frGFP LEE#1 – M280
- 11.) frGFP LEE#2 - M280
- 12.) ASFV113F1 - M280
- 13.) GFP-HA in pET 32 - M280

Out of the 13 reagents mentioned above, only proteins 3, 5, 6, 7, 12 and 13 were expressed and observed on a protein gel during pre-printing quality control. Reagents numbered 8 and 9 are negative controls to allow estimation of background fluorescence from spots due to either the beads themselves or the IVT reagent mixture. All proteins represented on the array have the folding reporter GFP tag on them. The same calibration file was used for all 13 solutions. However sample 9 did not print consistently with these conditions in initial tests. It was removed from the map and printed afterwards with a slight increase in energy onto the same slide.

Slide 1: 400787

5 μ L of each bead-PBS buffer solution were placed in a 1536 well plate. Each sample was laid out in a square pattern of 4 replicates. A dot pitch of 0.5mm was used, which is the distance between IVTT bead protein spots on array. The samples were printed in a randomized manner with each well ejecting 10 times and hitting 10 different blocks of 4 in order to ensure even drying on the surface. The rapid cycling through the sets of 13 samples was an attempt to ensure that the beads remained in suspension in the solution over the entire time of the print (~20 minutes.) Slide 3 (400931) was printed using this same protocol.

Slide 2: 400940

The print plate from slide 1 was used for slide 2 and a pitch of 0.5mm was used for printing the slide. However, in order to test the quality of the suspension over time, each sample was printed completely (~350 prints) before moving on to the next sample. Additionally, each well was primed onto a disposable surface between each print on the final slide. Visually this produced worse alignment of reagents on the slide as compared to slide 1. This might perhaps be due to the loading and unloading of the target plate. The plate map for the 0.5mm pitch is included in Figure A3- 10.

	1	2	3	4	5	6	7	8	9	10	11	12	13	14	15	16	17	18	19	20	21	22	23	24	25	26	27	28	29	30	31	32	33	34	35	36	37	38	39	40	41	42	43	44		Neg
A	1	1	2	2	3	3	4	4	5	5	6	6	7	7	8	8	9	9	10	10	11	11	12	12	13	13	1	1	2	2	3	3	4	4	5	5	6	6	7	7	8	8	9	9	1	Pos
B	1	1	2	2	3	3	4	4	5	5	6	6	7	7	8	8	9	9	10	10	11	11	12	12	13	13	1	1	2	2	3	3	4	4	5	5	6	6	7	7	8	8	9	9	2	
C	10	10	11	11	12	12	13	13	1	1	2	2	3	3	4	4	5	5	6	6	7	7	8	8	9	9	10	10	11	11	12	12	13	13	1	1	2	2	3	3	4	4	5	5	3	
D	10	10	11	11	12	12	13	13	1	1	2	2	3	3	4	4	5	5	6	6	7	7	8	8	9	9	10	10	11	11	12	12	13	13	1	1	2	2	3	3	4	4	5	5	4	
E	6	6	7	7	8	8	9	9	10	10	11	11	12	12	13	13	1	1	2	2	3	3	4	4	5	5	6	6	7	7	8	8	9	9	10	10	11	11	12	12	13	13	1	1	5	
F	6	6	7	7	8	8	9	9	10	10	11	11	12	12	13	13	1	1	2	2	3	3	4	4	5	5	6	6	7	7	8	8	9	9	10	10	11	11	12	12	13	13	1	1	6	
G	2	2	3	3	4	4	5	5	6	6	7	7	8	8	9	9	10	10	11	11	12	12	13	13	1	1	2	2	3	3	4	4	5	5	6	6	7	7	8	8	9	9	10	10	7	
H	2	2	3	3	4	4	5	5	6	6	7	7	8	8	9	9	10	10	11	11	12	12	13	13	1	1	2	2	3	3	4	4	5	5	6	6	7	7	8	8	9	9	10	10	8	
I	11	11	12	12	13	13	1	1	2	2	3	3	4	4	5	5	6	6	7	7	8	8	9	9	10	10	11	11	12	12	13	13	1	1	2	2	3	3	4	4	5	5	6	6	9	
J	11	11	12	12	13	13	1	1	2	2	3	3	4	4	5	5	6	6	7	7	8	8	9	9	10	10	11	11	12	12	13	13	1	1	2	2	3	3	4	4	5	5	6	6	10	
K	7	7	8	8	9	9	10	10	11	11	12	12	13	13	1	1	2	2	3	3	4	4	5	5	6	6	7	7	8	8	9	9	10	10	11	11	12	12	13	13	1	1	2	2	11	
L	7	7	8	8	9	9	10	10	11	11	12	12	13	13	1	1	2	2	3	3	4	4	5	5	6	6	7	7	8	8	9	9	10	10	11	11	12	12	13	13	1	1	2	2	12	
M	3	3	4	4	5	5	6	6	7	7	8	8	9	9	10	10	11	11	12	12	13	13	1	1	2	2	3	3	4	4	5	5	6	6	7	7	8	8	9	9	10	10	11	11	13	
N	3	3	4	4	5	5	6	6	7	7	8	8	9	9	10	10	11	11	12	12	13	13	1	1	2	2	3	3	4	4	5	5	6	6	7	7	8	8	9	9	10	10	11	11	14	
O	12	12	13	13	1	1	2	2	3	3	4	4	5	5	6	6	7	7	8	8	9	9	10	10	11	11	12	12	13	13	1	1	2	2	3	3	4	4	5	5	6	6	7	7	15	
P	12	12	13	13	1	1	2	2	3	3	4	4	5	5	6	6	7	7	8	8	9	9	10	10	11	11	12	12	13	13	1	1	2	2	3	3	4	4	5	5	6	6	7	7	16	
Q	8	8	9	9	10	10	11	11	12	12	13	13	1	1	2	2	3	3	4	4	5	5	6	6	7	7	8	8	9	9	10	10	11	11	12	12	13	13	1	1	2	2	3	3	17	
R	8	8	9	9	10	10	11	11	12	12	13	13	1	1	2	2	3	3	4	4	5	5	6	6	7	7	8	8	9	9	10	10	11	11	12	12	13	13	1	1	2	2	3	3	18	
S	4	4	5	5	6	6	7	7	8	8	9	9	10	10	11	11	12	12	13	13	1	1	2	2	3	3	4	4	5	5	6	6	7	7	8	8	9	9	10	10	11	11	12	12	19	
T	4	4	5	5	6	6	7	7	8	8	9	9	10	10	11	11	12	12	13	13	1	1	2	2	3	3	4	4	5	5	6	6	7	7	8	8	9	9	10	10	11	11	12	12	20	
U	13	13	1	1	2	2	3	3	4	4	5	5	6	6	7	7	8	8	9	9	10	10	11	11	12	12	13	13	1	1	2	2	3	3	4	4	5	5	6	6	7	7	8	8	21	
V	13	13	1	1	2	2	3	3	4	4	5	5	6	6	7	7	8	8	9	9	10	10	11	11	12	12	13	13	1	1	2	2	3	3	4	4	5	5	6	6	7	7	8	8	22	
W	9	9	10	10	11	11	12	12	13	13	1	1	2	2	3	3	4	4	5	5	6	6	7	7	8	8	9	9	10	10	11	11	12	12	13	13	1	1	2	2	3	3	4	4	23	

Figure A3- 10 Plate map for 0.5 mm pitch sonication printing protocol.

The red and white squares in a 'Z' pattern show location of proteins expressed in IVTT on the array, green show the location of negative control and un-expressed proteins.

Slide 4: 400941

The slide was printed with a pitch of 0.75mm. The printing was done with 5 prints from each source well. Sample 9 printed slightly off target alignment but within register from the rest of samples. This is most likely due to the unloading of the target for priming. The plate map for the 0.75mm pitch is included in Figure A3- 11.

	1	2	3	4	5	6	7	8	9	10	11	12	13	14	15	16	17	18	19	20	21	22	23	24	25	26	27	28	29	30	31	32
1	1	1	2	2	3	3	4	4	5	5	6	6	7	7	8	8	9	9	10	10	11	11	12	12	13	13	1	1	2	2	3	3
2	1	1	2	2	3	3	4	4	5	5	6	6	7	7	8	8	9	9	10	10	11	11	12	12	13	13	1	1	2	2	3	3
3	4	4	5	5	6	6	7	7	8	8	9	9	10	10	11	11	12	12	13	13	1	1	2	2	3	3	4	4	5	5	6	6
4	4	4	5	5	6	6	7	7	8	8	9	9	10	10	11	11	12	12	13	13	1	1	2	2	3	3	4	4	5	5	6	6
5	7	7	8	8	9	9	10	10	11	11	12	12	13	13	1	1	2	2	3	3	4	4	5	5	6	6	7	7	8	8	9	9
6	7	7	8	8	9	9	10	10	11	11	12	12	13	13	1	1	2	2	3	3	4	4	5	5	6	6	7	7	8	8	9	9
7	10	10	11	11	12	12	13	13	1	1	2	2	3	3	4	4	5	5	6	6	7	7	8	8	9	9	10	10	11	11	12	12
8	10	10	11	11	12	12	13	13	1	1	2	2	3	3	4	4	5	5	6	6	7	7	8	8	9	9	10	10	11	11	12	12
9	13	13	1	1	2	2	3	3	4	4	5	5	6	6	7	7	8	8	9	9	10	10	11	11	12	12	13	13	1	1	2	2
10	13	13	1	1	2	2	3	3	4	4	5	5	6	6	7	7	8	8	9	9	10	10	11	11	12	12	13	13	1	1	2	2
11	3	3	4	4	5	5	6	6	7	7	8	8	9	9	10	10	11	11	12	12	13	13	1	1	2	2	3	3	4	4	5	5
12	3	3	4	4	5	5	6	6	7	7	8	8	9	9	10	10	11	11	12	12	13	13	1	1	2	2	3	3	4	4	5	5
13	6	6	7	7	8	8	9	9	10	10	11	11	12	12	13	13	1	1	2	2	3	3	4	4	5	5	6	6	7	7	8	8
14	6	6	7	7	8	8	9	9	10	10	11	11	12	12	13	13	1	1	2	2	3	3	4	4	5	5	6	6	7	7	8	8
15	9	9	10	10	11	11	12	12	13	13	1	1	2	2	3	3	4	4	5	5	6	6	7	7	8	8	9	9	10	10	11	11
16	9	9	10	10	11	11	12	12	13	13	1	1	2	2	3	3	4	4	5	5	6	6	7	7	8	8	9	9	10	10	11	11
17	12	12	13	13	1	1	2	2	3	3	4	4	5	5	6	6	7	7	8	8	9	9	10	10	11	11	12	12	13	13	1	1
18	12	12	13	13	1	1	2	2	3	3	4	4	5	5	6	6	7	7	8	8	9	9	10	10	11	11	12	12	13	13	1	1
19	2	2	3	3	4	4	5	5	6	6	7	7	8	8	9	9	10	10	11	11	12	12	13	13	1	1	2	2	3	3	4	4
20	2	2	3	3	4	4	5	5	6	6	7	7	8	8	9	9	10	10	11	11	12	12	13	13	1	1	2	2	3	3	4	4
21	5	5	6	6	7	7	8	8	9	9	10	10	11	11	12	12	13	13	1	1	2	2	3	3	4	4	5	5	6	6	7	7
22	5	5	6	6	7	7	8	8	9	9	10	10	11	11	12	12	13	13	1	1	2	2	3	3	4	4	5	5	6	6	7	7
23	8	8	9	9	10	10	11	11	12	12	13	13	1	1	2	2	3	3	4	4	5	5	6	6	7	7	8	8	9	9	10	10
24	8	8	9	9	10	10	11	11	12	12	13	13	1	1	2	2	3	3	4	4	5	5	6	6	7	7	8	8	9	9	10	10
25	11	11	12	12	13	13	1	1	2	2	3	3	4	4	5	5	6	6	7	7	8	8	9	9	10	10	11	11	12	12	13	13
26	11	11	12	12	13	13	1	1	2	2	3	3	4	4	5	5	6	6	7	7	8	8	9	9	10	10	11	11	12	12	13	13
27	1	1	2	2	3	3	4	4	5	5	6	6	7	7	8	8	9	9	10	10	11	11	12	12	13	13	1	1	2	2	3	3
28	1	1	2	2	3	3	4	4	5	5	6	6	7	7	8	8	9	9	10	10	11	11	12	12	13	13	1	1	2	2	3	3
29	4	4	5	5	6	6	7	7	8	8	9	9	10	10	11	11	12	12	13	13	1	1	2	2	3	3	4	4	5	5	6	6
30	4	4	5	5	6	6	7	7	8	8	9	9	10	10	11	11	12	12	13	13	1	1	2	2	3	3	4	4	5	5	6	6
31	7	7	8	8	9	9	10	10	11	11	12	12	13	13	1	1	2	2	3	3	4	4	5	5	6	6	7	7	8	8	9	9
32	7	7	8	8	9	9	10	10	11	11	12	12	13	13	1	1	2	2	3	3	4	4	5	5	6	6	7	7	8	8	9	9
33	10	10	11	11	12	12	13	13	1	1	2	2	3	3	4	4	5	5	6	6	7	7	8	8	9	9	10	10	11	11	12	12
34	10	10	11	11	12	12	13	13	1	1	2	2	3	3	4	4	5	5	6	6	7	7	8	8	9	9	10	10	11	11	12	12
35	13	13	1	1	2	2	3	3	4	4	5	5	6	6	7	7	8	8	9	9	10	10	11	11	12	12	13	13	1	1	2	2
36	13	13	1	1	2	2	3	3	4	4	5	5	6	6	7	7	8	8	9	9	10	10	11	11	12	12	13	13	1	1	2	2
37	3	3	4	4	5	5	6	6	7	7	8	8	9	9	10	10	11	11	12	12	13	13	1	1	2	2	3	3	4	4	5	5
38	3	3	4	4	5	5	6	6	7	7	8	8	9	9	10	10	11	11	12	12	13	13	1	1	2	2	3	3	4	4	5	5

Figure A3- 11 Plate map for 0.75 mm pitch sonication printing protocol.

The red and white squares in a number '1' pattern show location of proteins expressed in IVTT on the array, green show the location of negative control and un-expressed proteins.

For quality control, the arrays were screened using a polyclonal Rabbit anti-frGFP primary antibody and appropriate reactivity detected using a secondary Alexa Fluor 647 conjugated antibody as seen in Figure A3-12, Panels A, B and C. In all four panels, the green spots are from bead-protein mixtures where the protein were not expressed and therefore the folding reporter GFP could not be detected with the anti-frGFP antibody. The orange-red

fluorescence is from the polyclonal rabbit anti-GFP antibody binding the GFP protein tag, detected using an Alexa Fluor 647 labeled anti-rabbit secondary antibody in panels A, B and C. In panel D the faint orange fluorescence from certain spots highlighted with white dotted lines is from the anti-mouse Alexa Fluor 647 labeled secondary antibody detecting mouse antibodies to cognate antigens used in immunization. The spot margins are much more regular at 0.75 mm pitch (Slide 4) instead of the 0.5 mm pitch (Slide 1, 2 and 3) The printing protocol used for Slide 2 produced some brighter spots due to the same protein being printed on the whole slide (~350 prints) first and then resuming other proteins sequentially. But the positioning of these spots was extremely irregular making alignment using the GenePix Pro (Molecular Dynamics, Sunnyvale, CA) program difficult. The signal intensities obtained from testing these 4 slides are represented in Table A3- 4 (Section A-D).

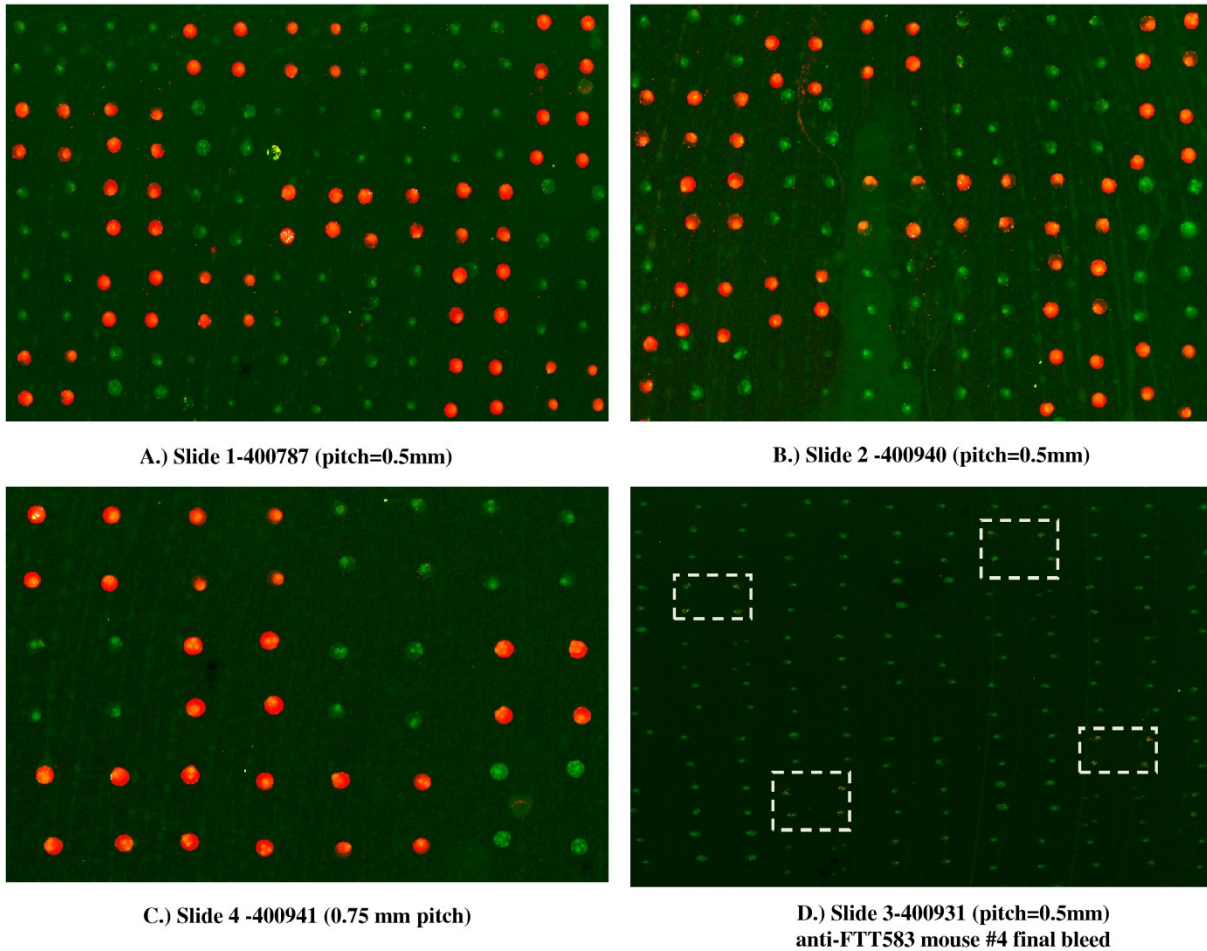


Figure A3-12 *Anti-GFP antibody reactivity captured from translated proteins on IVTT bead protein array.*

Panels A, B and C show orange dots representing anti-GFP antibody recognizing the GFP tag on IVTT proteins on beads being detected by an Alexa Fluor 647 labeled secondary antibody. Panel D shows the anti-FTT583 protein polyclonal mouse sera detected using an anti-mouse secondary binding cognate bead-protein spots (highlighted using grey dotted squares).

Table A3- 4 Signal captured from slides included in the printing protocol comparison in Fluorescence intensity units (FIU).

The count *N* represents the number of replicates printed & measured per reagent on a given slide.

A.) Rabbit anti-GFP (polyclonal) - 5nM (Slide 1-400787, pitch=0.5 mm)

Reagent No.	Reagent	Protein Expression	Count(N)	Min (FIU)	Max (FIU)	Mean (FIU)	Median (FIU)
1	rGFP_LEE#1 (MyOne)	-ve	167	98	220	137	132
2	rGFP_LEE#2 (MyOne)	-ve	169	112	263	147	141
3	ASFV113-F1 (MyOne)	+ve	170	236	9952	2656	1721
4	ASFV113-F2 (MyOne)	-ve	176	104	268	138	136
5	FTT0583 in GFP (MyOne)	+ve	171	859	18593	4142	3290
6	FTT1258 in GFP (MyOne)	+ve	171	152	6416	1661	1032
7	GFP-HA-in pET32 (MyOne)	+ve	168	378	5045	1352	1111
8	Mock IVT (IVT reaction/no template) (MyOne)	-ve	174	112	296	168	166
9	MyOne beads clean	-ve	170	99	165	121	119
10	rGFP_LEE#1 (M280)	-ve	166	107	228	147	143
11	rGFP_LEE#2 (M280)	-ve	167	104	237	131	127

12	ASFV113-F1 (M280)	+ve	174	139	4277	2096	1978
13	GFP-HA-in pET32 (M280)	+ve	172	203	1553	431	379

B.) Rabbit anti-GFP (polyclonal) - 5nM (Slide 2-400940, pitch=0.5 mm)

Reagent No.	Reagent	Protein Expression	Count(N)	Min (FIU)	Max (FIU)	Mean (FIU)	Median (FIU)
1	rGFP_LEE#1 (MyOne)	-ve	305	123	378	203	201
2	rGFP_LEE#2 (MyOne)	-ve	312	132	405	201	200
3	ASFV113-F1 (MyOne)	+ve	312	518	16820	2812	1403
4	ASFV113-F2 (MyOne)	-ve	307	119	371	174	170
5	FTT0583 in GFP (MyOne)	+ve	312	238	6064	2170	1637
6	FTT1258 in GFP (MyOne)	+ve	312	331	8450	1702	1016
7	GFP-HA-in pET32 (MyOne)	+ve	312	342	8017	2123	1614
8	Mock IVT (IVT reaction/no template) (MyOne)	-ve	305	127	338	171	166
9	MyOne beads clean	-ve	300	111	318	197	197
10	rGFP_LEE#1 (M280)	-ve	308	135	290	204	203
11	rGFP_LEE#2 (M280)	-ve	313	0	376	204	200
12	ASFV113-F1 (M280)	+ve	312	741	41258	6338	4710

13	GFP-HA-in pET32 (M280)	+ve	312	352	14723	2654	1658
----	------------------------------	-----	-----	-----	--------------	------	------

C.) Rabbit anti-GFP (polyclonal) - 5nM (Slide 4-400941, pitch=0.75 mm)

Reagent No.	Reagent	Protein Expression	Count(N)	Min (FIU)	Max (FIU)	Mean (FIU)	Median (FIU)
1	rGFP_LEE#1 (MyOne)	-ve	164	76	224	149	157
2	rGFP_LEE#2 (MyOne)	-ve	166	79	237	143	140
3	ASFV113-F1 (MyOne)	+ve	164	181	13491	2080	1632
4	ASFV113-F2 (MyOne)	-ve	164	76	208	139	143
5	FTT0583 in GFP (MyOne)	+ve	164	217	18515	2623	1701
6	FTT1258 in GFP (MyOne)	+ve	166	140	6143	1484	1391
7	GFP-HA-in pET32 (MyOne)	+ve	164	110	2657	673	561
8	Mock IVT (IVT reaction/no template) (MyOne)	-ve	164	92	225	172	184
9	MyOne beads clean	-ve	166	66	229	137	138
10	rGFP_LEE#1 (M280)	-ve	164	72	251	152	161
11	rGFP_LEE#2 (M280)	-ve	164	75	218	141	144
12	ASFV113-F1 (M280)	+ve	166	178	10222	2645	2383
13	GFP-HA-in pET32 (M280)	+ve	162	89	1777	434	344

D.) Polyclonal mouse anti-FTT0583 sera (1:500 diluted) - (Slide 3-400931, pitch=0.5mm)

Reagent No.	Reagent	Protein Expression	Count	Min (FIU)	Max (FIU)	Mean (FIU)	Median (FIU)
5	FTT0583 in GFP (MyOne)	+ve	168	108	505	190	156

On slide 1-400787 (Table A3- 4, Section A), from the maximum signal captured, MyOne bead-proteins showed higher signal as compared to M280 for 2 antigens ASFV113-F1 and Hemagglutinin (HA). This is an unexpected result given that M280 beads have a larger surface area as compared to MyOne beads. One reason why this might have happened could be due to lesser retention of M280 (larger) beads on the aminosilane surface as compared to MyOne beads during slide processing. Bead run-off before and after microarray processing would be difficult to estimate. Alternatively, the suspension time of beads in buffer during printing might be more important for M280 (heavier) beads. The effect of suspension time on beads is tested in Section B on slide 2-400940 whereby one reagent is printed on the complete slide before moving onto the second reagent. Here as expected M280 bead-proteins show higher signal intensity as compared to MyOne for both proteins ASFV113-F1 and HA. The quality of suspension decreases over time as observed when comparing intensities obtained from these two proteins between Section A and B. Higher sonication energy was used to deposit beads in slide 4 – 400941 (Table A3- 4, Section C) to estimate if doing so would equalize the amount of deposited bead-proteins regardless of the bead diameter. Increase in sonication energy was sufficient to overcome the difference in spotting between M280 and MyOne bead-proteins and resulted in better spot morphology as compared to Slides 1 and 2.

We also probed the array with polyclonal sera from mice immunized with protein # 5 (FTT0583) and protein # 6 (FTT1258). The overall signal obtained from polyclonal sera was low and very close to background as depicted in Figure A3-12, Panel D and Table A3- 4, Section D. This observation might be because polyclonal sera takes longer to equilibrate as observed from the pathogen proteome peptide (PPP) microarray in Chapter 4 and we only incubated the primary polyclonal sera for 1 hour during our initial test. Going forward, we would be testing polyclonal sera reactivity observed after 16 hours of incubation, which is recommended for protein microarrays [214].

For the next set of experiments, I would recommend testing different slide surfaces and using the print protocol that was approved in this first round of comparison. Again quality control testing should be repeated using the polyclonal anti-tag antibody so as to decide which slide surface provides maximum retention of beads. This technology could potentially be used for screening proteins from a pathogen whose epitope peptides have not been empirically mapped in literature or the Immune Epitope DataBase (IEDB) to rapidly identify both immunoreactive and immunodominant antigens.

Acknowledgements

I would like to thank Dr. Kathryn Sykes for involving me on these projects that help highlight some of the potential uses for the PPP array technology. I would also like to thank Dr. Linda Dixon from The Pirbright Institute, UK for providing ASFV sera.

I am grateful everyone listed below for providing data towards this appendix. The ELISA data for the TVDC project was obtained from Dr. Andrey Loskutov and Miss. Felicia

Craciunescu. The ELISA data for the ASFV project was obtained from Dr. Mark Robida and Dr. Debbie Tumbula Hansen. The sonication based printing was done by Matt Greving and the printing protocols were contributed by him in this manuscript. The polyclonal mouse sera data was obtained from Dr. Debbie Tumbula Hansen using Dr. Mark Robida's mouse immunization experiment. Miss Felicia Craciunescu completed a quality control assessment before sending out the 13 printing reagents using protein gel electrophoresis.

Bibliography

1. Chan KH, To KKW, Hung IFN, Zhang AJX, Chan JFW, et al. (2011) Differences in Antibody Responses of Individuals with Natural Infection and Those Vaccinated against Pandemic H1N1 2009 Influenza. *Clinical and Vaccine Immunology* 18: 867-873.
2. Prim D, Rebeaud F, Cosandey V, Marti R, Passeraub P, et al. (2013) ADIBO-Based "Click" Chemistry for Diagnostic Peptide Micro-Array Fabrication: Physicochemical and Assay Characteristics. *Molecules* 18: 9833-9849.
3. Cretich M, Damin F, Longhi R, Gotti C, Galati C, et al. (2010) Peptide Microarrays on Coated Silicon Slides for Highly Sensitive Antibody Detection. *Small Molecule Microarrays: Methods and Protocols* 669: 147-160.
4. Hjelm B, Forsström B, Löfblom J, Rockberg J, Uhlén M (2012) Parallel Immunizations of Rabbits Using the Same Antigen Yield Antibodies with Similar, but Not Identical, Epitopes. *PLoS ONE* 7: e45817.
5. Loh J, Zhao GY, Presti RM, Holtz LR, Finkbeiner SR, et al. (2009) Detection of Novel Sequences Related to African Swine Fever Virus in Human Serum and Sewage. *Journal of Virology* 83: 13019-13025.
6. Registry NSA HHS and USDA Select Agents and Toxins List.
7. Whitlock GC, Robida MD, Judy BM, Qazi O, Brown KA, et al. (2011) Protective antigens against glanders identified by expression library immunization. *Frontiers in Microbiology* 2.
8. Borca MV, Irusta P, Carrillo C, Afonso CL, Burrage T, et al. (1994) African swine fever virus structural protein p72 contains a conformational neutralizing epitope. *Virology* 201: 413-418.
9. GomezPuertas P, Rodriguez F, Oviedo JM, RamiroIbanez F, RuizGonzalvo F, et al. (1996) Neutralizing antibodies to different proteins of African swine fever virus inhibit both virus attachment and internalization. *Journal of Virology* 70: 5689-5694.
10. Neilan JG, Zsak L, Lu Z, Burrage TG, Kutish GF, et al. (2004) Neutralizing antibodies to African swine fever virus proteins p30, p54, and p72 are not sufficient for antibody-mediated protection. *Virology* 319: 337-342.

11. Barderas MG, Rodriguez F, Gomez-Puertas P, Aviles M, Beitia F, et al. (2001) Antigenic and immunogenic properties of a chimera of two immunodominant African swine fever virus proteins. *Archives of Virology* 146: 1681-1691.
12. Legutki JB, Johnston SA (2013) Immunosignatures can predict vaccine efficacy. *Proceedings of the National Academy of Sciences of the United States of America* 110: 18614-18619.
13. Pedelacq JD, Cabantous S, Tran T, Terwilliger TC, Waldo GS (2006) Engineering and characterization of a superfolder green fluorescent protein. *Nature Biotechnology* 24: 79-88.
14. Sykes KF, Johnston SA (1999) Linear expression elements: a rapid, in vivo, method to screen for gene functions. *Nature Biotechnology* 17: 355-359.
15. Montor WR, Huang J, Hu YH, Hainsworth E, Lynch S, et al. (2009) Genome-Wide Study of *Pseudomonas aeruginosa* Outer Membrane Protein Immunogenicity Using Self-Assembling Protein Microarrays. *Infection and Immunity* 77: 4877-4886.

APPENDIX IV
INSTITUTIONAL REVIEW BOARD (IRB) APPROVAL



ARIZONA STATE UNIVERSITY

Office of Research Integrity and Assurance
 660 S. Mill Avenue Suite 315
 Arizona State University
 Tempe AZ 85287-6111
 (Mail Code 6111)
 Phone: 480-965-6788
 Fax: (480) 965-7772

CONTINUING REVIEW FORM- IRB

- In accordance with Federal Regulations 45CFR46, the IRB must review nonexempt protocols at least annually, or more frequently if warranted.
- Please type your responses in the boxes provided. Use as much space as necessary (the boxes will expand). Please answer each question – if a question is not applicable, please put N/A in the box.
- Studies that are in the data analysis phase are considered open, researchers must complete this form.

1. Principal Investigator	
Principal Investigator: Stephen Albert Johnston	
ASU department address: Center for Innovations in Medicine, Biosign Institute B230 MC5901	
E-mail address: Stephen.johnston@asu.edu	
Phone number: 480-727-0792	Fax Number: 480-727-0782
Co-investigator(s) Name(s) and Contact Information: Phillip Stafford, Phillip.stafford@asu.edu; Kathryn Sykes, Kathryn.sykes@asu.edu; Lucas Restrepo, lucas.restrepo@asu.edu; Muskan Kukreja, muskan.kukreja@asu.edu	
2. Protocol Information	
2a) Title of protocol: Profiling Human Sera for Unique Antibody signatures	
2b) HS #: 0912004625	
2c) If project is funded or funding is being sought, provide list of all sponsors and grant numbers: DTRA HDTRA1-11-1-0010; DoD BCRP W81XWHO710549; Please indicate the grant status for each source of funding: <input checked="" type="checkbox"/> Active <input type="checkbox"/> Pending	
2d) ASU account number/project number: FQS0052, FQS0030	
2e) Location(s) of research activity: Biosign Center for Innovations in Medicine B225, B229, B233, B237	
2f) IRB approval dates from additional institutions: All samples are provided to us from institutions that are current with their IRB approval. We currently do not have that information but can obtain if needed. <i>*Please note that copies of current IRB approvals from additional institutions are required.</i>	
3. Protocol Status	
3a) Active: <input checked="" type="checkbox"/> Yes <input type="checkbox"/> No (If no, submit a close out report: http://researchintegrity.asu.edu/humans/forms)	
3b) Please indicate remaining duration of the study: 9 years	
4. Participant Information	
4a) Is this study closed to enrollment of new subjects: <input checked="" type="checkbox"/> Yes <input type="checkbox"/> No	

4b) Total number of participants approved for the study (to be enrolled): N/A
4c) Number of participants enrolled (e.g. signed a consent form) during the past approval period : N/A
4d) Total number of participants enrolled since study began : N/A
4e) Total number of individuals screened (e.g. individuals that responded to study advertisements or other recruitment practices and were questioned by investigators) in the past approval period (if applicable): N/A (this includes the number that was later enrolled)
4f) Of the total number of individuals screened in the past approval period, what percentage has been ineligible to participate in the study (if applicable)? N/A
4g) Number of enrolled participants who withdrew from the study: N/A Please state the reason(s) the participant(s) withdrew.
4h) Number of participants still to be enrolled: N/A (If this brings the sample to greater than what is listed in 4b, submit a request for modification see 7d).
4i) Participant enrollment breakdown by gender, age and ethnicity: (This information is required for all studies that are NIH-sponsored. It is recommended, but not required, that other researchers provide this information). N/A

5. Data Sources	
Check all categories that apply to your protocol.	
<input type="checkbox"/>	Human subjects intervention with use of informed consent form
<input type="checkbox"/>	Discarded, identified pathological materials, no intervention
<input type="checkbox"/>	Genetic analysis
<input type="checkbox"/>	Interviews or questionnaires
<input type="checkbox"/>	Medical records or other records from human subjects
<input checked="" type="checkbox"/>	Other please specify: We have clinical diagnosis and treatment status, genotype information and maybe smoking history. All information though is provided to us.

6. Adverse Events or Unexpected Problems	
6a) Have there been any complaints from subjects in the past approval period? <input type="checkbox"/> Yes If yes, describe <input checked="" type="checkbox"/> No	
6b) Have there been any adverse events or unexpected problems in the past approval period? <input type="checkbox"/> Yes <input checked="" type="checkbox"/> No If yes, please explain in detail and indicate when the IRB was notified of the event or problem. If the IRB was not notified, please explain why this was not done.	
6c) Does the study have a Data Safety Monitoring Board (DSMB)? <input type="checkbox"/> Yes <input checked="" type="checkbox"/> No If yes, please indicate the date of the last DSMB review: <i>Please note that investigators are required to submit DSMB reports to the ASU IRB at the time they are made available to the investigator.</i>	

7. Protocol Modifications or Revisions

Revised 8/11

7a) Have there been any modifications or revisions to the protocol in the past approval period?
 Yes No
 If yes, please indicate the date of the approval from the Committee for the modification or revision and provide a brief description.

7b) Have there been any deviations from the approved protocol? Yes No
 If yes, please describe to self-report the protocol violation.

7c) Do you want to add any new co-investigators to the study? Yes No
 If yes, submit their names and copies of the human subjects training required by the IRB:
<http://researchintegrity.asu.edu/training/humans>

7d) Do you wish to submit a modification at this time? Yes No
 If yes, please describe the modification request and rationale for the changes. Please remove Dr. Patricia Carrigan from the protocol. She has left ASU.

8. Current Consent Form

8a) Please attach a copy of your current consent form for renewal if you are enrolling new subjects. N/A

8b) Is this the original consent form or a revised form? Original Revised (If revised, please provide date of ASU IRB approval for the revision. Attach a copy of the stamped form and unstamped form)

9. Protocol Progress Report

9) Please submit a *detailed* progress report. The progress report must be substantive and complete, and include the goal(s) of the study, findings to-date, how data is being stored, and plans for the next year/review period. If this project is funded, please send a copy of the most recent progress report that was sent to the funding agency.

The last year, our team has optimized the immunosignature microarray and has contracted with Applied Microarrays (AMI) in Tempe, AZ to print our arrays. We obtained a new set of 10,000 different random peptides, as the last set had been depleted. We ensured that the new peptides were carefully diluted in a new buffer/organic mix that is compatible with AMI's printing process. The added precision of commercial printing has allowed us to obtain higher reproducibility across patients, and find much more subtle changes in antibody responses. We have completed the Valley Fever project by printing a set of 100-peptide 'diagnostic arrays' to do the test-training sample sets. We have obtained 65 look-back blinded samples from John Galgiani at U of A in Tucson that were all false negative samples from his clinic. We classified these samples with 0% error (after excluding problematic samples that were inherently high-background or had been subject to degradation effects). We are in the process of writing these data up in a manuscript.

We completed a project on glioblastoma multiformae, using blinded samples from Barrow Neurological Institute (BNI) in which we were able to identify brain cancer grade as well as presence or absence of an important methylation enzyme, MGMT. This enzyme's status has been shown to be an effective predictor of response to Temozolamide. We have submitted this manuscript to NeuroOncology.

We have completed a project on Esophageal Cancer, using blinded samples obtained from Mayo Clinic, in which we were able to distinguish presence or absence of Esophageal cancer in patients. We are currently examining samples from patients with Barrett's Esophagus, to determine whether we can detect early cancer predisposition.

We have built a pathogen microarray, in which 5K peptides from human pathogens were tiled on a standard glass slide. We are currently optimizing this platform to distinguish patients who are convalescent from one or another infectious agent. We have found that printing methods that enhance the immunosignaturing effect are deleterious to the discrimination of our pathogen epitope arrays. Thus we are altering the printing characteristics for these arrays, and are using a slide surface that spaces the peptides out much further than our aminosilane slides allow.

10. Publications, Presentations and Recent Findings

10a) Have there been any presentations or publications resulting from this study during the past approval

Revised 8/11

period? Yes No If yes, please submit a copy of the abstract, or the publication, with this application.

"Immunosignaturing can detect products from molecular markers in brain cancer" – submitted to NeuroOncology
"Physical parameters Affecting Antibody Profiles as Biomarkers of Health Status" – revision resubmitted to Molecular and Cellular Proteomics
"Sample Preparation for Immunosignaturing" – revision resubmitted to Vaccine

Presentations:

BRP FY11 Vision Setting Meeting, November 2010 – Panel Member
3rd Annual Oncology Biomarker Conference, January 2011 – Invited speaker
Leading Innovation and Knowledge Sharing (LINKS) BCMRP meeting, February, 2011 - Panel member
BCRP FY10 Programmatic Review Meeting, March 2011 – Panel member
Canary Foundation, March 2011 – Invited participant
Era of Hope Abstract Placement Meeting, April 2011 – Committee member
NBCC Artemis Project, April 2011 – Workshop participant
Era of Hope Meeting, Orlando, August 2011 – Invited speaker, Organizing committee member

10b) Have there been any recent findings either from this study, or a related study (through a literature review for example), that would have an effect on this study's risk/benefit analysis? Yes No
If yes, please describe and cite references:

11. Conflicts of Interest and Commercialization

11. Does any member of the research team have a potential conflict of interest with this study that could affect study participants and/or study outcome? For more information about examples of conflicts of interests, please visit the ASU objectivity website: <http://researchintegrity.asu.edu/col>
 Yes (If yes, please describe and disclose in the consent form) No

b) Does the PI or Co-I have a current conflict disclosure form on file at the ASU Office of Research Integrity and Assurance?
 Yes No

c) If there are conflicts of interests, please describe the ways in which you have and will minimize harm to research subjects and/or the objectivity of research. No prospective human trials have been proposed, only blinded retrospective samples are currently being run on the immunosignaturing platform.

12. Training

12. The research team must verify completion of human subjects training within the last 3 years. (<http://researchintegrity.asu.edu/training/humans>)

CITI training – Provide the date that the PI and Co-I's completed the training:
If you completed NIH training prior to 9/15/10 this will be accepted. Provide a copy of the certificate.

13. Required Signatures

Revised 8/11

Principal Investigator:



Date: 10/18/11

FOR IRB USE

Chair or Committee member name:

Signature:

Date:

Office of Research Integrity and Assurance

To: Stephen Johnston
BDB

From: Carol Johnston, Chair
Biosci IRB

Date: 10/24/2011

Committee Action: Renewal

Renewal Date: 10/24/2011

Review Type: Expedited F5

IRB Protocol #: 0912004625

Study Title: Profiling Human Sera for Unique Antibody Signatures

Expiration Date: 11/21/2012

The above-referenced protocol was given renewed approval following Expedited Review by the Institutional Review Board.

It is the Principal Investigator's responsibility to obtain review and continued approval of ongoing research before the expiration noted above. Please allow sufficient time for reapproval. Research activity of any sort may not continue beyond the expiration date without committee approval. Failure to receive approval for continuation before the expiration date will result in the automatic suspension of the approval of this protocol on the expiration date. Information collected following suspension is unapproved research and cannot be reported or published as research data. If you do not wish continued approval, please notify the Committee of the study termination.

This approval by the Biosci IRB does not replace or supersede any departmental or oversight committee review that may be required by institutional policy.

Adverse Reactions: If any untoward incidents or severe reactions should develop as a result of this study, you are required to notify the Biosci IRB immediately. If necessary a member of the IRB will be assigned to look into the matter. If the problem is serious, approval may be withdrawn pending IRB review.

Amendments: If you wish to change any aspect of this study, such as the procedures, the consent forms, or the investigators, please communicate your requested changes to the Biosci IRB. The new procedure is not to be initiated until the IRB approval has been given.

Biosci IRB

To: Johnston, Stephen Albert

Date: 09 / 26 / 2011

From: Biosci IRB

Expiration Date: 11 / 22 / 2011

Re: Protocol # 0912004625: Profiling Human Sera for Unique Antibody Signatures

This letter serves as a IRB notification reminder by the Biosci IRB. It is the primary responsibility of the Principal Investigator to ensure that the re-approval status for lapsed protocols is achieved. All protocols must be re-approved annually by the IRB unless shorter intervals have been specified.

Please note that the level of review given to the continuing review process is the same as that of any new protocol. All requests for re-approval must be reviewed at a convened IRB meeting, except for those protocols that meet the criteria for expedited review.

Please submit the following documents at least three weeks prior to the expiration date to allow for full committee review:

- 1) A completed Continuing Review Form.
- 2) Two (2) copies of each consent form(s) used in the study (If data collection is ongoing).

Please note that you can obtain a copy of the Continuing Review Form through our web site:

<http://researchintegrity.asu.edu/humans>.

As of July 1, 2003, all personnel involved in human subjects research must complete the Human Subjects training course. It is the responsibility of the Principal Investigator to make sure all personnel associated with this study have completed the human subjects training course (see the Office of Research Integrity and Assurance website for a link to the NIH training).

It is a violation of Arizona State University policy and federal regulations to continue research activities after the approval period has expired. If the IRB has not reviewed and re-approved this research by its current expiration date, all enrollment, research activities and intervention on previously enrolled subjects must stop. If you believe that the health and welfare of the subjects will be jeopardized if the study treatment is discontinued, you may submit a written request to the IRB to continue treatment activities with currently enrolled subjects.

Your assistance and cooperation in ensuring that the above-mentioned protocol is received for re-approval evaluation at the Office of Research Integrity and Assurance before the lapse date is greatly appreciated.

*sent to Office of Research
Integrity
10/18/11*

APPENDIX V
INSTITUTIONAL ANIMAL CARE & USE COMMITTEE

ational Animal Care and Use Committee (IACUC)
Arizona State University

me

Tempe, Arizona 85287-3503
(480) 965-2179 FAX: (480) 965-8013

Animal Protocol Review

Protocol Number: 05-817R
Protocol Title: Genetic Cancer Vaccines
Principal Investigator: Stephen Johnston
Date of Action: 06/17/2005 Final Action Date: 06/17/2005

The animal protocol review was considered by the Committee and the following decisions were made:

- The original protocol was APPROVED as presented.
- The revised protocol was APPROVED as presented.
- The protocol was APPROVED with RESTRICTIONS or CHANGES as listed below. The project can only be pursued, subject to your acceptance of these restriction or changes. If you are not agreeable, contact the IACUC Chairperson immediately.
- The Committee requests CLARIFICATIONS or CHANGES in the protocol as described below. Approval is contingent upon review and approval of the required revisions by the IACUC Chair.
- The protocol was approved, subject to the approval of a WAIVER of provisions of NIH policy as noted below. Waivers require written approval from the granting agencies.
- The protocol was DISAPPROVED for reasons outlined in the attached memorandum.
- The Committee requests you to contact _____ to discuss this proposal.
- A copy of this correspondence has been sent to the Vice President for Research.

RESTRICTIONS, CHANGES OR WAIVER REQUIREMENT:

Approved Number of Animals: 3,000 Mice

Approval Period: 06/17/2005 - 06/16/2008

Signature: *me*
IACUC Chair or Designee

Date: 06/17/2005

Investigator cc: IACUC Office, IACUC Chair, ORSPA

VI. DUPLICATION AND ALTERNATIVES

- A. Provide the following details for the most recent literature search used to explore for duplicative research, alternatives to painful procedures and most currently relevant teaching use of animals.

Date that search was conducted: 4/5/2005
 Database used: Medline
 Publication years covered by the search: Last 5 years
 Keywords used: Genetic immunization, cancer vaccine, tumor antigens, melanoma, and breast cancer

- B. Describe any other procedures (e.g., participation in meetings, review of journals) that are used to evaluate duplication and explore alternatives:

We will continue to monitor commercial sources should one be available. In addition, we will monitor scientific literature for comparable reagents as needed. Journals that we routinely monitor include Science, Nature groups, Vaccine, PNAS, EMBO, Cancer Research, to name a few. In addition, Dr. Johnston attends multiple scientific meetings each year to keep abreast of new developments.


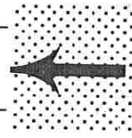
- C. Does this research replicate previous work? **NOTE: Teaching protocols need not address Item VI.c.**

- No. Proceed to section VII.
- Yes. Explain why the replication is necessary:

VII. ASSURANCE:

The information contained herein is accurate to the best of my knowledge. I have carefully compared the proposed work with the current state of knowledge in this field by reviewing the literature and it is my professional opinion that the proposed work meets high standards of scientific merit. If the study involves pain and distress to the animal, whether or not it is relieved by anesthetics or analgesics, I have (1) reviewed the literature related to this work and have found no significant studies which could make this protocol unnecessarily duplicative, and (2) considered alternatives to animal use and found none available, as described above. Procedures involving animals will be carried out humanely and all procedures will be performed by or under the direction of trained or experienced persons. Any revisions to animal care and use in this project will be promptly forwarded to the Animal Care and Use Committee for review. Revised protocols will not be used until Committee clearance is received. The use of alternatives to animal models has been considered and found to be unacceptable at this time.

The principal investigator, by signing below, and the IACUC recognize that other medications may be given to the animals for veterinary care purposes (including humane euthanasia of animals in pain that cannot be controlled, as determined by the University Veterinarian or a euthanasia-certified principal investigator).


 Individual listed on I.A. _____ Date 6/30/05

Stephen Albert Johnston, Director CIM
 Insert Name and Title Here - copy and paste as necessary _____ Date 6/30/05

 ***Department Chair _____ Date _____

 ***College Dean _____ Date _____

***ASU East requires these signatures.

NOTE: Principal investigators are requested to attach a two-page biosketch reflecting their most recent pertinent experience.

Institutional Animal Care and Use Committee (IACUC)
Arizona State University

Tempe, Arizona 85287-1103
(480) 965-2179 FAX: (480) 965-7772


Animal Protocol Review

ASU Protocol Number: 08-1000R
Protocol Title: Genetic Cancer Vaccines
Principal Investigator: Stephen Johnston
Date of Action: 07/01/2008

The animal protocol review was considered by the Committee and the following decisions were made:

- The original protocol was APPROVED as presented.
- The revised protocol was APPROVED as presented.
- The protocol was APPROVED with RESTRICTIONS or CHANGES as noted below. The project can only be pursued, subject to your acceptance of these restriction or changes. If you are not agreeable, contact the IACUC Chairperson immediately.
- The Committee requests CLARIFICATIONS or CHANGES in the protocol as described in the attached memorandum. The protocol will be reconsidered when these issues are clarified and the revised protocol is submitted.
- The protocol was approved, subject to the approval of a WAIVER of provisions of NIH policy as noted below. Waivers require written approval from the granting agencies.
- The protocol was DISAPPROVED for reasons outlined in the attached memorandum.
- The Committee requests you to contact _____ to discuss this proposal.
- A copy of this correspondence has been sent to the Vice President for Research.
- Amendment was approved as presented.

Approved # of Animals: 6,336 Mice **Pain Level:** D
Approval Period: 07/01/2008 - 06/29/2011
Funded: Department of Defense
Title: Towards Developing a Prophylactic Breast Cancer Vaccine

Signature:  Date: 7/1/08
IACUC Chair or Designee

Original: Principal Investigator
cc: IACUC Office
IACUC Chair
ORSPA/SPS

Institutional Animal Care and Use Committee (IACUC)

Office of Research Integrity and Assurance

Arizona State University

660 South Mill Avenue, Suite 315

Tempe, Arizona 85287-6111

Phone: (480) 965-4387 FAX: (480) 965-7772

Animal Protocol Review

ASU Protocol Number: 11-1197R
Protocol Title: Genetic Cancer Vaccines
Principal Investigator: Stephen Johnston
Date of Action: 06/24/2011

The animal protocol review was considered by the Committee and the following decisions were made:

- The original protocol was APPROVED as presented.
- The revised protocol was APPROVED as presented.
- The protocol was APPROVED with RESTRICTIONS or CHANGES as noted below. The project can only be pursued, subject to your acceptance of these restriction or changes. If you are not agreeable, contact the IACUC Chairperson immediately.
- The Committee requests CLARIFICATIONS or CHANGES in the protocol as described in the attached memorandum. The protocol will be considered when these issues are clarified and the revised protocol is submitted.
- The protocol was approved, subject to the approval of a WAIVER of provisions of NIH policy as noted below. Waivers require written approval from the granting agencies.
- The protocol was DISAPPROVED for reasons outlined in the attached memorandum.
- The Committee requests you to contact _____ to discuss this proposal.
- A copy of this correspondence has been sent to the Vice President for Research.
- Amendment was approved as presented.

RESTRICTIONS, CHANGES OR WAIVER REQUIREMENTS:

Total # of Animals: 9,024 **Pain Level:** B-720; C-3,074; D-5,230 **Species:** Mice
Sponsor: Department of Defense
Title: Towards Developing a Prophylactic Breast Cancer Vaccine
Proposal #: W81XWH0710549
Approval Period: 06/24/2011 – 06/23/2014

Signature: _____ Date: 6/24/11
IACUC Chair or Designee

Original: Principal Investigator
Cc: IACUC Office
IACUC Chair

Date: 6/7/2012

**ARIZONA STATE UNIVERSITY
IACUC ANNUAL REVIEW**

I. Currently approved protocol

Protocol Number: 11-1197R
 Protocol Title: Genetic Cancer Vaccine
 Principal Investigator: Stephen Johnston

II. Status of Project**A. Was the research or teaching conducted?**

- i. No. If no,
1. Will the protocol be terminated?
 - a. Yes. Proceed to item VI.
 - b. No. Proceed to item II B.
- ii. Yes. If yes,
1. Were there any significant animal welfare issues (morbidity or mortality, complications, etc.) encountered over the past 12 months?
 - a. Yes. Please describe (include the problem, approximate number of animals affected, and resolution). Proceed to item II B when completed.
About 5% of the FVB/N-NeuT females spontaneously died. This is a common characteristic of this transgenic mouse strain. All of the other mice behaved normally.
 - b. No. Proceed to item II B.

B. Will the research or teaching continue with no anticipated protocol changes in animal species, animal numbers, or categories listed below for the next 12-month period?

- Procedures
- Criteria to Measure/Monitor Pain or Distress
- Alternatives to Painful Procedures
- Restraint
- Amelioration and Control of Painful Procedures
- Estimation of Potential Postoperative/Intervention Pain
- Postoperative/Chronic Care
- Euthanasia/Disposition of Animals
- Animal Care and/or Use Sites

- i. Yes. Proceed to item III.
- ii. No. If there will be proposed changes, you must complete an Amendment Request form describing all proposed changes as well as the scientific rationale for these changes. Proceed to item III.

III. Updated Information**A. Please evaluate the Category of Pain as stated in your currently approved protocol. Do you feel it remains appropriate for the procedures performed?**

- i. Yes. Proceed to item III B.
- ii. No. If no, please describe: Proceed to item III B when completed.

Revision 1/12

B. Have there been any recent findings, either from this study or a related study, that would change the planned use of animals?

i. Yes. If yes, cite references below or in an attachment and submit an Amendment Request form. Proceed to item IV when completed.

ii. No. Proceed to item IV.

IV. Progress Report

Provide a statement on progress of your teaching or research under this protocol over the past 12 months. Include any presentations or publications that have resulted from this protocol during the past 12 months.

We optimized the immunization regime for our prophylactic cancer vaccine candidates. The protection by individual and pool FS antigens were confirmed in both FVB/NeuT and BALB/NeuT mice models. We are currently working on further optimization of the immunization to achieve the additive protection by pooling more FS antigen candidates. We presented "Frameshift Peptides as Prophylactic Cancer Vaccines Antigens" at 2012 annual meeting of American Association for Cancer Research at April 2012.

V. Personnel

All personnel who work with animals are required to have animal care training within the last three years. ASU IACUC training modules can be completed at the LATA ASU homepage. Training dates can also be verified by users at this site: <http://balsam.forest.net/latanet/records/asut/search3.htm>

A. List the names, titles, affiliations, and roles of ALL persons currently involved in the research or teaching activity.

<u>Name</u>	<u>Title</u>	<u>ASURITE name</u>	<u>Role in Protocol (What procedures will each person be doing?)</u>	<u>Species with which individual will have direct contact ("all" or list species)*</u>	<u>IACUC USE ONLY Training (mm/yy)</u>
Stephen Johnston, Ph.D.	PI, Center Director, CIM		Design experiments	None	4/10 HSQ
Kathryn Sykes, Ph.D.	Adjunct Professor		Design Experiments, interpret data, troubleshoot	None	11/11 HSQ
Christopher Diehnelt, Ph.D.	Res. Asst. Professor		Design Experiments	None	Basic 9/09, Mice 4/10 HSQ
Danielle Lussier	Graduate Student		Immunization, /bleed mice /Euthanasia	Mouse	HSQ 11/11
Andrey Loskutov, Ph.D.	Research Scientist		Immunization, /bleed mice /Euthanasia	Mouse	2/11 HSQ

Revision 1/12

Luhui Shen	Graduate Student		Immunization, /bleed mice /Euthanasia/Breed Tg mice/tumor cell injection/monitoring	Mouse	11/11 H5Q
Felicia Craciunescu	Researcher		Immunization, /bleed mice /Euthanasia/tumor cell injection/monitoring	Mouse	10/09 H5Q
John Charles Rodenberry	Researcher		Immunization, /bleed mice /Euthanasia/Breed Tg mice/tumor cell injection/monitoring	Mouse	2/11 H5Q
Kurt Whittemore	Graduate Student		Immunization, /bleed mice /Euthanasia/Breed Tg mice/tumor cell injection/monitoring	Mouse	6/12 H5Q
Kari Kotlarczyk	Technician		Immunization, /bleed mice /Euthanasia/Breed Tg mice/tumor cell injection/monitoring	Mouse	7/10 H5Q
Hu Duan	Graduate Student		Immunization, /bleed mice /Euthanasia/Breed Tg mice/tumor cell injection/monitoring	Mouse	6/10 H5Q

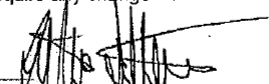
B. List the names of any individuals no longer involved with the research (these individuals will be removed from the protocol and DACT will be notified):

Mark Robida, Kristen (Day) Seifert

4

VI. Certification

By signing this report, I certify that, to the best of my knowledge, the information included herein is accurate and complete. I understand that continued animal use past the scheduled termination date of the protocol requires IACUC approval. I also understand that should the animal use under this protocol require any change from that stated in the protocol, prior approval by the IACUC is required.


Principal Investigator's Signature

6/7/12
Date


FOR IACUC USE ONLY
Annual Review Determination

ANNUAL REVIEW APPROVAL SIGNATURES:



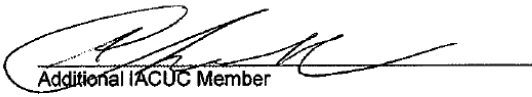
Chair, IACUC

6-28-12
Date



Attending Veterinarian

6-28-12
Date



Additional IACUC Member

6-28-12
Date

BIOGRAPHICAL SKETCH

I earned my Bachelor of Science degree majoring in Microbiology from the University of Mumbai in India. During my bachelors degree I simultaneously completed 2 diplomas in computer programming with the intention of pursuing a career in the field of Bioinformatics. My bachelors in Microbiology piqued my interest in medical diagnostics applied to diagnose infections caused by the microorganisms I was studying at the time. This led me to obtaining a Post Graduate Diploma in Medical Laboratory Technology (PGDMLT). As part of the culminating experience of this diploma I had the fine opportunity of interning and later working at a Harvard Medical International (HMI) affiliate hospital in India where I learnt first-hand how differential diagnosis is applied in the field of infectious disease. Pursing my aspirations for higher education, I came to Arizona State University to complete my Professional Science Masters (PSM) in Computational Biosciences. My mentors at the time encouraged enrolling into the Biological Design PhD program during which time at the Center for Innovation in Medicine in Biodesign, I learnt how diagnostics are made for infectious diseases. From having seen both perspectives (end-users and manufacturing) of medical diagnostics I hope to continue to apply my expertise to create novel forms of diagnostic interventions enabling earlier resolution of disease.